VERTICAL DISTRIBUTION OF TRAFFIC-GENERATED $PM_{2.5}$ AND NO_2 IN A TROPICAL URBAN ENVIRONMENT

P. MANO KALAIARASAN

(B. Eng (Civil) (Hons), University of Liverpool;
MSc (Building Science), National University of Singapore)

A THESIS SUBMITTED

FOR THE DEGREE OF DOCTOR OF PHILOSOPHY

DEPARTMENT OF BUILDING

SCHOOL OF DESIGN AND ENVIRONMENT

NATIONAL UNIVERSITY OF SINGAPORE

2010

ACKNOWLEDGEMENTS

I wish to dedicate this thesis to my beloved wife Hemalatha for her strong support and motivation and my children for their love and patience.

This dissertation would not have been possible without assistance, support and encouragement of many wonderful people to whom I wish to convey my sincere appreciation.

I wish to express my deepest gratitude to Associate Professor Cheong Kok Wai David, Associate Professor Tham Kwok Wai from the Department of Building and Associate Professor Rajasekhar Balasubramanian from the Department of Environmental Science and Engineering for their invaluable guidance and inspiration.

I would like to thank Mr Jovan Pantelic for his invaluable advice on Computational Fluid Dynamics modeling. Many thanks to all the undergraduate students who have helped me in the field studies. Last but not least, I would like to thank the National University of Singapore for their generous financial support.

DEDICATION

To my beloved wife Hemalatha & Children

TABLE OF CONTENTS

EXECUTIVE SUMMARY

The research study focuses on the vertical distribution profiles of traffic-generated $PM_{2.5}/NO_2$ concentration in several typical naturally-ventilated high-rise public residential buildings of point and slab block designs, at different parts of Singapore. A total of six buildings were selected for the study and these buildings are located in close proximity to expressways that had high traffic volume.

A combination of measurement strategies, i.e. passive sampling for NO_2 and active and passive sampling for $PM_{2.5}$ were employed to find the vertical distribution profiles of traffic-generated $PM_{2.5}/NO_2$ at the point and slab block designs. Experimental results showed that $PM_{2.5}$ mass/number concentration and NO_2 concentration was highest at the mid floor of the building as compared to those measured at high and low floors. $PM_{2.5}/NO_2$ emitted from hot vehicle exhaust rises due to buoyancy and blown towards the building by the upstream wind. $PM_{2.5}/NO_2$ motion in the upward and sideways direction is further assisted by the wind turbulence additionally amplified by the fast moving vehicles along the expressway. Upon reaching the trees, some of the $PM_{2.5}/NO_2$ is being intercepted by tree leaves. Most of the $PM_{2.5}/NO_2$ flow over the top of the trees and keep moving upwards and towards the building carried by airflow streamlines. This could explain the reason for the $PM_{2.5}$ mass/ number concentration and NO_2 concentration being the highest at the mid floor of the buildings as compared to those measured at high and low floors. Although the lower floors were closest to traffic emissions, the $PM_{2.5}$ mass/number concentration and NO_2 concentration was lower

there than that at the mid floors, which is due to the buoyancy rise at the source point, interception of $PM_{2.5}$/NO_2 by tree leaves or the vortices at the wake region of the trees diluting the traffic-polluted air behind the trees or all three. The high floors had the least $PM_{2.5}$ mass/number concentration and NO_2 concentration due to dilution following pronounced mixing of traffic-polluted air with ambient air. The only difference between the point block and slab block configurations is that at corresponding floors, the $PM_{2.5}$ mass/number concentration /NO_2 concentration for slab block is much higher than that of point block under similar traffic and meteorological conditions. This is attributable to the slab block configuration which tends to slow down wind speed. The vertical distribution profile of $PM_{2.5}$ mass/number concentration and NO_2 concentration in this study differs from the vertical distribution profile of several studies which found that $PM_{2.5}$ mass/number concentration and NO_2 concentration usually decreased with increasing height. However, in previous studies, there were no trees in between the motorways and buildings.

The health risk model show for both the blocks, residents at the mid floors of the buildings have the highest health risk for all age categories: infants, children (1yr), children (8 - 10 yr) and adults in the mid floor compared to the high (lowest) and low floors (second highest) due to $PM_{2.5}$/NO_2 inhalation. This was expected since the highest concentration of to $PM_{2.5}$/NO_2 concentration occurred at the mid floors of the buildings. For both the blocks, new born babies, one year old children, and adults had similar potential health risk while teenage children (8 - 10yr) had the lowest potential health risk due to $PM_{2.5}$ inhalation. For NO_2 inhalation, one year old children in both the blocks suffer from the highest health risk followed by 8 - 10 year old children. New born infants had the least health risk. The health risk model results also showed that for the point block, NO_2 and the combined effect of $PM_{2.5}$

and NO_2 is about 2.3 and 3.3 times more risky than $PM_{2.5}$ respectively and for the slab block, NO_2 and the combined effect of $PM_{2.5}$ and NO_2 is about 2.1 and 3.2 times more risky than $PM_{2.5}$ respectively. Living in a slab block is about 1.37 times more risky due to $PM_{2.5}$ and about 1.27 times more risky due to NO_2 in contracting a respiratory disease compared to living in a point block

LIST OF TABLES

LIST OF FIGURES

LIST OF SYMBOLS

PM_1	particles less than or equal to 1 micrometer in diameter
$PM_{2.5}$	particles less than or equal to 2.5 micrometers in diameter
PM_{10}	particles less than or equal to 10 micrometers in diameter
μ	micro
NO_2	nitrogen dioxide
RH	relative humidity
I/O	indoor / outdoor ratio
D	the age-specific dose rate (μg kg^{-1})
BR	age-specific breathing rate (L min^{-1})
BW	age-specific body weight (kg)
C(*t*)	diurnal concentration of the pollutant (μg m^{-3})
OF (*t*)	occupancy factor of zone
Loael	lowest tested dose of a pollutant that has been reported to cause harmful or adverse health effects on people or animal
HR	health risk value
Vw	Wind velocity
L	The distance between two transducers
tf	The transit time in the forward direction
tr	The transit time in the reverse direction
MΩ	resistivity
°C	degree centigrade
Al	aluminium
Co	cobalt
Cr	chrominium
Cu	copper
Fe	iron
Mn	manganese
Pb	lead

Cd	cadmium
Ni	nickel
As	arsenic
Ag	silver
Ti	titanium
Zn	zinc
V	vanadium
TC	total carbon
EC	elemental carbon
OC	organic carbon
IC	ionic carbon
G	the gradient of a standard curve for NO_2 analysis
[T]	ambient temperature in ^{o}C
[RH]	relative humidity in %
P_N	vapour pressure in mm Hg at $20^{o}C$
P_T	vapour pressure of water at ambient temperature [T] in mm Hg
Nss SO_4^{2-}	non-sea-salt (nss) sulphate
$[SO_4^{2-}]$	sulphate ion concentration
$[Na^{+}]$	sodium ion concentration
F^{-}	Fluoride
Cl^{-}	Chloride
NO_2^{-}	Nitrite
NO_3^{-}	Nitrate
PO_4^{3-}	Phosphate
SO_4^{2-}	Sulphate
Li^{+}	Lithium
Na^{+}	Sodium
NH_4^{+}	Ammonium
Ca^{2+}	Calcium
Mg^{2+}	Magnesium
K^{+}	Potassium

Nap	Naphthalene
Ace	Acenaphthene
Acy	Acenaphthylen
Flu	Fluorene
Phe	Phenanthren
Ant	Anthracene
Flt	Fluoranthene
Pyr	Pyrene
BaA	Benzo[*a*]anthracen
Chr	Chrysene
BbF	Benzo[*b*]fluoranthene
BkF	Benzo[*k*]fluoranthene
BaP	Benzo[*a*]pyrene
Ind	Indeno[*1,2,3,cd*]pyrene
DBA	Dibenzo[*a,h*]anthracene
BPe	Benzo[*g,h,i*]perylene
H	height of storey

LIST OF APPENDICES

CHAPTER 1: INTRODUCTION

1.1 Background

Airborne particulate matter is a complex mixture of components from various sources. Anthropogenic particles are produced by human activities such as fossil fuel combustion and industrial processes. Particles are also produced from natural processes such as forest fires, volcanic activities, sea spray and from secondary processes such as chemical reactions and condensation. Particles formed from anthropogenic process are generally fine particles whilst particles formed from natural process are generally coarse particles. Atmospheric aerosols refer to solid and liquid particles suspended in the atmosphere. They encompass a wide range of sizes, the smallest being only a couple of nanometres in diameter and the largest range to about 100µm in diameter (Harrison, 2004). Particles greater than 10µm in diameter deposit quickly under gravitational influence and particles less than 10µm in diameter have a longer atmospheric lifetime and tend to be more uniformly dispersed across urban areas (Hester and Harrison, 1998).

There are considerable quantities of primary particles composing mainly of soot and organic material due to the intensity of traffic in urban areas. Studies show the majority of particles from the vehicle exhausts were found to be in the range of 0.02 - 0.13µm for diesel and 0.04 - 0.06µm for petrol (Morawska et al., 1998a and Ristovski et al., 1998). A small fraction of the total emissions is in the coarse mode which is generally less than 30% (Rogak et al., 1994 and

Weingartner et al., 1997). Thus, a large number of the emitted particles have a high chance of depositing in the vulnerable parts of the respiratory system of human. Many studies have been done on Total Suspended Particles (TSP) which consist of particles of diameter less than 100μm and on particle size of diameter less than 10μm (PM_{10}) since 1980s (Winchester et al., 1981; Cheng et al., 2000; Kim et al., 2002; Xiao and Liu, 2004). However, there have been significantly fewer studies on particles of diameter less than 2.5μm ($PM_{2.5}$). This size fraction is commonly known as fine particles. Particle size determines in which part of the respiratory system the particles will be deposited. Particles less than 10μm could be inhaled. Coarse particles and part of the fine particles in the size range 0.5 - 2.5μm are usually deposited in the extra-thoracic and trachea-bronchial parts of the lung system. Particles less than 1μm could penetrate into the pulmonary alveoli of the lungs and end up in the interstitial spaces of the alveolar lung tissue where they cannot be reached by the macrophages. Characterisation of the chemical composition of $PM_{2.5}$ helps to identify any toxicological constituents and can provide hints on the origins of $PM_{2.5}$ since certain compounds are characteristic of specific sources.

Fine particles are believed to pose a larger health risk compared to PM_{10} particles as they can penetrate deeper into the human lung system (Etkin, 1994 and American Lung Association, 1994). A study by Churg and Brauer (1997) found that only 5% of the number of particles in human lungs appeared to be ultrafine and that 96% was smaller than 2.5μm. Thus, fine particulate matter has become the focus of much of the research lately. Also, many epidemiological studies correlate particulate pollution with acute health effects

and even premature death. Particles inside the respiratory tract can cause acute respiratory symptoms such as cough, asthma, constriction and over-secretion of mucus and bronchitis. Chronic exposure may result in the impairment of lung elasticity, gaseous exchange efficiency and in extreme cases cause the lung tissue to become fibrotic (Burnett et al., 1998; Loomis et al., 1999; Hoek et al., 1997; Brunekreef, 2000; United Nations, 1979 and US EPA 1996).

Currently, Singapore has a population of 4.99 million and is the fourth most densely populated country in the world (Department of Statistic Singapore, 2009). With a very high population density of 6489 persons/km^2 as at 2010 and a land area of 707.1 square kilometers, Singapore can be considered a land scarce country. The projected resident population is 6.5 million by 2020. Almost 83% of the residents live in high-rise residential buildings which are mostly naturally-ventilated. Although there is no precise definition on high-rise buildings that is universally accepted, various bodies have tried to define what 'high-rise' means. Massachusetts General Laws (2009)**,** define a high-rise as being higher than 21m. The Encyclopedia of Britannica (2009) define a high-rise building as a multistory building tall enough to require the use of a system of mechanical vertical transportation such as elevators. Due to the lack of land space, residential buildings are usually high-rise and in close proximity to each other. Some of these buildings are located very close to busy expressways and major roads which have very high traffic volume. To cater for the 894682 vehicles owned (Department of Statistic of Singapore, 2009), Singapore has a comprehensive transport infrastructure with roads occupying 12% of the total area (Tai and Chong, 1998). With the expected increase in the population growth and in the motor vehicle numbers in Singapore, there is

an increasing concern over both ambient and indoor air quality in the urban areas, especially in naturally-ventilated high-rise residential buildings located near expressways and major roads as on-road vehicles are main sources of fine traffic-generated particles in urban areas. The fine traffic-generated particles could be inhaled by the residents of the buildings and thus this could affect their health over time.

The government of Singapore has taken various steps to ensure the particulate matter exposure be kept to the minimum. In an attempt to curb the increasing motor vehicle pollution, the government has implemented various policies and measures such as improved public transport system, restricted car ownership, decentralisation to get people to live nearer their work place, and having green belts to absorb some of the polluted air. Unleaded petrol was introduced in 1991 to replace leaded petrol which was eventually phased out in 1998. Diesel vehicles which make up of about 20% of Singapore's motor vehicle population emit about 50% of total $PM_{2.5}$ to the atmosphere. The National Environmental Agency (NEA) tasked by the Singapore government introduced Euro IV emission standards for new diesel vehicles such as taxis, buses and commercial vehicles, in an attempt to lower concentrations of $PM_{2.5}$ to acceptable standards. This was put in force in 1st October 2006. NEA also encourages its citizen to adopt Compressed Natural Gas (CNG) vehicles by providing incentive package such as substantial tax rebates for purchasing new CNG vehicles(NEA of Singapore Annual Report, 2005). These measures show a growing concern of the government in keeping particulate matter level to the minimum.

To date, there is however a lack of comprehensive data on the vertical distribution profile of fine traffic-generated particulate matter in the apartments of buildings, with respect to the different floor heights of naturally-ventilated high-rise residential buildings located in close proximity to busy expressways in the tropics. To bridge this gap, the research study focuses on the vertical distribution profiles of fine traffic-generated particulate matter in several typical naturally-ventilated high-rise public residential buildings of point and slab block configurations, at different parts of Singapore. In addition, the health impacts associated with particulate matter is investigated. The few available studies on buildings located near expressways or major roads dealt primarily with the vertical distribution profile of traffic-generated particles in buildings that were air-conditioned (office) and were located in cities or in street canyons with either dry, subtropical, or temperate climatic conditions. For example, Morawska et al. (1999) found no significant height dependence of particle number concentration for an office block from 3rd to 25th floor which was located 80 m from the motorway in Brisbane, Australia. However, for a building located 15 m from motorway, they found the particle number concentration at the building envelope was very high comparable to those in the immediate vicinity of the motorway. Wu et al. (2002) observed at the building height of 79m, the mass concentration levels of $PM_{1,}$ $PM_{2.5}$, and PM_{10} decreased to about 80%, 62% and 60% respectively, of the maximum concentration level occurring at 2m from the ground in Macau, China. Other investigators including Rubino et al. (1998) of Italy, Hitchins et al. (2001) of Australia, Chan and Kwok (2000) of Hong Kong have also found that particle mass/number concentrations decreased with increasing height of a building. It

is therefore critically important to conduct field-based investigation in the tropics to gain a better understanding of the relationship between the vertical transport of fine traffic-generated particulate matter and their potential health impacts on the indoor air quality in naturally-ventilated high-rise residential buildings. Studies by Chao and Wong (2002) and Morawska et al. (2001) have shown that outdoor particulate matter concentration levels could be used to predict indoor concentration levels.

1.2 Objectives

The objectives of this research study are:

a To determine the vertical distribution profile of traffic-generated $PM_{2.5}$ in naturally-ventilated high-rise residential buildings of typical building designs close to expressways. In some of the buildings, the indoor and outdoor vertical distribution profile as well as the horizontal distribution profile of traffic-generated nitrogen dioxide (NO_2) and its indoor and outdoor (I/O) ratio values were determined. The study includes NO_2 measurement as it is a good surrogate indicator of traffic-generated pollutants.

b To assess the health impacts due to exposure of traffic-generated $PM_{2.5}$ on residents living in point and slab blocks (Case Studies 2 and 3) and the potential health risk of residents due to inhalation of traffic-generated $PM_{2.5}$ and particulate PAHs using well known health risk models. Also, the chemical composition of $PM_{2.5}$ is measured at the various floors of the buildings to assess the toxicity of the $PM_{2.5}$.

c To study the effect of building configuration on the transmission of airborne $PM_{2.5}/NO_2$ to the buildings.

d To examine and recommend measures and design principles to minimize the transmission of traffic-generated $PM_{2.5}/NO_2$ from expressways to naturally-ventilated residential buildings.

e To assess the health risk of residents using health risk model due to exposure to traffic-generated $PM_{2.5}/NO_2$ in naturally-ventilated high-rise residential buildings close to expressways.

1.3 Scope of Research

The scope of research work includes substantial fieldwork on naturally-ventilated high-rise buildings located in close proximity to expressways i.e. within 30m from expressway. The objective measurements offer an insight on the vertical distribution profile of $PM_{2.5}/NO_2$ at the various floors of the buildings in terms of particle mass, particle number concentration, particle chemical compositions, NO_2 mass concentration, relationship of ambient conditions such as wind speed, temperature, RH and obstacles like trees with regards to $PM_{2.5}/NO_2$ concentrations in typical building designs. The air displacement effect by fast moving traffic on two typical building configurations is studied using Computational Fluid Dynamics (CFD) modelling. Finally, the health risk of residents in contracting respiratory disease is assessed using health risk model due to exposure to traffic-generated

$PM_{2.5}$/NO_2 in naturally-ventilated high-rise residential buildings close to expressways.

1.4 Outline of Dissertation

Chapter One states the background, the objectives and scope of study. This study focuses on the vertical distribution profile of traffic-generated $PM_{2.5}$/NO_2 in naturally-ventilated high-rise residential buildings close to expressways and its impact on the health of residents living in these buildings. Only limited work has been performed in the tropics on this topic. The uniqueness of local context is described.

Chapter Two describes the various ways of characterizing particulate pollution and the importance of particle number concentration. The meteorological influence on the transmission and dispersion of particulate mass and NO_2 and its vertical and horizontal distribution profiles around the buildings are described. The migration of particulate mass and NO_2 indoors and their associated health risk are examined. Correlation of NO_2 and $PM_{2.5}$, CFD modelling of air pollution distribution around buildings and trees and exposure and health risk models are reviewed. This is substantiated by past research findings. Finally, the hypothesis is stated.

Chapter Three details the methodology that includes research design and instrumentation for the objective measurement of traffic-generated $PM_{2.5}$ (physical and chemical measurements)/NO_2, and the environmental parameters such as wind speed, wind direction, air temperature and RH. The various case studies, established health risk assessment models for inhalation

of particulate PAHs and $PM_{2.5}$ and computation and meshing parameters of a point and slab block configuration for the CFD modelling of air displacement effect by fast moving traffic is described.

Chapter Four presents the Case Studies 1 - 3 to evaluate the effects of environmental parameters such as ambient temperature, RH and wind speed on the vertical distribution profile of traffic-generated $PM_{2.5}$ in residential buildings located near the Central Expressway (CTE). All these buildings are located in the same precinct. The chemical compositions of $PM_{2.5}$ at the various floors of the buildings were determined. For Case Studies 2 (point block) and 3 (slab block), health risk assessment due to inhalation of $PM_{2.5}$ and particulate PAHs is studied using established health risk models. The results of the CFD modelling of air displacement effect by fast moving traffic in a point and slab block is discussed. Finally, the chemical composition of $PM_{2.5}$ mass concentration at the various floors of a point and slab block is reconstructed with the elemental composition determined using an established method.

Chapter Five presents the Case Studies 4 - 6 where the residential buildings are located close to different expressways such as the Ayer Rajah Expressway (AYE) and Pan Island Expressway(PIE). The study includes NO_2 measurement as it is a good surrogate indicator of traffic-generated pollutants. The findings are used to substantiate the findings of Case Studies 1 - 3. The effect of environmental parameters such as temperature, RH and wind speed on the vertical distribution profile of traffic-generated NO_2 in residential buildings is evaluated. The horizontal distribution profile, $PM_{2.5}$ number

concentration at the floor with highest NO_2 concentration as well as the indoor/outdoor ratio of NO_2 is determined for the buildings.

Chapter Six presents the health risk assessment of residents in contracting respiratory disease due to $PM_{2.5}/NO_2$ inhalation living in a typical 22 - storeys point block and a 16 - storeys slab block located close to expressways using established health risk model.

Chapter Seven summarizes all the results in the study and suggests recommendations for future research work.

CHAPTER 2: LITERATURE REVIEW

2.1 Particulate Matter

Fine and ultra fine particles emitted from petrol as well as diesel engines are formed at high temperature in the engines, in the exhaust pipe or immediately after emission to the atmosphere. Some of these particles may be in the nucleation mode. These particles are often formed by coagulation of primary particles and by condensation of gases on particles. Fine particles (accumulation mode) are typically secondary particles formed by chemical reactions (e.g. SO_2 and NO_x to form sulphates and nitrates). The coarse mode of particles are typically formed mechanically by abrasion of road material, tyres and brake linings, soil dust raised by wind and traffic turbulence.

High concentrations of fine and ultra fine particles in urban environments, especially in the vicinity of major streets and roads have raised the interest to study the physical and chemical transformation of particles **(**Buzorius et al., 1999; Morawska et al., 1999**;** Pakkanen et al., 2001). Toxicological studies suggest fine and ultra fine particles have considerably enhanced toxicity per unit mass and their toxicity increased as particle size decrease (Donalson and MacNee, 1998; Minnesota Department of Health, 2009). A study also reported fine particles have large surface-to-diameter ratio allowing toxic substances to be released quickly (Diabaté, 2000).

Particles can be inhaled when they are smaller than 10μm. In general, smaller particles penetrate deeper into the lungs (US EPA, 2005). Particles in the size

range of 0.5 - 2.5µm are usually deposited in the extra-thoracic and the trachea-bronchial parts of the respiratory system due to impaction, settling and sedimentation. Particles of size less than 0.2µm can even deposit in the alveoli by diffusion. So far, there is no indication if one size fraction is more important than another size fraction in terms of health effects (Bree and Cassee, 2000). A study has found only 5% of the number of particles in human lungs appeared to be ultrafine and that 96% was smaller than 2.5µm (Churg and Brauer, 1997).

2.1.1 Physical Characterization

2.1.1.1 Gravimetric Mass

In ambient air quality standards and characterization of indoor and outdoor particle mass concentration, $PM_{2.5}$ and PM_{10} are commonly used. $PM_{2.5}$ is the mass concentration of particles with aerodynamic diameters lesser than 2.5µm, while PM_{10} is the mass concentration of particles with aerodynamic diameters lesser than 10µm. $PM_{2.5-10}$ is the mass concentration of particles with aerodynamic diameter greater than 2.5µm but equal to or less than 10µm. Further classification of particle size is shown in Table 2.1.

Table 2.1 Classification of Particles (Baron and Willeke, 2001)

Particle Classification	Size (in µm)
Coarse	Particles larger than 2.5
Fine	Particles smaller than 2.5
Ultra-fine	Particles smaller than 0.1

2.1.1.2 Particle Number Concentration

Most of the time, particles are reported in gravimetric terms. Recent studies have shown that particle number concentration can be more significant than particle mass concentration as small sized particles have small mass but are large in numbers. For instance, a study on characterization of airborne particles in Beijing showed 99% of airborne particles are in the respirable zone and gravimetrically, $PM_{2.5}$ constituted 46% of PM_{10} (Shi et al., 2003). Other epidemiological studies have found particle number concentration is a better indicator than particle mass concentration for health effects (Peters et al., 1997; Oberdörster et al., 1992; Oberdörster, 1995).

2.1.2 Chemical Characterization

Chemical characterization of fine particles is an essential step to identify toxicological constituents. Chemical compositions provide hints on the origins of fine particles since certain compounds are characteristic of specific sources. Toxic effect of particles depends on its size fraction. The major mass fraction of inorganic compounds such as sulphates and nitrates is present in the fine fraction. Carbonaceous compounds such as elemental carbon, organic carbon and polycyclic aromatic hydrocarbons (PAHs) usually occur in the ultrafine, fine and coarse fraction. Metals are present in the fine and ultrafine fraction. Many researchers have confirmed the importance of carbonaceous compounds in particles above that of inorganic compound in terms of health (Gordon et al., 1998; Rombout et al., 2000; Bree and Cassee, 2000). Elemental carbon causes acute and chronic effects. Studies have shown the relative risk on premature death increased with 1% per 1$\mu g/m^3$ of elemental carbon (Sunyer et

al., 1991) which is 5 - 10 times higher than the relative risk of PM_{10}. It has been extensively shown that PAHs are genotoxic and carcinogenic (Raat, 1994). Toxicological studies have shown metals in particulate matter can cause damage to the alveoli of lungs by producing ROS and interacting with the macrophages (Goldsmith, et al., 1998). The presence of the toxic groups, elemental carbon and particulate PAHs in the carbonaceous compounds and metals which are emitted by motor vehicles is the reason to believe traffic emissions may play a crucial role in inducing adverse health effects.

2.2 Factors Affecting Particle Concentration

2.2.1 Traffic Volume

A study conducted along road sides has revealed that concentration of fine particles are much greater closer to the sources such as vehicular traffic, than that at more distant locations (Jones and Harrison, 1994). Li et al. (1993) reported that higher level of particles coincided mostly during peak traffic hours whereas lowest particle number concentration occurred in the absence of traffic activity.

2.2.2 Meteorological Conditions

The particle concentration in urban areas has different characteristics on account of the changing meteorological factors depending on the geographical and topographical peculiarities of the urban areas. Meteorological parameters like ambient air temperature, RH, wind speed and wind direction play an important role in the migration of particles. Many papers discussed the

influence of these meteorological parameters on air pollution concentration. These studies marked the role of ambient meteorological parameters and how they can effect the particle concentration. Cuhadaroglu and Demirci (1997) investigated the influence of some meteorological factors on air pollution in Turkey and found that the airborne particle concentration increased with increasing temperature and decreased with decreasing RH. In Hong Kong, indoor-outdoor ratios of particle concentrations tend to increase with increase of temperature, RH and solar irradiation, but little effect from wind speed (Chan, 2002). In Hanoi, Vietnam, a study showed that the most important determinants of $PM_{2.5}$ are wind velocity and air temperature, while rainfall and RH largely control the daily variations of $PM_{2.5-10}$ (Hien et al., 2002). Rain was found to influence $PM_{2.5}$ and PM_{10} particle concentration, which decreased with heavy rain and increased during drought periods (Charron and Harrison, 2000).

Latini et al. (2002) identified two major classes of meteorological parameters which have a significant impact on the type of particles and how it dispersed to the indoor environment. Temperature, humidity and solar radiation affect chemical transformations of particles and hence the type of particles entering the indoor environment. Wind speed, wind direction, atmospheric stability by mixing height, stability class, vertical temperature gradient, solar radiation affect the dispersion of particles. Similarly, another study found that wind speed, direction, temperature, RH and precipitation all play a significant role in the formation, transportation and dispersion of particulate matter (Jung et al., 2004).

Jonsson et al. (2004) found that urbanisation have an influence on the climate and concentration of particles. Due to urban heat island effect, the city temperature increases, making it warmer than its surroundings. Land-ocean temperature difference generates a diurnal sea breeze. It was observed that concentration of particle was the highest in the urban area during the dry season. Harrison et al. (2004) reported that airborne particle mass concentration varies with street geometry and atmospheric conditions, and that atmospheric conditions are influenced by street geometry.

2.3 Distribution Profile of Particles

2.3.1 Horizontal Distribution Profile of Particles

The horizontal distribution of particles is of interest because it helps town planners to decide on the location of buildings and amenities considering the degree of exposure of occupants to fine and ultra fine particles. Studies have generally shown fine and ultra fine particle concentration decreases with increased distance away from the road (Hitchin et al., 2000; Wu et al., 2002). Hitchin et al. (2000) observed $PM_{2.5}$ levels decreased with distance to around 75% of the maximum for wind blowing across the road and to 65% for wind blowing parallel to the road, at a distance of 375m in their study. Wu et al. (2002) found no significant trend of decrease in concentrations of particulate matter as the distance from the road increases. Over the total measured distance (0 - 228m), the maximum decreases of PM_{10}, $PM_{2.5}$ and PM_1 were only 7%, 9% and 10%, of the maximum occurring at 2m from the road, respectively. Studies have also shown that particle concentrations of fine and ultra fine particles dropped to background levels at a distance of about 200 -

300m away from heavily trafficked roads where motor vehicle particulate pollution is prevalent (Levy et al., 2003; Morawska et al., 1999 and Zhu et al., 2002).

2.3.2 Vertical Distribution Profile of Particles

Understanding how particles are distributed with respect to the height of a building is of major importance in deciding the location of the natural air intake of the building or its orientation to the source of particulate matter pollution. Variation in the concentration of particles at the different floors of building depend on several factors such as vehicle generated turbulence, variation in traffic flow, meteorological parameter, configuration of buildings and geometry of the street. In a study by Morawska (2003), it was found that there are two factors affecting the particle concentration profile as a function of height of building. First factor is that particulate matter that is emitted at ground level gets diluted with urban air and therefore its concentration with increasing distance from the source (i.e. with height) is expected to decrease, and the second factor is the temperature gradient between ground and upper level may affect the upward convective transport of particulate pollution emitted at ground level. This promotes the mixing of urban air and contributes to the decrease in concentration difference between the ground level and the upper level.

Rubino et al. (1998) investigated the vertical profile of pollutants emitted by motor vehicles, measured on the façade of a 100m urban office tower, 'Grattacielo Pirelli', located in an open square in Milan, Italy, with a high

traffic density. The results showed a decrease in PM_{10} concentration levels from approximately 40μg/m^3 at ground level to approximately 32μg/m^3 at 80m above level. It is interesting to note that the indoor PM_{10} concentration was homogenous at 25 ± 1.8μg/m^3 on all floors of the buildings.

In Brisbane, Australia, Morawska et al. (1999) attempted to isolate the fine particle contribution of the freeway from the contribution of other sources by allocating three test sites with different distances from the freeway and street configuration. The study found no significant height dependence of particle number concentration for an office block from 3rd - 25th floor, which was located 80m from the motorway. However, for a building located 15m from motorway, they found the particle number concentration at the building envelope was very high comparable to those in the immediate vicinity of the motorway.

In Macau, China, Wu et al. (2002) found that there was a significant decrease in the concentration of PM_{10}, $PM_{2.5}$ and PM_1, as the height above the ground increased from 2m to 79m. At the height of 79m, the concentration levels of PM_{10}, $PM_{2.5}$ and PM_1 decreased to about 60%, 62% and 80% respectively, of the maximum occurring at 2m. The vertical profile at the roadside suggested that particle concentrations were affected significantly by sources at ground level from traffic, e.g. resuspended road dust and vehicular emissions. In Hong Kong, Chan and Kwok (2000) found similar results.

A study on concentrations of submicrometer particles measured around low-rise and high-rise buildings was conducted by Hitchins et al. (2001) in Brisbane, Australia. This study includes measurements of the vertical profile

of particulate matter in three high-rise buildings. The results showed clear decreases of around 50 - 60% in particle number concentration between ground and roof-top levels for the three high-rise buildings.

2.4 Outdoor to Indoor Migration of Particles to Buildings

Most people spend their time indoors. Traffic emissions not only contribute to outdoor particulate matter concentration levels, but also to indoor levels. EPA Victoria (2009) has reported that motor vehicles emit 30% of the particulate matter. Since traffic-generated particles mostly fall in the fine and ultra fine range, the particles can easily penetrate the buildings via open windows, cracks and mechanical filter systems (Koponen, 2001). Generally, the indoor particle concentrations depends on the generation rate of particles indoors, the outdoor particle concentration, air exchange rate, particle penetration efficiency from the outdoor to the indoor environment, and the particle deposition rate on indoor surfaces (Shair and Heitner, 1974; Kamens et al., 1991; Thatcher and Layton, 1995). Studies conducted show that outdoor particle concentration could be used to predict indoor concentration levels (Morawska et al., 2001; Chao and Wong, 2002). Having knowledge about the influence of ambient particulate matter pollution on the concentration in indoor environment is, therefore, crucial for assessment of human health effects from traffic particulate pollution. Studies suggest that respiratory illness or reduced lung function is associated with proximity to main roads, road traffic density, or exposure to pollutants derived from motor vehicles (Burr et al., 2004). In urban areas, it has been shown that traffic is the dominating source of ultrafine particles in busy street, and the penetration of

traffic particles into houses along streets is significant for particles in the size range below 100nm (Palmgren et al., 2003).

Studies on the relationship between indoor and outdoor particles showed that the ratio of indoor and outdoor (I/O) total suspended particle matter varied from 0.20 to about 1.00 (Andersen, 1972). Monn et al. (1997) studied 17 naturally-ventilated homes in Switzerland on the relationship between I/O for PM_{10} and $PM_{2.5}$ particles and found that in homes without any indoor sources and where human activity was low, PM_{10} I/O ratios was about 0.7. The study also showed that indoor source like smoking had the highest influence on I/O ratios where the I/O ratio was greater than 1.8. Other studies indicate that the I/O ratio particle mass concentrations varied from 0.5 - 2 in the absence of indoor particle sources (Spengler et al., 1981; Quackenboss et al., 1989; Wallace, 1996). It should be noted that indoor activities such as smoking or cooking may play an important role in affecting the relationship (Spengler et al., 1981; Monn et al., 1995; Ross et al., 1999). Studies in Singapore suggest that the I/O ratio in naturally-ventilated building was close to unity (Gupta and Cheong, 2007) indicating particulate pollution migration was from outdoors to indoors rather than its emission from internal sources and that an I/O ratio close to unity indicate outdoor pollution significantly affects the indoor air quality of the building. This was supported by Benson et al. (1972) who concluded in general that the I/O ratio of particle concentration was about one.

2.5 Chemical Characterization of Traffic-Generated Particles

Traffic-generated particles can be divided into three main classes namely, inorganic compounds (sulphates and nitrates), carbonaceous compounds (elemental carbon, organic carbon and PAHs) and metals. Inorganic compounds are produced by secondary production mechanisms and are generally uniformly distributed over large distances. Carbonaceous particles are largely emitted as primary particles and the concentration of these particles increases in their source areas.

A study by Wang (2003) on the chemical characterisation of water soluble components of PM_{10} and $PM_{2.5}$ atmospheric aerosols in Nanjing city found higher portion of water soluble fraction in the traffic center and downtown area. Kirchstetter et al., (1999) found the chemical composition of traffic-generated particles mainly consisted of carbonaceous compounds and metals and that elementary carbon made up more than the emitted mass. Weingartner (1997) found particulate PAHs contribute about 1% of the particulate mass. Lonati (2005) studied into the chemical composition of $PM_{2.5}$ and showed the primary contribution by traffic source, in terms of carbonaceous matter, elemental carbon and primary organic aerosols, was estimated at 6% and 11% of the total $PM_{2.5}$ mass respectively in cold and warm season. Other studies also found trace metals such as chromium (Cr), copper (Cu), zinc (Zn), cadmium (Cd) and lead (Pb) in traffic emissions (Vermeulen et al., 1999). From the above studies it can be seen that traffic-generated particles contribute to the toxicity of outdoor and indoor aerosols.

2.6 Traffic-Generated Particles and its Health Implications

As people become more aware and concern of pollution issues, there is a need to study the impact of such emissions in the environment and the effect on human health. There is growing evidence of associations of traffic pollution and adverse health effects (NRC, 1998). In Singapore, only PM_{10} is monitored and the outdoor air quality threshold level of PM_{10} is 150μg/m^3 (24hr average) and 50μg/m^3 (annual average) for short and long term health protection purpose. The US EPA national standards (NAAQS) for PM_{10} and $PM_{2.5}$ are 150μg/m^3 and 35μg/m^3 (24hr average), respectively and 15μg/m^3 (annual average) for $PM_{2.5}$ (US EPA, 2009).

Motor vehicle emissions constitute a main source of fine and ultrafine particles in urban area (Gupta et al., 2003; Weingartner et al., 1997; Kittelson et al., 2000; Harrison et al., 2001; Shi et al., 2001; Wehner et al., 2002; Palmgren et al., 2003). A study reported that ultra fine particles in motor vehicle emissions have the largest surface area and the highest content of potentially toxic hydrocarbons among all particulate matter sources (Oberdörster and Utell, 2002). Another study reported that particle size, surface area, and chemical composition determine the health risk posed by particulate matter, and combustion particles such as from vehicle exhaust have a core of elemental carbon that is coated with a layer of chemicals, including organic hydrocarbons, metals, nitrates, and sulphates which may play a role in particle toxicity (Donaldson and Tran, 2002). These particles will be deposited deep in the lungs and the residence time will be very long, up to several months (WHO, 2000; James et al., 1991; Owen and Ensor 1992; Berico et al.,

1997) and cause adverse health effects. Some examples of adverse health effects due to motor vehicle particulate matter pollution are that chronic exposures to particulate matter may result in the impairment of lung elasticity, gaseous exchange efficiency and increase susceptibility to infections.

Risom et al. (2005), suggest that the mechanisms of particulate matter induced health effects were believed to involve inflammation and oxidative stress. The oxidative stress mediated by particulate matter might arise from direct generation of reactive oxygen species (ROS) from the surface of particles, soluble compounds such as transition metals or organic compounds and activation of inflammatory cells capable of generating ROS and reactive nitrogen species. The study also suggested that the surface area is the most important determinant of effect for ultra fine particles (diameter less than 100nm), whereas chemical composition may be more important for larger particles.

The health statistics issued by the Ministry of Health, Singapore, has revealed that about 24% of the deaths in Singapore is due to cardiovascular disease and 0.7% of the total deaths were due to bronchitis, emphysema and asthma (Ministry of Health Singapore, 2009). Studies have implicated that the daily concentrations of PM_{10} and $PM_{2.5}$ have been linked with cardio-respiratory health effects and even with mortality (Le Tertre et al., 2002; Schwartz, 1994 and Dockery et al., 1993). Another study showed that each 10 $\mu g/m^3$ increase in fine particulate pollution has been associated with approximately 6% - 8% increased risk of cardiopulmonary and lung cancer mortality respectively (Pope et al., 2002). In extreme cases, lung tissue may become fibrotic (United

Nations, 1979). Neuberger et al. (2004) showed acute impairments of respiratory function and health in elderly and children were associated with fine particulates and sub-fractions related to motor vehicle traffic. Peters et al. (2004) reported that transient exposure to traffic might increase the risk of myocardial infarction in a susceptible person. Particles could also circumvent many of the respiratory system's defence mechanisms, such as cilia, and are capable of delivering relatively high concentrations of potentially harmful substances, often causing severe damage at the cellular level (Etkin, 1994).

2.7 Nitrogen Dioxide (NO_2)

In urban air, the presence of NO_2 is mostly from vehicular traffic (Raducan and Stefan, 2009; Ryan et al., 2009; LTP, 2006; Chaix et al., 2006, Hochadel et al. 2006). NO_2 is produced when nitric oxide (NO) emitted from combustion process of motor vehicles combines with ozone in the atmosphere. NO_2 not only affects the health of people but it is also a good surrogate indicator of traffic pollutants. In urban areas NO_2 concentration can be high, both in indoors and outdoors. WHO (2005) guidelines state the maximum acceptable NO_2 concentration is 40μg/m^3 for the annual mean and 200μg/m^3 for the 1hr mean concentration. For example, in the United Kingdom, the mean NO_2 concentration level measured at 363 urban sites ranged from less than 10 ppb (18.8μg/m^3) in northern Scotland to around 50ppb (93.9μg/m^3) at near-road sites in London (Ekberg, 1996). In Seoul and its suburbs, a study reported that the mean NO_2 levels were 60.2ppb (113.0μg/m^3) and ranged from 43 to 79 ppb (80.7 - 148.2μg/m^3) (Sohn et al., 1995). In Hong Kong, 12 residential premises studied showed the mean NO_2 level in the indoor

environment (living room, bedroom and kitchen) was 55.2μg/m^3 while the corresponding outdoor NO_2 level was 71.8μg/m^3. The study indicated that cooking activities in the kitchen had strong impact on the NO_2 level. When cooking existed, the mean indoor NO_2 level was 59.7μg/m^3 and when cooking did not exist, the NO_2 level was 41.8μg/m^3 (Chao and Law, 2000). A large scale study of human exposure to NO_2 in the Los Angeles Basin found the median outdoor level was 35ppb (65.7μg/m^3) and the median indoor level was 24ppb (45μg/m^3) (Spengler et al., 1994). Other studies conducted in the UK showed the mean concentration of NO_2 was 12.7ppb (27.6μg/m^3) in 12 homes (Ross, 1996).

2.8 Factors Affecting NO_2 Concentration

2.8.1 Traffic Volume

Traffic-generated NO_2 are generally highest in urban rather than rural areas. It was reported that NO_2 levels vary significantly in the United States of America and China throughout the day from September - November 2004, with peaks generally occurring twice daily as a consequence of rush hour traffic (NASA, Goddard Space Flight Centre, 2010). Another study from Bahrain showed NO_2 levels decreased where traffic volume and density also decreased (Danish and Madany, 1992).

2.8.2 Meteorological Conditions

Correlation between NO_2 and meteorological parameters such as wind speed, temperature and RH has been studied. The results showed that the

concentrations of NO_2 is strongly correlated with wind speed but weakly correlated with temperature (Hargreaves et al., 2000; Wehner and Wiedensohler, 2003; Gupta et al., 2004 and Turalioglu et al., 2005). It appears to be that there is a simple inverse relationship between NO_2 and wind speed, indicating the dilution and transport by wind (Elminir, 2005). However, there is no significant relation between RH and NO_2 concentrations (Turkoglu et al., 2004).

2.9 Distribution Profile of NO_2

2.9.1 Horizontal and Vertical Distribution NO_2

The horizontal distribution of NO_2 is of interest because it helps town planners to decide on the location of buildings and amenities considering the degree of exposure of occupants to NO_2 concentration levels. The vertical distribution of NO_2 concentration levels also merits consideration because it provides an understanding how the NO_2 concentration levels are distributed with respect to the height of a building so that one can decide on the location of the natural air intake of the building, or the building orientation based on the NO_2 pollution source. Studies showed the concentration of NO_2 decreased with increasing distance from the highway (Roorda-Knappe et al., 1998; Gilbert et al., 2003 and Maruo et al., 2003). For the vertical distribution profile of NO_2, a study at the Gustavii Cathedral in Göteborg, Sweden, showed NO_2 concentrations were the same at 10m and 32m height levels (Janhäll et al., 2003). Another study reported the concentration of NO_2 decreased with increasing height of the building (Costabile et al., 2006).

2.10 Outdoor to Indoor Migration of NO_2 to Buildings

Studies show the indoor air contaminant levels depending on ventilation rate, source and sink strengths, as well as outdoor condition which influence the outdoor air contaminant level. The relationship usually has a strong temporal component as the parameters that influence these two levels change with time (Ekberg, 1996). A study on 12 residential homes in Hong Kong reported the mean indoor and outdoor (I/O) ratio of NO_2 was 0.80 (Chao and Law, 2000). Another study in Hong Kong reported the mean I/O ratio of in homes of 10 non-smoking residential buildings in Hong Kong was 0.79 (Chao, 2001). In Swedish homes, the mean I/O ratio ranged from about 0.4 - 0.7 (Hagenbjork-Gustafsson et al., 1996).

2.11 Deposition Velocity of NO_2

A very important factor in establishing I/O ratios and indoor concentration levels is the deposition velocities of the gases to the room surfaces. In the absence of indoor sources, indoor air concentrations are determined by the outdoor concentrations, by homogeneous gas phase chemistry in the indoor air, by the air exchange rate due to natural ventilation and by the deposition velocity of the pollutant gases to the room surfaces. The deposition velocities vary for material surfaces and depend on air humidity and temperature. The IMPACT model can be used to estimate the steady state I/O ratio from the simple equation (Nazaroff et al., 1993):

$$\frac{I}{O} = \frac{\lambda}{\lambda + (1/V)\Sigma v_{d,i} S_i'} \quad \text{.....(1)}$$

where I is the indoor air gas concentration (ppb), O is the outdoor air gas concentration (ppb), λ is the air exchange rate (s^{-1}), vd,i is the total deposition velocity to the i^{th} room surface (ms^{-1}), Si is the area of the i^{th} room surface (m^2), V is the room volume (m^3).

2.12 Estimation of Removal of NO_2 Using Deposition Algorithms

Removal of NO_2 by tree canopies can be estimated using dry deposition algorithms. A gridded photochemical model (Comprehensive Air Quality Model with extensions, CAMx) uses such algorithms. Dry deposition estimation methods in CAMx are based on the work of Wesely et al. (1989) and Walmsley and Wesely (1996). In this model, dry deposition rates are influenced by resistances due to three mechanisms namely aerodynamic transport, diffusion across a quasi-laminar sub-layer, and surface uptake.

The dry deposition flux is found as:

$$F_c = V_d \cdot C_z \quad \text{.....(2)}$$

where F_c is the dry deposition flux of the gas of interest, V_d is the dry deposition velocity, and C_z is the concentration or mixing ratio at the mid-point of first vertical layer height in CAMx.

For gases, the dry deposition velocity is calculated as follow:

$$V_d = \frac{1}{r_a + r_d + r_s} \quad \text{.....(3)}$$

where r_a is the aerodynamic resistance above the surface, r_d is the deposition layer (or quasi-laminar sub-layer) resistance and r_s is the bulk surface (or canopy) resistance. r_a and r_d are expressed as follow:

$$r_a = \frac{1}{\kappa \cdot u_*}\left[\ln\left(\frac{\Delta z}{z_o}\right) - \phi_h\right]$$

$$r_d = \frac{2S_c^{2/3}}{\kappa \cdot u_*} \qquad \ldots(4)$$

where u_* is friction velocity (m/s), κ is von Karman constant (value of 0.4, dimensionless), Δz is the lowest model layer midpoint height which has the value of 20 m, z_o is land use-dependent aerodynamic surface roughness length (m), Φ_h is the stability correction function for trace gases, S_c is the Schmidt number or the ratio of kinematic viscosity of air to species molecular diffusivity.

Bulk surface (or canopy) resistance is expressed as several serial and parallel resistances that are influenced by land cover type.

$$r_s = \frac{1}{\frac{1}{r_{st}+r_m} + \frac{1}{r_{uc}} + \frac{1}{r_{dc}+r_{lc}} + \frac{1}{r_{ac}+r_{gs}}} \qquad \ldots(5)$$

where the first serial resistance set represents the pathway into stomatal and mesophyllic portions of active plants, the second is the pathway into the upper canopy, the third is the pathway into the lower canopy, and the fourth is the pathway to the ground surface.

The stomatal resistance is estimated as:

$$r_{st} = diffrat \times r_j \times \left(1 + \left(\frac{200}{solflux + 0.1}\right)^2\right) \times \left(\frac{400}{t_s(40 - t_s)}\right) \qquad \ldots(6)$$

where diffrat is ratio of molecular diffusivity of water to the molecular diffusivity of the species of interest (NO: 1.29; NO_2: 1.60; and O_3: 1.63), r_j is the baseline minimum stomatal resistance (sm^{-1}), solflux is the solar irradiation flux (Wm^{-2}), and t_s is the surface air temperature (^oC).

The mesophyll resistance, r_m, the leaf cuticular resistance in healthy vegetation, r_{uc}, the resistance to buoyant convection, r_{dc}, the resistance of exposed surfaces in lower canopy, r_{lc}, the baseline canopy height/density resistance, r_{ac}, and is the resistance of ground surface, r_{gs}, are calculated as:

$$r_m = \left(\frac{Henry_i}{3000} + 100 \cdot fo^i \right)^{-1}$$

$$r_{uc} = \frac{r_{lu}}{\frac{Henry_i}{Henry_{so2}} + fo^i}$$

$$r_{dc} = 100 \cdot \left(1 + \frac{1000}{solflux + 10} \right)$$

$$r_{lc} = \left(\frac{Henry_i}{Henry_{so2} \cdot r_{lcs}} + \frac{fo^i}{r_{lco}} \right)^{-1}$$

$$r_{gs} = \left(\frac{Henry_i}{Henry_{so2} \cdot r_{gss}} + \frac{fo^i}{r_{gso}} \right)^{-1} \quad \text{.....(7)}$$

where $Henry_i$ is Henry's law constant for each species i, $HENRY_{SO2}$ is Henry's 200 law constant for SO_2, and fo is the normalized reactivity parameter for each species i.

These algorithms could be used to estimate the maximum removal of NO_2 by tree canopies if it is assumed all the airflow went through the trees. This gives the maximum 'filtering' effect by the trees.

2.13 Correlation of NO_2 and $PM_{2.5}$

In a study of air pollution near major highways in the Netherlands, Roorda-Knape et al. (1999) reported that NO_2 was one of the easiest ways to measure as it could be monitored by passive diffusion samplers that made it good to use

as an index of traffic related pollutants. A study by Hazenkamp-von Arx et al. (2004) showed there was a positive correlation between NO_2 and $PM_{2.5}$ (Spearman correlation coefficient r_s = 0.75). This was supported by other studies which also showed a moderate to fair correlation between NO_2 and $PM_{2.5}$ (Kumar et al., 2006 and Beckerman et al., 2008).

2.14 NO_2 and its Health Implications

The evidence linking NO_2 and health mainly comes from epidemiological studies. NO_2 acts as an irritant affecting the mucosa of the eyes, nose, throat, and respiratory tract. Continuous exposure to high NO_2 concentrations may contribute to the development of acute or chronic bronchitis while exposure to low NO_2 concentrations may cause increased bronchial reactivity in asthmatics, decreased lung function in patients with chronic obstructive pulmonary disease and increased risk of respiratory infections, especially in young children (U.S. EPA, 2010).

2.15 Modelling Air Pollution Distribution Around Buildings and Trees Using Computational Fluid Dynamics (CFD)

In most of the CFD modelling studies, air pollution dispersion around buildings and trees are done separately. There is little information on air pollution dispersion around buildings with trees as obstacles in front of the building. This is due to the very complex nature of the problem. CFD has been widely used to predict indoor particle and droplet transport and dispersion (Shimada et al., 1996; Chung, 1999; Béghein, 2005). For outdoors, due to the complexity of pollutant dispersion around buildings, much of the research with CFD has focused on the urban street canyon (Leitl et al., 1997; Kastner-

Klein and Plate, 1999) and the isolated building (Li and Meroney, 1983; Leitl et al., 1997; Tominaga and Stathopoulos, 2007a; 2007b; 2008 and Blocken et al., 2008). In the studies, trees were not included in CFD analysis.

Airflow in and around trees tends to be strongly complex three-dimensional, inhomogeneous and turbulent. Even modelling of the trees itself is very complex. Trees have been modelled in a number of ways. In a study, a row of trees is modelled as a solid cylindrical stem and a conic porous canopy (Rosenfeld et al., 2010). In another study, CFD modelling of airflow within model plant canopies was performed with separate models for the leaves and the branches of the canopy. The effect of the branches on airflow was modelled by introducing the 3D architecture of the canopies into the model and that of the leaves was modelled by adding drag force terms in the momentum and turbulent energy equations in porous sub-domains created around the branches (Endalew et al., 2009). In this study, trees were not considered in the modelling due to the complex nature of the actual problem and computational limitation. CFD modelling was performed to provide a visual perspective of airflow patterns around a point block and slab block building configurations at various upstream wind speeds coupled with the air displacement effect from the fast moving traffic.

2.16 Exposure and Health Risk Model for Inhalation Exposure to Pollutants

Most of the exposure assessment models are often based on the outdoor pollutant concentration levels which are used as the input parameter for predicting total human exposure (Colls and Micallef, 1997). The indoor

concentration levels may differ from the outdoor ones even in the absence of any significant indoor pollution sources. Epidemiology has shown mass concentrations of urban ambient particles are associated with relative mortality risks for long-term exposures (10% increase in mortality risks per $10\mu gm^{-3}$ for $PM_{2.5}$) and daily exposures (0.6% increase in mortality risks per $10\mu gm^{-3}$ for PM_{10}) (Pope and Dockery, 2006). Stölzel et al. (2007) showed that particle number concentrations of ultrafine particles are associated with mortality (2.8% of increase in mortality risks per 10^4 cm^3).

The US EPA has developed several computer-based exposure models applicable to pollutants which are directly or indirectly linked to mobile sources (Johnson, 1995; Graham and Burke, 2004; Ozkaynak et al., 1999; McCurdy, 1995). Probabilistic modeling can be used to assess exposure distributions in selected target populations (Bruinen de Bruin et al., 2004; Hanninen et al., 2003; Zidek et al. 2005; Burke et al., 2001; Kruize et al., 2003; MacIntosh et al., 1995). A comparison of some of the models for human exposure to air pollution is discussed by Duan (1982). Some indirect exposure method for estimating population exposures to indoor pollutants have been developed (Klepeis, 1999).

Only a few health risk assessment methods have been developed for the inhalation of particles. The US EPA has been developing a total risk integrated methodology (US EPA, 2005) which is a set of models for assessing exposure and risk for criteria air pollutants and hazardous air pollutants. For low toxicity low solubility particles (LTLS) such as black carbon, the toxicological data are used as a baseline for the risk assessment. The upper limit of particle-

related health risks is estimated by using the dose-response function of quartz, a known high toxicity compound with 60 time higher toxicity than the LTLS particles (Duffin et al., 2007). Another health risk model by Hänninen et al. (2009) converted the risk factors per ambient particle concentration into risks per accumulated dose of non-soluble particles in the alveolar lung region by using an attenuation model (Wilson and Brauer, 2006; Hänninen et al., 2004 and Hussein et al. 2006), respiratory physiological data, an alveolar particle deposition model (ICRP, 1994) and an exponential model for particle clearance from the lungs (Kreyling, 1994). In the model, it is assumed the mortality in the general population is caused by the retained alveolar dose of the non-soluble fraction of ambient particles. The health risk model used by Pandey et al. (2005) and described in Chapter 3 (sec.3.4) is based on the analysis of the potential health risk of a person under three age-specific categories namely, infants, children and adults associated with inhalation exposure of a pollutant. It gives dimensionless values which can be used for relative risk assessments of a resident in contracting a respiratory disease due to the inhalation of traffic-generated pollution. The strength on this model is that it is easy to use and does not involve elobrate statistical analysis and its weakness is that it is dependent on the accuracy of the lowest observed adverse effect levels (loael) value. Loael is defined as the lowest tested dose of a pollutant that has been reported to cause harmful or adverse health effects on people or animal.

2.17 Hypothesis

a) Previous studies show that $PM_{2.5}$ and NO_2 concentration levels reduced with the height of the buildings. All the buildings did not have trees in between the buildings and motorways. For this study, there are trees in between the naturally-ventilated residential buildings and expressways. It is hypothesized that trees will affect the vertical distribution profile of $PM_{2.5}$ and NO_2 concentration in naturally-ventilated residential buildings (Hypothesis 1).

b) The row of trees along the expressways in all the studies has dense complex canopy structure and their heights are slightly above the low floors. $PM_{2.5}/NO_2$ emitted from hot vehicle exhaust rises due to buoyancy and the hot road surface before being blown towards the building by the upstream wind. $PM_{2.5}/NO_2$ motion in the upward and sideways direction is further assisted by the wind turbulence additionally amplified by the fast moving vehicles along the expressway. Upon reaching the trees, some of the $PM_{2.5}/NO_2$ are presumably being intercepted by tree leaves (Beckett et al., 2000; Impens and Delcarte, 1979). Most of the $PM_{2.5}/NO_2$ flow over the top of the trees and keep moving upwards carried by airflow streamlines (Cleugh, 1998; Judd et al., 1996 and McNaughton, 1988). Thus, it was hypothesized that the highest concentration of $PM_{2.5}$ and NO_2 occur at the mid floor of the naturally-ventilated residential buildings (Hypothesis 2).

c) As a corollary to Hypotheses 1 and 2, it is hypothesized that the associated health risk of residents at the mid floors is higher than the other floors (Hypothesis 3).

CHAPTER 3: RESEARCH METHODOLOGY

3.1 Research Design

A total of six case studies were performed to achieve the objectives set forth in this study. The research approach is outlined in Figure 3.1. The first three case studies were selected for $PM_{2.5}$ measurements whilst the last three case studies were selected for NO_2 measurements.

Table 3.1 Summary of Measurement Sites

Case	Pollutant	Expressway	Block Configuration
1	$PM_{2.5}$	Central Expressway	Point Block
2	$PM_{2.5}$	Central Expressway	Point Block
3	$PM_{2.5}$	Central Expressway	Slab Block
4	NO_2	Ayer Rajah	Point Block
5	NO_2	Ayer Rajah	Slab Block
6	NO_2	Pan Island	Slab Block

Case studies 1 and 2 are selected to confirm the measurement results of $PM_{2.5}$. Case studies 2 and 3 are selected to study the difference in measurement results of $PM_{2.5}$ between a point block and a slab block configuration. Case studies 4 - 6 are selected to see if there is a difference in the vertical distribution profile of $PM_{2.5}$ and NO_2 for the same block configuration. NO_2 is used because studies have shown that it is a good surrogate indicator of traffic-generated pollutants. To generalize the results, the studies were carried out at different major expressways which are located at different parts of Singapore.

3.1.1 Site Selection

The six sites were selected based on the following criteria:

- Naturally-ventilated high-rise residential buildings because about 83% of the population reside in these type of buildings.
- Building's proximity to expressway is less than or equal to 30m downstream of expressway. The expressways of Singapore are special roads that allow motorists to travel quickly from one urban area to another (Wikipedia, 2009).
- Expressway has high traffic volume. A road that carries around 12000 - 30000 vehicles per day in urban areas can be considered a road that carries a high traffic volume (Christchurch City Council, 2009).
- Two typical building design configurations. The point block is a high-rise apartment-building with the circulation and services in the central core and the residential areas grouped around it on several storeys (Wong and Yeh, 1985). The heights of the selected point block buildings range from 20 - 22 storeys. The slab block has exterior access corridors with only one layer of flats being lined along the corridor (Wong and Yeh, 1985). The heights of the selected slab block buildings range from 10 - 16 storeys. For both the building designs, their storey height is about 2.8m.
- The ground on which the buildings stood was reasonably flat and almost the same level as the road.

- The predominant wind blows almost perpendicularly towards the building facades where the living rooms are located. In this way, most traffic-generated pollutants would be advected into the buildings.
- The adjacent buildings nearby the site did not interfere with the predominant wind flow direction.

Once the building has been selected, sampling locations in each building were identified so as to give a good representation of the physical, chemical and environmental parameters measured at different heights of the building for both indoor and outdoor spaces. The objective study comprises of physical and chemical measurements. Physical measurement includes size and number concentration of traffic-generated $PM_{2.5}$ particles, temperature, RH, wind speed and wind direction. The chemical measurement includes NO_2 mass concentration, trace metals, elemental carbon, organic carbon, water soluble ions and particulate PAHs. The objective measurement procedure is shown in Figure 3.1. After data analysis, results are presented in tabular, graphs and charts for discussion and the conclusions are drawn. The instrumentation and the analysis procedure used are discussed in the next section.

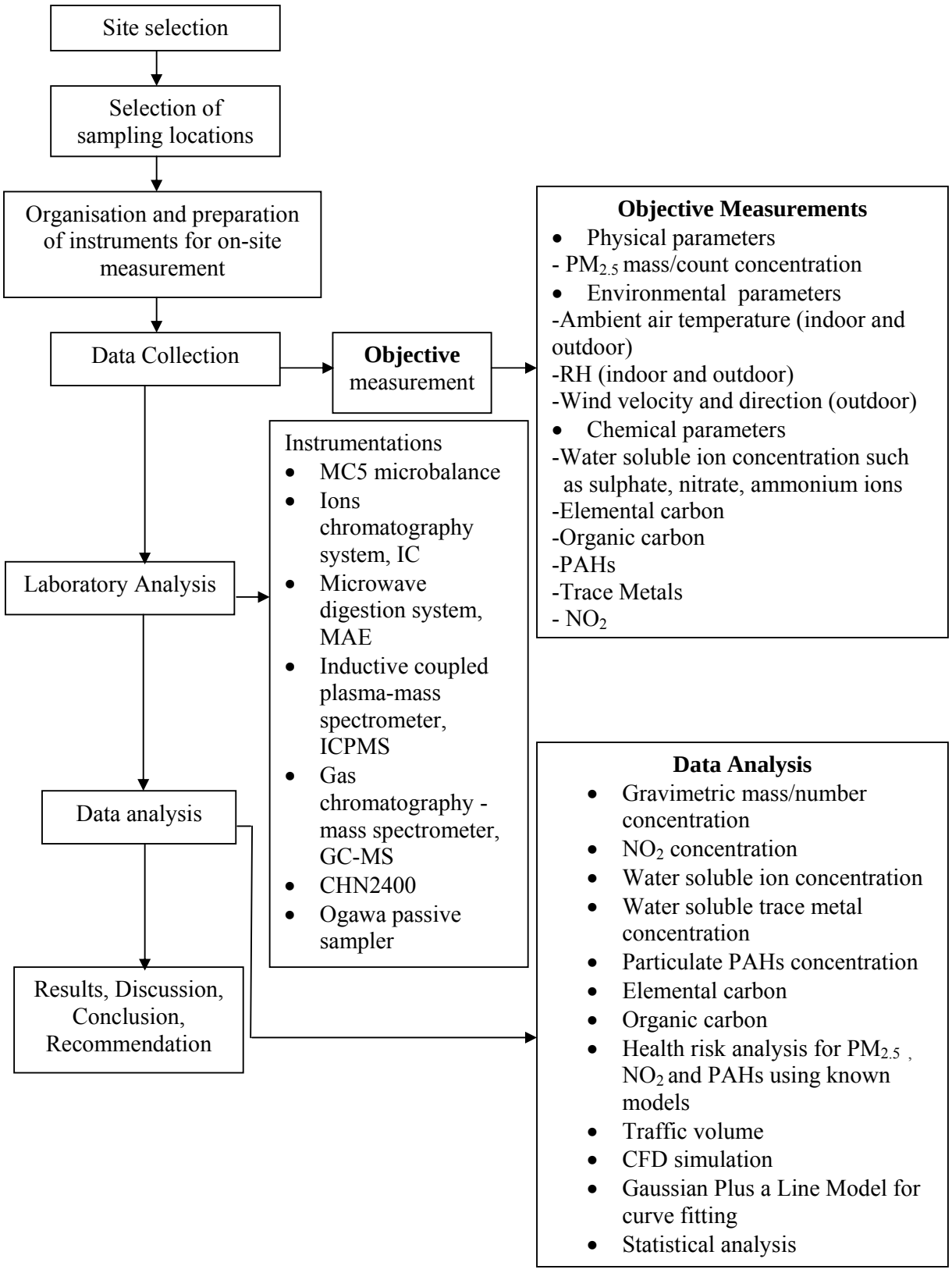

Figure 3.1 Flowchart of the Research Design Approach

3.1.2 Site Characterization and Sampling Strategy

3.1.2.1 Case Study 1

For Case Studies 1 - 3, the predominant wind is south-east direction. Block 96 as shown in Figure 3.2, is a 22 - storeys point block residential building selected for the study. The block was selected as it is about 7m from the Central Expressway (CTE). CTE is one of the most highly-utilized expressways which link many residential towns to the Central Business District of Singapore. The expressway is a dual carriageway with each carriageway having 3 lanes. The traffic volume is between 11000 - 16000 vehicles per hr.

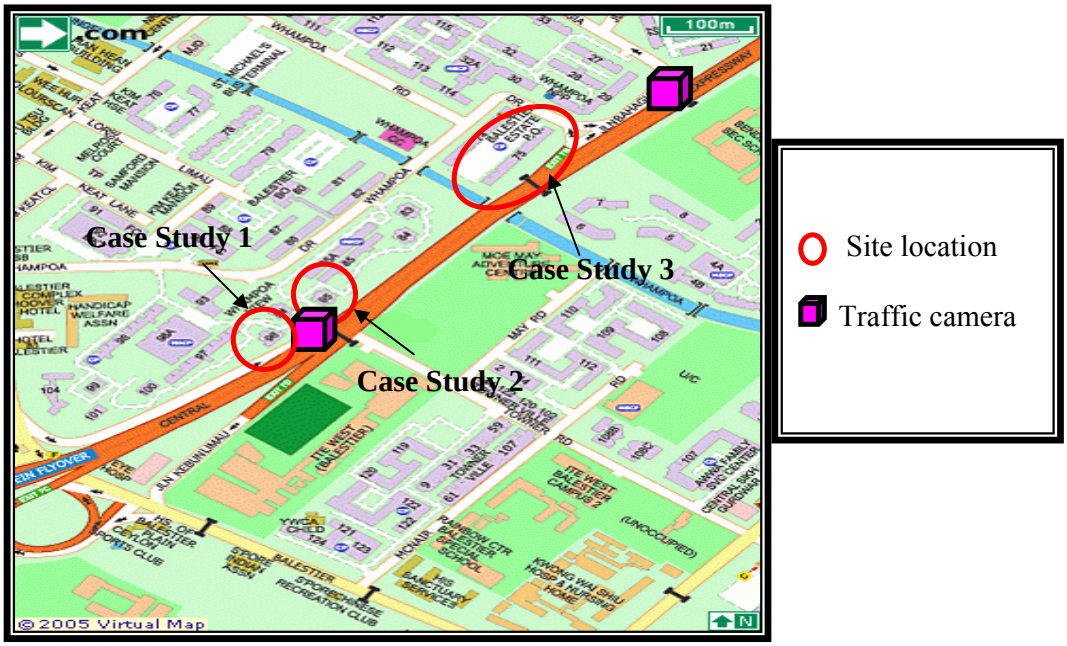

Figure 3.2 Site Location of Measurement Sites (Streetdirectory.com, 2009)

An aerial view of Case Study 1 measurement site is shown in Figure 3.3. The block is 'H 'shaped' and has 4 households in each horizontal storey with 2 of them (units # XX - 236 and #XX - 238) having living rooms facing south-east direction i.e. towards the expressway while the other two households north-west facing living rooms. XX represents the storey height whereas the number following XX is the unit number. The building is about 30 years old and standing on a reasonably flat ground. The actual dimensions of the point block is about 23.82 m(L) x 23.71m(W) x 52.87m(H).

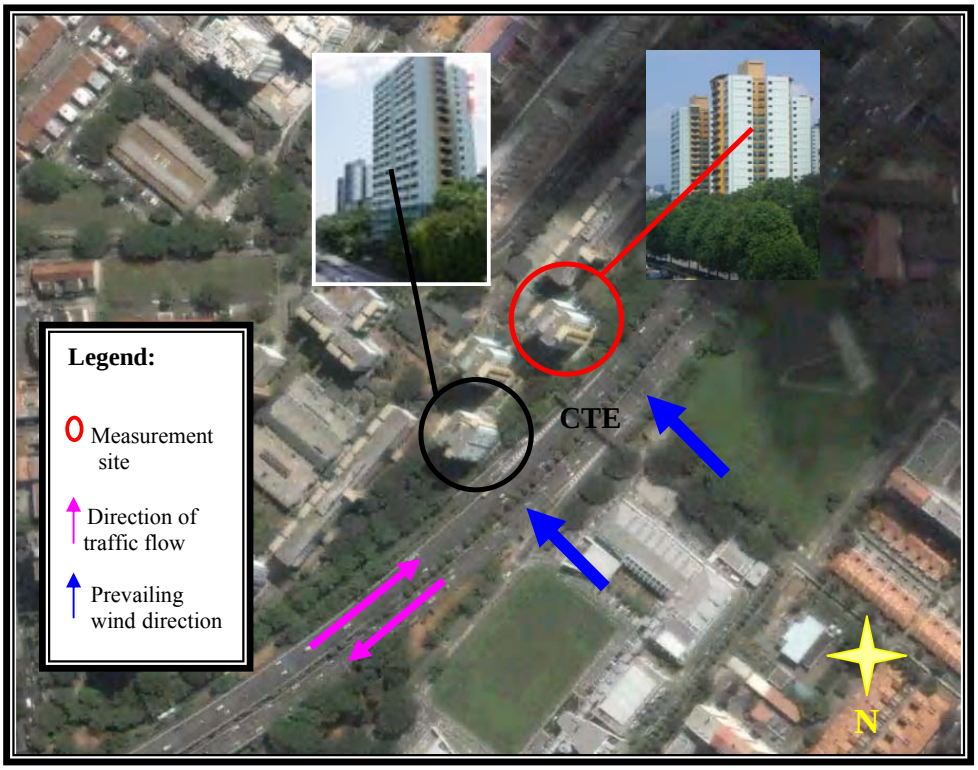

Figure 3.3 Plan view of Blocks 95 (in red) and 96(in black), near Jalan Bahagia

3.1.2.2 Case Study 2

The 2nd measurement site, Block 95, is located not far from Block 96 as shown in Figure 3.2. It is also a 22 - storeys point-block residential building and is located about 20m from CTE. Although the 2 blocks are located alongside each other with about 50m apart, contributions of pollutants from motor vehicles can vary due to the different distance of the buildings from the expressways and the difference in some of the physical characteristics of the sites. Hence, the 2nd measurement site was treated on an individual basis. The two households having their living rooms facing the south-east direction have unit numbers # XX - 244 and #XX - 246 i.e. towards the expressway. The aerial view of Case Study 2 measurement site is shown in Figure 3.3. In addition, Computational Fluid Dynamics (CFD) modelling was performed to study the air displacement effect by fast moving traffic towards the block at various upstream wind speeds. However, the drawback of modelling was that trees were not included in the CFD model due to the complex nature of the actual problem and computational limitation.

3.1.2.3 Case Study 3

The 3rd measurement site, Block 75 is located in the same precinct as the two earlier blocks (Case Studies 1 and 2). It is a 16-storeys slab block residential building and is located about 20m from CTE. The only difference between building in the 3rd measurement site and those in the previous two measurement sites is the building configuration. Figure 3.2 shows the site location of Block 75. The block is 126.90m(L) x 12.57m(W) x 42.40m(H) and

has 18 households (# XX - 346 to #XX - 380) on each floor with all the living rooms facing south-east direction i.e. towards the expressway. The front elevation of the block is shown in Figure 3.4. The distance between the end walls of Blocks 95 and 75 is about 300m. The schematic illustration of the locations and characteristics of the 2nd (Case Study 2) and 3rd (Case Study 3) measurement sites is shown in Figure 3.5. CFD modelling was also performed to study the air displacement effect by fast moving traffic towards the block at various upstream wind speeds. The results of the CFD analysis were compared to those obtained in Case Study 2.

On the opposite side of the expressway is the Balestier Institute of Technical Education which comprise mainly of low-rise buildings and behind the measurement sites (Case studies 1 - 3), the other buildings are some distance away from the buildings where measurements were taken as indicated in Figure 3.2. This made it ideal to study the effects of unobstructed airflow on the concentration level of $PM_{2.5}$ at the various floors of the buildings, i.e. these experiments can be considered as being conducted in an open street geometry and street-canyon effect is negligible.

Figure 3.4 Elevation View of Block 75, near Jalan Bahagia

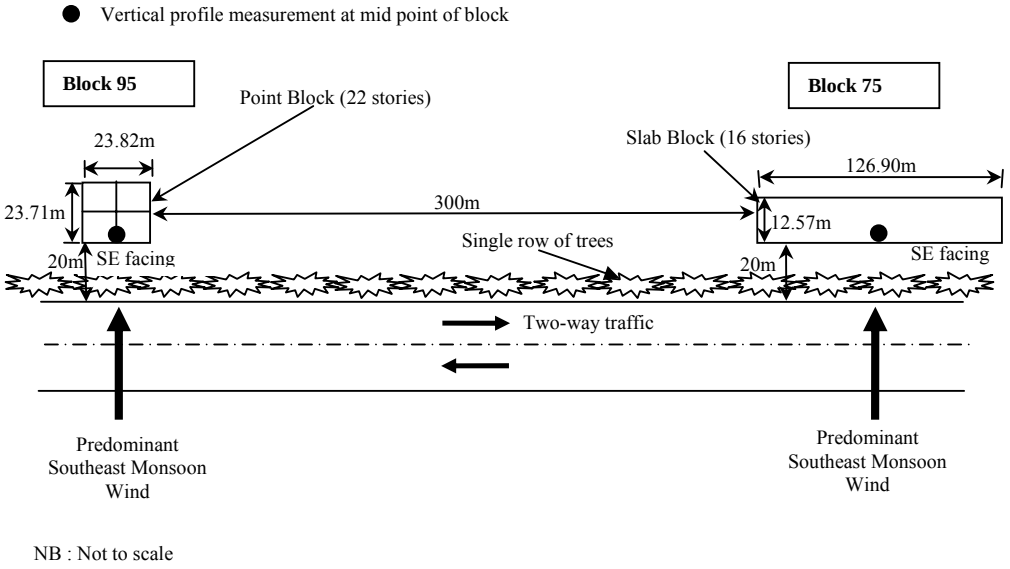

Figure 3.5 Schematic Illustration of the Locations and Characteristics of Measurement Sites (Case Studies 2 and 3)

3.1.2.4 Case Study 4

For Case Studies 4 - 6, the predominant wind is in the north-east direction. From Case Study 4 onwards, NO_2 a surrogate indicator of traffic-generated

pollutants, was used to determine the horizontal as well as the vertical distribution profiles of traffic-generated pollutants at the residential high-rise buildings. Block 39 as shown in Figures 3.6 - 3.7, is a 20 - storeys point block residential building selected for the study. The block is located about 20m from the Ayer Rajah Expressway (AYE). The AYE is located at the southern-western part of Singapore. It enables traffic movement from the city to the residential area along the west and ends at Tuas checkpoint before going to Malaysia. The expressway is a dual carriageway with each carriageway having 3 lanes. The traffic volume can range from 5000 - 9000 vehicles per hr. The actual dimensions of the point block is 23.82m(L) x 23.71m(W) x 47.27m(H). The two households having their living rooms facing the north-east direction have unit numbers # XX - 249 and #XX - 251 i.e. towards the expressway while the other 2 households have their living rooms facing the south-west direction. On the opposite side of the expressway is the National University of Singapore which mainly comprised of several low-rise buildings and behind the measurement site, the other buildings are some distance away from the building where measurements were taken as shown in Figure 3.6. This made it ideal to study the effects of unobstructed airflow on the concentration level of NO_2 at the various floors of the buildings, i.e. these experiments can be considered as being conducted in an open street geometry and street–canyon effect is negligible.

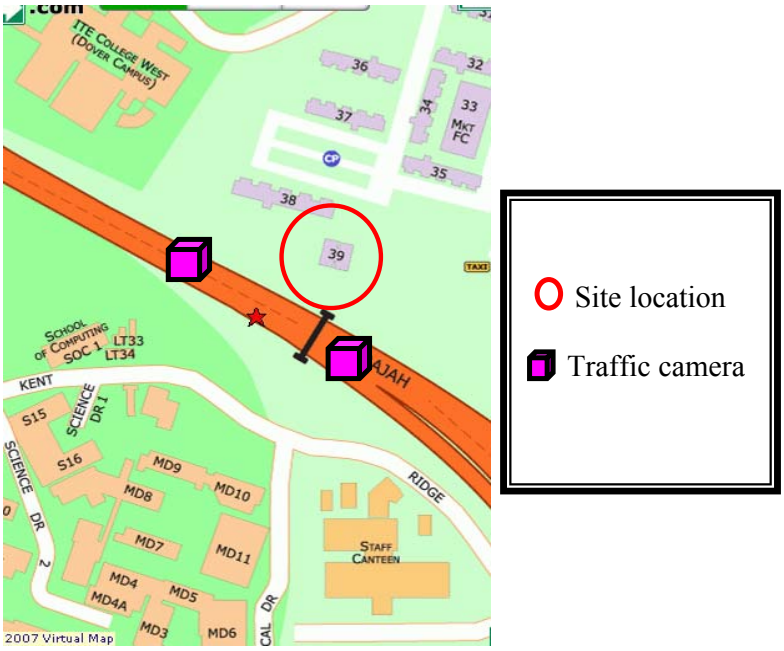

Figure 3.6 Site Location of Block 39, Dover Drive (Streetdirectory.com, 2009)

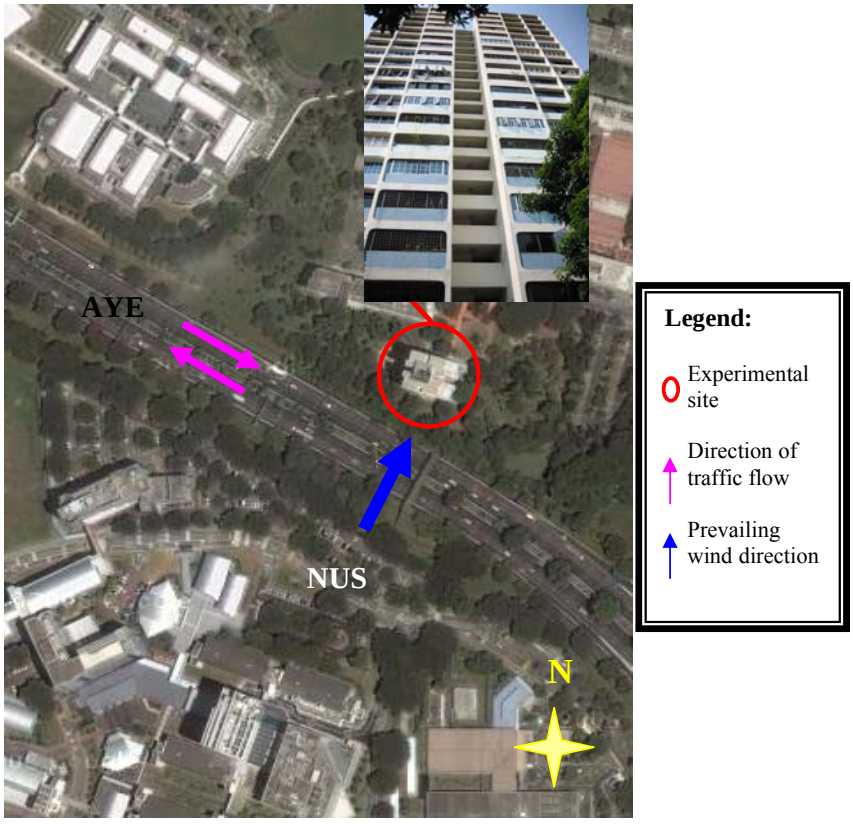

Figure 3.7 Plan View of Block 39, Dover Drive

3.1.2.5 Case Study 5

Block 401 is a 13 - storeys high-rise residential building located about 20m from AYE. It is about 4.5km away from the measurement site of Case study 4. The location and elevations of the block are shown in Figures 3.8 and 3.9 respectively. The actual dimensions slab block is 139.90m(L) x 12.57m(W) x 34.45m(H). The slab block consisted of a main rectangular block (12 units with unit numbers from # XX - 262 to #XX - 284) and two slightly inclined 'wing' blocks (4 units with unit numbers from # XX - 254 to #XX - 260 and # XX - 286 to #XX -292) on either ends of the main block. Each floor has a total of 20 households, with the living room of each unit in the main block facing the north-east direction. Objective measurements were only conducted on the main block. On the opposite side of the expressway are mainly low-rise private housing and behind the measurement site, the other buildings are some distance away from the building where measurements were taken as shown in Figure 3.8. This made it ideal to study the effects of unobstructed airflow on the concentration level of NO_2 at the various floors of the buildings, i.e. these experiments can be considered as being conducted in an open street geometry and street-canyon effect is negligible.

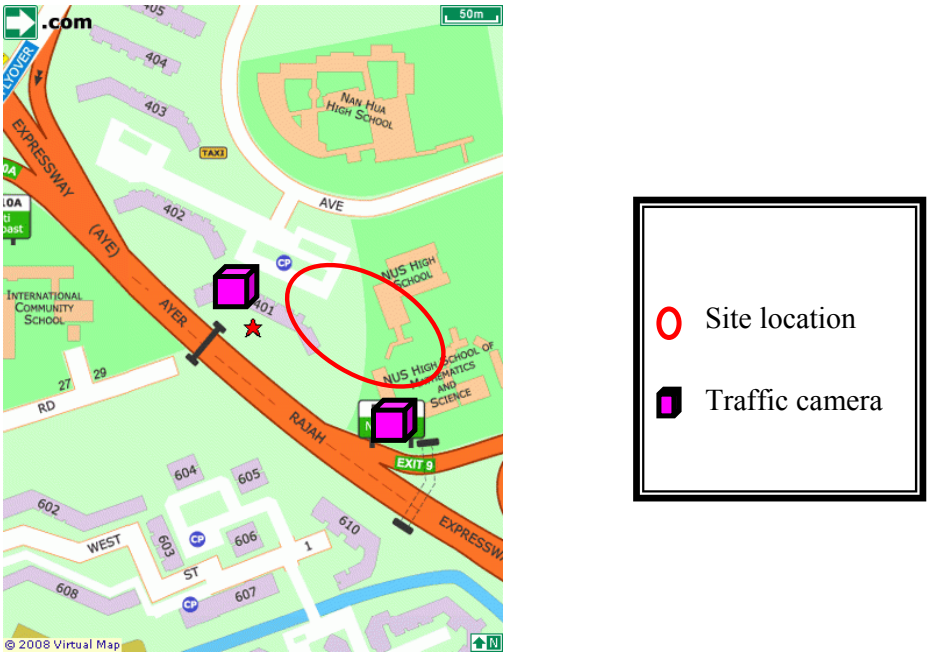

Figure 3.8 Site Location of Block 401, Clementi Avenue 1 (Streetdirectory.com, 2009)

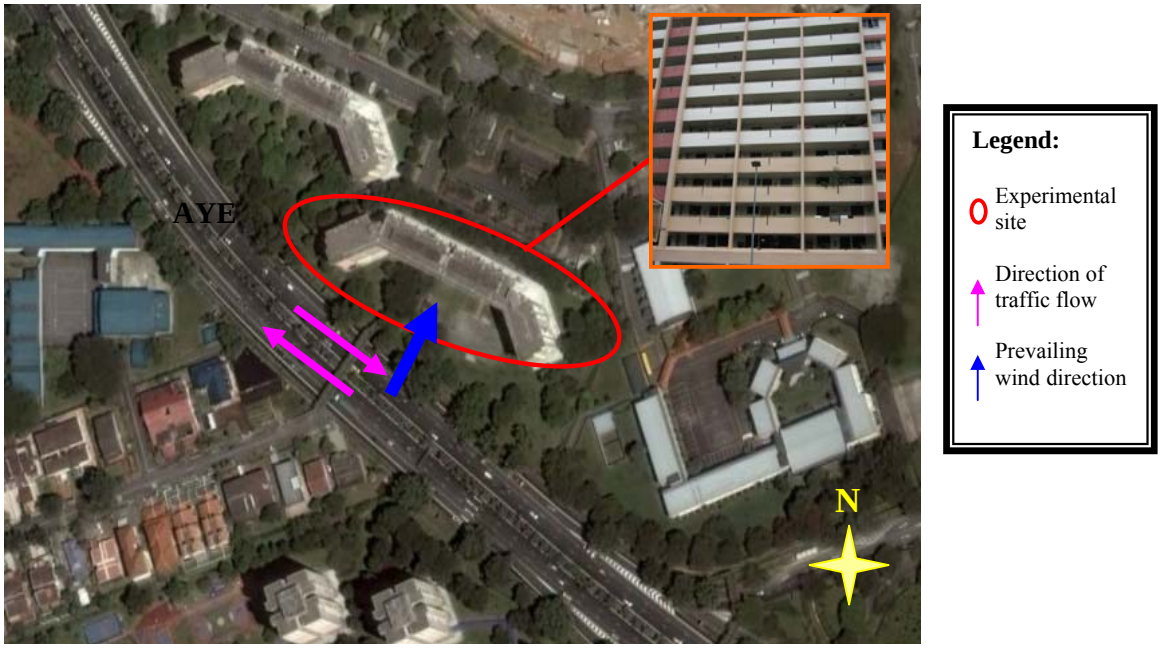

Figure 3.9 Plan View of Block 401, Clementi Avenue 1

3.1.2.6 Case Study 6

Block 93 is a 10 - storeys slab block and is located approximately about 15m from the Pan Island Expressway (PIE). The PIE is the oldest and longest expressway in Singapore. It extends along the length of the island, connecting Tuas in the west to Singapore Changi Airport in the east. The expressway is a dual carriageway with each carriageway having 3 lanes. The traffic volume can range from 8500 - 11000 vehicles per hr. The location and elevations of the block are shown in Figures 3.10 and 3.11 respectively. The actual dimensions slab block is 133.30m(L) x 12.57m(W) x 28.75m(H). The slab block consisted of a main rectangular block (12 units with unit numbers from # XX - 3033 to #XX - 3055) and a slightly inclined 'wing' block (4 units with unit numbers from # XX - 3057 to #XX - 3063) at one end of the main block. Each floor has a total of 16 homes, with the living rooms of the main block are facing in the north-east direction. Measurements were conducted on the straight portion of the block. On the opposite side of the expressway are mainly low-rise buildings and behind the measurement site, the other buildings are some distance away from the building where measurements were taken as shown in Figure 3.10. This made it ideal to study the effects of unobstructed airflow on the concentration level of NO_2 at the various floors of the buildings, i.e. these experiments can be considered as being conducted in an open street geometry and street-canyon effect is negligible.

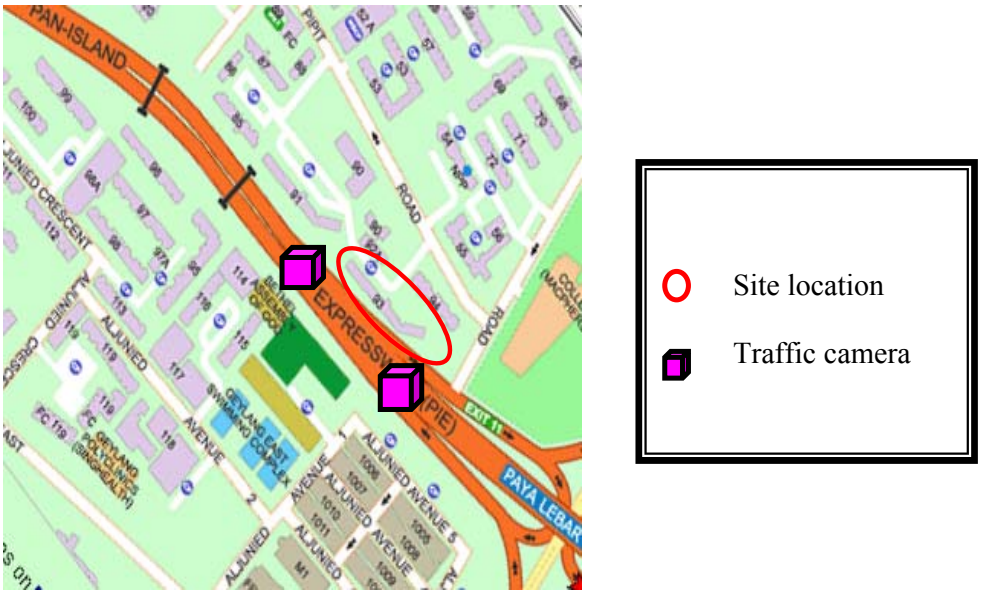

Figure 3.10 Site Location of Block 93, Pipit Road (Streetdirectory.com, 2009)

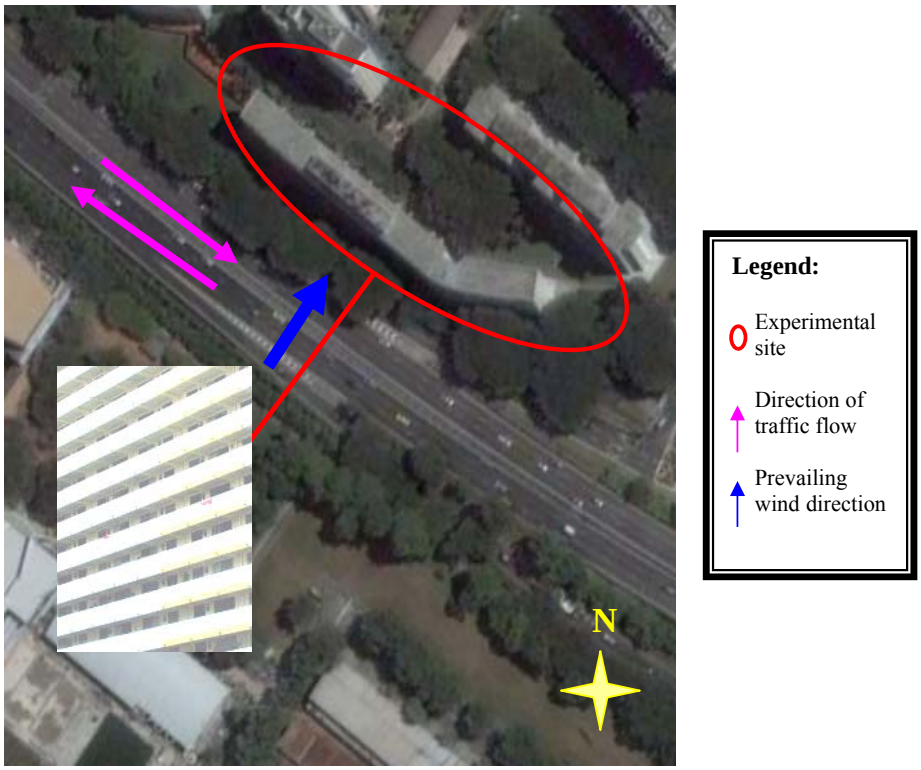

Figure 3.11 Plan View of Block 93, Pipit Road

For all measurement sites, the number of occupants in each household varies from 2 - 6. The main obstacles for airflow towards the buildings are the trees and hedges planted along the expressways. In each expressway, the trees are planted in a single row and have drooping branches with dense and complex canopy structure. For all the sites, the average tree canopy spans up to about 4 - 5 storeys high. Fronting the tree canopy is 1m tall hedges which is about 0.7m wide as shown in Figures 3.12 - 3.14.

Figure 3.12 Dense Complex Canopy Structure in Front of Block 75 (CTE) (Case Study 3)

Figure 3.13 Dense Complex Canopy Structure in Front of Block 39 (AYE) (Case Study 4)

Figure 3.14 Dense Complex Canopy Structure in Front of Block 93 (PIE)(Case Study 6)

3.1.2.7 Particulate Matter Measurement (Case Studies 1 - 3)

For the three blocks, mass concentration and chemical samples were collected in the middle of each building on three representative floors, i.e. low, mid and high floors and at the upstream of the measurement sites to determine the background concentration levels using portable MiniVol® low volume samplers. For chemical analysis of $PM_{2.5}$ particles, Teflon (PTFE) samples were used for water soluble ions and trace metal concentration determination whilst the Whatman high quality quartz microfibre filter samples were used for elemental carbon (EC), organic carbon (OC) and Polycyclic aromatic hydrocarbons (PAHs) concentration determination. The samples were collected during the period in which the island experienced the predominant south-east monsoon winds which tend to transport the traffic-generated particulate matter from the expressway to the residential apartments. Figures 3.15 - 3.18 show the locations of instruments at the representative floors. For case studies 2 and 3, real-time particle count concentrations related to the engine combustions were quantified using Grimm Dust Monitors (model

1.108, Grimm Technologies Inc., Douglasville, GA) at the various representative floors of the buildings. For these measurements, the instruments were set to particle count concentration mode and therefore they cannot measure particle concentration in $\mu g/m^3$. It should be noted that the dust monitors cannot measure particle sizes below 0.3µm. $PM_{2.5}$ count concentration levels were measured between 1000 - 2200hr.

The instruments were placed about 1.5 - 1.8m high from the floor (Li et al., 2005; IDEM, 2009 and Quackenboss et al., 1986) in the building's outdoor balcony/corridor to simulate the breathing zone, at least 1m away from the parapet wall of the building and away from lighting heat sources as recommended by the manufacturer. Outdoor measurements were taken because the previous studies in Singapore (Gupta and Cheong, 2007) reported that the indoor/outdoor (I/O) ratio in naturally-ventilated building was close to unity indicating that pollution migration was from outdoors into indoors rather than its emission from internal sources. All these measurements were made at the windward face of the buildings and strategically located to allow free flow of outdoor air laden with particulate matter which subsequently penetrates into the homes of the buildings. Field blanks were collected in all the representative floors to determine any potential contamination during sampling, transport and storage.

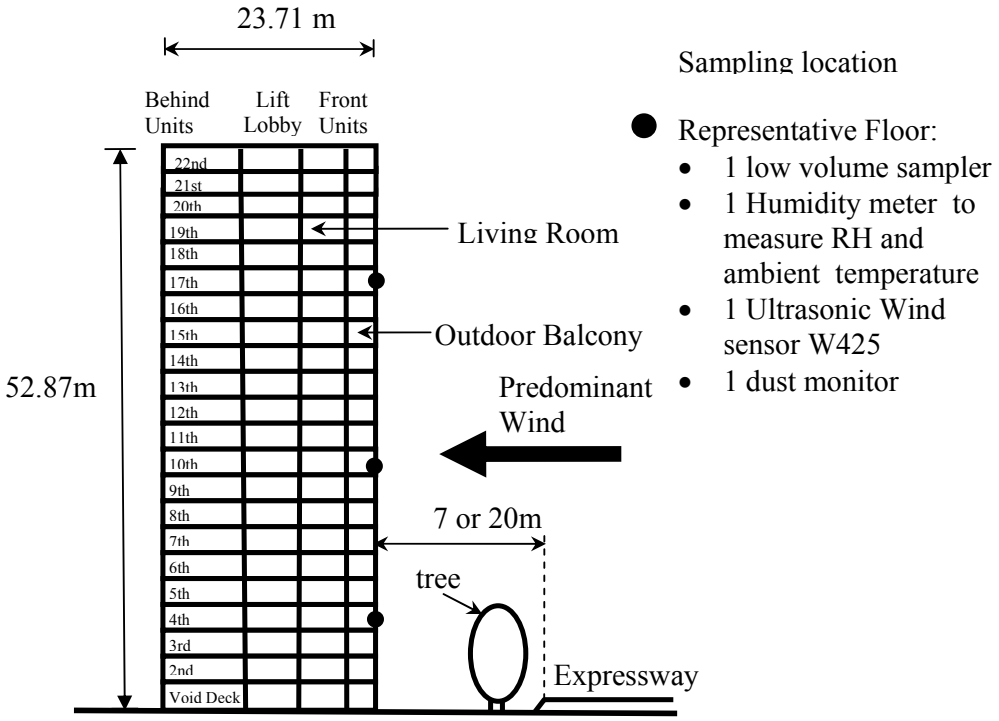

Figure 3.15 End Elevation of Block 96 (Case Study 1) and Block 95 (Case Study 2)

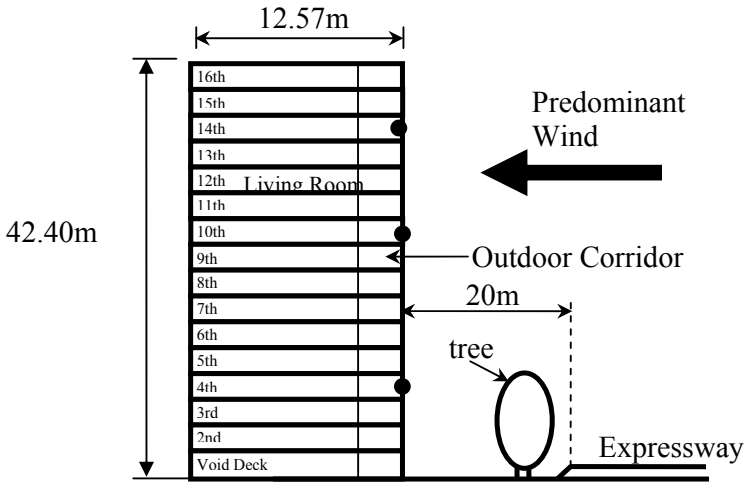

Figure 3.16 End Elevation of Block 75 (Case Study 3)

Figure 3.17 Instruments at the Low Floor Outdoor Balcony of Block 96 (Case Study 1)

Figure 3.18 Instruments at the High Floor Outdoor Corridor of Block 75 (Case Study 3)

Key meteorological parameters such as wind speed, wind direction, ambient temperature, and RH were also concurrently measured at the sampling locations. Ultrasonic Vaisala Wind Sensors (WS425) were used to measure

wind speed and wind direction from 1000 - 2200hr daily. HOBO® Data Loggers were used to record the ambient temperature and relative humidity for 24hr daily. For meteorological parameters, the frequency of measurement was five minute average readings whilst for mass concentration and chemical samples, filters were exposed for 24hr daily. Cross calibration checks were made for all the instruments of the same kind e.g. HOBO® Data Loggers and Grimm Dust Monitors in a controlled environment over a period of one week before they were taken to the field. The difference between the readings of each type of instrument was less than 5%. Cross calibration checks were not performed for the Ultrasonic Vaisala Wind Sensors. On site calibration checks of the instruments were also performed before and after each measurement day. All the measurements were taken when there was no precipitation and no measurements were made during the weekends. Information regarding traffic flow was obtained from the Land Transport Authority of Singapore (LTA).

3.1.2.8 NO_2 Measurement (Case Studies 4 - 6)

For last three case studies, measurements were conducted during the predominant north-easterly wind which blew perpendicularly towards the building facades. Households with no /minimal smoking activity were selected for the measurement. Cooking hours per day ranged from 0.5 - 3hr mostly in the evenings as most of the adults were working during the day and children were at schools. Windows were kept open when the residents were in their apartments during the measurement period to encourage ventilation.

The measurements were made at the windward face of the building over a period of 5 weeks for each building. Ogawa PS-100 passive samplers were used to measure indoor and outdoor NO_2 concentration levels of building as well as map out the outdoor horizontal distribution profile of NO_2 from expressway to building façade. For Case Study 4, the selected households for measurements are unit numbers #XX - 251 (right side) and # XX - 249 (left side). Based on the measurements, the indoor and outdoor vertical distribution profiles of NO_2 concentration were obtained at these units. The horizontal distribution profile of NO_2 concentration levels from the building façade to the expressway was obtained in the middle of the building. For Case Study 5, the indoor and outdoor the vertical distribution profiles of NO_2 concentration were measured at units #XX - 268 (left side) and # XX - 278 (right side) of the block. The horizontal distribution profiles of NO_2 concentration from the building façade to the expressway were measured at the locations where the vertical distribution profiles were measured. Similarly for Case Study 6, the indoor and outdoor the vertical distribution profiles of NO_2 concentration were measured at the units #XX - 3037 (left side) and # XX - 3051 (right side) of the block. The horizontal distribution profiles of NO_2 concentration from the building façade to the expressway were also measured at the locations where the vertical distribution profiles were measured.

For the indoor measurements, the passive samplers were located in the living room and for outdoor measurements, the passive samplers were located at the outdoor balcony and the lift lobby. The upstream background NO_2 levels were also measured using the passive samplers. All the passive samplers were exposed to exposure protection air for 1 week and kept refrigerated after each

test. The samplers were sent back to the laboratory for chemical analysis within three days after the samples were collected. For outdoor, all the outdoor passive samplers were protected using improvised shelters as shown in Figure 3.19. Field blanks were collected at the measured locations to determine any potential background contamination during sampling, transport and storage.

All the instruments were placed about 1.5 - 1.8m high from the floor (breathing zone) and at least 1m away from the any wall obstructions The locations of all the instruments in all the case studies are shown in Figures 3.20, 3.21(a), 3.21(b), 3.22(a) and 3.22(b). Figure 3.23 show an Ogawa PS-100 passive sampler. Indoor and outdoor $PM_{2.5}$ number concentration levels were measured at the apartment of the building where the highest concentration level of NO_2 had occurred using two Grimm Dust Monitors from 1000 - 2000hr. 24hr temperature and RH data were obtained from both indoors and outdoors using HOBO® Data Loggers placed at the living rooms, lift lobby areas and outdoor balconies of the selected households. The outdoor wind speed and direction were obtained using Ultrasonic Vaisala Wind Sensors (WS425) at three representative floors (low, mid and high floors) from 1000 - 2000hr. Cross-calibration checks were made between the various instruments a week before the measurement commenced. These tests were done in a controlled environment. The difference between the readings of the respective instruments was found to be less than 5%. Calibration checks of the instruments were also performed before and after each measurement day. Information regarding traffic flow was obtained from the Land Transport Authority of Singapore (LTA).

Figure 3.19 Ogawa Samplers strapped to Lamp Post in Front of Block 39 (Case Study 4)

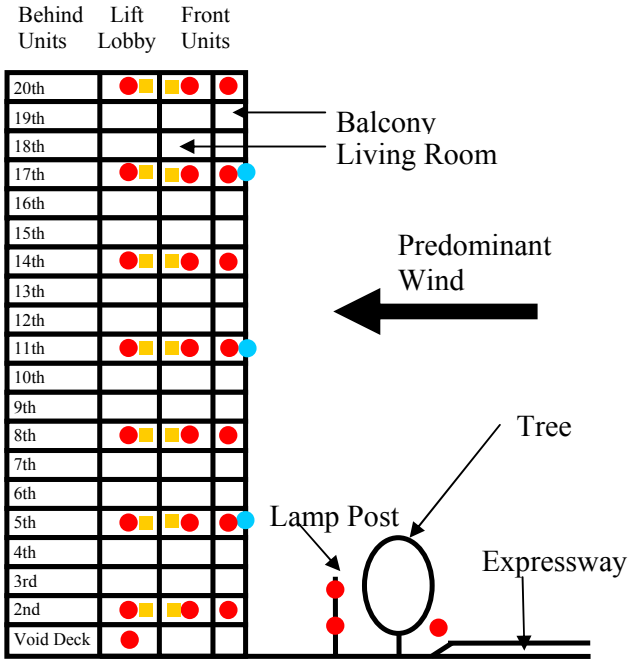

Figure 3.20 End Elevation Showing Location of Instruments at Block 39 (Case Study 4)

Ultrasonic wind sensor

Humidity meter

Ogawa passive sampler

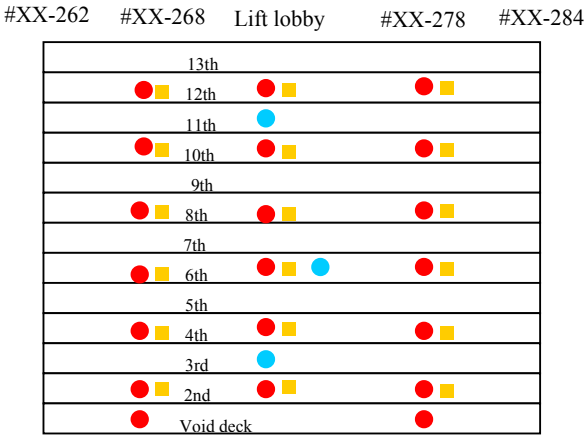

Figure 3.21 (a) Front Elevation of Main Block of Block 401 showing Location of Instruments

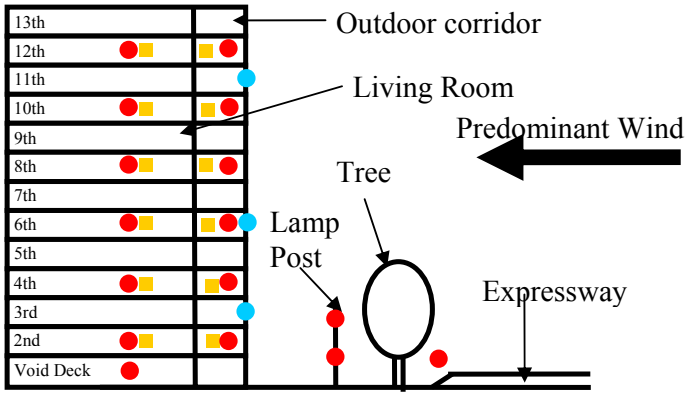

Figure 3.21(b) End Elevation Showing Location of Instruments at Block 401 (Case Study 5)

Ultrasonic wind sensor

Humidity meter

Ogawa passive sampler

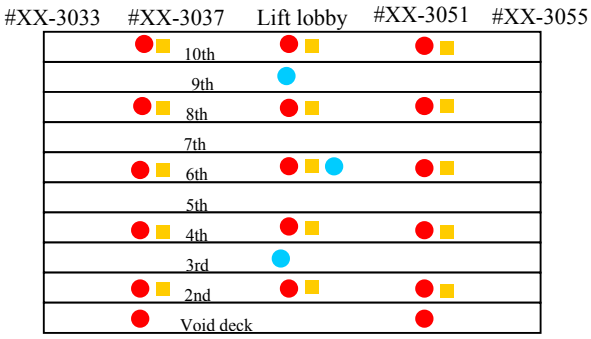

Figure 3.22 (a) Front Elevation of Main Block of Block 93 showing Location of Instruments

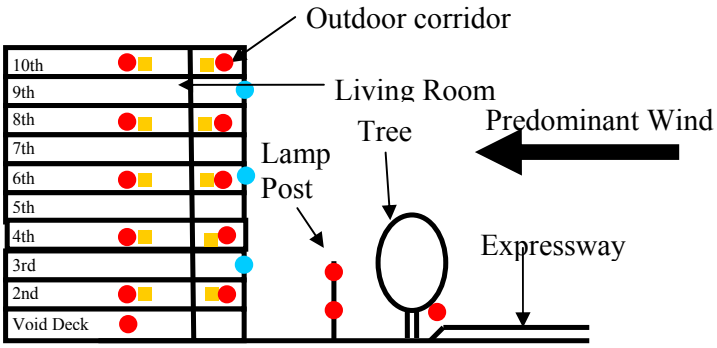

Figure 3.22(b) End Elevation Showing Location of Instruments at Block 93 (Case Study 6)

Ultrasonic wind sensor

Humidity meter

Ogawa passive sampler

Figure 3.23 Ogawa PS-100 Passive Sampler at the 10th Floor Outdoor Corridor in Front of Unit of #XX-268 at Block 401 (Case Study 4)

3.2 Objective Measurements

Objective measurements include physical and environmental parameters and chemical composition of traffic-generated $PM_{2.5.}$

3.2.1 Instrumentation

3.2.1.1 Grimm Dust Monitor - $PM_{2.5}$ Measurement

The Grimm dust monitor (model 1.108, Grimm Technologies Inc., Douglasville, GA) as shown in Figure 3.24 is an aerosol measuring system. The operating principle of the Grimm dust monitor is shown in Figures 3.25 and 3.26. Air sample [1] is constantly being drawn via a volume controlled pump [3 & 4] through a flat beam of light produced by a focused laser diode. The vibration insensitive optical bench [5 - 7] system assures the same accurate reading in the field. Each scattered signal generated crossing this

beam is detected with a high speed photo diode [8] at 90°, so the particle colour changes can be neglected. This pulse is analyzed by an integrated pulse height analyzer [9] and is classified in 8 (or 15) different size ranges [10] and then counted. These counts or masses (per size range) are stored on the data storage card [11] and are displayed in intervals every six seconds (or minute) on the display [12]. In addition a filter is incorporated [2] collecting all the measured particles, so that at any later date an appropriate density verification/correction is possible. After the data has been downloaded to the computer, it is analyzed by the Grimm 1.174 software program and classified into various sizes and concentration levels. The specifications of Grimm dust monitor is shown in Table A1 of Appendix A. The laser technology used also avoids moisture counts as moisture is emitted at special wavelength.

Figure 3.24 Grimm Dust Monitor, model 1.108

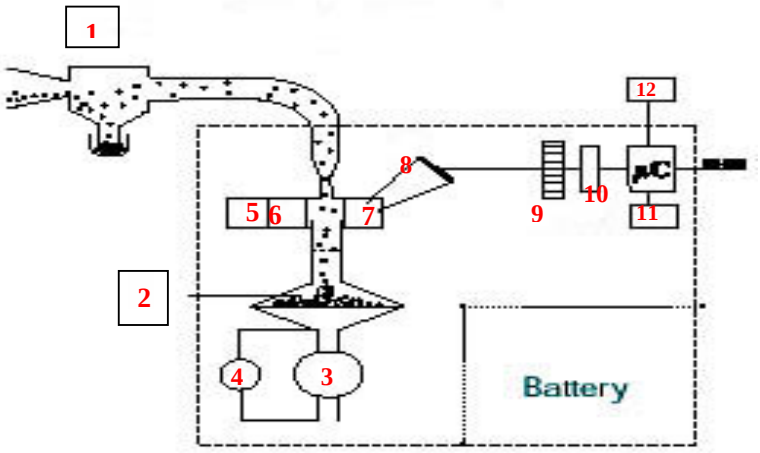

(Source: GRIMM Technologies, Inc., 2009)

Figure 3.25 Operation of Grimm Dust Monitor

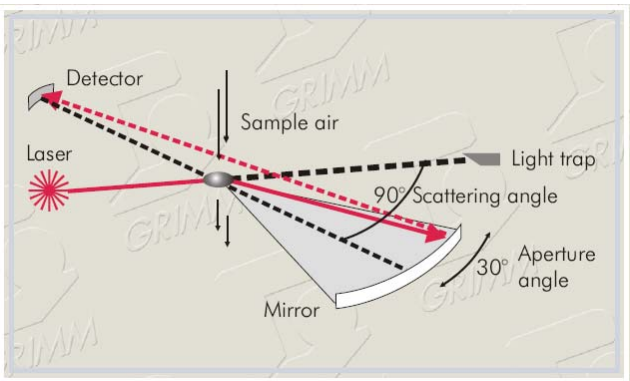

(Source: GRIMM Technologies, Inc., 2009)

Figure 3.26 Optical Light Scattering Technology

3.2.1.2 HOBO® Data Loggers - Temperature and Relative Humidity (RH) Measurement

The HOBO® Data Logger is a two-channel logger with an internal temperature and user-replaceable relative humidity sensor (HOBO® by onset, 2009). Figure 3.27 shows a HOBO® Data Logger which is equipped with onboard memory that will measure and record up to 7943 readings. The reading rate can be selected at sampling intervals of 0.5 seconds to 9 hours, recording times up to 1 year. The temperature measurement range of the logger is between -20ºC and 70ºC, with a temperature accuracy of ± 0.7°C at 21°C. It measures a RH between 25 - 95% with an accuracy of ± 5% RH.

Figure 3.27 HOBO® Data Logger

3.2.1.3 WS425 Ultrasonic Wind Sensor - Wind Speed and Direction Measurement

Figure 3.28(a) Ultrasonic Wind Sensor WS425 Vaisala **Figure 3.28(b) Data logger**

The Ultrasonic Vaisala Wind Sensor WS425 (Vaisala, 2009) and its data logger is shown in Figures 3.28a and 3.28b. The wind sensor has an on-board microcontroller that captures and processes data and performs serial communications. The instrument was set to measure wind speed and its direction at every 6 seconds. The wind sensor has an array of three equally spaced ultrasonic transducers on a horizontal plane as depicted in Figure 3.29 The sensor measures transit time which is the time that it takes for the ultrasound to travel from one transducer to another. The transit time is measured in both directions and depends on the wind velocity along the ultrasonic path. For zero wind velocity, both the forward and reverse transit times are the same. With wind along the sound path, the up-wind transit time increases and the down-wind transit time decreases.

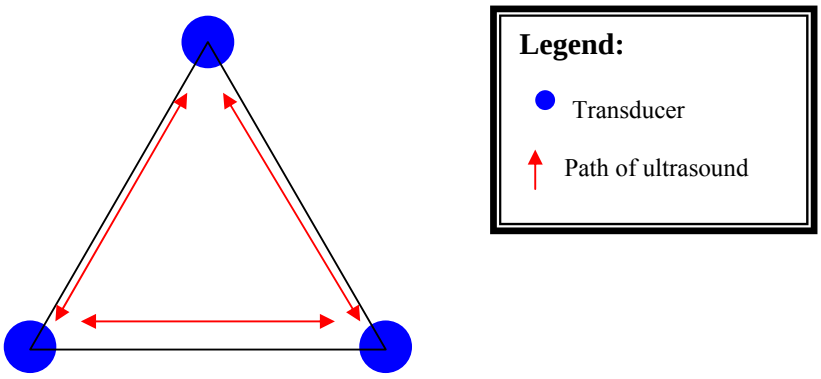

(Source: VAISALA, 2009)

Figure 3.29 Principle of function of the Vaisala Wind Sensor

The microprocessor of the microcontroller calculates the wind speed from the transit times using the following formula:

$$Vw = 0.5 \times L \times (1/tf - 1/tr)$$

where:

Vw = Wind velocity
L = The distance between two transducers
tf = The transit time in the forward direction
tr = The transit time in the reverse direction

Measuring the six transit times allows wind velocity to be calculated for each of the three ultrasonic paths, which are offset to each other by 120°. The calculated wind speeds are independent of altitude, temperature, and humidity because they cancel out with the six measurements even though the velocity of sound affects individual transit times. Incorrect readings may occur when a large raindrop or ice pellet hits a transducer. They are eliminated by a proprietary signal processing technique. The wind velocity that is most affected by turbulence error is eliminated so that wind speed and wind direction are calculated from the best two vectors. The data received from the wind sensor is transmitted into the laptop computers and recorded using Microsoft's Hyper Terminal program. Table A2 of Appendix A shows the

specifications of the Ultrasonic Vaisala Wind Sensor. Data from the sensor was captured in a data logger and then exported to Microsoft Excel for analysis. The instrument was calibrated before the start of each experiment. The orientation of the instrument was made with the aid of a magnetic compass.

3.2.1.4 MiniVol® Portable Air Sampler - Collection of PM $_{2.5}$ Samples

Figure 3.30 MiniVol® low volume Sampler

The particulate samples were collected using MiniVol® portable, battery-operated low volume samplers (AIRMETRICS, 2009) as shown in Figure 3.30. MiniVol® is designed to operate from either AC line power or DC battery pact power sources. This makes the sampler portable for use in many sampling fields that have no access to line power. Air flow rate is to be maintained at a pre-determined value to ensure consistent collection efficiency of the correct particle size through the impactor. Generally, the low volume sampler shows smaller mass concentration values than a standard high volume

sampler. The difference in mass concentration of particles collected ($PM_{2.5}$) by a low volume sampler could be as much as 12% lesser than that of a high volume sampler. This difference could be due to different inlet systems (virtual impactors), different filter material used etc. (Spindler, 2004). The samplers draw air continuously for 24hr through a 47mm Teflon (PTFE) filter with 2.0μm pore size or Whatman high quality quartz microfibre filters (47 mm diameter) at a pre-calibrated flow rate of 5 litres per minute via a $PM_{2.5}$ inlet. Before and after sampling, the samplers were calibrated with a Gilibrator-2 standard flow Primary Air Flow Calibrator (Gilian Instrument Co, NJ, USA). The samplers were left running 24hr a day to collect particles continuously and the filters were changed daily. The PTFE samples were used for the determination of mass concentration, water soluble trace metal and water soluble inorganic ion analysis while the Whatman high quality quartz microfibre filters samples were used for elemental carbon, organic carbon and polycyclic aromatic hydrocarbons determination. The airflow rates were checked before and at the end of each measurement to ensure that a constant flow rate was maintained throughout the sampling period.

3.2.1.5 Ogawa Passive Air Sampler - Collection of NO_2 Samples

The Ogawa passive air sampler as shown in Figure 3.31 was used to measure NO_2 concentrations (Ogawa & Company USA, Inc., 2009). Weather propriety shelters were used for the Ogawa sampler placed outdoor to protect the filter from winds and rain. The Ogawa Sampler can be reused for countless times except that the pre-coated filter pad which is a consumable. Laboratory

analysis of these pads has to be carried out to obtain the NO_2 concentration levels.

(a)

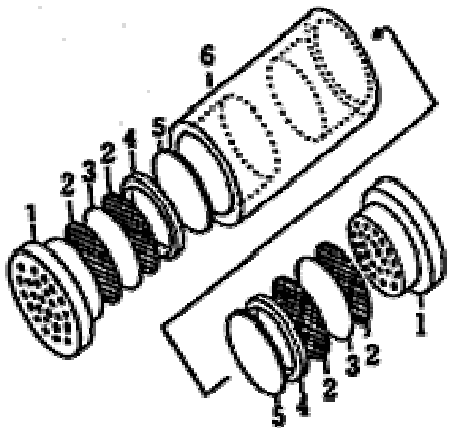

(b)

(Source: Ogawa & Company USA, Inc., 2009)

Figure 3.31 Ogawa Passive Air Sampler

1. End Cap
2. Stainless Steel Screen
3. Pre-Coated Collection Pad
4. Retainer Ring
5. Inner Base Pad
6. Sampler Body

3.2.2 Analytical Methodology

3.2.2.1 Gravimetric Analysis

The filters were weighed with MC-5 microbalance (Sartorius AG, Goettingen, Germany, 2009) with 1 μg sensitivity before and after sampling. Figure 3.32 shows the MC-5 microbalance used in the study. The microbalance was calibrated with a primary standard traceable to NIST mass standard. Before

sampling, the filters were maintained in a dry box at a constant temperature of 25°C and constant humidity of 35% for at least 24hr before the actual weighing. After sampling, the exposed filters were stored in sterile petri-dishes (Gelman Sciences Inc., MI, USA) and again they were placed in the dry box for at least 24hr before final weight measurements. They were then stored in the refrigerator at 4°C until extraction and chemical analyses. This is done to prevent loss of semi-volatile species like organic carbon and ammonium nitrate. Field and laboratory blanks were also weighed. Mass concentrations are then calculated using the actual weight of the particulates collected. This is obtained by subtracting the pre-collection weight from post-collection weight. The weight is then divided by the volume of air that was pulled through the filter over the sampling period to obtain the mass concentration.

Figure 3.32 MC-5 Microbalance

$PM_{2.5}$ mass concentration($\mu g/m^3$) :

$$\left[\frac{Actual\ weight\ of\ \ particles\ on\ \ filter(\mu g)}{Flow\ rate\ of\ \ air\left(m^3\ \min^{-1}\right)\times\ sampling\ time(\min)}\right]$$

Since the flow rate of the sampler was calibrated at room temperature of 24°C and an atmospheric pressure of 101325Pa, the actual flow rate of air was

adjusted for different temperatures and pressures that existed at the measurement sites using the ideal gas law.

3.2.2.2 Chemical Analysis

For the chemical analysis, all exposed filters and field blanks were conditioned for a minimum of 24hr in a dry box maintained at a constant temperature of 25^{o}C and a RH of 30%. The filters were stored in the dark at 4^{o}C until further extraction and chemical analysis to minimize possible degradation and volatilization losses.

3.2.2.2.1 Analysis of Water Soluble Inorganic Ions

One half of the PTFE filters were analyzed for water soluble inorganic ions. For the ions analysis, a pair of forceps was used to place all the Teflon filter samples in 50ml conical flasks. About 0.1ml of iso-propanol was added into each conical flask, using an auto pipette, onto each filter surface so as to wet the filter surface completely since PTFE filters are hydrophobic in nature. Next 15ml of ultra pure deionized water (resistivity > 17.8MΩ) was added into the conical flask. The conical flasks were then capped and place into an ultrasonic bath (ULTRAsonik, 57X, ITS Science & Medical Pte Ltd), at a temperature of 60°C for about 1hr after which the solutions were transferred into 20ml volumetric flasks. About 5ml more ultra pure deionized water was added to the solutions and they were filtered through a special Whatman filter with 0.45μm PTFE membrane in order to remove any particles present, so as not to clog up the Ion Chromatography (IC) system.

For the separation and quantification of the cations and anions, a Metrohm AG ion chromatograph (IC), was utilized as shown in Figure 3.33. All the ions analyzed are listed in Table 3.2. The instrument was equipped with a 733 IC analytical separation systems, a 732 IC detector, 709 IC pump, 753 Suppressor module and a 750 Auto sampler. A Metrosep Anion Dual 2 column is used for anion detection with the suppressor module at a flow rate of 0.8mL min^{-1} while Metrosep C2 - 100 is used for the cation detection without the suppressor unit at a flow rate of 1.0mL min^{-1}. The IC operating parameters are given in Table A3 of Appendix A. Before doing an ion analysis, the IC was calibrated using a series of standard solutions of different concentrations containing the same ion. Distilled water and the standard solutions were placed into small vials and onto the tray of the IC. A five point calibration graph in the range of 0.5 - 10mgL^{-1} was obtained for all the ions and the concentration of each ion was calculated using their respective calibration graphs. It should be noted that only when calibration graph was almost linear ($r^2 > 0.995$), then the ionic analysis begun.

.

Figure 3.33 Metrohm AG Ion Chromatograph (IC) System

Table 3.2 Ion Chromatography Analysis Species

Anion	Cation
Fluoride, F^-	Lithium, Li^+
Chloride, Cl^-	Sodium, Na^+
Nitrite, NO_2^-	Ammonium, NH_4^+
Nitrate, NO_3^-	Calcium, Ca^{2+}
Phosphate, PO_4^{3-}	Magnesium, Mg^{2+}
Sulphate, SO_4^{2-}	Potassium, K^+

3.2.2.2.2 Analysis of Water Soluble Trace Metals

The remaining halves of the filters were placed in Teflon vessels, and 15mL of ultrapure water was added. Extractions were performed using microwave energy of 100W for 5 min. After cooling, the extracts were carefully filtered through 0.2µm PTFE syringe filters, acidified with supra pure HNO_3 (20µL of 1:1), and refrigerated at 4°C until analysis. Microwave digestion is commonly

used to extract trace metals from airborne particles (Yang et al., 2002). The microwave oven used for the study (Figure 3.34) was a MLS-1200 MEGA Microwave Digestion System (Mileston, Italy), which consisted of a compact terminal touch-screen display with operator selectable 0-800 W output, temperature control up to 300˚C, five-layer PTFE coated microwave cavity, HPR/1000/10S Rotor and ten 100mL Teflon vessels. The Teflon vessels were cleaned with 10% nitric acid and washed with deionized water prior to usage.

Coupled plasma mass spectrometer (ICP-MS, Model ELAN 6100, Perkin Elmer, USA) as depicted in Figure 3.35 was used to analyze for 14 metals, i.e. Al, Co, Cr, Cu, Fe, Mn, Pb, Cd, Ni, As, Ag, Ti, Zn and V. The instrumental settings used for the analysis were similar to those recommended by the manufacturer. The instrument is equipped with a standard pneumatic nebulizer and an automatic sampler AS 90. The instrumental settings used for the analysis are shown in Table A4 of Appendix A. The instrumental detection limits of most metals were found at sub-ppb levels of analyte solution, which correspond to a few tens to hundreds of picogram of analyte in an absolute sense. Prior to each analytical batch, the ICP-MS was calibrated with multi-element standards at different concentrations, prepared from serial dilution of 1000mg/l of individual standard solutions, and its response was regularly verified by a calibration standard. Slopes ($r^2 > 0.995$) for the standard curve were computed for all elements and used to calculate the concentrations in unknown samples. The final concentrations were corrected with field blank values.

Figure 3.34 MLS -1200 MEGA Microwave Digestion System

Figure 3.35 Inductive Coupled Plasma - Mass Spectrometry (ICP-MS)

3.2.2.2.3 Analysis of PAHs

Three-quarters of the Whatman high quality quartz microfibre filters were used for the PAHs analysis. The 16 PAHs identified by the US EPA as priority pollutant were analyzed. The priority pollutant PAHs are naphthalene (Nap), acenaphthene (Ace), acenaphthylene (Acy), fluorene (Flu), phenanthrene (Phe), anthracene (Ant), fluoranthene (Flt), pyrene (Pyr), benzo (a) anthracene (BaA), chrysene (Chr), benzo (b) fluoranthene (BbF), benzo (k) fluoranthene (BkF), benzo (a) pyrene (BaP), indeno (1,2,3,cd) pyrene (Ind), dibenzo (a,h) anthracene (DBA), and benzo (g,h,i) perylene (Bpe) (US EPA, 2009). The Whatman high quality quartz microfibre filters were extracted and analyzed for PAHs following the procedures described by Karthikeyan et al. (2005). Firstly, the filters were treated with 20 ml of 1:1 v/v reagent grade acetone:hexane (J.T. Baker, NJ, USA) in MLS-1200 MEGA closed vessel Microwave Digestion System (Milestone srl, Sorisole (BG), Italy) for 20 min at 150 W microwave irradiation. The extracts were then concentrated to 3 ml using a rotary evaporator and then to near dryness with a gentle stream of nitrogen under low temperature at 20°C. Subsequently, the concentrate is then re-dissolved in 1ml of the extraction solvent for PAHs analysis using gas chromatograph-mass spectrometer (GC-MS) as shown in Figure 3.36. The evaporative loss of PAHs was minimized by carrying out the drying process carefully at low temperature using a small steady flow of nitrogen. Acenaphthene-d_{10} was used as a surrogate, and its recovery efficiency evaluated, which was in the range of 90 ± 10%.

Figure 3.36 Gas Chromatograph-Mass Spectrometer (GC-MS)

Prior to the analysis of the filter extracts, the Hewlett Packard 6890 series GC System and Mass Selective Detector (Agilent Technologies, CA, USA) fitted with a DB-5MS 5%-phenyl-methylpolysiloxane 30m long x 0.2mm internal diameter x 0.25µm film thickness capillary column (J&W Scientific, CA, USA), was calibrated with three different concentrations (200, 500 and 1000 times dilution) of an EPA 610 Polynuclear Aromatic Hydrocarbons Mix containing the 16 PAHs (Supleco, 100 ppm for Phe, Ant, Pyr, BaA, Chr, BkF, BaP, Ind; 200 ppm for Flu, Flt, BbF, DBA, BPe, 1000 ppm for Nap and Acy, 2000 ppm for Ace) The GC-MS was operated under the following conditions: splitless injection of 2µl, split opening after 30 s and injector temperature at 280°C; the oven temperature program was 50°C (hold 2 min); 50 - 200°C at 10°Cmin^{-1} (hold 1 min); 200 - 300°C at 5°Cmin^{-1} (hold 8 min). The detector was run in electron impact mode with an electron energy of 70eV and ion source temperature of 230°C. Helium at a constant flow rate of 0.8mlmin^{-1} was used as carrier gas. PAHs were monitored using selected ion

monitoring mode (SIM). In order to get maximum sensitivity, the 16 ions were divided into groups (seven intervals of retention time), and the detector monitors only the ions programmed for each group. The identification of individual PAHs was based on the comparison of retention times (chromatographic column) and mass spectra (mass detector) of PAHs in aerosol samples with those of PAH standards (full scan mode). Information on the limit of detection (0.3×10^{-3}ppm (BaP) to 8.81×10^{-3}ppm (Flt)) and limit of quantification (0.59×10^{-3}ppm (BaP) - 17.63×10^{-3}ppm (Flt)) is given in one of our recent publications by Karthikeyan et al. (2005).

3.2.2.2.4 Analysis of Carbonaceous Species

To investigate the different forms of carbonaceous species, circular punches of 6mm diameter were taken from the remainder one quarter of the Whatman high quality quartz microfibre filters. The total carbon (TC) can be categorized as the sum of organic carbon (OC), elemental carbon (EC), and ionic carbon (IC).

$$TC = EC + OC + IC$$

The contribution of IC to atmospheric aerosol mass is usually < 5%, at least for samples collected in urban areas (Mueller et al., 1972; Appel et al., 1983). The different forms of carbon (TC, EC, IC and OC) were analyzed using the 2400 series II CHNS/O analyzer (Perkin-Elmer Life and Analytical Sciences Inc.), which was operated in CHN mode with acetanilide (71.09% C, 6.71% H, 10.36% H) as a calibration standard and with helium plus 8% oxygen as carrier gas (Figure 3.37). Each calibration curve had five points, and the instrument background value was measured after analyzing each standard. The

details of experimental procedure for their determination are described elsewhere (Balasubramanian et al., 2003; Zappoli, et al., 1999). Briefly, after removal of IC from filter with 1 M HCl, this amount was deducted from that of TC. The resultant mass of carbon is now due to both EC and OC (TC minus IC). For EC determination, the filter was placed in a crucible and heated in a Carbolite Oven as shown in Figure 3.38 at 350°C for 24hr after acidification to remove completely the IC and OC. The amount of OC was obtained by the difference [TC-TIC-EC]. TIC is the total ionic carbon. The detection limits of TC, EC, and OC were 0.03, 0.03, and 0.06μg/m^3 respectively. The steps for carbon extraction are shown in Table 3.3. Although there was no absolute standard available to assess the accuracy of carbon measurement, the results obtained were highly reproducible.

Table 3.3 Steps for Carbon Extraction

Step	Description for TC	Description for EC
1	Place filter in the dry box	Place filters in crucibles and heat them in Carbolite Oven at 350°C for 24hr - for OC removal.
2	-	The filters are conditioned again in the dedicator.
3	Weigh conditioned filters	Weigh conditioned punched filters
4	Send for CHN 2400 analyzer	Send for CHN 2400 analyzer to determine EC concentration.

Figure 3.37 2400 series II CHNS/O Analyzer

Figure 3.38 Carbolite Oven

3.2.2.2.5 NO_2 Analysis

The laboratory analysis required to extract the NO_2 concentration adsorbed by the filter is shown in Figure 3.39. Before the exposed filters were tested, sulfanilamide solution was prepared by dissolving 80g of reagent grade sulphanilamide in a mixture of 200ml of concentrated phosphoric acid and

700ml of water. The solution was then diluted with water to make a total of 1000ml. NEDA solution was prepared by dissolving 0.56g N-(1-Naphthyl)-ethylenediamine dihydrochloride into 100ml of water and stored in the refrigerator. Then sulfanilamide solution and NEDA solution were mixed together in a ratio of 10 parts of sulfanilamide solution to 1 part of NEDA solution to form a colour producing reagent.

Sodium nitrite was dried for over 4hr at a temperature of 105^{o}C. Then 1.5g of the dried sodium nitrite was dissolved in one litre of water. This created a contained 1000µg of nitrite/ml solution. The nitrite standard solution was diluted by 100 times with water. Then 0, 2, 4, 6, 8 and 10ml samples were diluted with water to make 100ml solutions. This produced working standard solutions of 0 - 1µg nitrite/ml.

The stainless steel screens and filters were put into 25ml glass vials containing 8ml of water and then shaken. Vials were sealed as per laboratory practice. At the end of first half an hour, the vials were cooled to 2 - 6^{o}C and 2ml of colour producing agent added and shaken. The vials were kept cool for an additional 30 minutes. Later, the vials were allowed to reach room temperature for another 20 minutes and the amount of colour derivative was determined with a spectrophotometer (UV-VIS-NIR Spectrophotometer, UV-3101 PC/3150, Shimadzu) at a wavelength of 545nm. Unexposed filters underwent the same procedure as exposed filters to obtain a blank value determination.

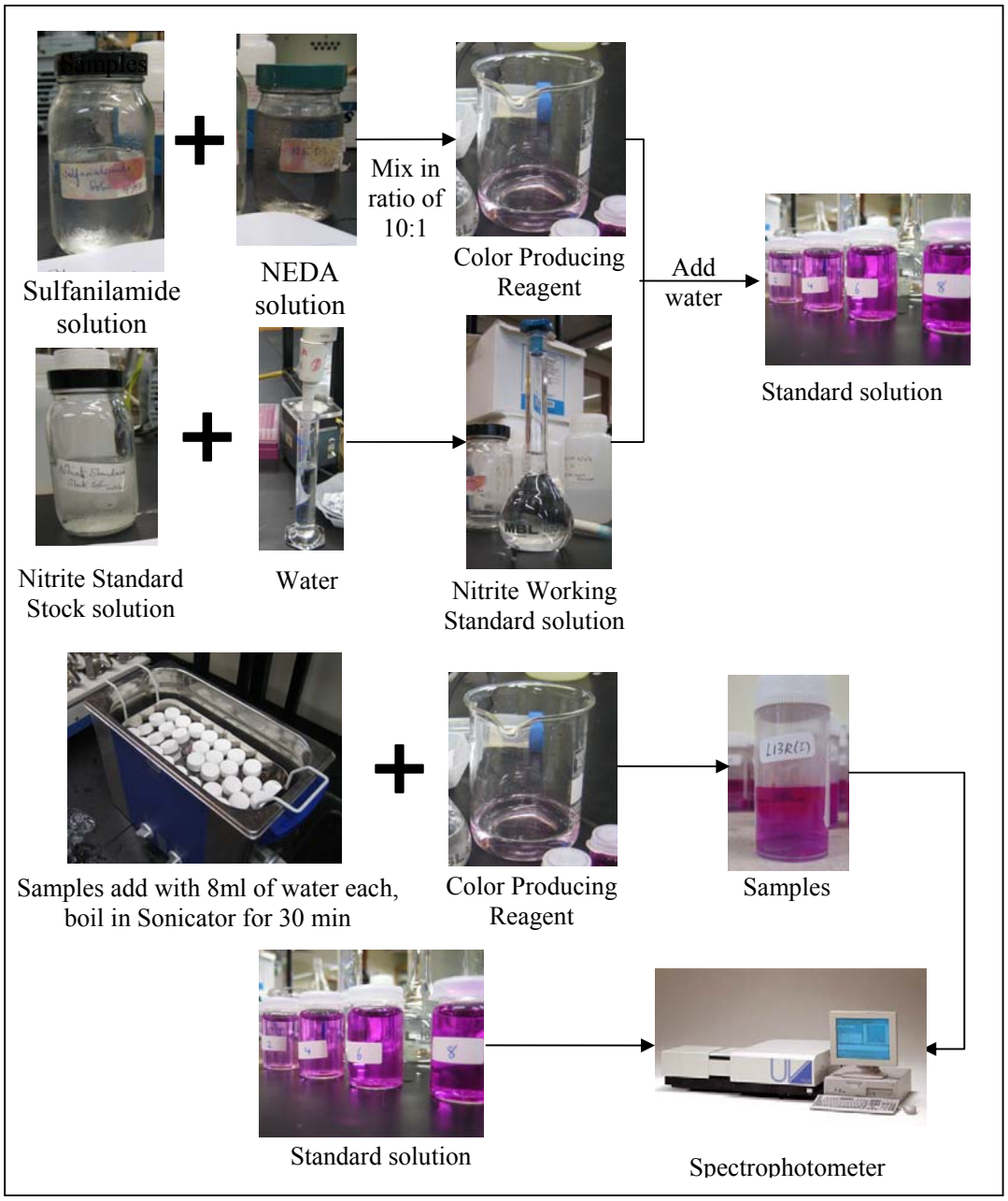

Figure 3.39 Laboratory Analysis of Ogawa Sample Filter

3.2.2.2.6 Data Analysis for Chemical Samples

The data analysis for chemical samples, other than NO_2 concentration calculation, depends on the amount of solution used during chemical extraction and the volume of air extracted during sampling. A general formula for all concentration data calculation is given below.

$$\text{Concentration} = \frac{(\textit{Concentration of solution}) \times (\textit{Volume of Solution})^{*}}{\text{Sampling flow rate } (\text{m}^3/\text{minute}) \times \text{duration (minute)}}$$

*Ions/water-soluble metals : $20\text{ml} \times \frac{4}{3}$

PAH : $1\text{ml} \times \frac{4}{3}$

Tracel metals : $50\text{ml} \times 4$

To obtain carbonaceous species concentration (mg/m^3), the formula used was as follow:

Concentration (mg/m^3):

$$\frac{(\frac{39}{6})^2 (\frac{C\%}{100}) Mass_{sample} - (\frac{39}{6})^2 (\frac{C\%}{100}) Mass_{blank}}{\text{Sampling flow rate } (\text{m}^3/\text{minute}) \times \text{duration (minute)}}$$

For NO_2 concentration data analysis, the gradient, G, of a standard curve was required. This was done by measuring the absorbance of 6 standard samples by a spectrometer. From the previously prepared nitrite working solution (0 - 1μg nitrite/ml), 8ml of it was mixed with 2ml of colour reagent and shaken to obtain the standard samples. The standard samples prepared had concentrations 0, 0.1, 0.2, 0.4, 0.6 and 0.8μg/ml NO_2.

Concentration(ppb):

$$\frac{[\frac{Absorbance_{\exp osed} - Absorbance_{blank}}{G} \times 8ml \times 1000 \times a_{NO_2}]}{Exposure\,time_{\min ute}}$$

$$a_{NO_2} = \frac{10000}{(0.677 \times [P] \times [RH]) + (2.009[T] + 89.8}$$

Where:

[T] = ambient temperature in ^{o}C
[RH] = relative humidity in %

$$[P] = \left[\frac{2P_N}{P_T + P_N}\right]^{\frac{2}{3}}$$

P_N = vapour pressure in mm Hg at 20^{o}C
P_T = vapour pressure of water at ambient temperature T in mm Hg

3.2.2.2.7 Quality Control and Quality Assurance

All chemical filters were weighed in a temperature and humidity-controlled room (25°C, 35 ± 5% RH). All filters were left to equilibrate for 24hr prior to pre-sampling weighing and for the post-sampling weighing. The filters were inspected for defects under bright illumination before exposure. Filters were installed in the low volume samplers using Teflon-tipped forceps. Soon after the end of the sampling period, exposed filters were retrieved to avoid potential for filter damage, changes in sample mass due to particle loss and passive deposition. To correct for the effects of filter handling, the mean net mass of the field blanks was deducted from the raw sampled filters' mass. The microbalance used to obtain the particulate mass had 1μg sensitivity, and was maintained at a relative humidity of 35.0 ± 3.0%. At the beginning of each weighing session, it was calibrated to NIST mass standards.

Field blanks (PTFE and Whatman high quality quartz microfibre filters) were collected in all the representative floors and background locations to determine any potential background contamination during sampling, transport and storage. They were removed during the deployment interval and were placed in air tight containers before returning them to the laboratory for testing. They were treated as regular samples. The field blanks accounted for about 50% of total number of PTFE and Whatman high quality quartz microfibre filter samples collected for each block. Experimental results show the mass concentration in the field blanks accounted for less than 1% of the corresponding mass concentrations of the PTFE and Whatman high quality quartz microfibre filter samples. All the samples were corrected for potential background contamination during sampling, transport, and storage.

Chemical analysis of samples began only when calibration graph was almost linear ($r^2 > 0.995$). For water soluble ions the summation of positive ions and summation of negative ions was 0.97 ± 0.09 indicating most of the ionic species measured. In trace metal analysis, the trace metals concentrations in some of the randomly selected samples obtained by graphite furnace atomic absorption spectrometry (GF-AAS) and ICP-MS were in good agreement (slope = 0.98; r = 0.97). For the carbon analysis using the 2400 series II CHNS/O analyzer, a standard (acetanilide) was combusted for every 5 samples to check the accuracy of the analysis. Although there is no absolute standard available to assess the accuracy of carbon measurements, the results obtained were highly reproducible. The average precision of the measurements for EC and OC based on repeated analysis of calibration standards were ± 6% and ± 5%, respectively.

For NO_2 measurements, field blanks were handled using similar procedures as for the chemical samples, but were kept in a plastic zip-lock bag throughout the 24hr sampling period. To adjust for filter handling and analysis procedures, NO_2 concentrations were corrected using field blank values. Five blanks were used each lot analyzed. Mean limit of detection (LOD) for indoor and outdoor measurements ranged between 8.5 - 11.9ppb (Bracho et al., 2002**).** All the indoor and outdoor NO_2 measurements were below their respective LODs.

3. 3 Health Risk Assessment due to Inhalation of Particulate PAHs (BAPeq Analysis)

The dose-response relationship for inhalation of all particulate PAHs is not currently available in the literature. The environmental risk assessment associated with particulate PAH inhalation is often estimated in terms of benzo[a]pyrene equivalent (BaP_{eq}) concentrations by using the list of toxic equivalent factors (TEFs) (Menichini, 1999). Most countries regulate benzo(a)pyrene since it is a well known experimental carcinogen, mutagen, tumorigen, neoplastigen and teratogen and a probable carcinogen in humans and a known human mutagen. Since Singapore has no regulations on benzo(a)pyrene, the proposed a maximum permissible risk level of $1ng/m^3$ of benzo(a)pyrene in ambient air, based on the carcinogenic potential of inhaled particulate PAHs as proposed by Slooff et al. (1989) has been adopted for this study. Of the various established TEF values, those reported by Nisbet and LaGoy (1992) seemed to accurately reflect the relative potency of individual PAHs (Petry et al., 1996; Castellano et al., 2003; Fang et al.,2004). Table A5 of Appendix A shows the TEF values of individual PAHs used in the analysis as proposed by Nisbet and LaGoy (1992). The carcinogenic potencies of

individual carcinogenic particulate PAHs were obtained by multiplying their respective concentrations with the appropriate TEF values. This converted the individual PAH concentrations to benzo(a) pyrene equivalence (BaP_{eq}) values. The overall carcinogenic potency for a mixture of PAHs is obtained by summing the individual PAH benzo(a) pyrene equivalence values. The TEF approach has been extensively used for hazard assessment of different classes of toxic PAH mixtures and is commonly used for cancer risk assessment.

3.4 Health Risk Assessment Due to Inhalation of Fine Particulate Matter

In this study, the health risk model by Pandey et al. (2005) is used to assess the potential relative health risk of residents living in the point and slab blocks in contracting respiratory disease. The model accounts for age specific dose rates, age-specific breathing rates, age-specific body weights, diurnal concentration of the pollutant, occupancy factor (percentage of population likely to be in the zone at a given interval of time) for the zone (residential, industrial and commercial) and the loael. A brief description of the health risk model used by Pandey et al. (2005) is given below.

The analysis of the potential health risk of occupants associated with inhalation exposure of particulate matter was based on estimated the dose rates and the lowest observed adverse effect levels (loael). Exposure occurs when a person comes in contact with a pollutant (Ott, 1985). A person's exposure to a pollutant is defined as the contact of the pollutant at one or more boundaries of the person i.e. mouth or skin at specific concentrations over a period of time. Dose occurs only when the pollutant crosses the physical boundary of a person. The analysis is age-specific, and it divides the occupants under three

age-specific categories namely, infants, children and adults. The dose rate of a pollutant in a zone has been estimated through the following expression over a day.

$$Dose\,rate\,(D) = [BR / BW] \int_0^{24} C(t) OF(t)\, dt \ldots\ldots\ldots\ldots\ldots (1)$$

where D is the age-specific dose rate (μg kg^{-1}); BR is age-specific breathing rate (L min^{-1}); BW is age-specific body weight (kg); $C(t)$ is diurnal concentration of the pollutant (μg m^{-3}); and OF (t) is occupancy factor of zone (percentage of population likely to be in the zone at a given interval of time).

For the estimation of the potential health risks of a person due to inhalation of a specific pollutant, the following expression is used.

$$Health\ \ risk\ \ (HR) = [Dose\,rate\,/\ pollu\tan t\ specific\,loael] \ldots\ldots\ldots\ldots\ldots\ldots (2)$$

The loael values for particulate matter and NO_2 were taken from Cerna et al. (1998) and Neuberger et al. (2002) respectively. The HR value is dimensionless and is useful for making relative comparisons.

3.5 Traffic Measurement

The traffic data obtained were recorded continuously by the Land Transport Authority of Singapore (LTA, 2009). The traffic count was made with the help of an intelligent management system that monitors and manages traffic along expressways, through cameras mounted on lamp posts. The cameras are located in front of the blocks and captured the traffic on the expressway. The number of vehicles was counted on an hourly basis for a period of 24hr.

3.6 CFD Modelling of Air Displacement Effect by Fast Moving Traffic

Fast moving traffic close to buildings tends to displace air towards the buildings. This may affect the traffic-generated pollutant concentration around the buildings. A study by Morawska et al. (1999) showed that for a building in very close proximity to freeway, the air flow around the building envelope is such that it drew air directly from the freeway. A CFD study was performed to provide a visual perspective of airflow patterns around the point block and slab block building configurations at various upstream wind speeds coupled with the air displacement effect from the fast moving traffic. In the study, it was assumed the pollutants move along with the airflow streamlines. Trees were not considered in the modelling due to the complex nature of the actual problem and computational limitation.

Architectural and structural drawings of Block 95 (Case Study 2-Point Block) and Block 75 (Case Study 3-Slab Block) were obtained from the Housing Development Board (HDB) of Singapore prior to CFD modelling. In the construction of the 2 CFD models, the walls, roof and ground of the building were zoned as wall boundary conditions. In selection of mesh type, issues such as set-up time, computational expense and computer memory space capabilities were considered. The ‘element’ parameter defines the shape of the element that is used to mesh the face. The ‘type’ parameter defines the pattern of mesh elements on the face. For example, ‘tri’ specifies that the mesh which includes triangular mesh elements. ‘Pave’ creates an unstructured grid of mesh elements. A tri-pave meshing scheme means GAMBIT creates a face mesh consisting of irregular triangular mesh elements. The outer domains of both

the buildings were meshed using Tet/Hybrid of Tgrid type. Tet/Hybrid specifies that the mesh is composed primarily of tetrahedral mesh elements but may include hexahedral, pyramidal, and wedge elements where appropriate. TGrid type is a highly efficient, easy-to-use, unstructured grid generation program that can handle grids of virtually unlimited size and complexity.

For the two buildings, the expressway was positioned at 20m in front of the building. The front vertical plane on the outer domain in front of the building was specified as a velocity-inlet for the prevailing wind. The plane was defined with an ambient air temperature of 28.5^{o}C. The rear vertical plane of the domain was specified as a pressure-outlet boundary condition. The two vertical planes along the width and the top of the domain were specified as symmetry planes. The air displacement effect by fast moving traffic was studied at various upstream wind velocities of 1m/s, 2m/s, 3m/s, 4m/s and 5m/s. For the expressway, the 2-D plane was zoned as a velocity-inlet condition type in GAMBIT software. A continuous traffic line source was assumed which had a velocity of 22.2m/s which is equivalent to 80km/h. The mean road surface temperature of 47^{o}C and the mean façade temperature of 37^{o}C as measured on site were used in the model analysis.

For the species boundary condition on RH, a moisture content value of 0.023 was used as estimated from the psychometric chart. This was based on a mean ambient temperature of 28.5ºC and a mean relative humidity of 84% the (NEA, 2007). CFD simulations were then performed by using the solver, Fluent 6.0 using the standard K-epsilon (2 eqn) turbulence model. A number of CFD simulations were performed for steady state airflow within the outer

domain. Some of the parameters used in the computations are shown in Table 3.4.

Table 3.4 Computation Parameters of the CFD Model (Blocks 75 and 95)

S/No.	Description	Type
1	Physical model	3 dimensional
2	Flow model	Steady State
3	Turbulent model	k-epsilon (2 eqn)
4	Species Model	Mulitple
5	Materials	Water and air
6	Gravity	Enable (in Y-direction)
7	Energy Equation	Enable

3.6.1 Block 95 (Case Study 2)

The actual dimension of Block 95, 23.82m(L) x 23.71m(W) x 52.87m(H) was created and meshed using GAMBIT software. Special attention was taken to ensure that the virtual geometry was similar to the actual geometry of the building as shown in Figure 3.40. An outer box domain which was 10 times larger than the actual dimensions of the building was created to allow accurate convergence of solutions (Ng, 2009; Planning Department of Hong Kong SAR, 2007; Ng et al., 2004; Fung et al., 2009). Figure 3.41 shows the 3-D view of the virtual building geometry in its outer domain. The building model, expressway and domain meshing parameters are shown in Table 3.5.

Table 3.5 Meshing Parameters for Block 95

S/No.	Description	Mesh Type	Element Type	Spacing
1	Roof of building	Face	Tri element (Pave)	0.3
2	Ground of building	Face	Tri element (Pave)	0.3
3	Walls of building	Face	Tri element (Pave)	0.3
4	Expressway	Face	Tri element (Pave)	0.5
5	Outer domain	Volume	Tet/Hybrid (TGrid)	5.0

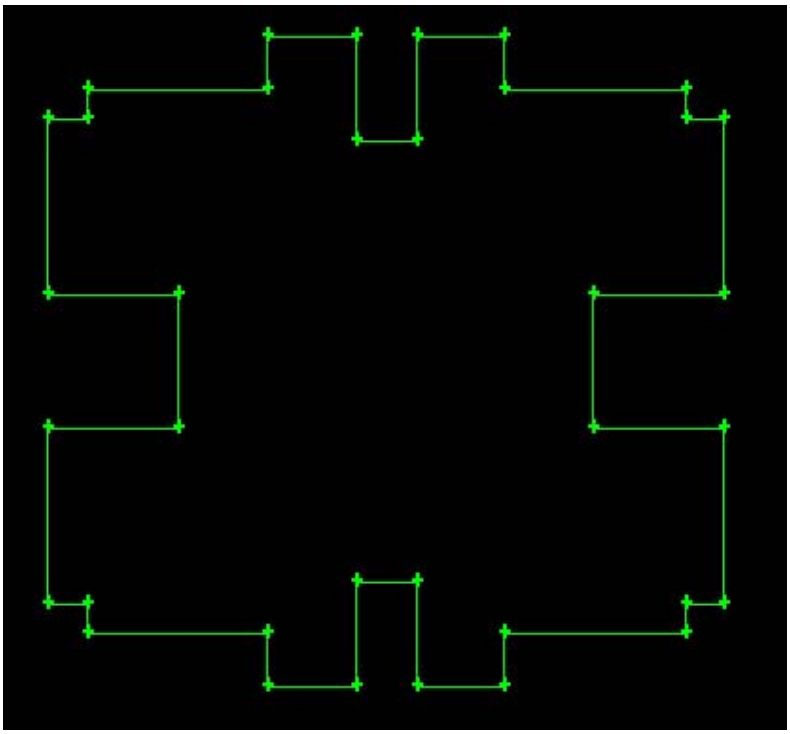

Figure 3.40 Plan view of Block 95 using GAMBIT Software (Case Study 2)

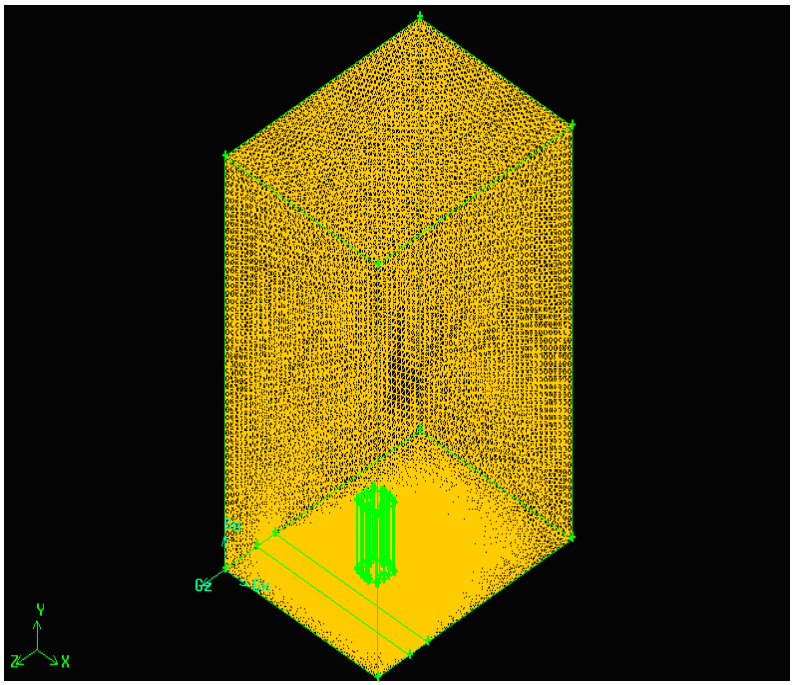

Figure 3.41 View of Block 95 in Outer Domain (Case Study 2)

3.6.2 Block 75 (Case Study 3)

A 3-D model of the Block 75 with dimension 126.9m(L) x 12.57m(W) x 42.4m(H) was created using the Gambit software. An additional rectangular shape of dimension 6.5m(L) x 6.62m(W) x 42.4m(H) was created for the lift landing positioned in the middle of the building. An outer box domain which was 5 times the length, 11 times the width and 4 times the height of the building was created to allow accurate convergence of solutions. Figure 3.42 shows the 3-D view of the virtual building geometry in its outer domain. The building model, expressway and domain meshing parameters are shown in Table 3.6.

Table 3.6 Meshing Parameters for Block 75

S/No.	Description	Mesh Type	Element Type	Spacing
1	Roof of building	Face	Quadrilateral (Pave)	0.8
2	Ground of building	Face	Quadrilateral (Pave)	0.8
3	Walls of building	Face	Quadrilateral (Pave)	0.8
4	Vehicular Traffic	Face	Quadrilateral (Pave)	1.0
5	Outer domain	Volume	Tex/Hybrid (TGrid)	6.0

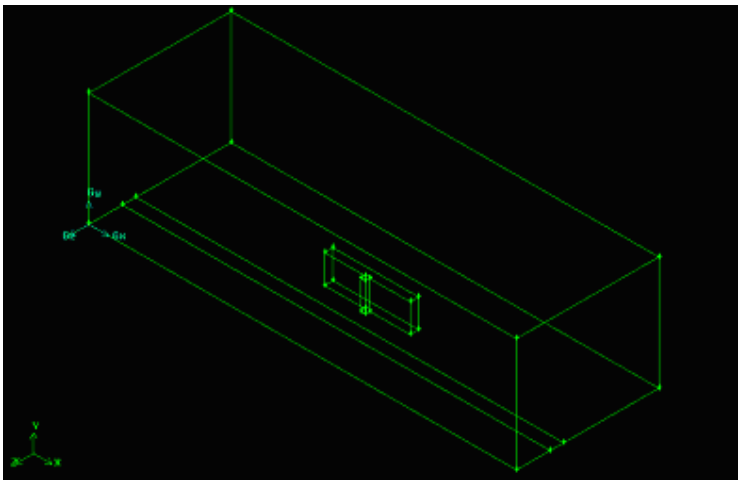

Figure 3.42View of Block 75 in Outer Domain (Case Study 3)

3.7 Statistical Analysis

The extent of statistical data analysis varies depending on the type of collated data. Some examples of statistical analysis include mean, standard deviation, significance testing such as t-test and A One-Way Analysis of Variance (ANOVA), pearson product-moment correlation coefficient, linear regression analysis, non linear regression using the gaussian plus a line model function etc. The linear, pearson product-moment correlation coefficient and non linear

regression was performed using the curve fitting program FindGraph, version 2.01 (UNIPHIZ Lab software, 2009).

CHAPTER 4: PARTICULATE MATTER MEASUREMENT

4.1 Introduction

Samples of Case Study 1 were collected from 26 July - 22 August 2005 while samples of Case Studies 2 and 3 were collected from 2 July - 27 July 2007 to assess the influence of building design configuration on the vertical distribution profile of $PM_{2.5}$ mass concentration at the various floors of the buildings under similar climatic and traffic conditions. A total of 80 PTFE samples (60 samples from the building and 20 samples from the background location) and 80 Whatman high quality quartz microfibre filter samples (60 samples from the building and 20 samples from the background location) were collected for each block. The methodology for the $PM_{2.5}$ measurement and description of Case Studies 1 - 3 is described in section 3.1. The measurement of background $PM_{2.5}$ levels was about 300 to 400m from the measurement sites.

Detailed chemical analysis of $PM_{2.5}$ and a health risk assessment due to the inhalation of $PM_{2.5}$ using the health risk model used by Pandey et al. (2005) was performed. The health risk model give dimensionless values which can be used for relative risk assessments of an occupant contracting a respiratory disease due to the inhalation of $PM_{2.5}$. In the assessment, residents were divided into four age group namely, infants, children (1 yr), children (8-10 yr) and adults. The analysis accounted for age-specific breathing rates, loael

values and body weights for the different age group. A brief description of the health risk model used by Pandey et al. (2005) is given in chapter 3, section 3.4. Similarly, a health risk assessment due to the inhalation of a cocktail of toxic particulate PAHs (US EPA priority components) using the TEF approach as described in chapter 3, section 3.3 was performed. The TEF approach has been extensively used for hazard assessment of different classes of toxic PAH mixtures inhaled by a person. Finally, a CFD study was performed to provide a visual perspective of airflow patterns around the point block and slab block building configurations at various upstream wind speeds coupled with the air displacement effect from the fast moving traffic as described in section 3.7.

4.2 Data Analysis

The measured data averaging over a period of 10 minutes is sufficient to be used for the analysis on any given day as any shorter averaging time will not improve the accuracy of the data but lead to large amount of data. The Grimm 1.177 software was used to download the particulate mass/number concentration data from the dust monitor while wind data was retrieved from the data logger of the ultrasonic wind vane using Microsoft's Hyper Terminal program. The Boxcar Pro 3.7 software was used to download data from the HOBO® Data Loggers. All the data were then analysed and converted into useful charts and diagrams using the Microsoft Excel program.

4.3 Results and Discussion

4.3.1 Traffic Volume

The contribution of various types of motor vehicles to the total fine traffic-generated particulate matter was not quantified in all these case studies. Traffic composition analysis along the CTE indicated approximately 62% of the vehicles were petrol-driven passenger cars fitted with catalytic converters. For Case Study 1, the daily traffic volume ranged from 11575 - 15631 vehicles/hr with a mean value of 13603 ± 2365 vehicles per hr. The traffic pattern on all days of a week had similar trend. Traffic volume generally peaked at around 1100 - 1300hr and 1600 - 1800hr which coincided with the lunch break and evening off-work periods respectively. Approaching the end of the day, the traffic condition worsens, leading to congestion with vehicles moving at low speed.

For Case Studies 2 and 3, a shift in traffic pattern was observed due to the introduction of Electronic Road Pricing (ERP) gantry which was commissioned by the LTA to control traffic flow during the evening peak period along the CTE. The daily traffic volume ranged from 14000 - 17000 vehicles per hr with a mean daily traffic volume of about 15500 ± 1200 vehicles per hr. The increase in vehicle volume could be due to the increase in car ownership. Traffic composition analysis indicated that petrol-driven passenger cars fitted with catalytic converters accounts for the majority of the vehicular traffic of about 60%. The daily traffic volume for a typical week is shown in Figure 4.1. Based on traffic data, the time periods of 1000 -

1300hr(Period 1), 1300 - 1700hr(Period 2) and 2000 - 2200hr(Period 3), had been classified as rising peak, afternoon peak and evening peak respectively. The reason for starting at 1000hr for Period 1 and ending at 2200hr for Period 3 was because this is the more critical time of the day for the study. 1700 - 2000hr was not included in the analysis as it registered a decreasing traffic volume which could be due to the diversion of vehicles towards other alternative routes as the ERP gantry operates between 1730 - 2000hr. Although there was a shift in traffic pattern, results showed that traffic pattern on all days of a week had similar trend. The traffic volume for Period 1 can reach as high as 15000 vehicles per hr. Thereafter, Period 2, the number of vehicles remained fairly constant at about 15000 - 16000 vehicles per hr. The traffic volume for Period 3 can be above 14000 vehicles per hr. Approaching towards the end of the day, the traffic condition became worst, leading to traffic congestion as vehicles are moving very slowly.

The daily mean mass concentration levels of the $PM_{2.5}$ at the representative floors was correlated against the total traffic volume for the same day. For all the case studies, traffic volume showed a poor correlation with the fine particles at each representative floor of all the buildings (Pearson's r = 0.15 - 0.26 for the low floor; r = 0.20 - 0.35 for the mid floor; r = 0.11 - 0.24 for the high floor). Other studies also showed no significant or poor correlations between traffic volume and fine particles (Namdeo et al., 1999; Kaur and Nieuwenhuijsen, 2009; Gietl and Klemm, 1995). Figure 4.2 shows an example of a poor correlation between traffic volume and $PM_{2.5}$ mass concentration. The reason for the poor correlation in this study could be due to the row of

trees and vegetation planted along the expressway which could have intercepted or modified the airflow patterns blowing towards the building.

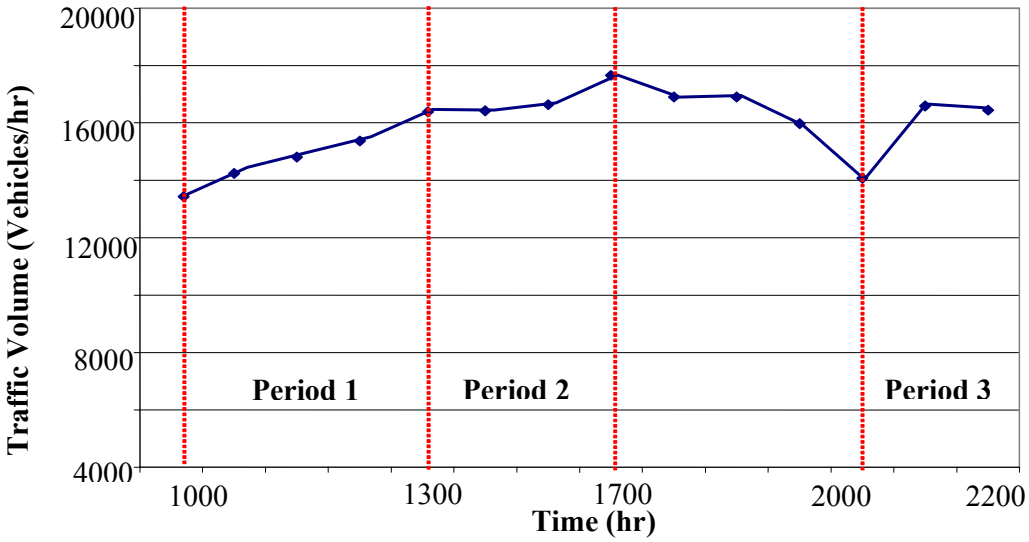

Figure 4.1 Daily Traffic Volume for a Typical Week for Blocks 75 (Case Study 3) and 95 (Case Study 2)

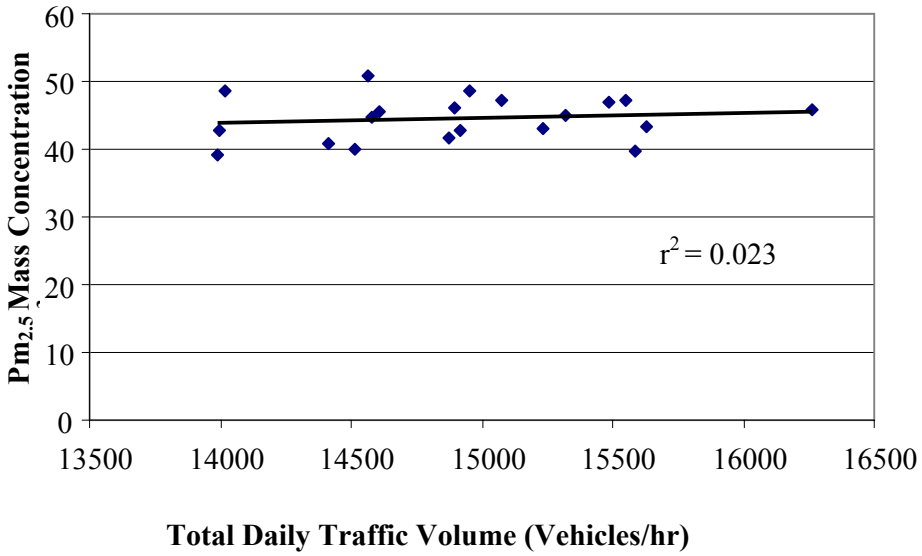

Figure 4.2 Regression of Daily $PM_{2.5}$ Mass Concentration and Traffic Volume at the Lower Floor of Block 95 (Case Study 2) in a Typical Day

4.3.2 Wind Speed and Direction

The wind direction measurements showed that the south-east monsoon winds were the dominant winds blowing at almost right angles towards the building façade for all the case studies. The wind azimuth and wind speed for Case Studies 1 - 3 is shown in Table 4.1. These prevailing wind conditions facilitated the transport of the fine traffic-generated particulate towards the residential apartments. A typical daily wind profile for a point and slab block is shown in Figures 4.3 and 4.4 respectively. The results showed the overall mean wind speed of slab block was slightly lower than that of the point block. Generally, the wind speed increased with the height of the building. It has been accepted that the wind velocity is low at the surface, and increases with height (Calvert, 2004).

Table 4.1 Wind Azimuth and Wind Speed for Case Studies 1 - 3

	Block 96 (Case Study 1)	**Block 95 (Case Study 2)**	**Block 75 (Case Study 3)**
Wind Azimuth	$136.2^o \pm 4.1^o$	$133.5^o \pm 6.4^o$	$134.9^o \pm 5.8^o$
Overall Mean Wind Speed	1.71 ± 0.35 m/s (0.94-2.89 m/s)*	1.75 ± 0.45 m/s (0.21-3.72 m/s)*	1.36 ± 0.42 m/s (0.16-2.01m/s)*
Low Floor	1.57 ± 0.42 m/s (0.94-2.49 m/s)*	1.65 ± 0.49 m/s (0.25-3.52 m/s)*	0.68 ± 0.37m/s (0.17-1.30 m/s)*
Mid Floor	1.73 ± 0.56 m/s (1.11-2.67 m/s)*	1.73 ± 0.32 m/s (0.28-3.68 m/s)*	1.49 ± 0.40 m/s (0.29-2.01 m/s)*
High Floor	1.86 ± 0.39 m/s (1.21-2.89 m/s)*	1.91 ± 0.47 m/s (0.21-3.72 m/s)*	1.72 ± 0.39 m/s (0.16-1.91m/s)*

* Minimum and maximum wind speed values obtained during these studies

The daily mean mass concentration of the $PM_{2.5}$ at the representative floors was correlated against the daily mean wind speed for the same day. The results did not show any significant correlation between wind speed and $PM_{2.5}$ mass concentration measured at each representative floor for all the case studies

(Pearson's r = -0.11- (-0.37) for the low floor; r = -0.25 - (-0.13) for the mid floor; and r = - 0.4 - (-0.16) for the high floor). Figure 4.5 show an example of a poor correlation between wind speed and $PM_{2.5}$ mass concentration (r^2 = 0.038).

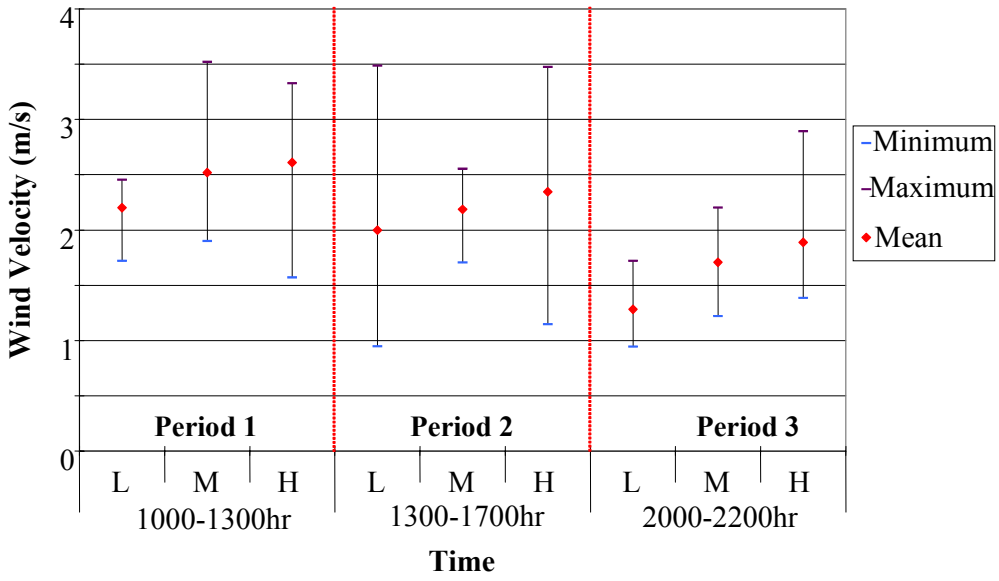

Figure 4.3 Typical Daily Wind Profile at Block 95 (Case Study 2)

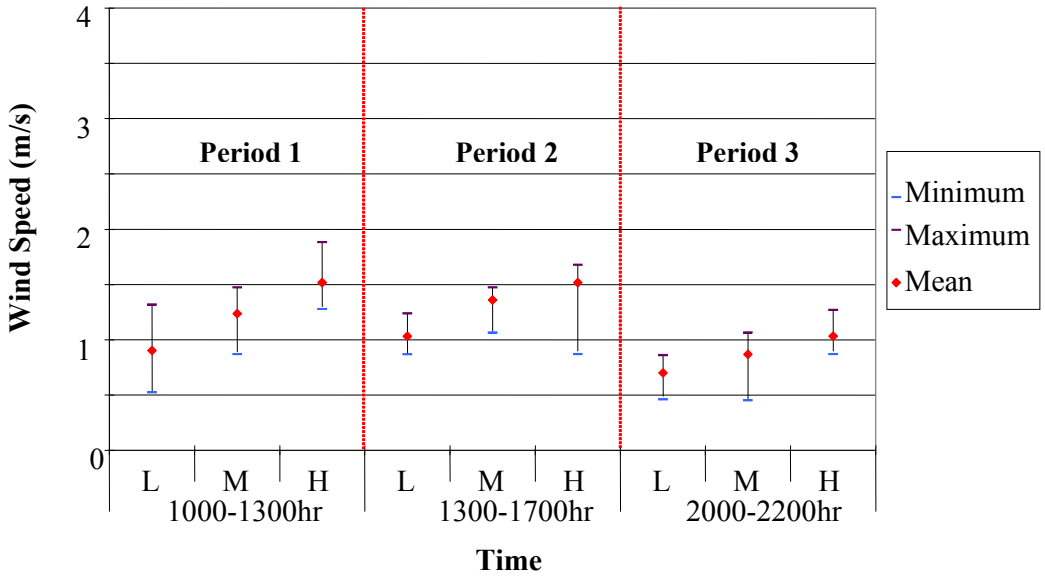

Figure 4.4 Typical Daily Wind Profile at Block 75 (Case Study 3)

L - low floor M - mid floor H - high floor

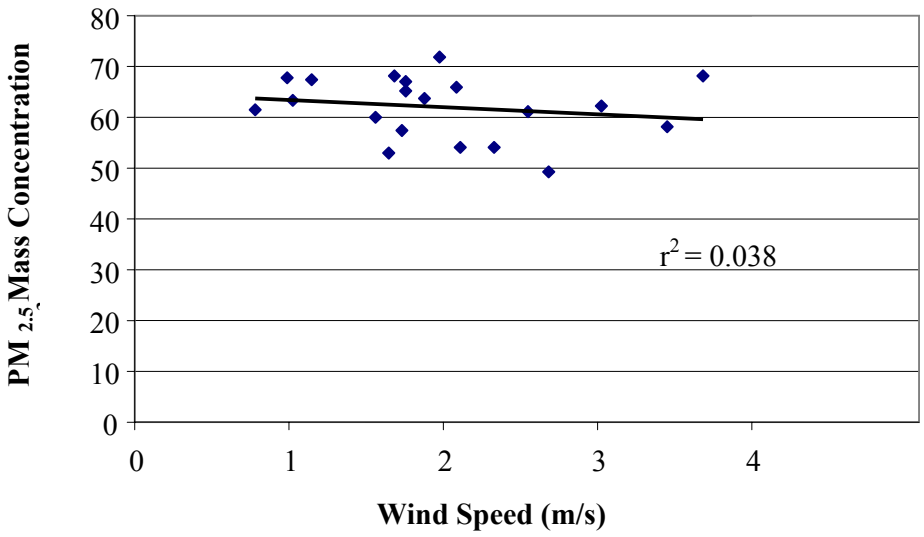

Figure 4.5 Regression of Daily $PM_{2.5}$ Mass Concentration and Wind Speed at the Mid Floor of Block 95 (Case Study 2) in a Typical Day

4.3.2.1 Air Displacement Effect by Fast Moving Traffic (CFD Analysis)

To study the air displacement effect by fast moving traffic towards a point and slab block configurations, CFD simulations were carried out. The drawback of the CFD analysis was that the row of trees planted along the expressway was not considered in the modelling. Although the actual site topology was not simulated, the main idea of the modelling was to provide a visual perspective of airflow patterns around the point block and slab block building configurations at various upstream wind speeds coupled with the air displacement effect from the fast moving traffic. For both the block configurations, the results showed the air displacement effect from the fast moving traffic coupled with low upstream wind velocity, caused wind velocity at the low floor to be relatively higher than other floors (Figures 4.6 and 4.7).

The air displacement effect by the fast moving traffic was less significant when the upstream wind speed increased as shown in Figures 4.8 and 4.9.

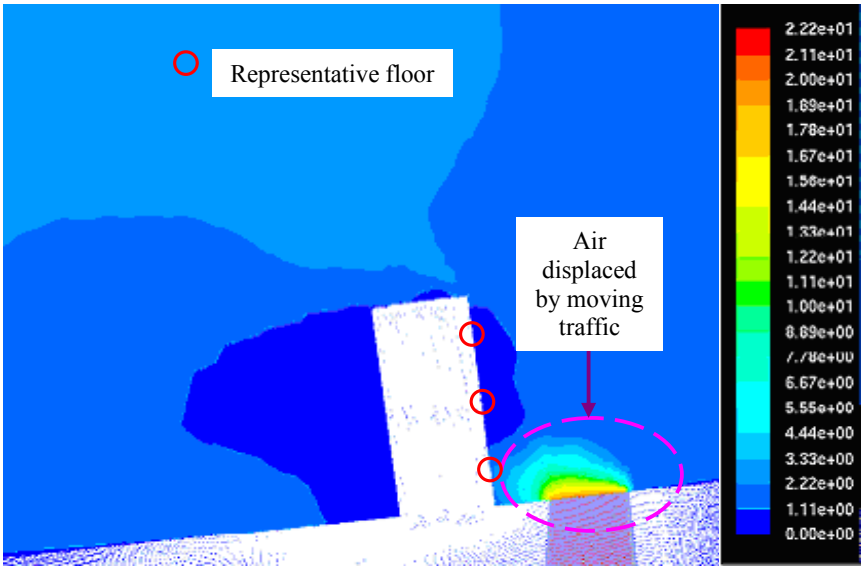

Figure 4.6 CFD Simulation with Upstream Wind Speed of 2m/s at Block 95 (Case Study 2)

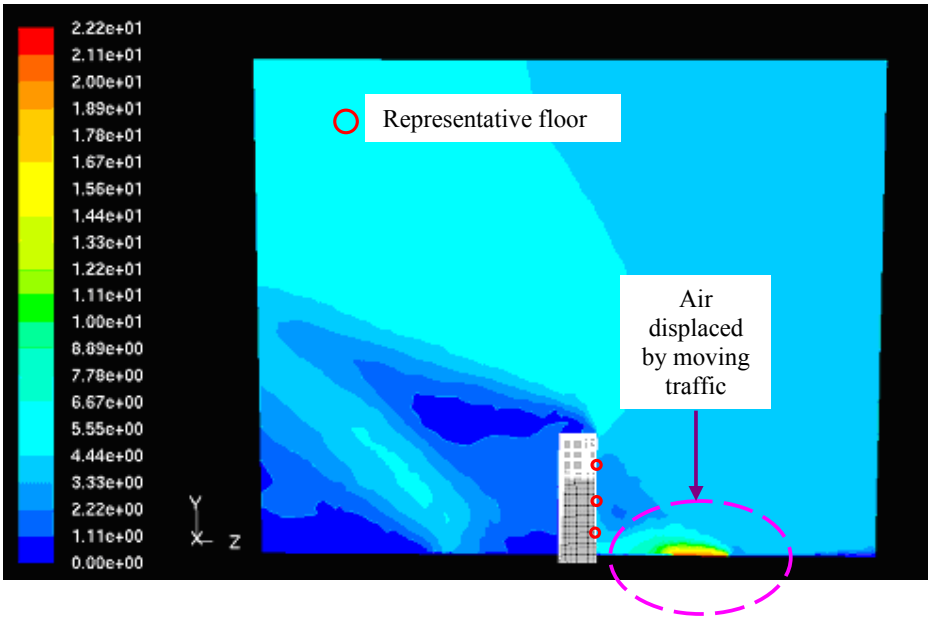

Figure 4.7 CFD Simulation with Upstream Wind Speed of 3m/s at Block 75 (Case Study 3)

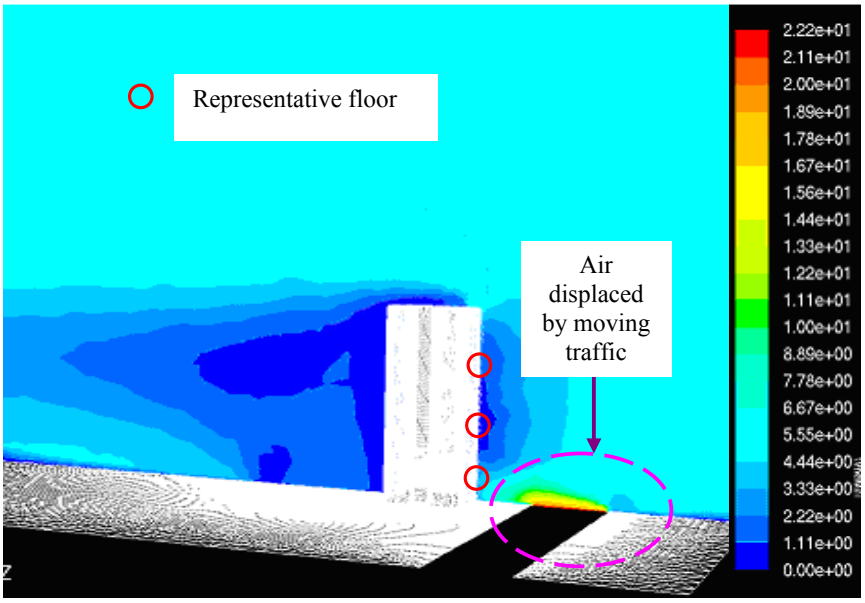

Figure 4.8 CFD Simulation with Upstream Wind Speed of 5m/s at Block 95 (Case Study 2)

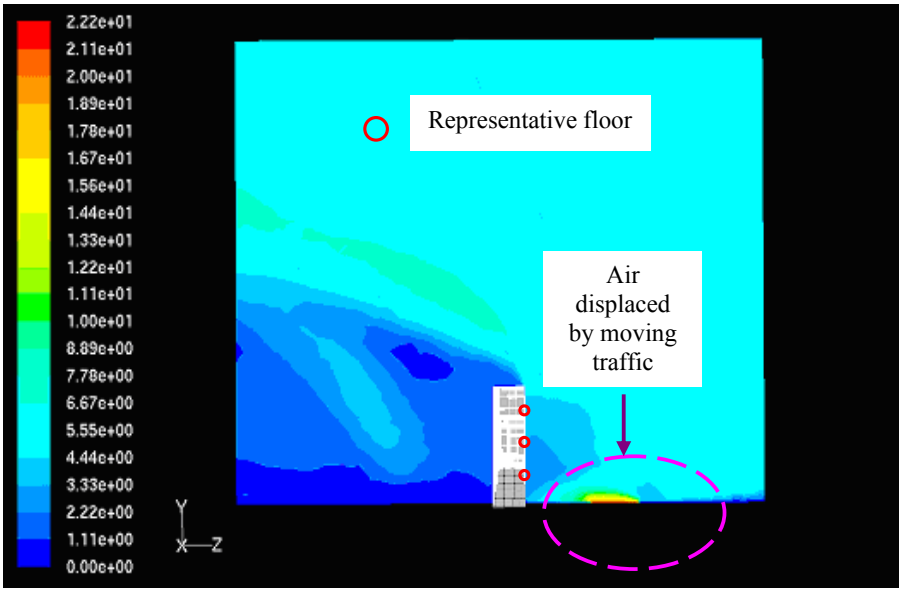

Figure 4.9 CFD Simulation with Upstream Wind Speed of 5m/s at Block 75 (Case Study 3)

4.3.3 Ambient Temperature and RH

Ambient temperature and RH was measured for 24hr daily during the measurement period. Generally, the ambient temperature decreased with increasing height of the building as shown in Table 4.2. Figure 4.10 shows a typical daily ambient temperature profile over the measurement period. The daily mean mass concentration of the $PM_{2.5}$ at the representative floors was correlated against the daily mean ambient temperature for the same day. For all the case studies, ambient temperature did not show any significant correlation with $PM_{2.5}$ mass concentration measured at each representative floor (Pearson's r = -0.03 - (-0.14) for the low floor; r = -0.39 - (-0.06) for the mid floor; r = -0.14 - (-0.20) for the high floor). Figure 4.11 shows an example of a poor correlation between ambient temperature and $PM_{2.5}$ mass concentration (r^2 = 0.096). The results were supported with other studies which show poor or very little significant correlations between temperature and fine particles (Gupta et al., 2006; Kaur and Nieuwenhuijsen, 2009).

Table 4.2 Ambient Temperature for Case Studies 1 - 3

	Block 96 (Case Study 1)	**Block 95 (Case Study 2)**	**Block 75 (Case Study 3)**
Overall Mean Ambient Temperature	28.9 ± 1.9 ^oC	29.9 ± 2.7 ^oC	30.2 ± 3.1 ^oC
Low Floor	29.1 ± 1.6 ^oC	30.2 ± 3.5 ^oC	30.5 ± 2.7 ^oC
Mid Floor	28.8 ± 1.5 ^oC	29.7 ± 2.5 ^oC	30.1 ± 2.9 ^oC
High Floor	28.4 ± 1.8 ^oC	29.4 ± 3.2 ^oC	29.8 ± 3.6 ^oC
Difference in temperature between high and low floor	0.7^oC	0.8^oC	0.7^oC
Difference in temperature between low and mid floor	0.3^oC	0.5^oC	0.4^oC
Difference in temperature between mid and high floor	0.4^oC	0.3^oC	0.3^oC

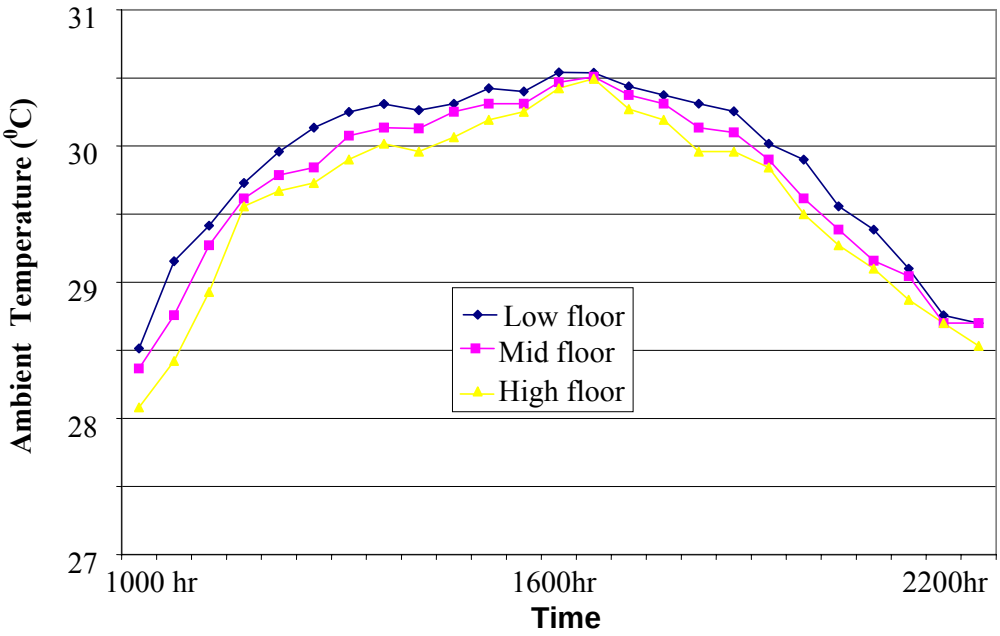

Figure 4.10 Typical Daily Ambient Temperature Profile on 18 July 2007 at Block 7(Case Study 3)

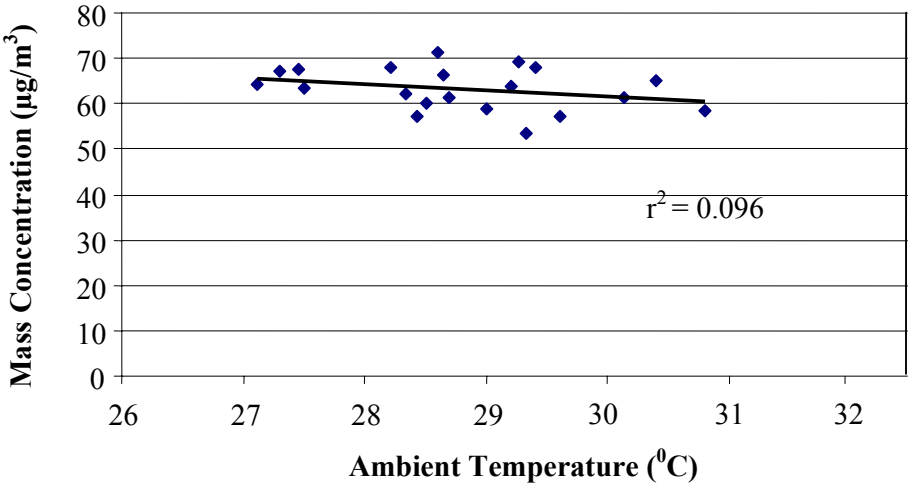

Figure 4.11 Regression of Daily $PM_{2.5}$ Mass Concentration and Ambient Temperature at the Mid Floor of Block 96 (Case Study 1) in a Typical Day

Table 4.3 RH for Case Studies 1 - 3

	Block 96 (Case Study 1)	Block 95 (Case Study 2)	Block 75 (Case Study 3)
Overall Mean RH	65.8 ± 3.8 %	71.7 ± 4.7 %	69.1 ± 4.1 %
Low Floor	62.4 ± 4.6 %	69.2 ± 3.9 %	65.0 ± 4.6 %
Mid Floor	67.3 ± 3.9 %	72.8 ± 4.2 %	68.1 ± 4.9 %
High Floor	68.9 ± 4.2 %	73.4 ± 3.2 %	70.3 ± 4.4 %
Difference in RH between high and low floor	6.5%	4.2%	5.3%
Difference in RH between low and mid floor	4.9%	3.6%	3.1%
Difference in RH between mid and high floor	1.6%	0.6%	2.2%

Figure 4.12 shows a typical daily RH profile over the measurement period. Generally, the RH increased with increasing height of the building as shown in Table 4.3. The daily mean mass concentration of $PM_{2.5}$ at the representative floors was correlated against the daily mean RH for the same day. RH did not show any significant correlation with the daily mean $PM_{2.5}$ mass concentrations measured at each representative floor of the buildings. Similarly for all the case studies, RH did not show any significant correlation with the $PM_{2.5}$ mass concentration measured at each representative floor (Pearson's r = 0.05 - 0.30 for the low floor; r = 0.12 - 0.23 for the mid floor; and r = 0.09 - 0.17 for the high floor). Figure 4.13 shows an example of a poor correlation between RH and $PM_{2.5}$ mass concentration (r^2 = 0.026). The results were supported with other studies which show poor or very little significant correlations between RH and fine particles (Gupta et al., 2006; Kaur and Nieuwenhuijsen, 2009).

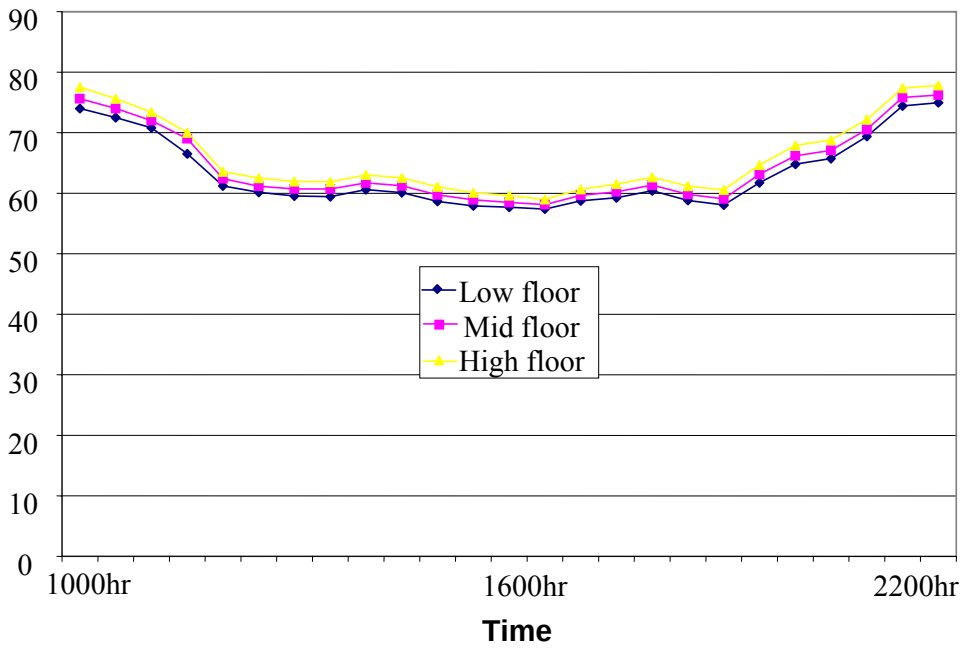

Figure 4.12 Typical Daily RH Profile on 18 July 2007 at Block 75 (Case Study 3)

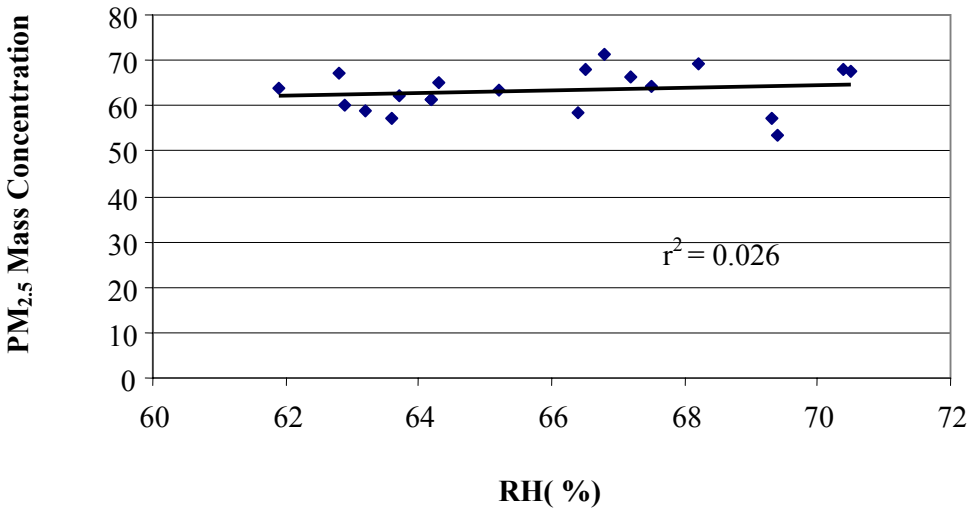

Figure 4.13 Regression of Daily $PM_{2.5}$ Mass Concentration and RH at the Mid Floor of Block 96 (Case Study 1) in a Typical Day

For all the case studies, the vertical temperature distribution profile and RH distribution profile showed very little stratification between the representative

floors. The insignificant RH and temperature stratifications observed between the three selected floors could be due to rapid mixing of air near the boundary layer of the building. The insignificant temperature stratification between the representative floors of the building reduced the buoyancy effect on the vertical transportation of fine traffic-generated particulate matter.

4.3.4 Proportion of Particulate Mass Concentration

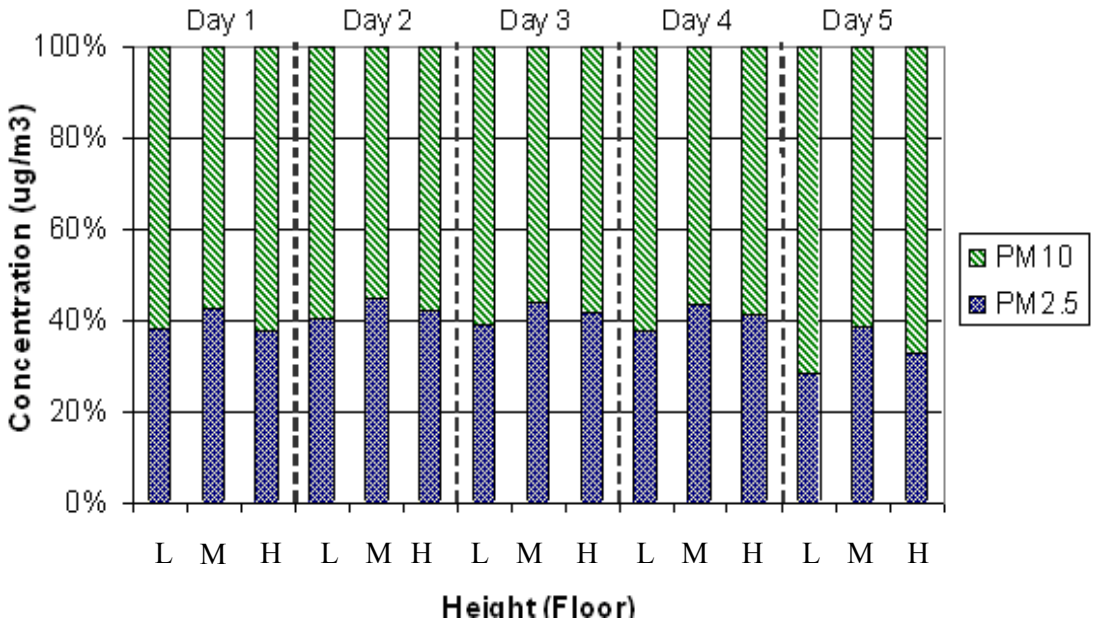

Figure 4.14 Proportion of PM_{10} and $PM_{2.5}$ Mass Concentration in Block 96 (Case Study 1) for a Typical Week

L - low floor M - mid floor H - high floor

Result indicated about 40 - 60% of PM_{10} was constituted by $PM_{2.5}$. For example, Figure 4.14 shows the proportion of the mass concentration of $PM_{2.5}$ and PM_{10} as measured by dust monitors at the various representative floors of Block 96 for a typical working week. The concentration of $PM_{2.5}$ is of concern

since the particles can penetrate deeper into the lungs and cause adverse health effects.

4.3.5 Vertical Distribution Profile of Fine Particulate Matter

For all the case studies, experimental results showed that $PM_{2.5}$ daily mean particulate mass/number concentration was highest at the mid floor of the building as compared to those measured at high and low floors during a typical day as shown in Tables 4.4 - 4.6. The mean daily mass concentration at the various floors exceeded the $PM_{2.5}$ National Ambient Air Quality Standard (NAAQS, 2009) annual average of 15μg/m^3 and 24 hour value of 35μg/m^3 most of the time during the measurement period. This is of major concern since the health of residents including the health of "sensitive" populations such as asthmatics, children, and the elderly are affected.

$PM_{2.5}$ emitted from hot vehicle exhaust (about 150 - 250^{o}C) rises due to buoyancy before being blown towards the building by the upstream wind. $PM_{2.5}$ motion in the upward and sideways direction is further assisted by the wind turbulence additionally amplified by the fast moving vehicles along the expressway. Upon reaching the trees, some of the $PM_{2.5}$ is presumably being intercepted by tree leaves (Beckett et al., 2000; Impens and Delcarte, 1979). Most of the $PM_{2.5}$ flow over the top of the trees and keep moving upwards carried by airflow streamlines. This could explain the reason for the daily mean $PM_{2.5}$ mass concentration being the highest at the mid floor of the building as compared to those measured at high and low floors. Although the lower floors were closest to traffic emissions, the mean $PM_{2.5}$ mass/number

concentration was lower there than that at the mid floors, which could presumably be due to the buoyancy rise at the source point, interception of $PM_{2.5}$ by tree leaves or the vortices at the wake region of the trees (Ishikawa et al., 2006) diluting the traffic-polluted air behind the trees or all three. The high floors had the least $PM_{2.5}$ mass/number concentration due to dilution following pronounced mixing of traffic-polluted air with ambient air. There is a significant difference between the mean $PM_{2.5}$ mass/number concentration values measured at the low and mid floors ($p < 0.02$ to 0.04) and the mid and high floors ($p < 0.01$ to 0.05) for all the case studies.

The vertical distribution profile of $PM_{2.5}$ mass/number concentration in this study contradicts the vertical distribution profile of several studies which found that particulate matter concentration usually decreased with increasing height (Morawska et al., 1999; Wu et al., 2002; Rubino et al., 1998; Hitchins et al., 2001). The buildings used in the previous studies were mainly air-conditioned or semi-air conditioned and the studies were conducted in temperate, subtropical and dry climates. Also, in the studies, there were no trees in between the roads and buildings. In this study, microclimatic conditions of the selected sites, such as the influence of trees planted along the expressway, could have had an influence on the vertical distribution profile of the $PM_{2.5}$ mass/number concentration in the buildings.

Table 4.4 Particulate Mass Concentration ($PM_{2.5}$) at Block 96 (Case Study 1) for a Typical Week

Day	Upstream Background level ($\mu g/m^3$)	Low floor ($\mu g/m^3$)	Mid floor ($\mu g/m^3$)	High floor ($\mu g/m^3$)
1	24.0 ± 4.8	46.0± 4.4	60.1 ± 5.1	35.6 ± 5.0
2	23.1 ± 5.1	48.5 ± 4.8	63.4 ± 5.7	40.2 ± 4.9
3	23.7 ± 4.4	41.7 ± 5.2	57.3 ± 4.2	32.7 ± 5.0
4	24.7 ± 4.2	50.6± 5.6	67.6 ± 4.9	40.7 ± 5.4
5	21.4 ± 5.3	44.7 ± 4.8	63.8 ± 4.6	37.2 ± 5.0

For the point block configuration (Case Study 2), the $PM_{2.5}$ number concentration ranged from 50 - 225 particles/cm^3 for the block. The daily mean $PM_{2.5}$ number concentration were 117.9 ± 26.0 particles/cm^3 at the low floor, 178.6 ± 34.1 particles/cm^3 at the mid floor and 79.0 ± 16.9 particles/cm^3 at the high floor of the building. So far, there is no ambient air quality standard for $PM_{2.5}$ number concentration. For the slab block configuration (Case Study 3), the $PM_{2.5}$ number concentration ranged from 98 - 255 particles/cm^3 for the block. The daily mean $PM_{2.5}$ number concentration were 169.4 ± 28.5 particles/cm^3 at the low floor, 229.7 ± 23.1 particles/cm^3 at the mid floor and 120.1 ± 21.1 particles/cm^3 at the high floor of the building. Figures 4.15 and 4.16 show the $PM_{2.5}$ number concentrations at the representative floors of the point and slab block configurations at all time periods for a typical day.

Table 4.5 Particulate Mass (M) and Number (N) Concentration in Block 95 (Case Study 2) for a Typical Week

Day		Upstream Background level ($\mu g/m^3$)	Low floor ($\mu g/m^3$ or particles/cm^3)	Mid floor ($\mu g/m^3$ or particles/cm^3)	High floor ($\mu g/m^3$ or particles/cm^3)
1	M	22.1 ± 4.9	45.6 ± 5.3	62.2 ± 6.1	33.4 ± 4.0
	N		145.9 ± 20.5	195.5 ± 22.4	92.4 ± 20.5
2	M	23.7 ± 5.2	48.8 ± 4.1	61.5 ± 5.1	35.6 ± 4.3
	N		141.8 ± 23.6	225.5 ± 21.1	90.2 ± 22.5
3	M	20. 8 ± 4.2	36.8 ± 4.9	49.3 ± 4.4	27.0± 3.4
	N		116.1 ± 19.1	142.3 ± 23.2	50.2 ± 17.6
4	M	23.0 ± 4.0	37.3 ± 4.8	53.9 ± 5.6	28.4 ± 4.1
	N		86.4 ± 20.5	180.0 ± 24.2	80.6 ± 16.3
5	M	24.0 ± 4.50	39.1 ± 5.8	54.1 ± 4.2	30.7 ± 4.6
	N		99.4 ± 18.8	149.7 ± 17.4	81.5 ± 15.1

Table 4.6 Particulate Mass (M) and Number (N) Concentration in Block 75 (Case Study 3) for a Typical Week

Day		Upstream Background level ($\mu g/m^3$)	Low floor ($\mu g/m^3$ or particles/cm^3)	Mid floor ($\mu g/m^3$ or particles/cm^3)	High floor ($\mu g/m^3$ or particles/cm^3)
1	M	24.3 ± 4.0	58.5 ± 4.5	73.9 ± 5.0	45.3 ± 5.4
	N		196.3 ± 21.8	248.4 ± 18.2	139.6 ± 23.9
2	M	23.0 ± 4.5	60.3 ± 5.5	75.9 ± 5.0	50.0± 4.7
	N		203.8 ± 19.1	256.2 ± 22.8	145.6 ± 18.4
3	M	23.7 ± 5.0	52.7 ± 5.0	65.4 ± 4.2	41.3 ± 5.1
	N		150.5± 16.5	201.2 ± 19.8	99.0 ± 18.3
4	M	24.0 ± 5.1	51.8 ± 5.2	66.8 ± 4.3	40.0 ± 3.9
	N		141.6 ± 23.4	212.0 ± 15.9	99.0 ± 18.3
5	M	22.8 ± 4.5	53.6 ± 5.8	68.8 ± 4.1	40.0 ± 5.0
	N		154.9 ± 20.0	231.4 ± 24.8	110.8 ± 22.6

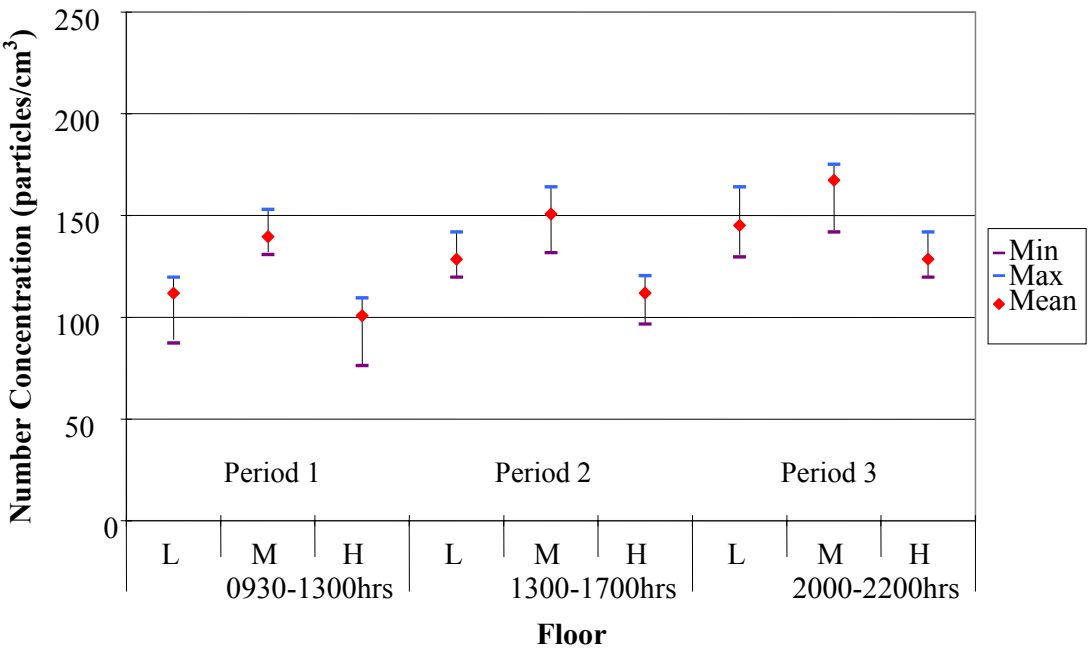

Figure 4.15 $PM_{2.5}$ Number Concentrations at the Various Floors of Block 95 (Case Study 2) in a Typical Day

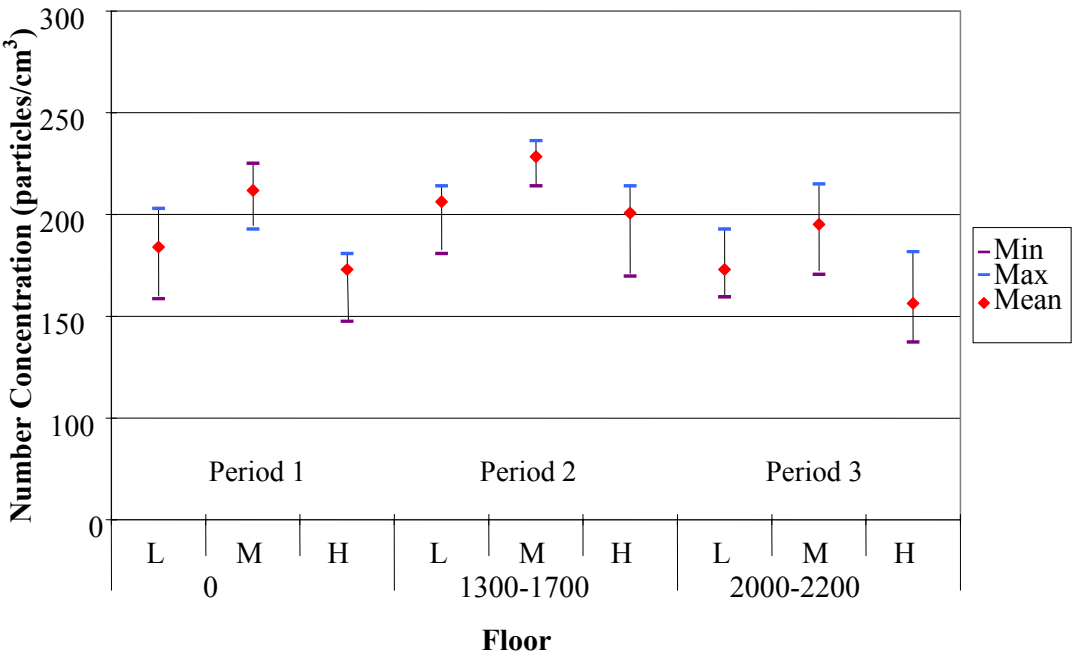

Figure 4.16 $PM_{2.5}$ Number Concentrations at the Various Floors of Block 75 (Case Study 3) in a Typical Day

L - low floor M - mid floor H - high floor

The only difference between the point block and slab block configurations is that at corresponding floors, the $PM_{2.5}$ mass/number concentration for slab block is much higher than that of point block under similar traffic and meteorological conditions. This could be attributed to the slab block configuration which tends to slow down wind speed. For the point block configuration, $PM_{2.5}$ number concentration showed a significant correlation with $PM_{2.5}$ mass concentration at the same floor (Pearson's r = 0.73 for the low floor; r = 0.75 for the mid floor; and r = 0.69 for the high floor). Figure 4.17 shows an example of a moderate correlation between $PM_{2.5}$ mass concentration and $PM_{2.5}$ number concentration ($r^2 = 0.534$). For the slab block configuration, $PM_{2.5}$ number concentration show a significant correlation with $PM_{2.5}$ mass concentration at the various floors (Pearson's r = 0.72 for the low floor; r = 0.69 for the mid floor; and r = 0.73 for the high floor). Figure 4.18 shows an example of a moderate correlation between $PM_{2.5}$ mass concentration and $PM_{2.5}$ number concentration ($r^2 = 0.518$).

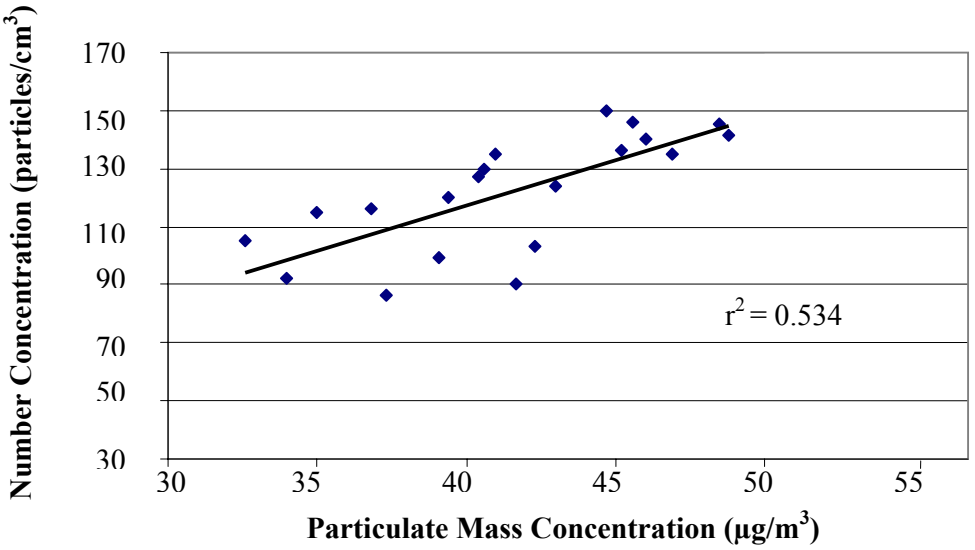

Figure 4.17 Regression of Mean Daily $PM_{2.5}$ Mass Concentration and Daily $PM_{2.5}$ Number Concentration at the Low Floor of Block 95 (Case Study 2) in a Typical Day

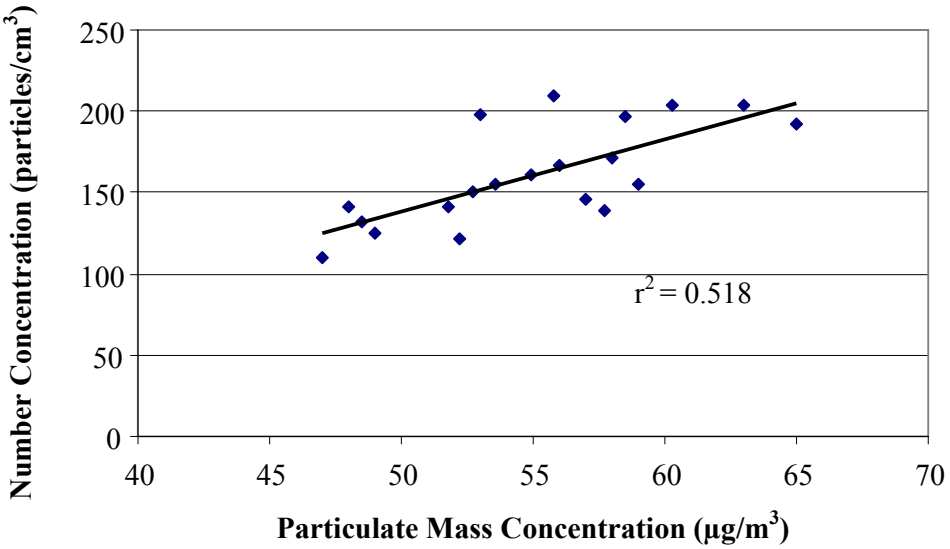

Figure 4.18 Regression of Mean Daily $PM_{2.5}$ Mass Concentration and Daily $PM_{2.5}$ Number Concentration at the Low Floor of Block 75 (Case Study 3) in a Typical Day

4.3.6 $PM_{2.5}$ Size Distribution

The size distribution of $PM_{2.5}$ at the various floors in a point block (Block 95) and a slab block (Block 75) configuration is similar. These results are based on $PM_{2.5}$ number concentration. The $PM_{2.5}$ size distribution at the various floors of both the building configurations is shown in Figures 4.19 and 4.20. About 93 - 95% of the $PM_{2.5}$ number concentration consisted of particles below the size range of 0.65 μm while the rest 5 - 7% of the particles fall in the size range 0.65 - 1.6μm. Of the 93 - 95% particles, about 73 - 75% particles were in the size range of 0.3 - 0.4μm, 14 - 16% in the size range of 0.4 - 0.5μm and 4 - 6% in the size range of 0.5 - 0.65μm at all the representative floors of both the buildings. The size distribution show majority particles in the $PM_{2.5}$ number concentration may have a very high chance of penetrating deeper into the lungs of residents. Toxicological studies have implicated fine and ultra fine particles have considerably enhanced toxicity per unit mass and their toxicity increased as particle size decrease (Donalson and MacNee, 1998).

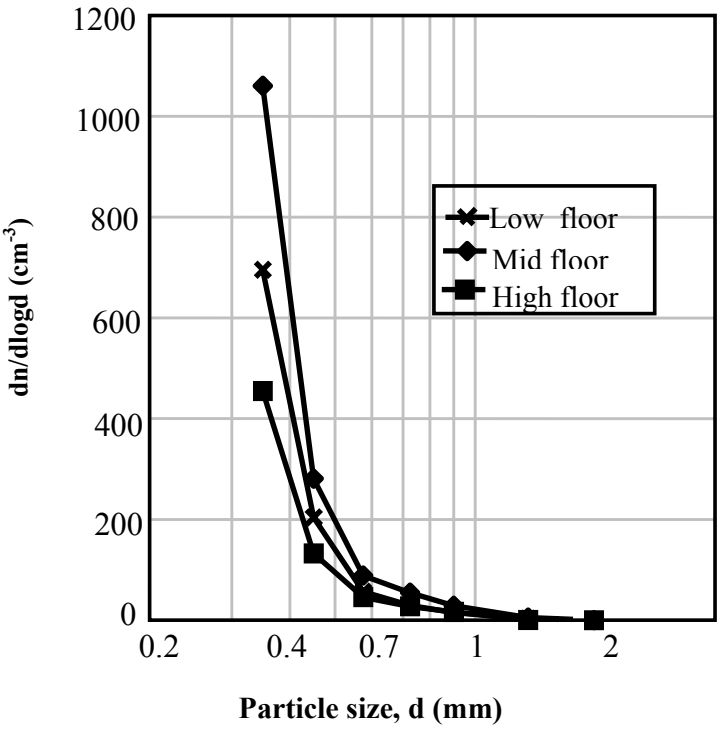

Figure 4.19 Size Distribution of $PM_{2.5}$ at Block 95 (Case Study 2)

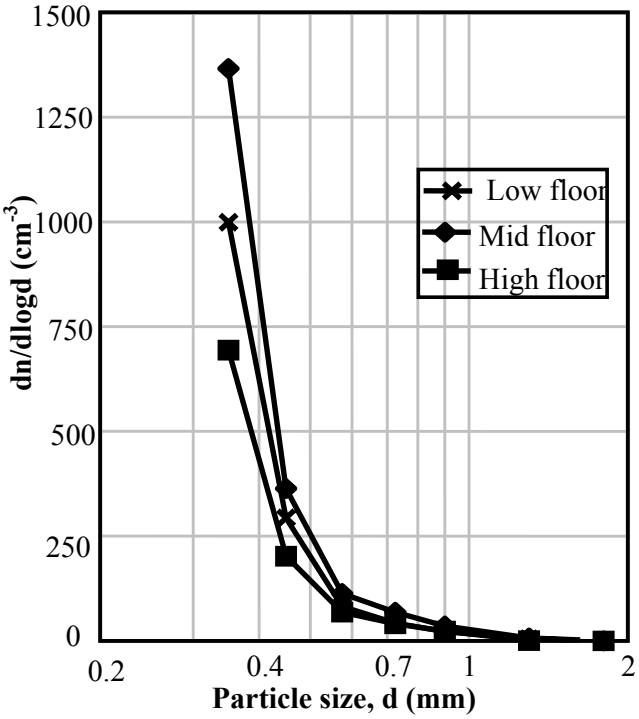

Figure 4.20 Size Distribution of $PM_{2.5}$ at Block 75 (Case study 3)

4.3.7 Potential Health Risk Assessment due to $PM_{2.5}$ Inhalation (Case Studies 2 and 3)

Dose rates and the potential health risk (HR) values for the point block (Block 95) and slab block (Block 75) are shown in Tables 4.7 - 4.8. For both the blocks, the analysis showed that the potential health risks to respiratory disease are highest for all age categories: infants, children (1 yr), children (8 - 10 yr) and adults) in the mid floor compared to the high (lowest) and low floor (second highest). New born babies, one year old children, and adults had similar potential health risk while teenage children (8 - 10yr) had the lowest potential health risk. The HR values at the mid and low floors of the point block indicate that residents living in these floors had 1.81 and 1.34 times more risk, respectively, in terms of developing respiratory diseases when

compared to residents living at the high floors for all age categories. For the slab block, the HR values at the mid and low floors indicate that residents living in these floors had 1.62 and 1.28 times more risk, respectively, in terms of developing respiratory diseases when compared to the residents living at the high floors for all age categories. The HR values are most likely to increase since the vehicle population in Singapore has increased over the years from 683204 vehicles in 1997 to 851336 vehicles in 2008 (Department of Statistics of Singapore, 2009). Given that the projected population growth will increase by about 50% in the near future and more residential buildings will be required to accommodate the growing population in a land scarce Singapore and therefore they could be built close to expressways and major roads. Hence, it is important to consider the possible penetration of fine traffic-generated particles into buildings at the design stage. The results of the potential health risk assessment due to particulate matter inhalation had been published elsewhere (Kalaiarasan et al. 2009).

Table 4.7 Dose Rates and HR values at Block 95 (Case Study 2)

Floor	**n = 80**							
	Dose Rate(μg kg^{-1})				**HR(dimensionless)**			
	New born	Children (1 year)	Children (8-10 years)	Adult	New born	Children (1 year)	Children (8-10 years)	Adult
Low floor	7.68 ± 1.00	10.95 ± 1.42	9.61 ± 1.24	8.24 ± 1.06	0.51 ± 0.06	0.52 ± 0.07	0.36 ± 0.04	0.54 ± 0.05
Mid floor	10.41 ± 1.02	14.83 ± 1.45	13.01 ± 1.27	11.15 ± 1.09	0.70 ± 0.07	0.72 ± 0.04	0.47 ± 0.05	0.71 ± 0.06
High floor	5.74 ± 0.66	8.18 ± 0.94	7.18 ± 0.82	6.15 ± 0.70	0.39 ± 0.04	0.38 ± 0.05	0.26 ± 0.03	0.40 ± 0.04

n = number of samples collected and analyzed for mass concentration

Table 4.8 Dose Rates and HR values at Block 75 (Case Study 3)

Floor	n = 80							
	Dose Rate (μg kg^{-1})				HR (dimensionless)			
	New born	Children (1 year)	Children (8-10 years)	Adult	New born	Children (1 year)	Children (8-10 years)	Adult
Low floor	10.25 ± 0.70	14.61 ± 1.00	12.81 ± 0.88	10.98 ± 0.75	0.70 ± 0.04	0.69 ± 0.05	0.47 ± 0.03	0.68 ± 0.07
Mid floor	12.99 ± 0.84	18.51 ± 1.20	16.24 ± 1.05	13.92 ± 0.90	0.88 ± 0.06	0.86 ± 0.04	0.59 ± 0.04	0.89 ± 0.03
High floor	8.02 ± 0.80	11.43 ± 1.14	10.03 ± 1.00	8.60 ± 0.86	0.55 ± 0.05	0.53 ± 0.07	0.36 ± 0.05	0.56 ± 0.04

n = number of samples collected and analyzed for mass concentration

4.3.8 Chemical Characterization of Particulate Matter

4.3.8.1 Carbonaceous species

Elemental carbon (EC) is emitted from combustion source and its transformation is limited. Thus, EC is a good indicator of primary anthropogenic air pollutants. Data on carbonaceous species, organic carbon (OC) and elemental carbon, were obtained and the ratio between these species i.e. OC/EC ratio was evaluated for actual traffic emissions. The mean EC and OC mass concentration for a typical week at the various floors of the case studies is given in Tables 4.9 - 4.12. For all the case studies, the highest EC and OC concentrations occurred at the mid floor of the buildings.

Table 4.9 EC and OC Mass Concentration in Block 96 (Case Study 1) in a Typical Week

Day	n = 80					
	EC			OC		
	Low floor ($\mu g/m^3$)	Mid floor ($\mu g/m^3$)	High floor ($\mu g/m^3$)	Lower floor ($\mu g/m^3$)	Mid floor ($\mu g/m^3$)	High floor ($\mu g/m^3$)
1	15.1 ±1.7	20.1± 2.1	10.2 ±2.7	13.1± 2.2	18.7 ±2.5	9.4 ± 2.0
2	16.4 ±2.5	21.5 ±3.1	11.2 ±2.9	16.5 ±3.0	22.9 ±3.3	12.8 ±2.9
3	14.1 ±2.6	19.1 ±2.0	8.3 ± 2.5	15.2 ±3.3	21.4 ±1.7	9.0 ± 2.3
4	17.6 ±2.0	21.5 ±3.3	12.8 ± 2.2	18.9 ±3.2	23.4 ±2.7	14.9 ± 3.0
5	15.8 ±2.4	22.9 ±3.5	9.9 ± 2.7	15.8 ± 2.5	21.1 ± 2.2	10.6 ± 2.6

n = number of samples collected and analyzed for mass concentration

Table 4.10 EC and OC Mass Concentration in Block 95 (Case Study 2) in a Typical Week

Day	n = 80					
	EC			OC		
	Low floor ($\mu g/m^3$)	Mid floor ($\mu g/m^3$)	High floor ($\mu g/m^3$)	Low floor ($\mu g/m^3$)	Mid floor ($\mu g/m^3$)	High floor ($\mu g/m^3$)
1	16.6 ±2.2	21.6 ±3.0	11.8± 2.9	13.8± 2.1	22.1± 3.1	11.4± 2.6
2	17.4 ±3.2	20.9 ±2.6	12.3 ±1.9	14.9± 2.7	21.4± 2.5	12.1± 2.0
3	12.5 ±2.2	17.6 ±2.9	9.0 ± 1.7	11.7± 3.4	16.2 ±2.1	8.7 ± 2.4
4	13.0 ±2.1	19.0±3.1	9.2 ± 2.5	12.6 ±2.8	18.3± 3.6	9.9 ± 2.3
5	13.2 ±1.6	18.2 ±2.5	9.9 ± 1.4	13.2 ±2.1	19.3 ±1.8	10.7 ±2.7

n = number of samples collected and analyzed for mass concentration

Table 4.11 EC and OC Mass Concentration in Block 75(Case Study 3) in a Typical Week

Day	n = 80					
	EC			OC		
	Low floor ($\mu g/m^3$)	Mid floor ($\mu g/m^3$)	High floor ($\mu g/m^3$)	Low floor ($\mu g/m^3$)	Mid floor ($\mu g/m^3$)	High floor ($\mu g/m^3$)
1	19.6 ± 3.1	26.7 ± 2.2	16.5 ±1.8	19.6 ± 2.0	25.9 ± 3.0	15.2 ± 2.9
2	21.7 ± 3.0	27.3 ± 2.0	18.0 ± 2.3	20.6 ± 3.2	26.8 ± 3.4	16.6 ± 3.1
3	17.4 ± 3.1	22.5 ± 2.4	14.5 ± 2.2	17.5 ± 2.3	23.3 ± 3.2	13.7 ±1.4
4	17.9 ± 2.89	22.9 ± 2.8	13.9 ± 3.2	16.8 ± 3.4	23.5 ± 2.0	14.6 ± 2.8
5	18.9 ± 2.3	23.3 ± 3.0	12.9 ± 2.5	18.6 ± 2.7	24.6 ± 2.3	14.9 ±3.5

n = number of samples collected and analyzed for mass concentration

Table 4.12 OC/EC Ratio for Case Studies 1 - 3

	Block 96 (Case Study 1)	Block 95 (Case Study 2)	Block 75 (Case Study 3)
Background EC concentration	7.1 ± 2.5 μg/m^3	6.7 ± 1.8 μg/m^3	6.7 ± 1.8 μg/m^3
Background OC concentration	6.8 ± 2.8 μg/m^3	5.8 ± 2.6μg/m^3	5.8 ± 2.6μg/m^3
Low Floor (Daily EC concentration)	15.8 ± 1.3 μg/m^3	14.5 ± 2.3 μg/m^3	19.1 ± 1.7 μg/m^3
Mid Floor (Daily EC concentration)	21.1 ± 1.5 μg/m^3	19.5 ± 1.7 μg/m^3	24.5 ± 2.2 μg/m^3
High Floor (Daily EC concentration)	10.5 ± 1.7μg/m^3	10.4 ± 1.5 μg/m^3	15.2 ± 2.1 μg/m^3
Low Floor (Daily OC concentration)	15.9 ± 2.1 μg/m^3	13.2 ± 1.2 μg/m^3	18.6 ± 2.1 μg/m^3
Mid Floor (Daily OC concentration)	21.5 ± 1.8 μg/m^3	19.5 ± 2.4 μg/m^3	24.8 ± 2.2 μg/m^3
High Floor (Daily OC concentration)	11.3 ± 2.5 μg/m^3	10.6 ± 1.3 μg/m^3	14.9 ± 1.5 μg/m^3
Low Floor (Daily OC/EC ratio)	1.00 ± 0.08 (0.86-1.07)	0.92 ± 0.07 (0.86-1.00)	0.97 ± 0.03 (0.94-1.01)
Mid Floor (Daily OC/EC ratio)	1.03 ± 0.09 (0.92-1.13)	1.00 ± 0.05 (0.92-1.05)	1.01 ± 0.04 (0.97-1.06)
High Floor (Daily OC/EC ratio)	1.07 ± 0.09 (0.92-1.17)	1.01 ± 0.06 (0.97-1.29)	0.99 ± 0.09 (0.92-1.12)

There was a significant difference between upstream background levels and those EC and OC values measured at the various floors of the blocks ($p < 0.02$ to 0.03 for OC and $p < 0.02$ to 0.05 for EC). OC mass concentration and EC mass concentrations were highly correlated at the various floors of the block (0.92 - 0.94 for the low floor, 0.90 - 0.96 at the mid floor and 0.89 - 0.95 at the high floor). The very high correlation suggested OC and EC mass concentrations came from the same anthropogenic source (Na et al., 2004).

Studies have shown EC causes acute and chronic effects. EC particles can adsorb transition metals such as antimony, barium, copper, iron and zinc

which are emitted from traffic exhaust, tyres and brake wear. These metals which are mainly generated by traffic in urban atmospheres (Steiner et al., 2007) have been shown to induce oxidative stress in the lung (Campbell, 2004). Other studies have shown the relative risk of premature death increases with 1% per 1μg/m^3 of EC (Sunyer et al., 1991). This is 5 - 10 times higher than the relative risk of PM_{10}. Although, EC is present in small aerosol fractions, its large surface area enhances its toxicity. OC can be emitted from primary emission source or produced from the condensation of low vapour pressure products during photo-oxidation of hydrocarbons (Seinfield, 1986). Figures 4.21 shows an example of a very high correlation between EC mass concentration and OC mass concentration at Block 96.

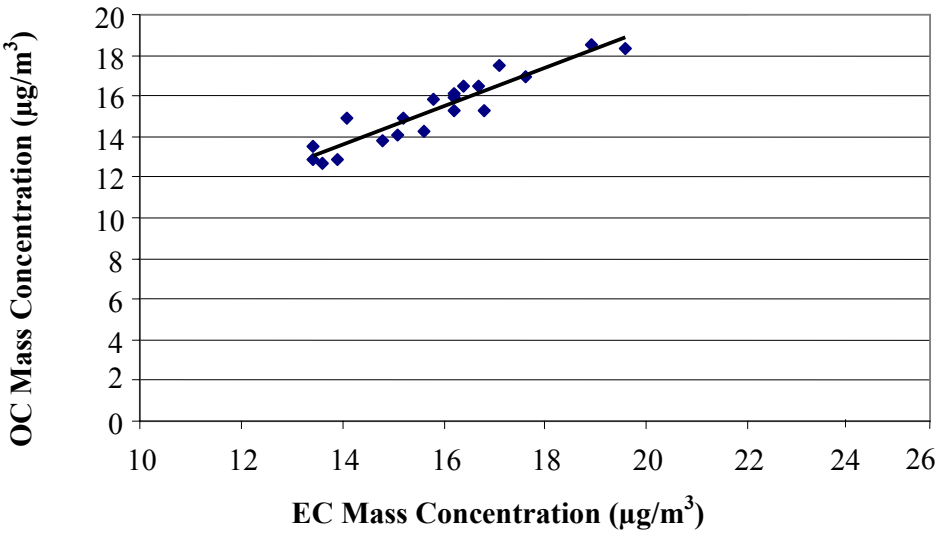

Figure 4.21 Regression of EC and OC Mass Concentrations at the Low Floor of Block 96 (Case Study 1) in a Typical Day

For all the case studies, the OC/EC ratio at all floors was less than the expected value of 3.7 for traffic emissions suggesting most of the particulate matter were from traffic (Cabada and Pandis, 2002). The lower values

suggested the expressway was dominated by vehicles with catalytic converter (Giugliano et al., 2005). An OC/EC ratio value of less than 2 also indicated no secondary organic aerosols were present (Chow et al., 1996; Turpin et al., 1990a and 1990b). The overall mean OC and EC mass concentration accounted for about 65 - 69% of the $PM_{2.5}$ mass concentration for the all the blocks. Yu (2002) reported OC and EC mass accounted for about 58 - 68% of $PM_{2.5}$ mass concentration in a sampling site close to a roadside in Hong Kong.

4.3.8.2 Water Soluble Inorganic Ions

The water soluble components of $PM_{2.5}$ contain many important compounds, which can change the size, composition and lifetime of aerosol owing to their hygroscopic nature. On the other hand, it can also increase the solubility of toxic organic compounds, such as polycyclic aromatic hydrocarbons (PAHs) by acting as surface active reagents and therefore increase their toxicity to human health (Wang et al.,2003). Hence, by understanding their chemical compositions, it is possible to evaluate their potential impact on the human health. Nitrate is one of the major constituents of urban atmospheric aerosols. The study by Fairley (1999) found strongest associations occur with particulates, especially ammonium nitrate and $PM_{2.5}$ mass concentration on daily mortality. Particulate nitrate is formed from the photo-oxidation of NO_2 derived from the combustion of fossil fuel (Logan, 1983). Some fraction of SO_2 is oxidized to sulphate aerosols before dry and wet deposition (Cheng et al., 2000). The non-sea-salt (nss) sulphate was calculated using the below formula (Millero and Sohn, 1992):

:

$$Nss\text{-}\ SO_4^{2-} = [SO_4^{2-}] - [\ Na^+\ ] \times 0.2516$$

In a study, it was found sulphate does not act as a direct toxicant but facilitates the toxicity of reactive metal constituents e.g. it may play a role in the generation of reactive oxygen species (ROS) by functioning as a ligand for particle associated iron (Ghio et al., 1999). Particulate ammonium mainly originates from ammonia vapour. Ammonium sulphate is the most stable compared to ammonium chloride which is volatile. Ammonia nitrate is also formed from the gas-phase reaction between ammonia and nitric acid (Stelson and Seinfield, 1982).

Among the 12 cations tested, sodium (Na^+), ammonium (NH_4^+), calcium (Ca^{2+}), potassium (K^+), chloride (Cl^-), nitrate (NO_3^-), sulphate (SO_4^{2-}) and phosphate (PO_4^{3-}) were detected for all the case studies. The daily mean concentrations of cations and anions for all the case studies are presented in Tables 4.13 - 4.18.

Table 4.13 Daily Mass Concentrations of Cation at Block 96 (Case Study 1)

Cation	Low floor µg/m^3	Mid floor µg/m^3	High floor µg/m^3
Sodium	0.44 ± 0.22	0.96 ± 0.32	0.53 ± 0.25
Ammonium	3.96 ± 1.43	2.85± 0.71	2.11 ± 1.21
Calcium	1.05 ± 0.29	1.35 ± 0.54	1.49 ± 0.67
Potassium	1.45 ± 0.27	2.30 ± 0.39	1.00 ± 0.42
Total mean mass	5.90	7.46	5.13

Table 4.14 Daily Mass Concentration of Anion at Block 96 (Case Study 1)

Anion	Lower floor $\mu g/m^3$	Mid floor $\mu g/m^3$	High floor $\mu g/m^3$
Chloride	0.25 ± 0.07	0.85 ± 0.16	0.27 ± 0.19
Nitrate	1.80 ± 0.25	1.34 ± 0.27	1.82 ± 0.37
Sulphate	4.65 ± 1.37	4.93 ± 2.26	3.54 ± 1.71
Phosphate	0.12 ± 0.02	0.17 ± 0.10	0.07 ± 0.02
Total mean mass	6.82	7.29	5.70

Table 4.15 Daily Mass Concentration of Cation at Block 95 (Case Study 2)

Cation	Low floor $\mu g/m^3$	Mid floor $\mu g/m^3$	High floor $\mu g/m^3$
Sodium	0.53 ± 0.28	1.16 ± 0.34	0.38 ± 0.26
Ammonium	2.95 ± 1.02	2.45 ± 0.89	2.04 ± 0.96
Calcium	1.36 ± 0.37	1.88 ± 0.43	1.70 ± 0.51
Potassium	1.26 ± 0.63	2.38 ± 0.57	1.93 ± 0.49
Total mean	7.10	7.87	6.05

Table 4.16 Daily Mass Concentration of Anion at Block 95 (Case Study 2)

Anion	Low floor $\mu g/m^3$	Mid floor $\mu g/m^3$	High floor $\mu g/m^3$
Chloride	0.43 ± 0.12	1.03 ± 0.39	0.32 ± 0.23
Nitrate	2.62 ± 0.86	3.15 ± 1.76	1.61 ± 1.49
Sulphate	5.60 ± 1.28	4.79 ± 1.51	3.85 ± 0.67
Phosphate	0.21 ± 0.09	0.29 ± 0.11	0.31 ± 0.05
Total mean	8.86	9.26	6.09

Table 4.17 Daily Mass Concentration of Cation at Block 75 (Case Study 3)

Cation	Low floor $\mu g/m^3$	Mid floor $\mu g/m^3$	High floor $\mu g/m^3$
Sodium	0.68 ± 0.13	1.21 ± 0.57	0.51 ± 0.36
Ammonium	3.61 ± 0.79	3.24 ± 0.64	2.80 ± 0.88
Calcium	1.65 ± 0.45	2.01 ± 0.55	1.43 ± 0.23
Potassium	1.42 ± 0.81	2.38 ± 0.70	1.67 ± 0.37
Total mean	7.36	8.84	6.41

Table 4.18 Daily Mass Concentration of Anion at Block 75 (Case Study 3)

Anion	Low floor $\mu g/m^3$	Mid floor $\mu g/m^3$	High floor $\mu g/m^3$
Chloride	0.51 ± 0.26	1.06 ± 0.44	0.43 ± 0.15
Nitrate	2.93 ± 2.15	2.47 ± 1.26	2.34 ± 1.83
Sulphate	5.27 ± 2.09	5.32 ± 2.33	4.89 ± 1.97
Phosphate	0.24 ± 0.18	0.29 ± 0.07	0.26 ± 0.12
Total mean	8.95	9.14	7.92

SO_4^{2-} accounted for most of the ionic mass followed by NH_4^+ and NO_3^- ions at all the floors of the buildings. Generally, the highest total mass concentration of cations and anions were observed at the mid floor of the buildings and the total mass concentrations of anions were slightly higher than that of cations at all the floors of all the building. A study showed the relatively high concentrations of anions are associated with urban particulate matter (Talebi and Abedi, 2005). Cation species accounted for about 13 - 17% of the $PM_{2.5}$ mass concentration at the low floor, 12 - 14% of the $PM_{2.5}$ mass concentration at the mid floor and 14 - 20% of the $PM_{2.5}$ mass concentration at the high floor whilst anion species accounted for about 13 - 21% of the $PM_{2.5}$ mass concentration at the low floor, 12 - 17% of the $PM_{2.5}$ mass concentration at the mid floor and 15 - 20% of the $PM_{2.5}$ mass concentration at the high floor of the buildings.

The nss-sulphates over the total sulphate in the $PM_{2.5}$ mass concentration were about 93 - 95% at the three different floors of the buildings indicating a substantial anthropogenic origin. For Case Study 1, SO_4^{2-}, Na^+, K^+, PO_4^{3-} and Cl^- ions had the highest mass concentration at the mid floor while for NO_3^- and Ca^{2+} ions, the highest of these concentrations were observed at the high floor.

Highest concentration of NH_4^+ ion was present at the low floor. In case Study 2, SO_4^{2-} and NH_4^+ ions had the highest mass concentration at the low floor while for NO_3^-, K^+, Na^+, Cl^- and Ca^{2+} ions, the highest of these concentrations were observed at the mid floor of the building. Highest concentration of PO_4^{3-} ion was observed at the high floor of the building. In Case Study 3, SO_4^{2-}, $NO^{3-}$and NH_4^+ ions, had the highest mass at the low floor while for K^+, Na^+, Cl^-, PO_4^{3-} and Ca^{2+} ions, the highest of these concentrations were observed at the mid floor of the building. Studies have also shown that NH_4^+ ions correlates well with sulphate (i.e. SO_4^{2-}) suggesting that ammonium sulphate may be the major ammonium salt (Wang et al., 2003; Lewin et al., 1986).

The mass concentrations of Na^+ were slightly more than that of Cl^- mass concentrations at all the floors of the buildings. A marginal excess of Na^+ over Cl^- could arise as a result of its reaction with acidic species present in the atmosphere or its additional source from the local dust particles with disproportionate Cl^-/Na^+ (Rastogi and Sarin, 2005). Correlation between of Na^+ and Cl^- showed both ions correlated well ($r = 0.991 - 0.995$) suggesting their origin may be due to sea spray.

4.3.8.3 Water Soluble (WS) Trace Metals

Trace elements are mostly associated with ultra-fine particulate matter which are non-volatile and are not prone to chemical transformation, hence they usually remain in their emitted forms (Morawska and Zhang, 2001). Many trace metals are present in leaded and unleaded petrol, diesel oil, anti-wear substances added to lubricants, brake pads and tyres, and are emitted by vehicle exhaust pipes (Caselles et al., 2002). Trace metals associated with fine

aerosol particles may contribute to particulate toxicity (Gao et al., 2002). Soluble metals have been implicated in particulate matter-associated respiratory or cardiopulmonary disease in healthy and compromised individuals (Frampton et al., 1999; Chapman et al., 1997). According to toxicological studies, metals present in particulate matter contribute significantly to two biological mechanisms i.e. the production of ROS and the interaction with macrophages (cytokine production), that cause damage in the alveoli (Goldsmith et al., 1998). Since man has about 70% of body mass as water and given the solubility of WS trace metals in water, WS metals possess an appreciative damage to our health.

High correlations were found among the crustal elements Al, Ca, Fe, Mg and Ti in a study in Hong Kong (Ho et al., 2003). Crustal matter originates from soil and road dust. In a study in Sicily, it was found traffic appeared to be responsible for the high levels of Ba, Cu, Cr, Mo, Pb, Sb and Zn (Manno et al., 2006). In a study done in Singapore by Balasubramanian and Qian (2003), it was reported that Al, Fe and Ti is attributed to construction activities and road dust. Ag, Cd, Cr and Mn appeared to be related to metallurgical industry and motor vehicles while Cu, Pb and Zn are from combustion sources such as biomass burning and vehicular emissions. Zn has been known to be emitted by from motor vehicles. V, Ni and Co are fuel-oil combustion-related pollutants and the sources are related to diesel-driven vehicles and industrial sources involving fossil fuel combustion. The daily mass concentrations of WS trace metals found in the $PM_{2.5}$ samples for all the case studies is presented in Tables 4.19 - 4.21. The WS trace metals accounted for about 1.9 - 3.6% of the $PM_{2.5}$ mass concentration at the low floor, 1.4 - 4.3% of the $PM_{2.5}$ mass

concentration at the mid floor and 2.3 - 2.9% of the $PM_{2.5}$ mass concentration at the high floor for all the buildings.

Table 4.19 Daily Mass Concentrations of WS Trace Metals at Block 96 (Case Study 1)

Metals	Low floor	Mid floor	High floor
Al	57.4 ± 6.2	41.8 ± 4.8	45.0 ± 5.5
Cr	232.9±18.8	234.2±20.3	110.7± 16.4
Cu	274.6±25.9	201.2±17.7	199.9± 23.5
Fe	112.5±16.4	95.3± 18.2	64.4± 8.8
Mn	2.7± 0.8	5.1± 1.4	ND
Pb	64.7± 11.5	51.2± 6.8	195.3± 22.3
Ni	3.8± 1.2	3.4± 0.9	1.0± 0.7
As	3.2± 2.3	2.6± 0.5	1.3± 0.5
Ag	ND	37.2± 6.9	ND
Ba	86.9± 9.8	119.6±12.4	157.6± 14.6
Bi	3.4± 0.8	10.5± 4.3	2.3± 0.6
Ga	5.3± 2.3	9.6± 3.1	9.2± 2.5
Mg	32.2± 7.5	50.0± 4.8	55.4± 7.5
Sr	1.5± 0.4	3.9± 1.0	2.7± 0.7
Total	881.0	865.6	844.8
Total in $\mu g/m^3$	0.88	0.87	0.85

All values in ng/m^3. ND denotes 'Not Detected'

For Case Study 1, the total mass concentration of WS trace metals measured at the representative floors were almost similar. Based on the simple comparison of the magnitude, the data sets have been grouped into 3 categories: (1) < 1 - 10ng/m^3 : Mn, Ni, As, Bi, Ga and Sr; (2) < 10 - 100ng/m^3 : Ag, Mg and Al; and (3) > 100ng/m^3 : Cr, Cu, Fe, Pb and Ba. Cu and Cr were the highest mass concentration observed at all the floors among all the trace metals. The relatively high concentrations of Al, Fe and Mg at all the floors could be due to roadside dust while the high concentrations of Cr, Cu and Ba could be due to traffic emissions. The International Agency for Research on Cancer (IARC, 1999) has classified Cr together with Ni, Cd and arsenic as known human

carcinogens and two others, Pb and cobolt, as probable human carcinogens. A high proportion of WS trace metal is suggestive of anthropogenic activities since anthropogenic metals usually arise from metal dominated abrasion or heat vapour which condenses onto the surface of other particles (Heal et al., 2005).

Table 4.20 Daily Mass Concentrations of WS Trace Metals at Block 95 (Case Study 2)

Metals	Low floor	Mid floor	High floor
Al	662.4 ±10.3	936.6 ±15.2	711.2 ±16.8
Co	3.7 ± 0.8	2.0 ± 0.2	4.7 ± 0.6
Cr	13.5 ± 3.4	14.6 ± 4.0	12.4 ± 2.5
Cu	201.6 ±25.5	161.0 ± 28.7	101.9 ±15.4
Fe	230.8 ±11.1	202.5 ±17.3	255.0 ± 21.0
Mn	43.7 ± 5.4	31.3 ± 5.4	13.59 ± 3.9
Pb	144.2 ±13.2	87.8 ± 8.5	28.4 ± 4.5
Cd	4.4 ± 1.1	6.8 ± 1.0	3.8 ± 1.3
Ni	5.1 ± 1.2	4.9± 0.6	3.8 ± 0.4
As	6.1 ± 2.5	5.2 ± 1.9	3.8 ± 1.2
Ag	4.8 ± 1.8	3.6 ± 0.9	4.1 ± 0.7
Ti	143.5 ±13.5	162.5 ±16.5	177.8 ±18.4
Zn	9.9 ± 3.6	5.5 ± 1.4	4.8 ± 1.7
V	3.0 ± 0.5	2.7 ± 0.5	1.9 ± 0.7
Total	1476.7	1620.1	1327.1
Total in $\mu g/m^3$	1.48	1.62	1.33

All values in ng/m^3.

For Case Study 2, the highest total mass concentration of WS trace metals occurred at the mid floor of the building. Based on the simple comparison of the magnitude, the data sets as grouped into the 3 categories are: (1) < 1 - 10ng/m^3 : Co, Cd, Mn, Ni, As, Ag, Zn and V; (2) < 10 - 100ng/m^3 : Cr and Mn; and (3) > 100ng/m^3 : Al, Cu, Fe, Pb, Ti. Al followed Fe dominated all the floors of the building. Cu and Ti were generally present in bulk amount at all the floors of the building.

Similar to Case Study 2, the highest total mass concentration of WS trace metals occurred at the mid floor of the building in Case Study 3. Based on the simple comparison of the magnitude, the data sets as grouped into the 3 categories are: (1) < 1 - 10ng/m^3 : Co, Cd, Ni, As, Ag and V; (2) < 10 - 100ng/m^3 : Cr, Zn and Mn; and (3) > 100ng/m^3 : Al, Cu, Fe, Pb, Ti . Al, Cu and Fe dominated all floors of the building. Ti is generally present in bulk amount at all the floors of the building.

Table 4.21 Daily Mass Concentrations of WS Trace Metals at Block 75 (Case Study 3)

Metals	Low floor	Mid floor	High floor
Al	702.9 ±15.1	995.4 ±20.6	689.3 ±13.1
Co	4.4 ± 0.5	3.7 ± 0.7	5.7 ± 0.2
Cr	20.6 ± 5.3	26.3 ± 3.9	18.2 ± 3.3
Cu	257.6 ±30.4	221.8 ±25.2	164.7 ±22.3
Fe	265.2 ±19.3	272.0 ±20.0	193.2 ±16.6
Mn	54.7 ± 6.7	44.9 ± 4.2	27.7 ± 6.0
Pb	128.4 ±15.5	98.4 ± 12.2	57.0 ± 10.5
Cd	5.2 ± 2.2	8.9 ± 0.8	5.0 ± 2.5
Ni	6.5 ± 0.6	6.5 ± 0.8	5.9 ± 1.2
As	6.3 ± 1.4	7.9 ± 2.0	4.9 ± 1.4
Ag	6.0 ± 1.3	5.3 ± 0.8	4.5 ± 1.1
Ti	179.4 ±16.8	186.2 ±19.0	194.7 ±14.6
Zn	13.4 ± 2.8	9.5 ± 1.9	6.8 ± 1.5
V	3.83 ± 0.6	3.65 ± 0.7	2.52 ± 0.5
Total	1654.4	1890.4	1380.1
Total in µg/m^3	1.65	1.89	1.38

All values in ng/m^3

4.3.8.4 Vertical Distribution Profile of PAHs

4.3.8.4.1 Block 95 (Case Study 2)

The mass concentrations of particulate PAH species at the representative floors of the block is presented in Table 4.22. The mean mass concentration of the total particulate PAHs ranged from 2.70 - 4.54ng/m^3 at the different floors of the block. The highest mean total PAH mass concentration occurred at the mid floor followed by the high floor of the block. The low floor had the least mean total PAH mass concentration. The overall total mass concentrations of particulate PAHs for the block is 3.32 ± 1.76ng/m^3 (0.56 - 7.2ng/m^3). The dominant particulate PAHs measured at the block are naphthalene (Nap), acenaphthylene (Acy), benzo(b)fluoranthene (BbF) and benzo(g,h,i)perylene (BPe). Many studies have reported the mutagenic and/or carcinogenic effects of PAHs. IARC (2002) identified benz(a) anthracene (BaA), benzo (a) pyrene (BaP), dibenz(a,h)anthracene (DBA), benzo (k) fluoranthene (BkF), indeno(1,2,3-cd)pyrene (Ind), including benzo(b)fluoranthene (BbF) and naphthalene (Nap) to be carcinogenic compounds.

PAH species with four or more ring structures (i.e. BPe, DBA, Ind, BaP, BkF, BbF, Chr, BaA and Pyr), are less volatile than those PAHs with two or three rings (Nap, Ace, Acy, Flu, Phe, Ant and Flt) which mainly exist in gaseous state (Beak et al., 1991). The vertical distribution profile of more volatile PAHs to total PAHs (sum of Nap-Flt as a % of total PAH) remained almost the same from the low to mid floors and increased from mid to the high floors as shown in Table 4.22. PAH concentration ratios can be used to identify possible emission sources (Kakimoto et al., 2002; Venkataraman et al., 1994).

Li and Kamens (1993) used the BPe/Ind ratio to distinguish emission of PAHs from different engine types. The study reported a ratio over the range of 3.5 - 3.8 for petrol engines and a ratio of 1.1 - 1.2 for diesel engines. Based on the results shown in Table 4.23, the ratio values suggested a mixture of both diesel and petrol engine type of vehicles contributed to the particulate PAH concentrations, with diesel engine vehicles contributing a higher percentage of particulate PAHs to the different floors of the building.

Table 4.22 Vertical Distribution Profile of Particulate PAHs at Block 95 (Case Study 2)

PAH	Mass Concentration (ng/m^3)		
	Low floor	Mid floor	High floor
Naphthalene(Nap)	0.08 ± 0.03 (0.08- 0.23)	0.35 ± 0.15 (0.21- 1.04)	1.15 ± 0.37 (0.24- 3.47)
Acenaphthene (Ace)	0.08 ± 0.02 (0.08- 0.29)	0.55 ± 0.25 (0.03- 1.69)	0.05 ± 0.02 (0.01- 0.08)
Acenaphthylen (Acy)	0.66 ± 0.33 (0.22- 1.17)	0.81 ± 0.37 (0.11- 1.34)	0.81 ± 0.41 (0.61- 1.44)
Fluorene (Flu)	0.32 ± 0.10 (0.16- 0.47)	0.37 ± 0.16 (0.03- 0.57)	0.33 ± 0.18 (0.21- 0.53)
Phenanthren (Phe)	0.22 ± 0.12 (0.07- 0.41)	0.30 ± 0.18 (0.14- 0.55)	0.22 ± 0.18 (0.03- 0.49)
Anthracene (Ant)	0.06 ± 0.02 (0.01- 0.07)	0.21 ± 0.09 (0.01- 0.61)	0.06 ± 0.02 (0.01- 0.10)
Fluoranthene (Flt)	0.09 ± 0.04 (0.02- 0.11)	0.15 ± 0.05 (0.09- 0.43)	0.16 ± 0.06 (0.01- 0.46)
Pyrene (Pyr)	0.13 ± 0.06 (0.09- 0.24)	0.19 ± 0.08 (0.05- 0.31)	0.12 ± 0.04 (0.04- 0.24)
Benzo[*a*]anthracen(BaA)	0.06 ± 0.03 (0.02- 0.10)	0.11 ± 0.03 (0.03- 0.58)	0.07 ± 0.03 (0.01- 0.15)
Chrysene (Chr)	0.09 ± 0.04 (0.01- 0.25)	0.08 ± 0.03 (0.02- 0.33)	0.09 ± 0.03 (0.01- 0.13)
Benzo[*b*]fluoranthene (BbF)	0.30 ± 0.13 (0.04- 0.93)	0.51 ± 0.15 (0.02- 1.74)	0.10 ± 0.03 (0.05- 0.25)
Benzo[*k*]fluoranthene (BkF)	0.07 ± 0.03 (0.03- 0.11)	0.13 ± 0.05 (0.06- 0.27)	0.06 ± 0.02 (0.03- 0.11)
Benzo[*a*]pyrene (BaP)	0.14 ± 0.08 (0.05- 0.26)	0.11 ± 0.04 (0.07- 0.22)	0.09 ± 0.03 (0.03- 0.14)
Indeno[*1,2,3,cd*]pyrene (Ind)	0.13 ± 0.06 (0.11- 0.50)	0.08 ± 0.04 (0.04- 0.13)	0.07 ± 0.02 (0.06- 0.22)
Dibenzo[*a,h*]anthracene (DBA)	0.10 ± 0.04 (0.01- 0.16)	0.23 ± 0.13 (0.05- 0.41)	0.18 ± 0.05 (0.03- 0.47)
Benzo[*g,h,i*]perylene (BPe)	0.17 ± 0.10 (0.06- 0.36)	0.36 ± 0.26 (0.06- 0.89)	0.11 ± 0.04 (0.01- 0.30)
ΣPAH	2.70 ± 1.23	4.54 ± 2.06	3.67 ± 1.53

Note: values in bracket are minimum and maximum values.

Table 4.23 Proportion of Nap - Flt species sum as a % of total PAH, ratio of BPe/Ind and BaP_{eq} values at Block 95 (Case Study 2)

Floor	Nap-Flt (% of total PAH)	BPe/Ind	BaP_{eq} ng/m^3
Low floor	54	1.36 ± 0.2	0.69 ± 0.33 (0.14-1.21)
Mid floor	56	1.63 ± 0.6	1.34 ± 0.63 (0.59-2.17)
High floor	78	1.57 ± 0.4	1.15 ± 0.78 (0.17-2.45)
Overall total			1.06 ± 0.64 (0.14-2.45)

4.3.8.4.2 Block 75 (Case Study 3)

The mean mass concentrations of particulate PAH species at each representative floor of the block is presented in Table 4.24. The mean mass concentration levels of total particulate PAHs ranged from 4.67 - 6.79ng/m^3 at the different floors of the block. The highest mean total PAH mass concentration occurred at the low floor which did not vary significantly up to the mid floor and thereafter gradually decreased all the way to the high floor of the building. The overall total mass concentration of particulate PAHs for the block was 6.0 ± 1.88ng/m^3 (3.19 - 10.26ng/m^3). The dominant particulate PAHs measured at the block were naphthalene (Nap), phenanthrene (Phe) fluoranthene (Flt) and benzo(g,h,i)perylene (BPe). The vertical distribution profile of more volatile PAHs to total PAHs (sum of Nap-Flt as a % of total PAH) remained almost the same from the low floor to mid floor and increased from the mid floor to the high floor as shown in Table 4.25. Based on the BPe/Ind ratio values shown in Table 4.24, the results also suggested a mixture of both diesel and petrol engine type of vehicles contributing to the particulate PAH concentrations, with diesel engine vehicles contributing a higher

percentage of particulate PAHs concentrations to the different floor levels of the building.

Table 4.24 Vertical Distribution Profile of Particulate PAHs at Block 75 (Case Study 3)

PAH	Mass Concentration (ng/m^3)		
	Low floor	Mid floor	High floor
Naphthalene(Nap)	1.54 ± 0.81 (0.69- 2.60)	1.16 ± 0.68 (0.56- 2.16)	0.93 ± 0.46 (0.50- 1.76)
Acenaphthene (Ace)	0.21 ± 0.18 (0.03- 0.54)	0.06 ± 0.03 (0.01- 0.11)	0.05 ± 0.02 (0.01- 0.11)
Acenaphthylen (Acy)	0.35 ± 0.25 (0.02- 0.58)	0.52 ± 0.17 (0.01- 2.17)	0.19 ± 0.04 (0.06- 0.42)
Fluorene (Flu)	0.38 ± 0.19 (0.18- 0.64)	0.56 ± 0.10 (0.16- 1.96)	0.23 ± 0.07 (0.08- 0.31)
Phenanthren (Phe)	0.76 ± 0.34 (0.38- 1.23)	0.68 ± 0.23 (0.42- 0.98)	0.52 ± 0.14 (0.35- 0.73)
Anthracene (Ant)	0.03 ± 0.01 (0.01- 0.08)	0.09 ± 0.02 (0.01- 0.13)	0.06 ± 0.02 (0.01- 0.11)
Fluoranthene (Flt)	0.98 ± 0.17 (0.76- 1.28)	0.95 ± 0.12 (0.71- 1.10)	0.98 ± 0.16 (0.73- 1.15)
Pyrene (Pyr)	0.23 ± 0.10 (0.01- 0.33)	0.21 ± 0.11 (0.02- 0.38)	0.14 ± 0.05 (0.01- 0.38)
Benzo[*a*]anthracen(BaA)	0.31 ± 0.25 (0.02- 0.70)	0.47 ± 0.12 (0.14- 0.81)	0.27 ± 0.10 (0.01- 0.64)
Chrysene (Chr)	0.40 ± 0.19 (0.13- 0.69)	0.28 ± 0.09 (0.01- 0.65)	0.31 ± 0.09 (0.01- 0.72)
Benzo[*b*]fluoranthene (BbF)	0.23 ± 0.09 (0.02- 0.50)	0.13 ± 0.05 (0.02- 0.30)	0.18 ± 0.06 (0.02- 0.48)
Benzo[*k*]fluoranthene (BkF)	0.17 ± 0.05 (0.01- 0.52)	0.43 ± 0.15 (0.03- 1.74)	0.08 ± 0.03 (0.04- 0.32)
Benzo[*a*]pyrene (BaP)	0.20 ± 0.07 (0.02- 0.46)	0.22 ± 0.07 (0.02- 0.38)	0.11 ± 0.05 (0.01- 0.57)
Indeno[*1,2,3,cd*]pyrene (Ind)	0.35 ± 0.10 (0.01 0.97)	0.39 ± 0.16 (0.03- 1.38)	0.30 ± 0.11 (0.02- 0.62)
Dibenzo[*a,h*]anthracene (DBA)	0.20 ± 0.06 (0.01- 0.84)	0.11 ± 0.04 (0.01- 0.31)	0.10 ± 0.04 (0.01- 0.25)
Benzo[*g,h,i*]perylene (BPe)	0.45 ± 0.13 (0.03- 1.13)	0.45 ± 0.22 (0.02- 1.22)	0.22 ± 0.08 (0.01- 0.61)
ΣPAH	6.79 ± 2.99	6.71 ± 2.36	4.67 ± 1.52

Note: values in bracket are minimum and maximum values

Table 4.25 Proportion of Nap - Flt species sum as a % of total PAH , ratio of BPe/Ind and BaP_{eq} values at Block 75 (Case Study 3)

Floor	Nap-Flt (% of total PAH)	BPe/Ind	BaP_{eq} ng/m^3
Low floor	62	1.36 ± 0.3	1.36 ± 1.86 (0.17-3.49)
Mid floor	60	0.92 ± 0.2	0.72 ± 0.54 (0.33-1.83)
High floor	65	1.41 ± 0.4	0.64 ± 0.67 (0.10-1.57)
Overall total			0.94 ± 1.22 (0.10-4.59)

4.3.8.4.3 Potential Health Risk Assessment Inhaling Particulate PAHs (Case Studies 2 and 3)

The overall total BaP_{eq} value for the Block 95 (Case Study 2) is $1.06 \pm 0.64 ng/m^3$ ($0.14 - 2.45\ ng/m^3$) as shown in Table 4.22. The total BaP_{eq} value at the mid and high floors exceeded the maximum permissible risk level of $1 ng/m^3$ of benzo(a)pyrene with the mid floor residents having the highest potential cancer risk compared to those residents living at the low and high floors of the building. Residents at the high floor had the second highest potential cancer risk followed by the residents at the low floor. The total BaP_{eq} value of the low floor was about 69% of maximum permissible risk level.

The overall total BaP_{eq} concentrations for the Block 75 (Case Study 3) was $0.94 \pm 1.22 ng/m^3$ ($0.10 - 4.59 ng/m^3$) as shown in Table 4.24. The total BaP_{eq} value at the low floor exceeded the maximum permissible risk level of $1 ng/m^3$ of benzo(a)pyrene showing residents at the low floor having the highest potential cancer risk compared to those residents living at the mid and high floors of the building. Residents at the mid floor had the second highest potential cancer risk followed by the residents at the high floor. The total

BaP_{eq} values at the mid and high floors were about 72% and 64% of maximum permissible risk level respectively.

For all the floors below the maximum permissible risk level, the maximum permissible risk level is most likely to be exceeded since the motor vehicle count and the number of trips per vehicle in Singapore keeps on increasing over the years. The World Health Organization (WHO, 1987; Doll and Peto, 1981) suggested that exposure to BaP at a concentration of 1ng of BaP per m^3 of air, throughout life, carried a risk of lung cancer of 1 in 10,000 or 0.0001%. Although particulate PAH accounted for less than 1% of $PM_{2.5}$ mass concentration, its negative impact on health cannot be discounted. Based on the total BaP_{eq} values at all the floors of both the blocks, particulate PAHs inhalation is of concern to the residents of the blocks due to the high potential cancer risk. The health risk assessment of the residents of the blocks inhaling particulate PAHs has been published elsewhere (Kalaiarasan, 2009).

4.3.8.5 Reconstruction of Chemical Composition of $PM_{2.5}$ Mass Concentration

4.3.8.5.1 Point Block

The reconstructed chemical composition using the procedure adopted in USA IMPROVE study (Eldred et al., 1988) at the various floors of the building is shown in Figure 4.22. In this study, the $PM_{2.5}$ mass concentration can be classified into seven major types: crustal matter, sea salt, ammonium, sulphate, nitrate, elemental carbon and organic matter. Aluminum (Al) is usually selected as a tracer material of the soil. The crustal matter concentration was

estimated to be [Al] / 7.26% (Cheng et al., 2000). Soluble Na in the aerosol samples is assumed to come solely from sea salt. The mass of sea salt is estimated by sea salt = 2.54 soluble Na. The conversion factor for organic substances is 1.4 for this study (Ho et al., 2000).

The combined mean results of Blocks 95 and 96 at the respective floors were used for the procedure. The seven major components of the reconstructed $PM_{2.5}$ mass concentration accounted for about 90% of the $PM_{2.5}$ mass concentration for the low floor, 91% of the $PM_{2.5}$ mass concentration for the mid floor and 90% of the $PM_{2.5}$ mass concentration for the high floor of the block. Based on the reconstructed $PM_{2.5}$ mass concentration, organic matter (26 -42%), elemental carbon (25 - 36%), ammonium (4 - 8%) and sulphate (7 - 10%) were the major chemical components at the floors of the building. Carbonaceous species alone accounted for about 69% of $PM_{2.5}$ mass concentration for the low floor, 67% of $PM_{2.5}$ mass concentration for the mid floor and 58% of $PM_{2.5}$ mass concentration for the high floor of the building.

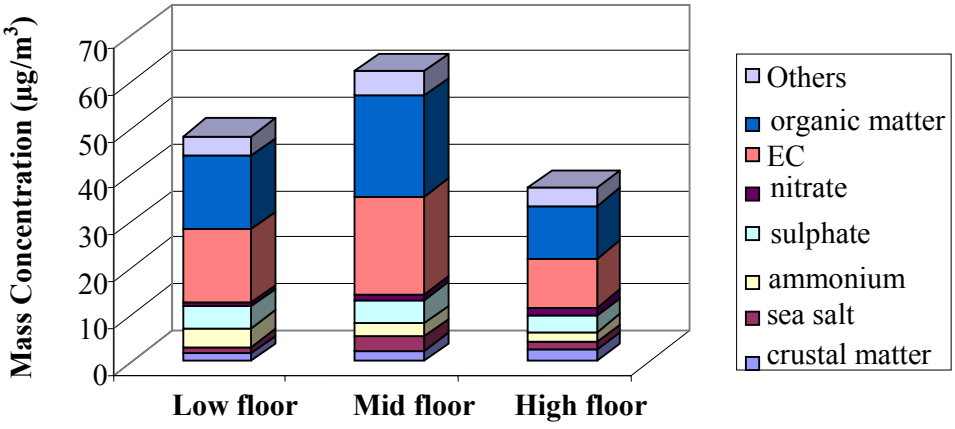

Figure 4.22 Mass Balance of $PM_{2.5}$ at Point Block

4.3.8.5.2 Slab Block

The reconstructed chemical composition using the procedure adopted in USA IMPROVE study (Eldred et al., 1988) at the various floors of the building is shown in Figure 4.23. The seven major components of the reconstructed $PM_{2.5}$ mass concentration accounted for about 89% of the $PM_{2.5}$ mass concentration for the low floor, 89% of the $PM_{2.5}$ mass concentration for the mid floor and 90% of the $PM_{2.5}$ mass concentration for the high floor of the block. Based on the reconstructed $PM_{2.5}$ mass concentration, organic matter (32 - 36%), elemental carbon (32 - 37%) and sulphate (7 - 12%) were the major chemical components at the floors of the building. Carbonaceous species alone accounted for about 68% of $PM_{2.5}$ mass concentration for the low floor, 70% of $PM_{2.5}$ mass concentration for the mid floor and 69% of $PM_{2.5}$ mass concentration for the high floor of the building.

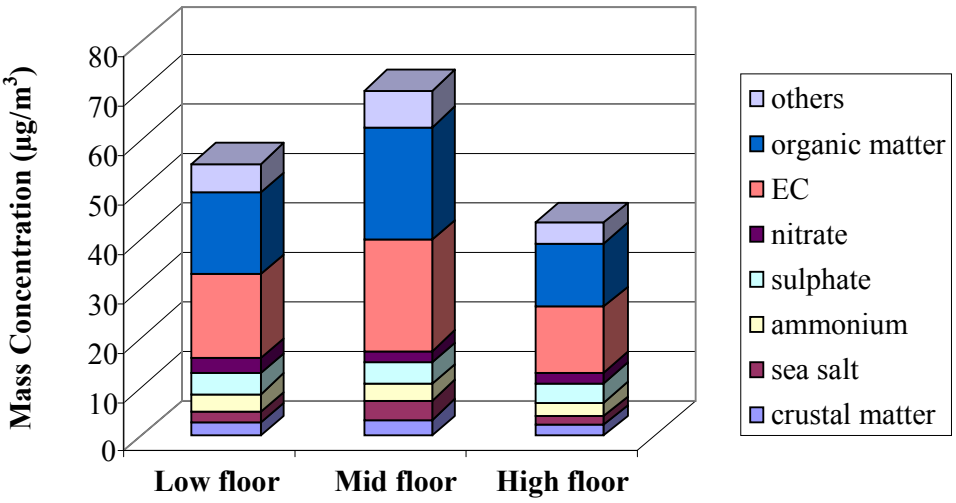

Figure 4.23 Mass Balance of $PM_{2.5}$ at Slab Block

The results of the physical and chemical characteristics of the traffic-generated $PM_{2.5}$ mass concentration of Case Studies 2 (Block 95) and 3 (Block 75) have been are published in the Springer book "Urban Airborne Particulate matter: Origins, Chemistry, Fate and Heath" in 2010 (Kalaiarasan et al., 2009).

4.4 Conclusion

4.4.1 Vertical Distribution Profile of Traffic-Generated $PM_{2.5}$ Mean Mass/Number Concentration

For all the case studies, experimental results showed that the daily mean $PM_{2.5}$ mass/number concentration was highest at the mid floor of the building when compared to those measured at the high and low floors of the building for a typical day regardless of the building configuration. There is a significant difference between the mean $PM_{2.5}$ mass/number concentration values measured at the low and mid floors ($p < 0.02$ to 0.04) and the mid and high floors ($p < 0.01$ to 0.05) for all the case studies. Although the lower floors were closest to traffic emissions, the mean $PM_{2.5}$ mass/number concentration was lower there than that at the mid floors, which could presumably be due to the buoyancy rise at the source point, interception of $PM_{2.5}$ by tree leaves or the vortices at the wake region of the trees diluting the traffic-polluted air behind the trees or all three. The high floors had the least $PM_{2.5}$ mass/number concentration due to dilution following pronounced mixing of traffic-polluted air with ambient air. The only difference between point and slab blocks is that at corresponding floors, the $PM_{2.5}$ mass/number concentration for slab block is much higher than that of point block. The results may suggest that $PM_{2.5}$

mass/number concentration decreasing with increasing height of building is not true with regards to this study. The reason could be that the buildings used in the other studies were mainly air-conditioned (e.g. office buildings) or semi-air conditioned (e.g. educational institutions) and most of the studies were conducted in temperate, subtropical and dry climates. Also, in the studies, there were no trees in between the roads and buildings. In this study, the buildings are naturally-ventilated high-rise residential buildings and the climate is tropical. The trees (dense and complex canopy structure) and vegetation planted along the expressways is a unique feature in Singapore for the naturally-ventilated high-rise residential buildings that are in close proximity to expressways. The trees and vegetation could have had an influence on the vertical distribution profile of the traffic-generated $PM_{2.5}$ mass/number concentration in these buildings. It was also found in all the case studies, traffic volume, wind speed, ambient temperature and RH did not show any significant correlation with the $PM_{2.5}$ mass/number concentration measured at the representative floors of the buildings.

4.4.2 Health Impacts of Traffic-Generated Particulate Matter

4.4.2.1 Physical Characteristics

For all these case studies, the daily mean mass concentration of traffic-generated $PM_{2.5}$ at the various floors of the buildings either exceeded the $PM_{2.5}$ NAAQS annual average value of 15μg/m^3 or the 24hr value of 35μg/m^3. This is of major concern since the health of residents including the health of "sensitive" populations such as asthmatics, children, and the elderly are affected. The study on $PM_{2.5}$ size distribution show about 93 - 95% of the

$PM_{2.5}$ number concentration consisted of particles below the size range of 0.65µm while the rest 5 - 7% of the particles fall in the size range 0.65 - 1.6µm. Of the 93 - 95% particles, about 73 - 75% particles were in the size range of 0.3 - 0.4µm, 14 - 16% in the size range of 0.4 - 0.5µm and 4 - 6% in the size range of 0.5 - 0.65µm at all the representative floors of the point block and slab block. The size distribution show that majority of particles in the traffic-generated $PM_{2.5}$ number concentration has a very high chance of penetrating deeper into the lungs. Toxicological studies have implicated fine and ultra fine particles have considerably enhanced toxicity per unit mass and their toxicity increased as particle size decrease.

4.4.2.2 Chemical Characteristics

Based on the reconstructed chemical composition using the procedure adopted in USA IMPROVE study (Eldred et al., 1988) at the various floors of the point and slab block buildings, carbonaceous species alone accounted for about 58 - 69% of $PM_{2.5}$ mass concentration at the point block and 68 - 70% at the slab block. Studies have shown the relative risk of premature death increases with 1% per 1µg/m^3 of elemental carbon. This is 5 -10 times higher than the relative risk of PM_{10}. Water soluble trace metals such as Cr, Cu, Ba etc. were detected in the traffic-generated particulate matter. IARC, Lyons, France has classified Cr together with Ni, Cd and arsenic as known human carcinogens and two others, Pb and cobolt, as probable human carcinogens. Since WS trace metal compounds are present in the fine fraction, they can not only penetrate deep into the lungs and cause serious pollution-related respiratory health problems but also they can easily be absorbed in the bloodstream and

be transported to the other parts of the human body and may cause other health related problems. The dominant particulate PAHs measured at the buildings are naphthalene (Nap), acenaphthylene (Acy), benzo(b)fluoranthene (BbF), phenanthrene (Phe), fluoranthene (Flt) and benzo(g,h,i)perylene (BPe). Many studies have reported the mutagenic and or carcinogenic effects of PAHs. IARC, Lyons, France has identified benz(a) anthracene (BaA), benzo (a) pyrene (BaP), dibenz(a,h)anthracene (DBA), benzo (k) fluoranthene (BkF), indeno(1,2,3-cd)pyrene (Ind), including benzo(b)fluoranthene (BbF) and naphthalene (Nap) to be carcinogenic compounds. Although particulate PAH accounted for less than 1% of $PM_{2.5}$ mass concentration, inhalation of particulate PAHs is of concern to the residents of the buildings close to expressways due to the high potential cancer risk.

On the whole, traffic generated $PM_{2.5}$ contributes to a large extent to the toxicity of outdoor aerosol and more effort should be taken towards the reduction of traffic-generated $PM_{2.5}$ in a roadside microenvironment since the expected increase in the population growth and in the motor vehicle numbers in Singapore in the near future poses an increasing concern over both ambient and indoor air quality in the urban areas, especially in high-rise naturally-ventilated residential buildings located near expressways as on-road vehicles are main sources of $PM_{2.5}$ in urban areas. The relevant authorities have taken many proactive approaches to curb the number of vehicles on road and reduce traffic congestion but unfortunately, no single solution can solve a decade long problem. As motor vehicle numbers and population increase in the land scarce country, more residential buildings have to be built closer to road and expressways to accommodate the increasing population and even minor roads

can become congested during non peak hours. The result will be similar to this study where the residential building is in close proximity to the busy expressway. Some methods to mitigate this problem is to increase the more row of trees and vegetation between residential buildings and roads as trees and vegetation can help to intercept the traffic-generated $PM_{2.5}$, use clean fuels and build even taller high-rise residential buildings which can be further away from major roads or expressways.

CHAPTER 5: NITROGEN DIOXIDE MEASUREMENT

5.1 Introduction

Case Studies 4 - 6 used NO_2 as a surrogate indicator of traffic-generated pollutants to determine the horizontal as well as the vertical distribution profiles of traffic pollutants at naturally-ventilated residential high-rise buildings located in close proximity to the expressways. After the vertical distribution profile of NO_2 concentration is determined, $PM_{2.5}$ number concentration is then measured at the floor where the maximum concentration of NO_2 is found, which means the most polluted level of the buildings. For Case Studies 4 and 5, field measurements were conducted simultaneously from 3 December 2007 - 4 January 2008 i.e. 5 weeks. Samples of Case Study 6 were collected from 7 January - 8 February 2008 i.e. 5 weeks. The measurement of the background NO_2 concentration was about 300 to 400m from the measurement sites.

5.2 Results and Discussion

5.2.1 Traffic Volume

For Case Studies 4 and 5, the traffic composition analysis along the AYE indicated that about 60% of the vehicles were petrol-driven passenger cars fitted with catalytic converters. The traffic volume ranged from 10470 - 14336 vehicles per hr with a mean around 12853 ± 1048 vehicles per hr in a typical

day. Traffic peaks occurred during the morning rush hour from 0730 - 0930hr and the evening rush hours from 1730 - 1930hr. Each peak lasted approximately two to three hours. Results showed that the traffic pattern on all days in a week had similar trends. For both the cases, the weekly mean traffic volume did not show any significant correlation with the weekly mean indoor and outdoor NO_2 concentration measured at each floor: Case Study 4 has mean Pearson's r = 0.21 ± 0.08 (outdoor) and mean Pearson's r = 0.13 ± 0.03 (indoor) while Case Study 5 has mean Pearson's r = 0.32 ± 0.05 (outdoor) and mean Pearson's r = 0.25 ± 0.06 (indoor).

For Case Study 6, the traffic composition analysis along the PIE indicated that about 63% of the vehicles were petrol-driven passenger cars fitted with catalytic converters were the major contributor to traffic volume. The traffic volume ranged from 9567 - 15848 vehicles per hr with a mean value of around 13356 ± 2215 vehicles per hr in a typical day. Traffic peaks occurred during the morning rush hour from 0700 - 0930hr and the evening rush hours from 1730 - 2000hr. Each peak lasted approximately two and a half hours. Results showed that the traffic pattern on all days in a week had similar trends. Similar to case study 4 and 5, the weekly mean traffic count did not show any significant correlation with the weekly mean indoor and outdoor NO_2 concentration measured at each floor: mean Pearson's r = 0.22 ± 0.04 (outdoor) and mean Pearson's r = 0.29 ± 0.05 (indoor). For all the case studies, the low correlation was supported by a study in Sweden (Modig et al., 2006).

5.2.2 Wind Speed and Direction

The wind direction measurements showed that the north-east monsoon winds were the dominant winds blowing at almost right angles towards the building façade for all the case studies. The wind azimuth and overall mean wind speed for Case Studies 4 - 6 is shown in Table 5.1. These prevailing wind conditions facilitated the transport of the fine traffic-generated NO_2 towards the residential apartments.

Table 5.1 Wind Azimuth and Overall Mean Wind Speed for Case Studies 4 - 6

	Block 39 (Case Study 4)	**Block 401 (Case Study 5)**	**Block 93 (Case Study 6)**
Wind Azimuth	$047.9^o \pm 6.1^o$	$043.6^o \pm 4.8^o$	$046.2^o \pm 5.1^o$
Overall Mean Wind Speed	1.63 ± 0.16 m/s	1.48 ± 0.19 m/s	1.46 ± 0.30 m/s

The daily mean wind speed for a typical week and weekly mean wind speeds for all the buildings are shown in Tables 5.2 - 5.7. Generally, the daily and weekly mean wind speeds increased with the height of the buildings. The weekly mean wind speed did not show any significant correlation with the weekly mean outdoor NO_2 concentration measured at each representative floor: low floor has mean Pearson's r = -0.28 - (-0.19); mid floor has r = -0.26 - (-0.10); and high floor has r = -0.36 - (-0.29). Studies reported no significant or weak correlation between wind speed and NO_2 concentration (Laurinavičienė, 2008 and Hargreaves et al., 2000).

Table 5.2 Daily Wind Speed for a Typical Week at Block 39 (Case Study 4)

Day	Low floor (m/s)	Mid floor (m/s)	High floor (m/s)
1	1.34± 0.24	1.51 ± 0.19	1.76 ± 0.17
2	1.24 ± 0.33	1.47 ± 0.28	1.80 ± 0.28
3	1.31 ± 0.19	1.52 ± 0.32	1.62 ± 0.23
4	1.27± 0.32	1.49 ± 0.25	1.55 ± 0.35
5	1.19 ± 0.29	1.36 ± 0.36	1.68 ± 0.14

Table 5.3 Weekly Mean Wind Speed at Block 39 (Case Study 4)

Week	Low floor (m/s)	Mid floor (m/s)	High floor (m/s)
1	1.26± 0.12	1.48 ± 0.36	1.70 ± 0.16
2	1.14 ± 0.17	1.51 ± 0.23	1.74 ± 0.14
3	1.33 ± 0.21	1.45 ± 0.27	1.53 ± 0.30
4	1.17± 0.25	1.52 ± 0.29	1.63 ± 0.27
5	1.26 ± 0.28	1.39 ± 0.19	1.65 ± 0.31

Table 5.4 Daily Wind Speed for a Typical Week at Block 401 (Case Study 5)

Day	Low floor (m/s)	Mid floor (m/s)	High floor (m/s)
1	0.90± 0.13	1.42 ± 0.19	1.62 ± 0.14
2	1.02 ± 0.12	1.33 ± 0.28	1.54 ± 0.18
3	0.65 ± 0.28	1.28 ± 0.21	1.56 ± 0.19
4	0.98± 0.21	1.30 ± 0.14	1.42 ± 0.26
5	1.17± 0.15	1.44 ± 0.10	1.55 ± 0.22

Table 5.5 Weekly Mean Wind Speed at Block 401 (Case Study 5)

Week	Low floor (m/s)	Mid floor (m/s)	High floor (m/s)
1	0.88 ± 0.21	1.38 ± 0.35	1.61 ± 0.11
2	0.93 ± 0.16	1.35 ± 013	1.49 ± 0.23
3	0.72 ± 0.20	1.26 ± 0.21	1.59 ± 0.18
4	1.11 ± 0.25	1.36 ± 0.19	1.47 ± 0.26
5	1.02 ± 0.12	1.41 ± 0.17	1.63 ± 0.10

Table 5.6 Daily Wind Speed for a Typical Week at Block 93 (Case Study 6)

Day	Low floor	Mid floor (m/s)	High floor (m/s)
1	0.78± 0.19	1.26 ± 0.11	1.66 ± 0.15
2	0.85 ± 0.15	1.47 ± 0.12	1.52 ± 0.09
3	0.69 ± 0.29	1.29 ± 0.36	1.58 ± 0.34
4	1.04 ± 0.27	1.42 ± 0.19	1.60 ± 0.25
5	0.95 ± 0.13	1.38 ± 0.18	1.45 ± 0.16

Table 5.7 Weekly Mean Wind Speed at Block 93 (Case Study 6)

Week	Low floor (m/s)	Mid floor (m/s)	High floor (m/s)
1	0.89 ± 0.26	1.31 ± 0.10	1.59 ± 0.17
2	0.79 ± 0.24	1.29 ± 0.18	1.48 ± 0.16
3	1.00 ± 0.12	1.36 ± 0.15	1.55 ± 0.24
4	0.66 ± 0.17	1.37 ± 0.09	1.66 ± 0.20
5	0.82 ± 0.25	1.42 ± 0.28	1.56 ± 0.11

5.2.3 Temperature and RH

Tables 5.8 - 5.11 show the weekly indoor and outdoor temperatures at the households of Case Studies 4 - 6. Generally, the outdoor temperature decreased with increasing height of the building and indoor temperatures did not show any trend. For all the case studies, there was no significance difference between the overall weekly mean indoor temperatures of both the right and left hand side units and between the overall weekly indoor and outdoor mean temperatures ($p > 0.05$). The vertical temperature and RH distribution profiles for Case Studies 4 - 6 showed very little stratification between the selected floors similar to the Case Studies 1 - 3.

Table 5.8 Weekly Mean Indoor and Outdoor temperatures for Case Studies 4 - 6

	Block 39 (Case Study 4 Units)		**Block 401(Case Study 5 Units)**		**Block 93 (Case Study 6 Units)**	
	#XX-251 (R)*	**# XX-249 (L)****	**#XX-278 (R)***	**# XX-268 (L)****	**#XX-3051 (R)***	**# XX-3037 (L)****
Weekly mean indoor temperature range (^{o}C)	27 - 29		26 - 28		28 - 29	
Overall weekly mean indoor temperature (^{o}C)	28.4 ± 0.4	28.4 ± 0.4	27.1 ± 0.6	27.1 ± 0.5	29.0 ± 0.5	28.8 ± 0.4
Difference in temperature between any two floors (^{o}C)	≤ 0.7		≤ 0.8		≤ 0.8	
Overall mean weekly outdoor temperature (^{o}C)	28.0 ± 0.6		26.6 ± 0.8		28.0 ± 0.5	
Outdoor temperature difference between highest and lowest floor in a week (^{o}C)	0.9 - 1.1 (0.9 ± 0.1) (2nd and 20th floor)		0.7 - 1.0 (0.9 ± 0.1) (2nd and 12th floor)		0.8 - 1.0 (0.9 ± 0.1) (2nd and 10th floor)	

L** - left R*-right

Table 5.9 Weekly Mean Indoor and Outdoor Temperatures (^{o}C) at the Households of Block 39(Case Study 4)

Indoor					
Location	**Left units (#XX-249)**				
Floor	**Week 1**	**Week 2**	**Week 3**	**Week 4**	**Week 5**
20	29.0 ± 0.9	28.3 ± 0.5	28.1 ± 0.6	28.6 ± 0.9	28.0 ± 0.7
17	29.3 ± 0.6	28.6 ± 0.3	28.1 ± 0.4	28.6 ± 0.6	28.0 ± 0.3
14	29.4 ± 0.7	28.6 ± 0.4	28.2 ± 0.4	28.7 ± 0.6	28.1 ± 0.3
11	29.1 ± 0.7	28.7 ± 0.5	28.7 ± 0.6	28.7 ± 0.5	28.0 ± 0.4
8	28.7 ± 0.4	28.7 ± 0.6	28.2 ± 0.4	28.4 ± 0.4	27.9 ± 0.7
5	29.0 ± 0.4	28.4 ± 0.5	28.1 ± 0.4	28.3 ± 0.5	28.0 ± 0.5
2	29.1 ± 0.6	28.1 ± 0.6	27.9 ± 0.4	28.0 ± 0.7	27.9 ± 0.5
Right units (#XX-251)					
20	29.4 ± 0.7	28.8 ± 0.5	28.5 ± 0.7	28.9 ± 0.9	28.2 ± 0.5
17	29.1 ± 0.7	28.6 ± 0.5	28.2 ± 0.6	28.6 ± 0.8	28.1 ± 0.6
14	28.9 ± 0.7	28.3 ± 0.5	28.0 ± 0.6	28.3 ± 0.8	27.9 ± 0.6
11	29.0 ± 0.7	28.5 ± 0.6	28.2 ± 0.6	28.6 ± 0.7	28.0 ± 0.6
8	28.8 ± 0.5	28.8 ± 0.7	28.4 ± 0.6	28.6 ± 0.6	28.0 ± 0.5
5	29.0 ± 0.6	28.3 ± 0.5	28.1 ± 0.4	28.3 ± 0.6	28.0 ± 0.5
2	29.2 ± 0.7	28.2 ± 0.6	27.9 ± 0.3	28.4 ± 0.7	27.8 ± 0.5
Outdoor (Lift lobby)					
20	28.2 ± 0.9	27.3 ± 0.8	27.1 ± 0.8	27.4 ± 0.8	26.9 ± 0.9
17	28.4 ± 0.9	27.5 ± 0.6	27.3 ± 0.6	27.6 ± 0.8	27.1 ± 0.7
14	28.6 ± 0.9	27.8 ± 0.6	27.5 ± 0.6	27.8 ± 0.8	27.3 ± 0.7
11	29.0 ± 1.0	28.1 ± 0.8	27.8 ± 0.7	27.9 ± 0.9	27.5 ± 0.8
8	29.0 ± 0.8	28.1 ± 0.6	27.9 ± 0.6	28.1 ± 0.8	27.6 ± 0.6
5	29.2 ± 0.9	28.3 ± 0.7	27.9 ± 0.6	28.3 ± 0.8	27.7 ± 0.7
2	29.2 ± 0.8	28.4 ± 0.6	27.9 ± 0.4	28.3 ± 0.8	27.8 ± 0.6

Table 5.10 Weekly Mean Indoor and Outdoor Temperatures (^{o}C) at the Households of Block 401 (Case Study 5)

Indoor					
Location	**Left units (#XX-268)**				
Floor	**Week 1**	**Week 2**	**Week 3**	**Week 4**	**Week 5**
12	26.9 ± 0.6	27.0 ± 0.6	26.2 ± 0.5	28.1 ± 0.7	27.1 ± 0.7
10	27.1 ± 0.5	26.8 ± 0.5	26.2 ± 0.4	27.8 ± 0.5	27.0 ± 0.6
6	27.3 ± 0.6	27.3 ± 0.6	27.0 ± 0.4	28.1 ± 0.5	27.5 ± 0.5
2	26.7 ± 0.4	26.9 ± 0.5	26.8 ± 0.4	27.9 ± 0.5	26.8 ± 0.4
Right units (#XX-278)					
12	26.7 ± 0.7	27.1 ± 0.6	26.3 ± 0.7	28.1 ± 0.6	27.0 ± 0.7
10	26.5± 0.6	26.9 ± 0.5	26.2 ± 0.5	27.8 ± 0.6	26.6 ± 0.5
8	26.4 ± 0.5	27.3 ± 0.4	26.6 ± 0.5	28.3 ± 0.5	27.2 ± 0.5
6	27.2 ± 0.5	26.9 ± 0.5	27.0 ± 0.5	28.3 ± 0.5	27.4 ± 0.4
2	26.8 ± 0.5	27.6 ± 0.4	26.9 ± 0.4	28.3 ± 0.4	26.9 ± 0.4
Outdoor (Lift lobby)					
12	25.5 ± 0.6	26.3 ± 0.5	25.3 ± 0.6	27.5 ± 0.5	26.2 ± 0.5
10	25.9 ± 0.4	26.6 ± 0.5	25.5 ± 0.7	27.6 ± 0.4	26.7 ± 0.5
8	25.9 ± 0.6	26.9 ± 0.6	25.7 ± 0.5	28.0 ± 0.6	26.6 ± 0.6
6	25.9 ± 0.5	26.9 ± 0.5	25.8 ± 0.5	28.1 ± 0.5	26.7 ± 0.4
4	25.9 ± 0.5	27.0 ± 0.4	25.8 ± 0.5	28.1 ± 0.5	26.7 ± 0.6
2	26.5 ± 0.4	27.1 ± 0.5	26.4 ± 0.4	28.3 ± 0.4	26.9 ± 0.5

Table 5.11 Weekly Mean Indoor and Outdoor Temperatures (^{o}C) at the Households of Block 93 (Case Study 6)

Indoor					
Location	**Left units (#XX-3037)**				
Floor	**Week 1**	**Week 2**	**Week 3**	**Week 4**	**Week 5**
10	28.4 ± 0.5	28.3 ± 0.6	28.4 ± 0.5	28.8 ± 0.6	29.3 ± 0.8
8	29.1 ± 0.7	28.4 ± 0.6	29.0 ± 0.5	28.6 ± 0.7	29.1 ± 0.7
6	28.6 ± 0.7	28.8 ± 0.5	28.7 ± 0.5	29.1 ± 0.7	29.0 ± 0.6
4	29.0 ± 0.5	29.1 ± 0.6	28.8 ± 0.5	28.5 ± 0.6	28.5 ± 0.6
2	28.5 ± 0.7	28.9 ± 0.7	28.7 ± 0.7	29.2 ± 0.8	28.9 ± 0.7
Right units (#XX-3051)					
10	28.7 ± 0.7	29.3 ± 0.6	28.4 ± 0.6	29.3 ± 0.8	29.2 ± 0.6
8	28.7± 0.7	28.7 ± 0.7	28.9 ± 0.8	28.7 ± 0.6	28.9 ± 0.7
6	28.8 ± 0.5	29.2 ± 0.5	28.5 ± 0.6	29.1 ± 0.5	29.5 ± 0.7
4	29.4 ± 0.6	28.7 ± 0.7	29.1 ± 0.8	29.4 ± 0.6	29.8 ± 0.7
2	29.0 ± 0.6	29.5 ± 0.6	28.7 ± 0.7	29.4 ± 0.6	29.0 ± 0.7
Outdoor (Lift lobby)					
10	27.3 ± 0.6	27.7 ± 0.7	27.4 ± 0.7	27.7 ± 0.7	27.2 ± 0.6
8	27.6 ± 0.5	27.8 ± 0.6	27.6 ± 0.7	27.9 ± 0.5	28.0 ± 0.6
6	27.8 ± 0.6	28.2 ± 0.7	27.7 ± 0.5	28.1 ± 0.7	28.3 ± 0.7
4	28.1 ± 0.6	28.5 ± 0.5	28.0 ± 0.6	28.3 ± 0.6	28.6 ± 0.7
2	28.3 ± 0.6	28.6 ± 0.7	28.2 ± 0.6	28.5 ± 0.7	28.1 ± 0.4

The weekly mean indoor temperature did not show any significant correlation with the weekly mean indoor NO_2 concentration measured at each floor: Case Study 4 has mean Pearson's r = -0.11 ± 0.05: Case Study 5 has mean Pearson's r = -0.22 ± 0.13; and Case Study 6 has mean Pearson's r = -0.14 ± 0.07. Similarly, the weekly mean outdoor temperature did not show any significant correlation with the weekly mean outdoor NO_2 concentration level measured at each floor: Case Study 4 has mean Pearson's r = -0.24 ± 0.07; Case Study 5 has mean Pearson's r = -0.27 ± 0.03; and Case Study 6 has mean Pearson's r = -0.18 ± 0.09. Tables 5.12 - 5.15 show the weekly indoor and outdoor RH at the households of Case Studies 4 - 6.

Table 5.12 Weekly Mean Indoor and Outdoor RH (%) for Case Studies 4 - 6

	Block 39 (Case Study 4 Units)		**Block 401 (Case Study 5 Units)**		**Block 93 (Case Study 6 Units)**	
	#XX-251 (R) *	**# XX-249**	**#XX-278**	**# XX-268**	**#XX-3051 (R)** *	**# XX-3037**
Weekly mean indoor temperature range (%)	67 - 73	66 - 72	65 - 83	66 - 81	67 - 73	65 - 73
Overall weekly mean indoor RH(%)	71.0 ± 4.6	69.5 ± 5.4	75.9 ± 4.6	76.1 ± 4.1	70.5 ± 4.8	70.3 ± 5.2
Difference in RH between any two floors (%)	≤ 3.7		≤ 6.9		≤ 5.9	
Overall weekly mean outdoor RH (%)	71.6 ± 4.8		78.2 ± 5.5		72.4 ± 4.9	
Outdoor RH difference between highest and lowest floor in a week (^{o}C)	3.9 - 6.1 (5.1 ± 1.1) (2^{nd} and 20^{th} floor)		4.6 - 6.7 (5.7 ± 0.8) (2^{nd} and 12^{th} floor)		2.7 - 6.1 (4.4 ± 1.3) (2^{nd} and 10^{th} floor)	

L** -left R* -right

Table 5.13 Weekly Mean Indoor and Outdoor RH (%) at the Households of Block 39 (Case Study 4)

Indoor					
Location	**Left units (#XX-249)**				
Floor	**Week 1**	**Week 2**	**Week 3**	**Week 4**	**Week 5**
20	68.9 ± 5.8	72.4 ± 3.8	71.2 ± 3.2	68.2 ± 4.6	70.3 ± 4.2
17	66.1 ± 4.5	69.8 ± 3.1	70.2 ± 3.0	67.2 ± 4.0	69.8 ± 3.9
14	66.9 ± 4.4	70.4 ± 3.0	70.6 ± 2.7	68.3 ± 3.5	70.4 ± 3.2
11	67.3 ± 5.0	71.4 ± 3.2	71.2 ± 3.0	68.3 ± 3.6	70.6 ± 3.5
8	67.2 ± 5.6	71.2 ± 3.1	71.0 ± 3.1	68.3 ± 3.7	70.3 ± 3.4
5	67.2 ± 5.1	71.1 ± 3.0	70.9 ± 3.1	68.4 ± 3.8	70.2 ± 3.3
2	67.0 ± 4.2	72.7 ± 3.9	70.1 ± 3.2	68.0 ± 3.0	70.3 ± 2.9
Right units (#XX-251)					
20	68.4 ± 5.3	71.1 ± 3.8	71.0 ± 3.7	67.8 ± 4.2	70.7 ± 3.8
17	69.0 ± 5.6	71.7 ± 4.1	71.5 ± 3.7	68.7 ± 4.4	71.1 ± 4.0
14	69.5 ± 5.9	72.4 ± 4.4	71.9 ± 3.8	69.6 ± 4.6	71.4 ± 4.3
11	69.5 ± 5.8	72.4 ± 4.4	72.1 ± 3.8	69.8 ± 4.5	71.5 ± 4.3
8	69.4 ± 5.7	72.2 ± 4.1	71.7 ± 3.8	69.3 ± 4.1	71.3 ± 4.1
5	69.1 ± 5.1	73.5 ± 4.0	73.0 ± 3.1	71.4 ± 4.0	73.5 ± 3.4
2	69.0 ± 4.1	73.7 ± 3.2	73.1 ± 2.1	71.4 ± 2.9	73.3 ± 2.8
Outdoor (Lift lobby)					
20	72.4 ± 6.3	74.8 ± 4.9	75.7 ± 4.1	74.1 ± 5.3	74.3 ± 4.9
17	71.4 ± 6.0	73.5 ± 4.6	73.6 ± 3.8	72.4 ± 4.9	74.2 ± 4.6
14	68.8 ± 8.1	73.0 ± 4.6	72.8 ± 3.4	70.8 ± 4.3	72.8 ± 4.4
11	68.6 ± 5.5	72.6 ± 6.6	72.3 ± 5.9	69.4 ± 7.6	72.5 ± 6.7
8	67.8 ± 6.0	72.1 ± 4.6	71.2 ± 3.9	68.9 ± 4.8	70.7 ± 4.7
5	67.2 ± 6.1	71.5 ± 4.8	70.5 ± 3.9	68.5 ± 4.8	70.5 ± 4.7
2	66.7 ± 6.2	70.9 ± 4.9	69.8 ± 3.9	68.0 ± 4.9	70.4 ± 4.7

Table 5.14 Weekly Mean Indoor and Outdoor RH (%) at the Households of Block 401 (Case Study 5)

Indoor					
Location	**Left units (#XX-268)**				
Floor	**Week 1**	**Week 2**	**Week 3**	**Week 4**	**Week 5**
12	76.9 ± 4.3	78.9 ± 5.1	77.5 ± 4.3	69.7 ± 5.0	75.8 ± 4.6
10	77.7 ± 3.9	80.9 ± 4.1	78.7 ± 3.2	68.5 ± 5.1	76.5 ± 3.6
6	76.5 ± 5.0	75.7 ± 3.6	74.2 ± 3.9	66.4 ± 3.9	73.2 ± 3.2
2	81.8 ± 4.9	81.3 ± 3.6	77.8 ± 4.2	72.7 ± 3.7	78.7 ± 4.2
Right units (#XX-278)					
12	79.2 ± 5.2	77.2 ± 4.7	77.5 ± 5.2	68.1 ± 4.9	75.5 ± 5.3
10	81.1 ± 4.6	80.2 ± 4.3	77.8 ± 4.4	70.5 ± 4.3	77.4 ± 4.6
8	81.3 ± 3.5	77.2 ± 4.2	79.2 ± 4.7	70.0 ± 4.7	76.9 ± 4.1
6	75.1 ± 3.9	72.7 ± 3.6	75.5 ± 4.0	65.7 ± 3.9	73.2 ± 3.9
2	83.0 ± 4.2	76.3 ± 3.8	81.5 ± 3.7	68.2 ± 4.3	77.3 ± 4.3
Outdoor (Lift lobby)					
12	86.1 ± 7.2	80.7 ± 5.4	81.7 ± 6.7	68.4 ± 5.2	79.2 ± 4.9
10	84.6 ± 6.1	78.3 ± 4.8	80.6 ± 7.2	67.2 ± 6.4	77.7 ± 5.3
8	82.6 ± 5.9	77.6 ± 5.4	79.1 ± 6.2	68.0 ± 4.7	76.8 ± 4.0
6	83.5 ± 5.0	78.9 ± 4.5	80.0 ± 5.6	68.8 ± 5.1	77.8 ± 4.1
4	86.1 ± 4.3	80.0 ± 3.9	81.3 ± 4.7	68.4 ± 4.9	79.0 ± 3.7
2	79.4 ± 5.1	85.6 ± 4.3	81.7 ± 5.0	71.9 ± 3.7	76.6 ± 3.8

Table 5.15 Weekly Mean Indoor and Outdoor RH (%) at the Households of Block 93 (Case Study 6)

Indoor					
Location	**Left units (#XX-3037)**				
Floor	**Week 1**	**Week 2**	**Week 3**	**Week 4**	**Week 5**
10	67.9 ± 5.5	69.7 ± 4.0	72.5 ± 4.5	74.1 ± 4.4	71.9 ± 3.5
8	68.3 ± 4.6	71.8 ± 5.2	70.0 ± 4.0	72.7 ± 4.0	70.4 ± 4.6
6	65.4 ± 5.7	73.8 ± 4.5	71.1 ± 4.8	72.6 ± 4.8	68.2 ± 4.1
4	69.8 ± 6.0	72.9 ± 4.4	67.9 ± 3.9	70.7 ± 4.1	70.7 ± 3.6
2	66.9 ± 4.8	70.6 ± 4.9	68.7 ± 4.1	68.3 ± 3.3	69.8 ± 4.6
Right units (#XX-3051)					
10	68.3 ± 5.0	71.1 ± 4.0	73.1 ± 3.7	71.9 ± 4.7	72.2 ± 4.3
8	68.0 ± 6.1	72.4 ± 4.9	71.5 ± 4.5	69.9 ± 5.3	72.1 ± 5.7
6	68.5 ± 4.7	71.7 ± 3.8	71.6 ± 5.3	72.4 ± 3.8	67.8 ± 5.3
4	69.1 ± 5.4	72.9 ± 4.6	68.3 ± 5.0	72.9 ± 3.5	70.2 ± 5.4
2	67.6 ± 5.3	70.7 ± 4.2	68.4 ± 4.6	71.4 ± 5.5	68.7 ± 3.73
Outdoor (Lift lobby)					
10	73.6 ± 5.1	75.4 ± 3.6	74.2 ± 5.2	76.9 ± 5.4	74.6 ± 4.5
8	73.2 ± 4.2	75.0 ± 4.8	73.8 ± 4.4	74.2 ± 4.4	73.4 ± 4.5
6	72.4 ± 4.6	74.4 ± 6.0	72.5 ± 3.5	73.7 ± 4.8	71.7 ± 4.6
4	70.5 ± 5.0	73.1 ± 4.9	72.1 ± 4.5	72.5 ± 3.9	70.4 ± 4.8
2	69.9 ± 3.8	70.3 ± 4.5	71.5 ± 4.1	72.4 ± 5.1	68.5 ± 3.9

Generally, the outdoor RH increased with increasing height of the building and indoor RH did not show any trend. There was no significance difference between the overall weekly mean RH of both the right and left units and between the overall weekly indoor and outdoor mean RH ($p > 0.05$). There was no significant correlation between the weekly mean indoor RH and the weekly mean indoor NO_2 concentration measured at each floor; Case Study 4 has mean Pearson's $r = 0.19 \pm 0.06$; Case Study 5 has mean Pearson's $r = 0.35 \pm 0.14$; and Case Study 6 has mean Pearson's $r = 0.11 \pm 0.04$). Similarly, the weekly mean outdoor RH did not show any significant correlation with the weekly mean outdoor NO_2 concentration level measured at each floor; Case Study 4 has mean Pearson's $r = 0.24 \pm 0.13$; Case Study 5 has mean Pearson's $r = 0.31 \pm 0.05$; and Case Study 6 has mean Pearson's $r = 0.15 \pm 0.10$). Studies

have shown no clear or insignificant correlations between NO_2 concentrations and temperature and RH (Turkoglu et al., 2004 and Zou et al., 2006).

5.2.4 Distribution Profile of NO_2 Concentration

The horizontal distribution of NO_2 is of interest because it helps town planners to decide on the location of buildings and amenities considering the degree of exposure of occupants to NO_2 concentration levels. The vertical distribution of NO_2 concentration also merits consideration because it provides an understanding how the NO_2 concentration are distributed with respect to the height of a building so that one can decide on the location of the natural air intake of the building, or the building orientation based on the NO_2 pollution source.

The weekly mean indoor and outdoor concentration levels of NO_2 obtained from Ogawa samplers for Case Studies 4 - 6 are shown in Tables 5.16 - 5.18. Although NO_2 may be contributed by some indoor sources such as smoking, cooking and incense burning, the residents of the selected households agreed not to smoke during the measurement period. However, there was minimal incense burning and cooking activities since majority of the residents preferred to eat out. Thus, the measured NO_2 concentration was mainly contributed by the nearby traffic.

Table 5.16 Weekly Mean Concentration of NO_2 at Block 39 (Case Study 4)

Location	Outdoor Concentration ($\mu g/m^3$)	Location	Outdoor Concentration ($\mu g/m^3$)	Location	Indoor Concentration ($\mu g/m^3$)
Horizontal		**Floor**	**Right Unit (#XX-251)**	**Floor**	**Right Unit (#XX-251)**
Expressway	77.72 ± 3.13	20	51.73 ± 4.57	20	47.31 ± 4.63
Lamp post	70.49 ± 4.68	17	54.88 ± 4.18	17	51.27 ± 4.94
Void deck	58.41 ± 4.02	14	57.78 ± 3.46	14	54.47 ± 4.41
		11	62.09 ± 4.62	11	59.48 ± 4.84
		8	66.97 ± 4.64	8	62.25 ± 4.98
		5	64.21 ± 4.63	5	58.88 ± 5.10
		2	59.66 ± 4.58	2	54.12 ± 4.70
Lift Lobby Area Floor		**Floor**	**Left Unit (#XX-249)**	**Floor**	**Left Unit (#XX-249)**
20	47.55 ± 2.76	20	51.37 ± 3.14	20	47.97 ± 1.80
17	50.61 ± 3.45	17	56.02 ± 4.01	17	52.17 ± 2.62
14	49.64 ± 4.34	14	59.91 ± 3.30	14	55.99 ± 3.40
11	49.03 ± 3.98	11	62.91 ± 4.05	11	59.99 ± 4.50
8	50.92 ± 4.09	8	66.78 ± 4.98	8	62.70 ± 4.79
5	47.53 ± 3.05	5	68.05 ± 2.27	5	63.46 ± 2.85
2	49.23 ± 3.64	2	61.94 ± 3.73	2	56.75 ± 4.91

Table 5.17 Weekly Mean Concentration of NO_2 at Block 401 (Case Study 5)

Location	Outdoor Concentration ($\mu g/m^3$)	Location	Outdoor Concentration ($\mu g/m^3$)	Location	Indoor Concentration ($\mu g/m^3$)
Horizontal		**Floor**	**Right Unit (#XX-278)**	**Floor**	**Right Unit (#XX-278)**
Left Unit (#XX-268)		12	70.41 ± 2.54	12	59.05 ± 1.91
Expressway	84.37 ± 3.62	10	74.18 ± 3.51	10	62.08 ± 2.87
Lamp post	78.62 ± 3.11	8	80.66 ± 2.72	8	64.67 ±3.68
Void deck	73.25 ± 2.60	6	85.11 ± 2.93	6	68.05 ± 3.12
Right Unit (#XX-278)		2	76.54 ± 4.59	2	63.43 ± 2.88
Expressway	84.12 ± 2.53				
Lamp post	77.79 ± 3.55				
Void deck	73.51 ± 4.99				
Lift lobby Area Floor		**Floor**	**Left Unit (#XX-268)**	**Floor**	**Left Unit (#XX-268)**
12	58.16 ± 2.07	12	68.56 ± 2.34	12	59.10 ± 2.56
10	60.98 ± 2.70	10	74.62 ± 2.60	10	63.58 ± 2.98
8	64.09 ± 2.73	6	82.68 ± 1.78	6	68.48 ± 2.49
6	65.70 ± 3.54	2	75.84 ± 2.21	2	65.48 ± 2.24
4	63.15 ± 3.49				
2	64.25 ± 2.97				

Table 5.18 Weekly Mean Concentration of NO_2 at Block 93 (Case Study 6)

Location	Outdoor Concentration ($\mu g/m^3$)	Location	Outdoor Concentration ($\mu g/m^3$)	Location	Indoor Concentration ($\mu g/m^3$)
Horizontal		**Floor**	**Right Unit (#XX-3051)**	**Floor**	**Right Unit (#XX-3051)**
Left Unit (#XX-3037)		10	68.05 ± 2.48	10	55.52 ± 2.63
Expressway	82.30 ± 2.67	8	81.20 ± 2.53	8	68.12 ± 1.99
Lamp post	75.54 ± 3.85	6	78.32 ± 3.12	6	65.71 ± 3.81
Void deck	70.80 ± 3.42	4	76.44 ± 2.76	4	63.24 ± 2.56
Right Unit (#XX-3051)		2	71.63 ± 2.75	2	60.90 ± 3.45
Expressway	82.27 ± 2.88				
Lamp post	76.16 ± 3.08				
Void deck	70.35 ± 2.95				
Lift lobby Area Floor		**Floor**	**Left Unit (#XX-3037)**	**Floor**	**Left Unit (#XX-3037)**
10	53.67 ± 2.55	10	67.08 ± 3.62	10	54.07 ± 2.84
8	58.83 ± 2.36	8	75.17 ± 3.15	8	60.21 ± 3.15
6	60.36± 2.49	6	82.87 ± 4.56	6	67.94 ± 3.71
4	56.56 ± 2.03	4	78.38 ± 2.25	4	63.76 ± 3.09
2	58.59 ± 3.52	2	72.73 ± 2.82	2	61.83 ± 2.56

5.2.4.1 Horizontal Distribution Profile of NO_2 Concentration

The horizontal distribution profile of the weekly mean NO_2 concentration of Case Studies 4 - 6 is shown in Figures 5.1 - 5.3. The weekly mean concentration of NO_2 from the expressway decreased with increasing downstream distance up to the building facade. Table 5.19 summarizes the percentage decrease of NO_2 concentration levels at the trees and from the trees to the building façade for Case Studies 4 - 6. For the point block configuration (Case Study 4), the decrease in NO_2 concentration from the trees to the building façade was higher than that of the slab block configurations (Case Studies 5 - 6). This could be attributed to the slab block configuration which

tends to slow down the wind speed thus allowing the accumulation of NO_2 concentration.

Table 5.19 Percentage Decrease of NO_2 Concentration Before and After Trees and from Trees to Building Façade for Case Studies 4 - 6

	Block 39(Case Study 4 Units)		Block 401(Case Study 5 Units)		Block 93 (Case Study 6 Units)	
	#XX-251 (R) *	# XX-249 (L) **	#XX-278 (R) *	# XX-268 (L) **	#XX-3051 (R) *	# XX-3037 (L) **
Weekly Mean NO_2 levels 1m from Expressway($\mu g/m^3$)	77.72 ± 3.13		84.12 ± 2.53	84.37 ± 3.62	82.27 ± 2.88	82.30 ± 2.67
Weekly Mean NO_2 levels at building façade ($\mu g/m^3$)	58.41 ± 4.02		73.51 ± 4.99	73.25 ± 2.60	70.35 ± 2.95	70.80 ± 3.42
Distance from Expressway to facade	20m		20m		15m	
% decrease just before and after trees	9		8	7	7	8
% decrease between tree and facade	17		6	7	8	6

L**-left R*-right

There was a decrease of about 7 - 9% in the weekly mean NO_2 concentration just before and after the trees and a further 6 - 17% from the trees to the building facade for all the case studies. The decrease in the values after the trees could be due to absorption of NO_2 by the trees and vegetation (Takahashi et al., 2005). Other studies on the horizontal distribution of traffic-generated NO_2 concentration also showed NO_2 concentration decreased with increasing distance from the highway (Roorda-Knappe et al., 1998; Gilbert et al., 2003 and Maruo et al., 2003).

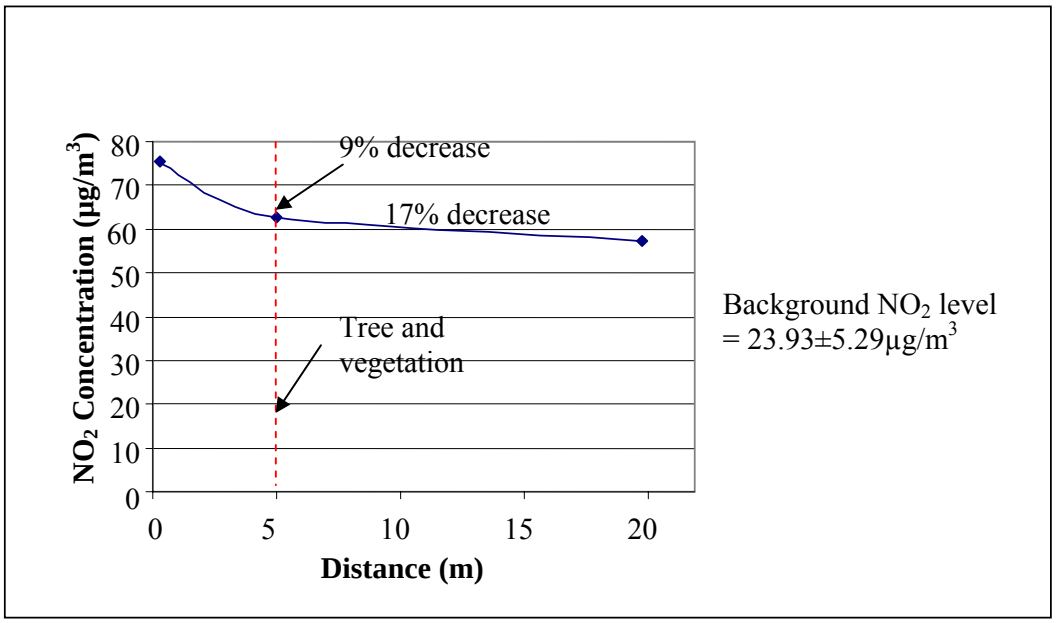

Figure 5.1 Horizontal Distribution Profile of Weekly Mean NO_2 Concentration from Expressway to Building Façade at the Middle of Block 39 (Case Study 4)

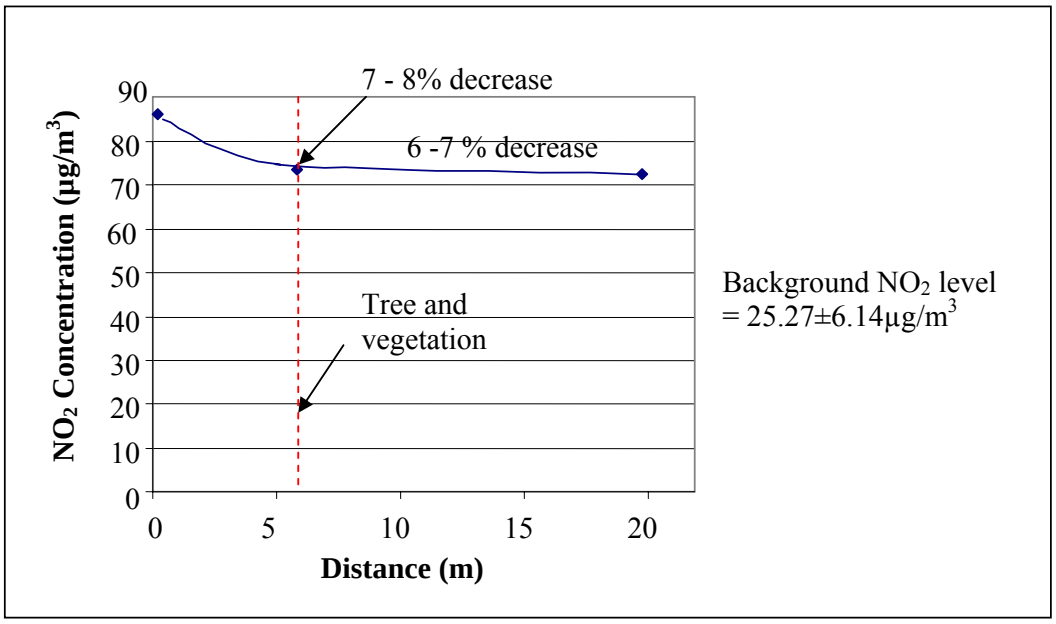

Figure 5.2 Mean Horizontal Distribution Profile of Weekly Mean NO_2 Concentration from Expressway to Building Façade at Block 401 (Case Study 5)

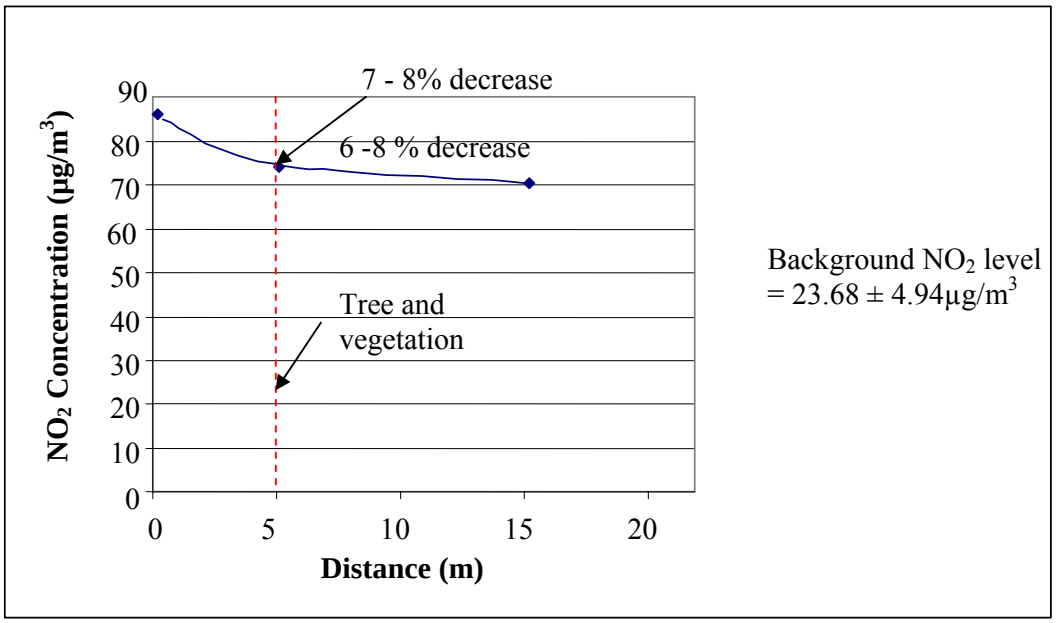

Figure 5.3 Mean Horizontal Distribution Profile of Weekly Mean NO_2 Concentration from Expressway to Building Façade at Block 93 (Case Study 6)

5.2.4.2 Vertical Distribution Profile of NO_2 Concentration

Figures 5.4 - 5.9 showed that the vertical distribution profile of NO_2 concentration at the right and left units of Case Studies 4 - 6. The results of Case Study 4 have been reported elsewhere (Kalaiarasan et al., 2008). Generally for a floor, the weekly mean outdoor concentration of NO_2 was higher than its indoor concentration. The results showed the weekly mean indoor concentration of NO_2 at all the floors in a building have exceeded the WHO (2005) maximum allowable annual mean value of 40µg/m^3. Statistical analysis showed there was no significant difference in the weekly mean indoor and outdoor concentrations of NO_2 at the corresponding floors of the right and left units of a building ($p > 0.05$).

The vertical distribution profiles of the weekly mean indoor/outdoor concentration of NO_2 in a building was similar to those profiles obtained for $PM_{2.5}$ mass/number concentration in Case Studies 1 - 3. Generally in a building, the highest weekly mean outdoor NO_2 concentration occurred at around the mid floors of the building (i.e. for the right units - 9th floor for Case Study 4 and 6th floor for Case studies 5 and 6 and for the left units - 7th floor for Case Study 4 and 6th floor for Case Studies 5 and 6) as compared to its lowest and highest floors during the measurement period. The NO_2 concentration value at the lowest floor was higher than that measured at the highest floor of the building. The vertical distribution profiles of the weekly mean indoor/outdoor concentration of NO_2 for a building was similar.

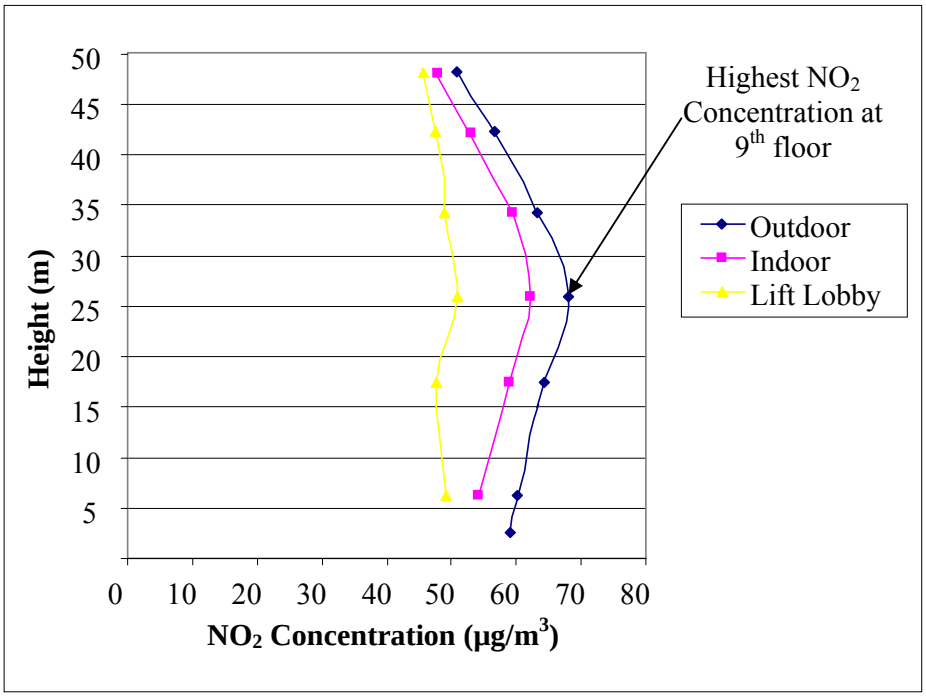

Figure 5.4 Vertical Distribution Profile of Weekly Mean NO_2 Concentration at the Right Unit (#XX - 251) of Block 39 (Case Study 4)

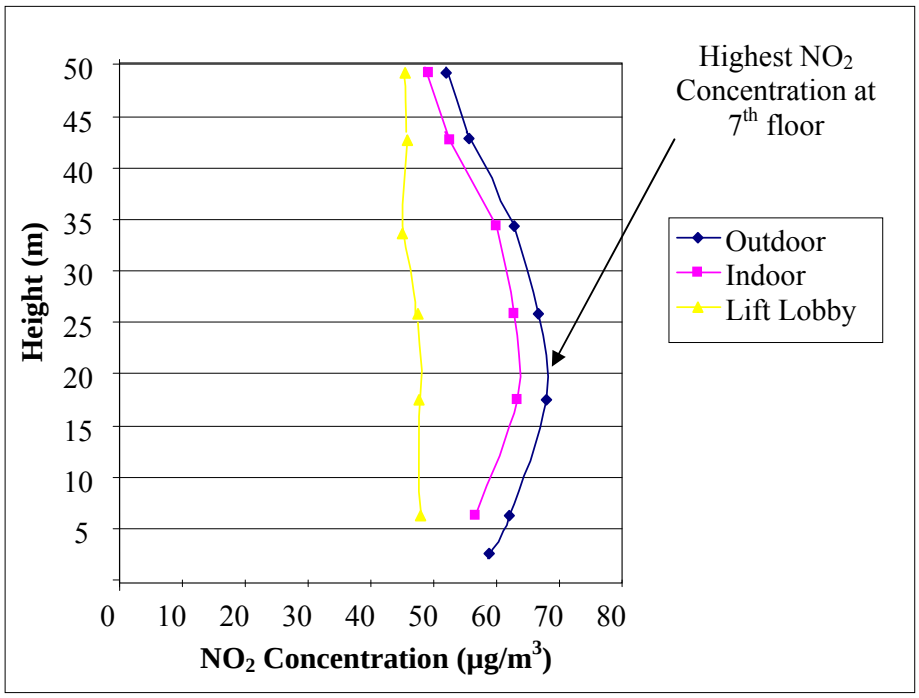

Figure 5.5 Vertical Distribution Profile of Weekly Mean NO_2 Concentration at the Left Unit (#XX - 249) of Block 39 (Case Study 4)

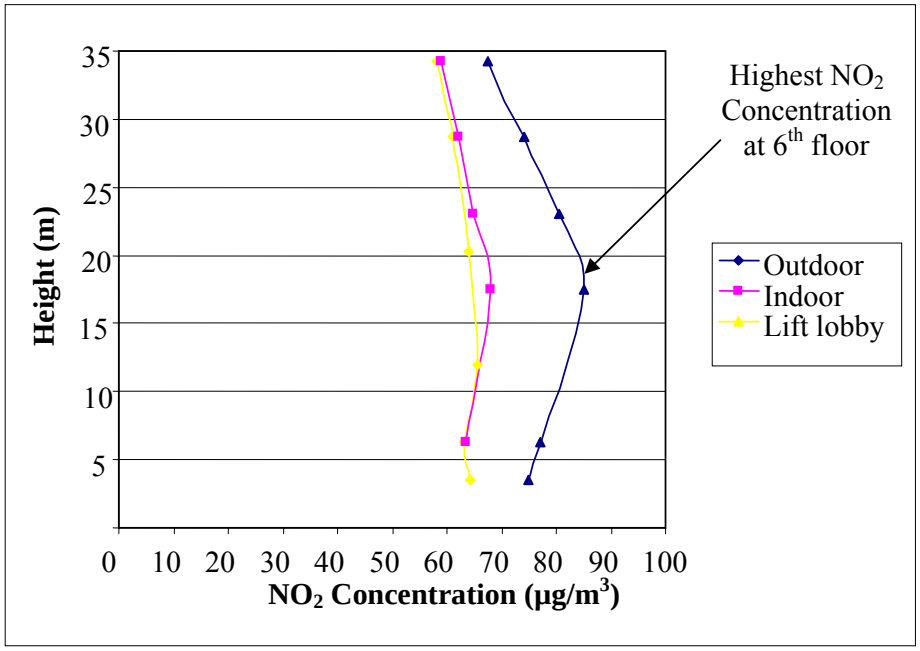

Figure 5.6 Vertical Distribution Profile of Weekly Mean NO_2 Concentration at the Right Unit (#XX - 278) of Block 401 (Case Study 5)

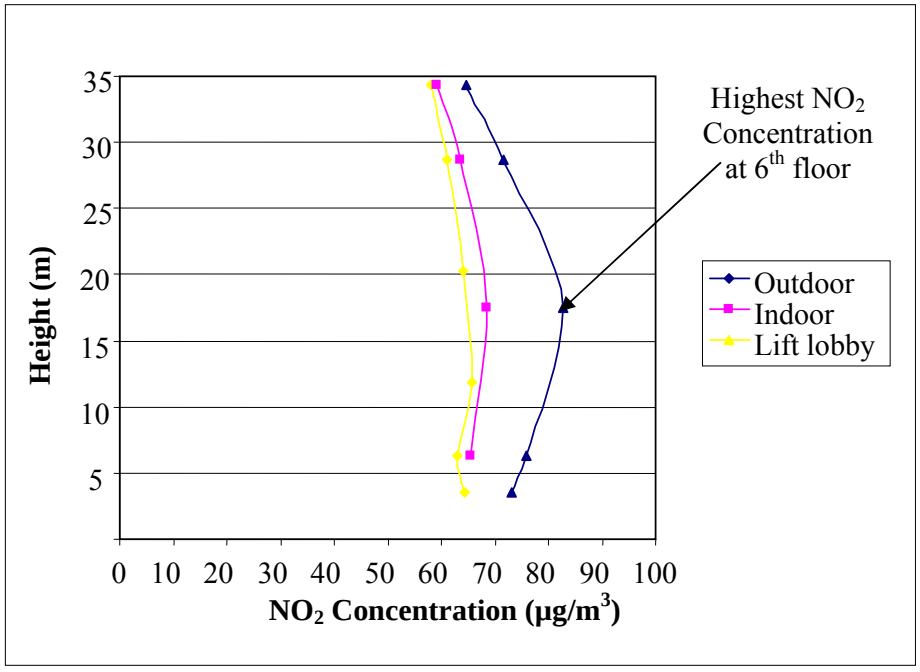

Figure 5.7 Vertical Distribution Profile of Weekly Mean NO_2 Concentration at the Left Unit (#XX - 268) of Block 401(Case Study 5)

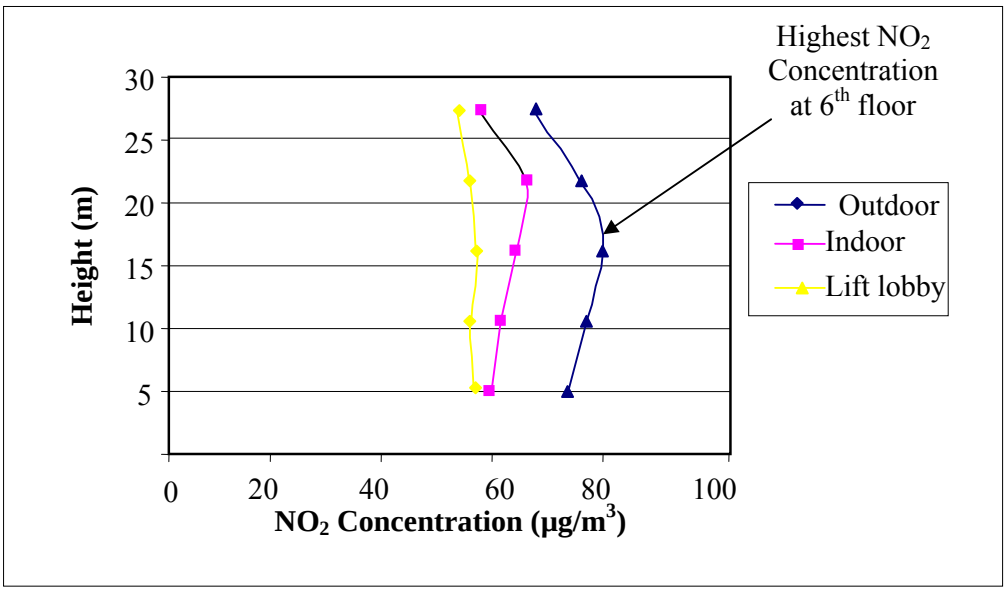

Figure 5.8 Vertical Distribution Profile of Weekly Mean NO_2 Concentration at the Right Unit (#XX - 3051) of Block 93 (Case Study 6)

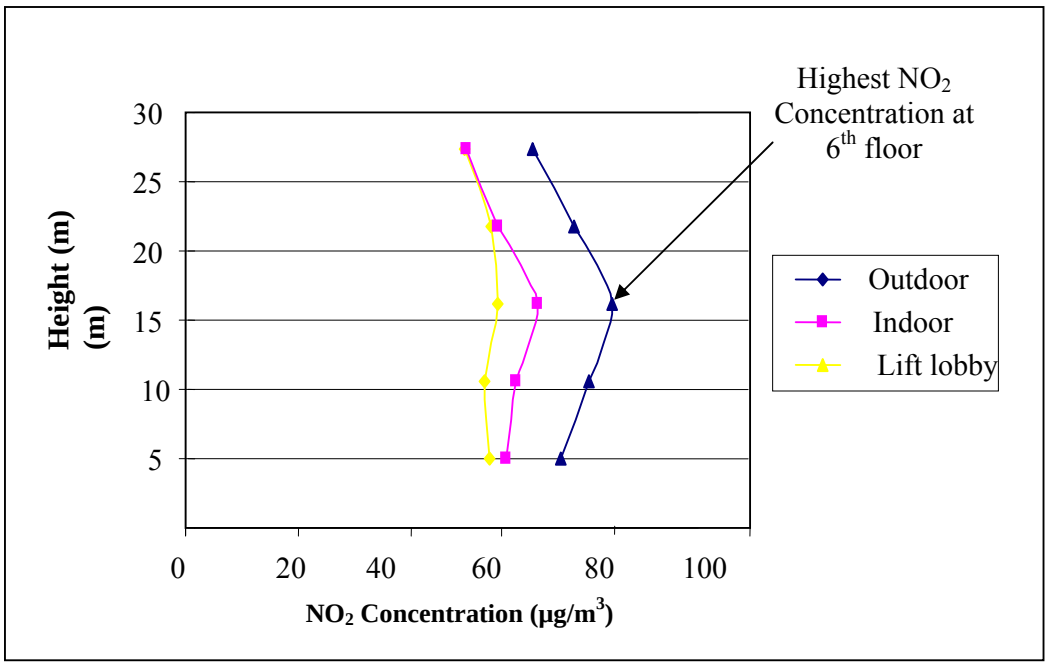

Figure 5.9 Vertical Distribution Profile of Weekly Mean NO_2 Concentration at the Left Unit (#XX - 3037) of Block 93 (Case Study 6)

5.2.5 Indoor/Outdoor (I/O) ratio of NO_2 Concentration

The indoor and outdoor air contaminant levels depend on ventilation rate, source and sink strengths, as well as outdoor conditions which influences the outdoor air contaminant level. In this study, the I/O ratio of NO_2 concentration for all the apartments in a building was less than unity indicating the transport of NO_2 was from outdoors to indoors rather than from internal sources. The outdoor source is mainly from the nearby traffic. Tables 5.20 - 5.22 show the I/O ratio values of NO_2 concentration in the apartments of the buildings for Case Studies 4 - 6. For Case Study 4 (point block configuration), the I/O ratio of NO_2 concentration was between 0.84 - 0.98 (0.93 ± 0.04). The mean I/O ratio was close to unity which could be due to the building being more permeable thus allowing equilibrium of the indoor and outdoor concentration to reach earlier. From observation and interview, it was found the doors and balcony windows of the selected apartments were left opened most of the time since residents felt less stuffy and warm with the doors and windows opened since during the measurement period it was hot and humid. An I/O ratio close to unity also indicates outdoor pollution significantly affects the indoor air quality of the building.

For Case Studies 5 and 6 (slab block configuration), the I/O ratios of NO_2 concentration for all the apartments in the buildings ranged from 0.723 - 0.899 (0.83 ± 0.04) and 0.665 to 0.896 (0.82 ± 0.05) respectively. The I/O ratio values of NO_2 concentration in the apartments of both these blocks were relatively lower than that of Case Study 4. This could imply that a slab block's façade has a better filtering effect of traffic-generated NO_2 as compared to a point block's façade. Other studies also reported the I/O ratio of NO_2

concentration for the apartments in a building to be less than unity. For example in Hong Kong, a study reported the I/O ratio of NO_2 concentration in homes of 10 non-smoking residential buildings was 0.79 (Chao, 2001). Another study reported that in Swedish homes, the mean I/O ratio of NO_2 concentration ranged from about 0.4 - 0.7 (Hagenbjork-Gustafsson et al., 1996).

Table 5.20 I/O Ratio of NO_2 Concentrations in Apartments of Block 39 (Case Study 4)

	I/O Ratio				
	Right Unit (#XX-251)				
Floor	**Week 1**	**Week 2**	**Week 3**	**Week 4**	**Week 5**
20	0.906	0.967	0.932	0.855	0.912
17	0.913	0.978	0.952	0.912	0.911
14	0.964	0.976	0.947	0.897	0.878
11	0.978	0.975	0.923	0.920	0.944
l 8	0.868	0.980	0.974	0.900	0.927
5	0.884	0.952	0.979	0.868	0.977
2	0.877	0.903	0.903	0.954	0.897
	Left Unit(#XX-249)				
20	0.979	0.903	0.967	0.903	0.924
17	0.839	0.969	0.973	0.879	0.982
14	0.866	0.980	0.964	0.937	0.929
11	0.950	0.957	0.950	0.971	0.938
8	0.926	0.933	0.969	0.955	0.912
5	0.890	0.936	0.941	0.956	0.939
2	0.844	0.949	0.920	0.934	0.931

Table 5.21 I/O Ratio of NO_2 Concentrations in Apartments of Block 401 (Case Study 5)

	I/O Ratio				
	Right Unit (#XX-278)				
Floor	**Week 1**	**Week 2**	**Week 3**	**Week 4**	**Week 5**
12	0.852	0.868	0.883	0.820	0.776
10	0.845	0.862	0.881	0.826	0.775
8	0.835	0.807	0.803	0.829	0.736
6	0.830	0.820	0.802	0.799	0.748
2	0.838	0.842	0.806	0.786	0.723
	Left Unit(#XX-268)				
12	0.860	0.863	0.868	0.899	0.821
10	0.874	0.810	0.842	0.867	0.868
6	0.846	0.813	0.829	0.855	0.798
2	0.863	0.853	0.868	0.879	0.855

Table 5.22 I/O Ratio of NO_2 Concentrations in Apartments of Block 93 (Case Study 6)

	I/O Ratio				
	Right Unit (#XX-3051)				
Floor	**Week 1**	**Week 2**	**Week 3**	**Week 4**	**Week 5**
10	0.779	0.808	0.815	0.866	0.811
8	0.824	0.845	0.859	0.715	0.799
6	0.867	0.863	0.828	0.881	0.755
4	0.840	0.816	0.767	0.818	0.896
2	0.877	0.861	0.854	0.836	0.822
	Left Unit(#XX-3037)				
10	0.821	0.890	0.745	0.844	0.805
8	0.796	0.764	0.837	0.823	0.785
6	0.872	0.833	0.748	0.842	0.865
4	0.665	0.888	0.786	0.803	0.797
2	0.812	0.886	0.835	0.849	0.869

5.2.6 $PM_{2.5}$ Number Concentration at Apartment with Highest NO_2 Concentration

The $PM_{2.5}$ number concentration was measured at the apartment of the building where the measured NO_2 concentration was the highest. The indoor and outdoor $PM_{2.5}$ number concentration for Case Studies 4 - 6 are shown in Tables 5.5 - 5.7. $PM_{2.5}$ number concentration measurement was used because studies like that of Penttinen et al. (2001) have suggested that particle count was more significant when fine particles are discussed as they are very small in mass but huge in numbers.

Table 5.23 $PM_{2.5}$ Number Concentration at the Floor with Highest NO_2 Concentration for a Typical Week at Block 39 (Case Study 4)

Day	Indoor Concentration (particles/cm^3)			Outdoor Concentration (particles/cm^3)		
	Min	Max	Mean	Min	Max	Mean
1	35.98	175.94	78.6 ± 37.62	45.24	136.78	79.04 ± 31.41
2	28.08	111.16	55.85 ± 21.08	31.75	143.21	67.81 ± 29.56
3	44.76	180.91	110.53 ± 21.87	63.64.	234.00	126.32 ±17.83
4	58.17	106.94	82.09 ± 11.49	71.75	233.77	100.19 ± 23.45
5	66.75	168.74	99.16 ± 23.02	78.09	186.94	110.84 ± 25.57

Table 5.24 $PM_{2.5}$ Number Concentration at the Floor with Highest NO_2 Concentration for a Typical Week at Block 401 (Case Study 5)

Day	Indoor Concentration (particles/cm^3)			Outdoor Concentration (particles/cm^3)		
	Min	Max	Mean	Min	Max	Mean
1	45.34	221.69	92.48 ± 39.57	56.99	172.34	99.60 ± 47.41
2	35.38	140.06	70.37 ± 26.56	40.64	183.31	86.79 ± 37.94
3	144.74	280.74	180.50 ± 21.86	206.19	294.84	239.28 ± 50.45
4	75.03	137.95	105.90 ± 14.82	91.84	299.22	128.25 ± 30.03
5	84.11	212.61	120.26 ± 30.45	98.39	232.54	138.57 ± 27.61

Table 5.25 $PM_{2.5}$ Number Concentration at the Floor with Highest NO_2 Concentration for a Typical Week at Block 93 (Case Study 6)

Day	Indoor Concentration (particles/cm^3)			Outdoor Concentration (particles/cm^3)		
	Min	Max	Mean	Min	Max	Mean
1	55.88	246.37	110.67 ± 25.86	80.81	232.63	129.41 ± 30.54
2	74.67	152.43	93.23 ± 15.98	82.46	212.79	119.52 ± 36.27
3	101.29	263.10	202.65 ± 35.75	112.75	287.90	240.92 ± 38.81
4	129.13	240.59	184.48 ± 20.19	165.84	280.16	227.73 ± 40.08
5	80.36	225.95	146.69 ± 29.54	86.77	210.73	169.19 ± 25.26

5.2.6.1 Indoor/Outdoor (I/O) ratio of $PM_{2.5}$ Number Concentration at Apartment

For all the Case Studies 4 - 6, the I/O ratio values of $PM_{2.5}$ number concentration was less than unity and ranged from 0.8 - 0.95 (0.88 ± 0.07) for Case Study 4, 0.75 - 0.92 (0.83 ± 0.06) for Case Study 5 and 0.78 - 0.86 (0.81 ± 0.04) for Case Study 6 for a typical working week. The variation of I/O ratio of $PM_{2.5}$ number concentrations at the apartments of the various case studies are shown in Figure 5.10. The I/O ratio was less than unity indicating the migration of $PM_{2.5}$ was from outdoors to indoors. The I/O ratio for the different size components of $PM_{2.5}$ for the various case studies in a typical day is shown in Figure 5.11.

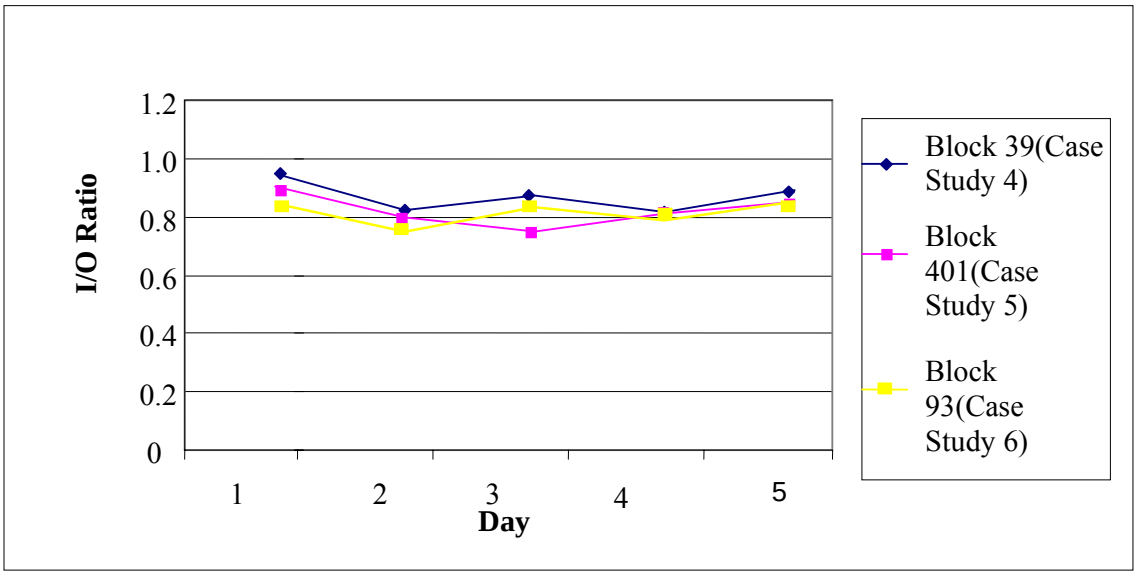

Figure 5.10 Variation of I/O Ratio of $PM_{2.5}$ Number Concentration at Apartments for a Typical Week

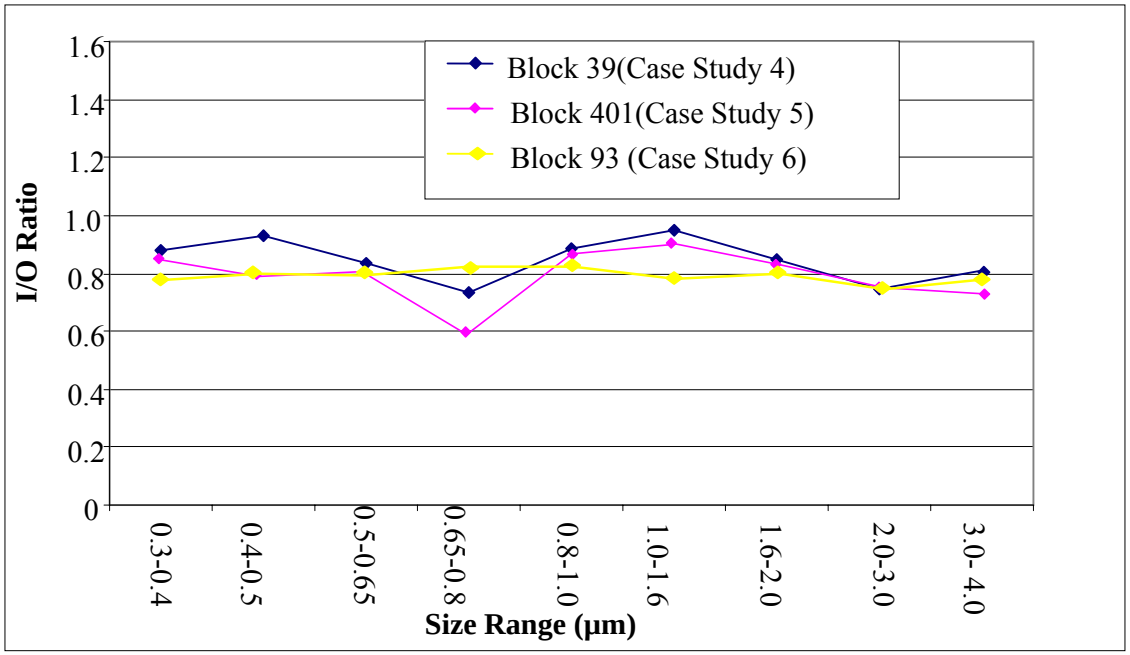

Figure 5.11 Variation of I/O Ratio for the Different Size Components of $PM_{2.5}$ Number Concentration in a Typical Day

5.2.6.2 Correlation of $PM_{2.5}$ and NO_2 Concentration at Apartment

For Case Studies 4 - 6, results showed there was a fairly good positive correlation between NO_2 concentration and $PM_{2.5}$ number concentration levels

at the apartments with r^2 = 0.69 - 0.88 for indoor concentrations and r^2 = 0.68 - 0.95 for outdoor concentrations. Studies by Beckerman et al. (2008) found that there was high correlation between NO_2 and $PM_{2.5}$ with regression from 0.7 - 0.96. Figures 5.12 - 5.13 show typical correlations of NO_2 and $PM_{2.5}$ number concentrations at the indoor and outdoor locations of Block 93 (Case Study 6) respectively. The fairly good correlation between NO_2 concentration levels and $PM_{2.5}$ number concentration in this study suggests NO_2 can be used as good surrogate indicator for $PM_{2.5}$ mass/number concentration.

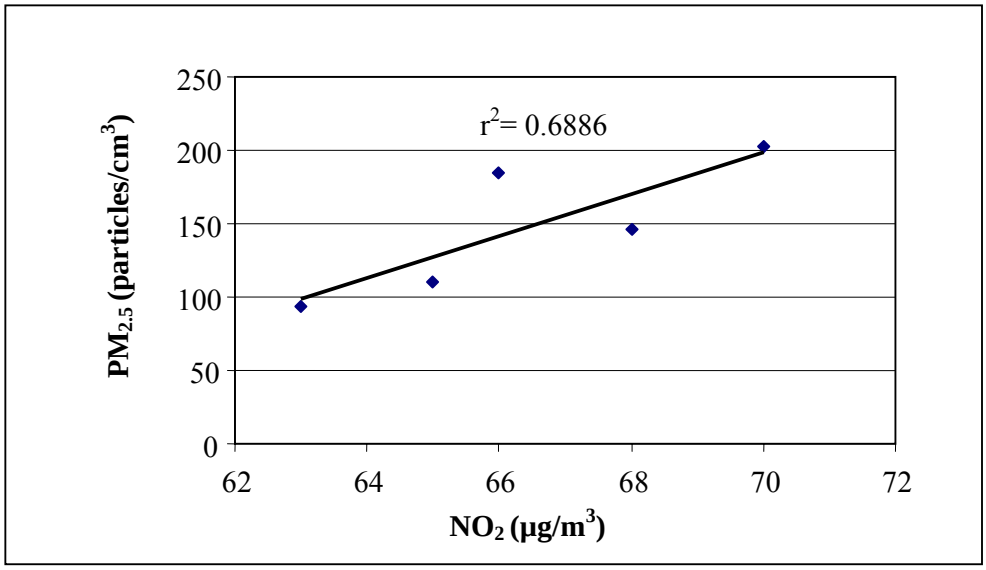

Figure 5.12 Correlation of Weekly Mean Indoor NO_2 and $PM_{2.5}$ Number Concentration at the Apartment of Block 93 (Case Study 6)

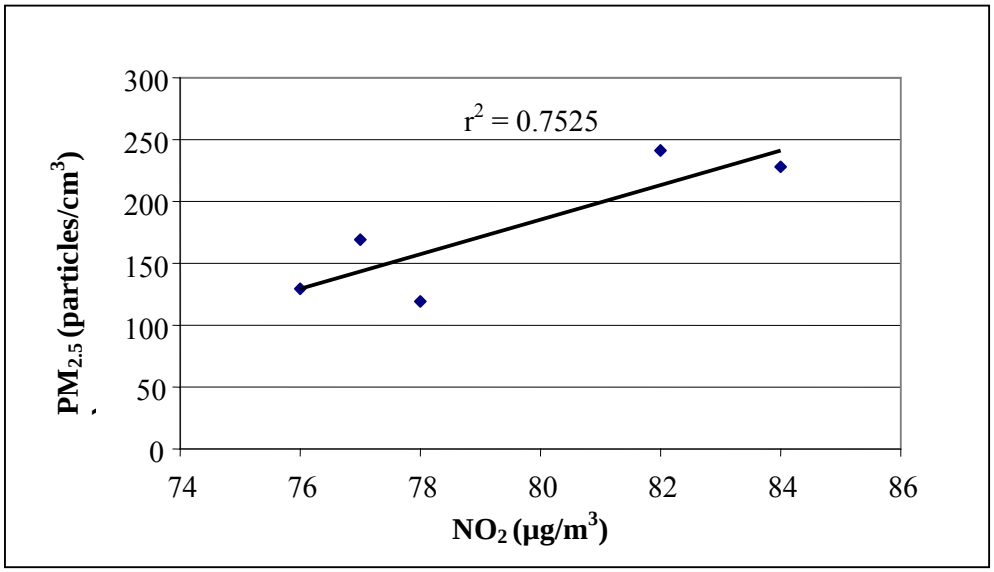

Figure 5.13 Correlation of Weekly Mean Outdoor NO_2 and $PM_{2.5}$ Number Concentration at the Apartment of Block 93 (Case Study 6)

5.3 Conclusion

5.3.1 Vertical and Horizontal Distribution Profile of Traffic-Generated NO_2 Concentration

The shape of the weekly mean indoor and outdoor vertical distribution profile of the traffic-generated NO_2 concentration in a building resembled that of a 'bell curve' with its abscissa in the vertical direction regardless of the configuration of the buildings. Experimental results showed the highest weekly mean indoor and outdoor concentration of NO_2 generally occurred at the mid floors of the buildings. Residents living at these floors could have an elevated chance of being exposed to a higher concentration of traffic-generated NO_2 compared to the other floors. Similar to traffic-generated $PM_{2.5}$, the low floors generally had the second highest NO_2 concentration and the high floors had the least weekly mean NO_2 concentration. For the horizontal distribution of NO_2 concentration levels in all the buildings, the weekly mean

concentration levels of NO_2 from the expressway decreased with increasing downstream distance up to the building facade. There was a decrease of about 7 - 9% in the weekly mean concentration level of NO_2 just before and after the trees and a further 6 - 17% from the trees to the building facade. The decrease in the values just before and after the trees suggested NO_2 could be absorbed by the row of trees and vegetation planted along the expressways.

5.3.2 I/O Ratio of Traffic-Generated NO_2 Concentration

The I/O ratio values of NO_2 concentration for all the apartments in a buildings were less than unity. The results indicate that the transport of NO_2 was from outdoors to indoors rather than from internal sources. The main outdoor source is from the nearby vehicular traffic. For the point block, the overall mean I/O value of NO_2 concentration was 0.93 ± 0.04 and this was close to unity. The close to unity I/O ratio value could be due to the building being more permeable thus allowing equilibrium of the indoor and outdoor concentration levels to reach earlier. A close to unity I/O ratio value also indicates outdoor pollution significantly affects the indoor air quality of the building. For both the slab blocks, the overall mean I/O ratio values of NO_2 concentration were 0.83 ± 0.04 and 0.82 ± 0.05. The I/O ratio values in the apartments of both the blocks were relatively lower than that of the point block. This showed a slab block's façade has a better filtering effect of traffic-generated NO_2 as compared to a point block's façade.

5.3.3 Correlation of Traffic-Generated NO_2 and $PM_{2.5}$ Concentration

Statistical results showed there was a fairly good positive correlation between the indoor and outdoor NO_2 concentration with $PM_{2.5}$ number concentration

levels at the apartments of the buildings where the highest concentration of NO_2 was measured. The results indicated NO_2 could be used as a surrogate indicator for traffic-generated $PM_{2.5}$.

5.3.4 Traffic-Generated NO_2 Concentration and Meteorological Factors

Generally, outdoor temperature reduced with increasing height of the building whilst outdoor RH and wind speed increased with increasing height of the building. Similar to earlier $PM_{2.5}$ mass/number concentration studies, traffic volume, wind speed, temperature and RH did not show any significant correlation with the indoor and outdoor NO_2 concentration levels measured at the floors for all the case studies.

CHAPTER 6: HEALTH RISK ASSESSMENT

6.1 Introduction

About 1 out of 5 children in Singapore are asthmatics and Singapore ranks number one in the Asia Pacific region in terms of the number of asthmatic kids between the ages 13 - 14 (ISSAC, 1998). Health risk differs from one pollutant to another. For example, NO_2 mainly acts as an irritant affecting the mucosa of the eyes, nose, throat and the respiratory tract. On the other hand, fine and ultra fine particles can penetrate deep into the lungs and cause serious health problems such as irritation of the breathing airways, difficulty in breathing, aggravated asthma, development of chronic bronchitis and also premature deaths in people with heart or lung disease (US EPA, 2009). Traffic-generated pollution constantly posed a health risk to people at all stages in life. The rising population and motor vehicle levels in Singapore pose a greater health risk to its citizens and hence it becomes imperative to carry out site-specific and age-specific health risk assessment with respect to traffic-generated particulate pollution so as to provide relatively accurate and representative estimates of health risk for residents living residential buildings close to major roads and expressways.

6.2 Health Risk Model for Exposure to $PM_{2.5}/NO_2$ for a Typical 22 - Storeys Point and a 16 - Storeys Slab Block

Indoor exposure models for $PM_{2.5}$ and NO_2 mass concentration are developed for a typical 22 - storeys point block and a 16 - storeys slab block as shown

in equations 1 - 4. The measured exposure levels at the various floors of the buildings were regressed using FindGrapH version 2.01. It is found the Gaussian plus a line model function was the best function to fit the measured daily mean vertical distribution profile of $PM_{2.5}$ (r^2 = 0.80) and the weekly mean vertical distribution profile of NO_2 regardless of the height and configuration of the buildings (r^2 = 0.80 - 0.94). The mean estimated dose rate and the dimensionless health risk value follow Pandey's et al. (2005) formulation as shown in chapter 3, section 3.4. For $PM_{2.5}$/NO_2 inhalation, conventionally employed somatic and respiration parameters for the various age as shown in Table 6.1 is adopted since there was no such available data in Singapore. Loael values for morbidity due particulate matter inhalation for the various age groups was obtained from Cerna et al. (1998) since there was also no such available data in Singapore. The loael values were obtained from a meta-analysis of data published in epidemiological studies (e.g. Xu et al., 1995; Pope, 1996; Sunyer et al., 1996, etc.) dealing with health effects (coughing, wheezing, decreased respiratory function, prevalence of respiratory illness, and acute mortality) and the median values for loael were calculated from the data referring to positive dose-response relationships. For NO_2 inhalation, a loael value of 1.5µg/kg per day for NO_2 as used by Pandey et al. (2005) is adopted for the model i.e. the dose value at which expiratory flow rate becomes lower than 100%. The loael value for NO_2 was estimated, based on the dose–response model constructed on the basis of data available in Neuberger et al. (2002). For all the blocks where the measurements were taken, the mean occupancy factor value was obtained based on the interview survey results i.e. about 25% of the residents were in their apartments from

about 8am - 8pm and for the rest of the time, about 95% of the residents were in their apartments. Occupancy factor is the percentage of residents likely to be in the building at a given interval of time. The computed mean occupancy factor for the point and slab block designs was found to be about 0.6.

For a 22 - storeys naturally-ventilated residential point block close to an expressway, the estimated mean indoor concentration at each floor of the building:

$$Diurnal\ mean\ indoor\ PM_{2.5}\ concentration = 30.891 + 30.394e^{-0.5\left[\frac{H-25.632}{11.881}\right]^2} - 0.059H$$

($\mu g/m^3$) ($r^2 = 0.80$).....(1)

$$Weekly\ mean\ indoor\ NO_2\ concentration = 55.074 + 12.212e^{-0.5\left[\frac{H-22.274}{14.456}\right]^2} - 0.071H$$

($\mu g/m^3$) ($r^2 = 0.94$).....(2)

For a 16 - storeys naturally-ventilated residential slab block close to an expressway, the estimated mean indoor concentration at each floor of the building:

$$Diurnal\ mean\ indoor\ PM_{2.5}\ concentration = 55.126 + 34.258e^{-0.5\left[\frac{H-24.349}{9.084}\right]^2} - 0.398H$$

($\mu g/m^3$) ($r^2 = 0.83$).....(3)

$$Weekly\ mean\ indoor\ NO_2\ concentration = 74.057 + 13.042e^{-0.5\left[\frac{H-16.836}{8.207}\right]^2} - 0.195H$$

($\mu g/m^3$) ($r^2 = 0.91$).....(4)

where H (m) indicates the height of storey measured from ground floor

The estimated mean dose rate at each floor of the building:

$$Dose\,rate_{(a,c,i)} = \left(\frac{BR_{(a,c,i)}}{BW_{(a,c,i)}}\right) \times Mean\ \ Indoor\ \ concentration \times Mean\ occupancy\ \ factor_{block}$$

$$= 0.6\left(\frac{BR_{(a,c,i)}}{BW_{(a,c,i)}}\right) \times Mean\ \ Indoor\ \ concentration$$

(μg/kg per day) ……(5)

where BR is age-specific breathing rate (L min^{-1}); BW is age-specific body weight (kg); a represents adults; c represents child and i represent infant.

For the estimation of the potential health risks of residents living at each floor of the building due to inhalation of $PM_{2.5}/NO_2$:

$$Health\ \ risk(HR)_{(a,c,i)} = \frac{Dose\,rate_{(a,c,i)}}{pollu\tan t\ \ specific\,loael_{(a,c,i)}} \quad \ldots\ldots (6)$$

HR is dimensionless and useful for making relative comparisons.

Table 6.1 Breathing Rates, Body Weights, and Loael Values for Morbidity (Particulate Matter)

Age Group	Inhalation Volume (m^3/day)	Body Weight (kg)	Loael for Morbidity (μg/kg per day)
Adult	20	70	15.7
Children 8-10	10	30	27.5
Children 1-year	3.8	10	20.9
New born	0.8	3	14.7

Source: Cerna et al. (1998)

6.2.1 Comparison of Predicted Health Risk (HR) between a Typical 22 - Storeys Point and a 16 - Storeys Slab Block using the Health Risk Model

The predicted dose rates and the potential health risk (HR) values for a typical 22 - storeys point block and a 16 - storeys slab block are shown in Tables 6.2 and 6.3. Table 6.4 shows the predicted HR values at the different floors of the 22 - storeys point block and the 16 - storeys slab block. For both the blocks, the model analysis indicates that residents at the mid floors of the buildings have the highest health risk for all age categories : infants, children (1 year), children (8 - 10 years) and adults in the mid floor compared to the high (lowest) and low floors (second highest) due to $PM_{2.5}/NO_2$ inhalation. For the point block, the overall mean HR value for $PM_{2.5,}$ NO_2 and combined effect of $PM_{2.5}$ and NO_2 is 0.46 ± 0.14, 1.06 ± 0.18 and 1.52 ± 0.26 respectively whereas for the slab block, the overall mean HR value for $PM_{2.5}$, NO_2 and combined effect of $PM_{2.5}$ and NO_2 is 0.63 ± 0.15, 1.35 ± 0.21 and 1.99 ± 0.27 respectively. For the point block, NO_2 and the combined effect of $PM_{2.5}$ and NO_2 is about 2.3 and 3.3 times more risky than $PM_{2.5}$ respectively and for the slab block, NO_2 and the combined effect of $PM_{2.5}$ and NO_2 is about 2.1 and 3.2 times more risky than $PM_{2.5}$ respectively. Living in a slab block is about 1.37 times more risky due to $PM_{2.5}$ and about 1.27 times more risky due to NO_2 in contracting a respiratory disease compared to living in a point block.

For both the blocks, new born babies, one year old children, and adults had similar potential health risk while teenage children (8 - 10yr) had the lowest potential health risk due to $PM_{2.5}$. The HR values at the mid and low floors of the point block indicate that residents living in these floors had 1.72 - 1.86 and

1.24 - 1.33 times more risk, respectively, in terms of developing respiratory diseases when compared to residents living at the high floors for all age categories. For the slab block, the HR values at the mid and low floors indicate that residents living in these floors had 1.44 - 1.48 and 1.10 - 1.17 times more risk, respectively, in terms of developing respiratory diseases when compared to the residents living at the high floors for all age categories.

One year old children in both the blocks suffer from the highest health risk due to NO_2 inhalation followed by 8 - 10yr old children. New born infants had the least health risk. The HR values at the mid and low floors of the point block indicate that residents living in these floors had 1.15 - 1.24 and 1.06 - 1.13 times more risk, respectively, in terms of developing respiratory diseases when compared to residents living at the high floors for all age categories. For the slab block, the HR values at the mid and low floors indicate that residents living in these floors had 1.15 - 1.17 and 1.08 - 1.11 times more risk, respectively, in terms of developing respiratory diseases when compared to the residents living at the high floors for all age categories.

Table 6.2 Predicted Dose Rates and HR Values Due to $PM_{2.5}/NO_2$ Inhalation Using the Health Risk Model for a Typical 22 - Storeys Point Block

Floor	Dose Rate(μg kg^{-1})				HR(dimensionless)			
	New born	Children (1 yr)	Children (8-10 yr)	Adult	New born	Children (1 yr)	Children (8-10 yr)	Adult
22	4.62 (8.32)	6.59 (11.86)	5.78 (10.40)	4.96 (8.91)	0.31 (0.79)	0.32 (1.13)	0.21 (0.99)	0.31 (0.78)
21	4.78 (8.41)	6.81 (11.98)	5.98 (10.52)	5.12 (9.01)	0.33 (0.80)	0.33 (1.14)	0.22 (1.00)	0.32 (0.80)
20	5.01 (8.53)	7.13 (12.15)	6.26 (10.66)	5.38 (9.13)	0.35 (0.81)	0.34 (1.16)	0.23 (1.01)	0.34 (0.82)
19	5.31 (8.68)	7.57 (12.35)	6.64 (10.83)	5.70 (9.28)	0.36 (0.83)	0.36 (1.18)	0.24 (1.03)	0.36 (0.84)
18	5.71 (8.83)	8.14 (12.58)	7.14 (11.04)	6.12 (9.46)	0.40 (0.84)	0.39 (1.20)	0.26 (1.05)	0.39 (0.86)
17	6.21 (9.02) (5.74)*	8.84 (12.86) (8.18)*	7.76 (11.28) (7.18)*	6.65 (9.67) (6.15)*	0.42 (0.86) (0.39)*	0.42 (1.22) (0.38)*	0.28 (1.07) (0.26)*	0.42 (0.87) (0.40)*
16	6.78 (9.23)	9.67 (13.16)	8.48 (11.54)	7.27 (9.89)	0.45 (0.88)	0.46 (1.25)	0.31 (1.10)	0.46 (0.89)
15	7.41 (9.46)	10.56 (13.48)	9.27 (11.82)	7.94 (10.13)	0.54 (0.90)	0.52 (1.28)	0.34 (1.13)	0.53 (0.93)
14	8.05 (9.69)	11.47 (13.81)	10.06 (12.11)	8.62 (10.39)	0.59 (0.92)	0.58 (1.31)	0.37 (1.15)	0.59 (0.97)
13	8.64 (9.92)	12.32 (14.14)	10.80 (12.40)	9.26 (10.63)	0.62 (0.94)	0.63 (1.35)	0.39 (1.18)	0.61 (1.01)
12	9.13 (10.13)	13.00 (14.43)	11.41 (12.66)	9.78 (10.85)	0.67 (0.96)	0.66 (1.37)	0.41 (1.21)	0.65 (1.03)
11	9.45 (10.3)	13.46 (14.68)	11.81 (12.88)	10.12 (11.03)	0.72 (0.98)	0.70 (1.40)	0.43 (1.22)	0.69 (1.05)
10	9.56 (10.43) (10.41)*	13.62 (14.86) (14.83)*	11.95 (13.04) (13.01)*	10.25 (11.17) (11.15)*	0.77 (0.99) (0.70)*	0.76 (1.42) (0.72)*	0.43 (1.24) (0.47)*	0.75 (1.06) (0.71)*
9	9.47 (10.50)	13.49 (14.97)	11.84 (13.12)	10.15 (11.25)	0.75 (1.00)	0.71 (1.43)	0.43 (1.25)	0.73 (1.07)
8	9.18 (10.52)	13.08 (14.99)	11.47 (13.14)	9.83 (11.27)	0.70 (0.97)	0.65 (1.43)	0.42 (1.25)	0.66 (1.05)
7	8.73 (10.48)	12.44 (14.93)	10.91 (13.10)	9.35 (11.23)	0.66 (0.94)	0.60 (1.39)	0.40 (1.20)	0.60 (1.03)
6	8.18 (10.39)	11.65 (14.80)	10.22 (12.98)	8.76 (11.13)	0.59 (0.92)	0.55 (1.36)	0.37 (1.15)	0.56 (0.99)
5	7.58 (10.25)	10.81 (14.61)	9.48 (12.81)	8.12 (10.99)	0.52 (0.91)	0.51 (1.33)	0.34 (1.12)	0.52 (0.97)
4	7.00 (10.09) (7.68)*	9.98 (14.39) (10.95)*	8.76 (12.62) (9.61)*	7.50 (10.82) (8.24)*	0.49 (0.89) (0.51)*	0.48 (1.29) (0.52)*	0.33 (1.09) (0.36)*	0.49 (0.95) (0.54)*
3	6.48 (9.92)	9.24 (14.13)	8.10 (12.40)	6.95 (10.63)	0.43 (0.87)	0.44 (1.25)	0.29 (1.08)	0.44 (0.92)
2	6.05 (9.74)	8.62 (13.89)	7.56 (12.18)	6.48 (10.44)	0.41 (0.86)	0.41 (1.24)	0.27 (1.07)	0.41 (0.89)
1	5.71 (9.58)	8.13 (13.65)	7.13 (11.98)	6.11 (10.26)	0.39 (0.85)	0.40 (1.22)	0.26 (1.04)	0.39 (0.86)

NB: Values in brackets are due to NO_2 inhalation and the values in bracket with asterisk are due to $PM_{2.5}$ inhalation which are published in Kalaiarasan et al., 2009 using Pandey's Model)

Table 6.3 Predicted Dose Rates and HR Values Due to $PM_{2.5}/NO_2$ Inhalation Using the Health Risk Model for a Typical 16 - Storeys Slab Block

Floor	Dose Rate(μg kg^{-1})				HR(dimensionless)			
	New born	Children (1 yr)	Children (8-10 yr)	Adult	New born	Children (1 yr)	Children (8-10 yr)	Adult
16	7.34 (10.61)	10.47 (15.13)	9.18 (13.27)	7.87 (11.38)	0.49 (1.01)	0.50 (1.44)	0.33 (1.26)	0.50 (1.08)
15	8.15 (10.74)	11.61 (15.30)	10.18 (13.42)	8.72 (11.51)	0.53 (1.02)	0.52 (1.46)	0.35 (1.28)	0.56 (1.10)
14	9.11 (10.90) (8.02)*	12.98 (15.53) (11.43)*	11.38 (13.62) (10.03)*	9.76 (11.68) (10.98)*	0.58 (1.04) (0.55)*	0.55 (1.48) (0.53)*	0.38 (1.30) (0.36)*	0.59 (1.11) (0.56)*
13	10.17 (11.12)	14.49 (15.84)	12.71 (13.90)	10.89 (11.91)	0.63 (1.06)	0.60 (1.51)	0.45 (1.32)	0.62 (1.13)
12	11.21 (11.43)	15.97 (16.27)	14.01 (14.27)	12.01 (12.36)	0.65 (1.09)	0.68 (1.54)	0.48 (1.36)	0.65 (1.16)
11	12.07 (11.80)	17.20 (16.82)	15.09 (14.75)	12.93 (12.65)	0.77 (1.12)	0.77 (1.60)	0.53 (1.41)	0.76 (1.20)
10	12.63 (12.25) (12.99)*	17.99 (17.45) (18.51)*	15.78 (15.31) (16.24)*	13.52 (13.12) (13.92)*	0.86 (1.17) (0.88)*	0.86 (1.66) (0.86)*	0.57 (1.46) (0.59)*	0.86 (1.24) (0.89)*
9	12.78 (12.71)	18.21 (18.11)	15.98 (15.88)	13.69 (13.61)	0.87 (1.21)	0.87 (1.72)	0.58 (1.51)	0.87 (1.30)
8	12.54 (13.10)	17.88 (18.67)	15.68 (16.37)	13.44 (14.03)	0.85 (1.25)	0.86 (1.78)	0.57 (1.56)	0.86 (1.34)
7	12.00 (13.35)	17.10 (19.03)	15.00 (16.69)	12.85 (14.31)	0.82 (1.27)	0.82 (1.81)	0.54 (1.59)	0.82 (1.36)
6	11.28 (13.42)	16.07 (19.13)	14.10 (16.78)	12.08 (14.38)	0.77 (1.28)	0.77 (1.82)	0.51 (1.53)	0.77 (1.37)
5	10.53 (13.31)	15.01 (18.97)	13.17 (16.64)	11.29 (14.26)	0.72 (1.22)	0.72 (1.75)	0.48 (1.49)	0.72 (1.32)
4	9.89 (13.07) (8.02)*	14.10 (18.63) (14.61)*	12.37 (16.34) (12.81)*	10.60 (14.00) (10.98)*	0.67 (1.18) (0.70)*	0.67 (1.65) (0.69)*	0.44 (1.56) (0.47)*	0.68 (1.29) (0.68)*
3	9.41 (12.77)	13.42 (18.20)	11.77 (15.96)	10.09 (13.68)	0.64 (1.16)	0.64 (1.62)	0.42 (1.46)	0.64 (1.26)
2	9.12 (12.48)	13.00 (17.79)	11.40 (15.60)	9.77 (13.37)	0.62 (1.13)	0.62 (1.59)	0.41 (1.43)	0.62 (1.23)
1	8.98 (12.26)	12.80 (17.47)	11.23 (15.32)	9.63 (13.12)	0.61 (1.11)	0.61 (1.53)	0.40 (1.41)	0.61 (1.20)

NB: Values in brackets are due to NO_2 inhalation and the values in bracket with asterisk are due to $PM_{2.5}$ inhalation which are published in Kalaiarasan et al., 2009 using Pandey's Model)

Table 6.4 Predicted HR Values at the Different Floors Risk Model of the 22 - Storeys Point Block and 16 - Storeys Slab Block Using the Health Model

	Point Block							
	HR for $PM_{2.5}$ (dimensionless)				**HR for NO_2 (dimensionless)**			
Floor	**New born**	**Children (1 yr)**	**Children (8-10 yr)**	**Adult**	**New born**	**Children (1 yr)**	**Children (8-10 yr)**	**Adult**
Low floor	0.48 ± 0.05	0.47 ± 0.04	0.33 ± 0.05	0.49 ± 0.02	0.90 ± 0.02	1.29 ± 0.04	1.10 ± 0.01	0.94 ± 0.03
Mid floor	0.67 ± 0.03	0.66 ± 0.03	0.43 ± 0.04	0.65 ± 0.04	0.98 ± 0.02	1.37 ± 0.03	1.20 ± 0.02	1.03 ± 0.01
High floor	0.36 ± 0.05	0.38 ± 0.04	0.25 ± 0.04	0.37 ± 0.05	0.83 ± 0.03	1.18 ± 0.02	1.04 ± 0.03	0.83 ± 0.03
$HR_{mid\ floor}/HR_{high\ floor}$	1.86	1.74	1.72	1.76	1.18	1.16	1.15	1.24
$HR_{low\ floor}/HR_{high\ floor}$	1.33	1.24	1.32	1.32	1.08	1.09	1.06	1.13
	Slab Block							
Low floor	0.68 ± 0.02	0.66 ± 0.03	0.43 ± 0.03	0.65 ± 0.04	1.14 ± 0.04	1.62 ± 0.03	1.44 ± 0.05	1.23 ± 0.04
Mid floor	0.84 ± 0.03	0.83 ± 0.04	0.56 ± 0.02	0.83 ± 0.03	1.21 ± 0.04	1.73 ± 0.02	1.52 ± 0.04	1.30 ± 0.04
High floor	0.58 ± 0.04	0.57 ± 0.03	0.39 ± 0.03	0.58 ± 0.02	1.04 ± 0.03	1.49 ± 0.04	1.30 ± 0.03	1.12 ± 0.03
$HR_{mid\ floor}/HR_{high\ floor}$	1.44	1.46	1.44	1.48	1.15	1.16	1.17	1.16
$HR_{low\ floor}/HR_{high\ floor}$	1.17	1.16	1.10	1.12	1.10	1.08	1.11	1.10

6.3 Conclusion

6.3.1 Health Risk Assessment Using Health Risk Model

The health risk model show for both the blocks, residents at the mid floors of the buildings have the highest health risk for all age categories: infants, children (1 yr), children (8 - 10 yr) and adults in the mid floor compared to the high (lowest) and low floors (second highest) due to $PM_{2.5}/NO_2$ inhalation. This was expected since the highest concentration of to $PM_{2.5}/NO_2$ concentration occurred at the mid floors of the buildings. For both the blocks, new born babies, one year old children, and adults had similar potential health risk while teenage children (8 - 10yr) had the lowest potential health risk due to $PM_{2.5}$ inhalation. For NO_2 inhalation, one year old children in both the blocks suffer from the highest health risk followed by 8 - 10yr old children. New born infants had the least health risk. The health risk model results also showed that for the point block, NO_2 and the combined effect of $PM_{2.5}$ and NO_2 is about 2.3 and 3.3 times more risky than $PM_{2.5}$ respectively and for the slab block, NO_2 and the combined effect of $PM_{2.5}$ and NO_2 is about 2.1 and 3.2 times more risky than $PM_{2.5}$ respectively. Living in a slab block is about 1.37 times more risky due to $PM_{2.5}$ and about 1.27 times more risky due to NO_2 in contracting a respiratory disease compared to living in a point block.

CHAPTER 7: CONCLUSIONS

7.1 Introduction

Existing studies show traffic-generated $PM_{2.5}$/NO_2 are readily inhalable and can penetrate deep into the cardiovascular and respiratory system and cause ill health. Their physical and chemical properties have a strong association with most types of respiratory illness and even mortality. Most of the previous and on-going researches on $PM_{2.5}$/NO_2 are mainly done in the United States of America, Europe, Australia and Asian countries like Hong Kong and China. Only a handful of these studies relate to the vertical distribution profile of $PM_{2.5}$/NO_2 concentration in high-rise buildings which were mainly air-conditioned or partially air-conditioned. In addition, most of these studies were done in temperate, semi-tropical or in dry climatic conditions. In this study, the buildings were naturally-ventilated high-rise residential buildings and the climatic condition was tropical i.e. hot and humid. The results of other studies may not be directly applicable to the local condition of Singapore due to differences in climatology, topography of the streets, building designs and ventilation strategies. The findings in this study can be very useful to building and town planning practitioners of highly urbanized cities and megacities for design and policy making for future cities. This chapter concludes the study by providing a summary of all important findings and recommends future research direction in this area.

7.2 Review and Achievement of Research Objectives

7.2.1 First Objective

7.2.1.1 To investigate the vertical distribution profile of traffic-generated fine particulate matter/NO_2 in the residential buildings of urban areas

The 6 case studies selected for this study provided a variety of settings to be investigated and the findings are comprehensive and substantial enough to draw some sound conclusions. Generally, traffic-generated $PM_{2.5}$ concentrations measured at three sites from the same precinct (Case Studies 1 - 3) showed that the daily mean outdoor $PM_{2.5}$ mass/number concentration of a building was highest at its mid floors when compared to those measured at low and high floors of the building. The low floor of the building had the second highest mass/number concentration whilst its high floor had the least mass/number concentration level. The vertical distribution profile of the traffic-generated $PM_{2.5}$ mass/number concentration could be influenced by the row of trees and vegetation planted along the expressway. In other studies, there were no trees and vegetation present in between the motorways and buildings which is unique in Singapore's town planning when the residential high-rise buildings are close to expressways.

In Case Studies 4 - 6, the shape of the weekly mean indoor and outdoor vertical distribution profile of NO_2 concentration in a building resembled that of a 'bell curve' with its abscissa in the vertical direction. Generally, the weekly mean indoor and outdoor peak concentration of NO_2 generally occurred just above the tree tops i.e. about 2 - 3 storeys. Residents living at

these floors could be exposed to a higher concentration of traffic- generated NO_2. Statistical results showed there was a fairly good positive correlation between NO_2 concentration and $PM_{2.5}$ number concentration at the floor where NO_2 concentration was measured the highest. The results indicate NO_2 can be used as a surrogate indicator for traffic-generated $PM_{2.5}$ mass/number concentration. The I/O ratio of NO_2 concentration in a building was less than unity. The results indicated the transport of NO_2 was from outdoors to indoors rather than from internal sources. The main outdoor source of NO_2 is from the nearby traffic. The I/O ratio values of NO_2 concentration in a slab block was comparatively lower than that of a point block suggesting that slab block's façade design has a better filtering effect of traffic-generated NO_2 compared to a point block's façade.

7.2.2 Second Objective

7.2.2.1 To assess the health impacts associated with traffic-generated $PM_{2.5}$

7.2.2.1.1 Physical Characteristics

The daily mean $PM_{2.5}$ mass concentration at the various floors of all the buildings (Case Studies 1 - 3) exceeded either the $PM_{2.5}$ NAAQS annual average of 15μg/m^3 or the 24hr value of 35μg/m^3. Similarly, the weekly mean NO_2 concentration levels at the various floors of all the buildings in Case Studies 4 - 6 has exceeded the WHO (2005) maximum allowable annual mean value of 40μg/m^3. This is of major concern since the health of residents including the "sensitive" population such as asthmatics, children, and the elderly will be affected. For the point and slab block designs, this study

showed the $PM_{2.5}$ number concentration comprised about 93 - 95% of the particles fall below the size range of 0.65µm while the rest 5 - 7% of the particles were in the size range of 0.65 - 1.6µm. The size distribution show that majority of the traffic-generated $PM_{2.5}$ has a very high chance of penetrating deeper into the lungs. Toxicological studies have shown fine and ultra fine particles have considerably enhanced toxicity per unit mass and their toxicity increased as particle size decrease. Residents living close to the expressway have a high chance of developing cancer or respiratory disease. This was supported by the health risk models used in the study.

7.2.2.1.2 Chemical Characteristics

Detailed chemical analyses on $PM_{2.5}$ were performed for Case Studies 1 - 3. For all the case studies, the daily mean OC/EC ratio values for the all the floors were less than the expected value of 3.7 for traffic emissions suggesting most of the particulate matter were from the nearby traffic. This was supported by the values of the BPe/Ind ratio in Case Studies 2 and 3 which also suggested a mixture of both diesel and petrol engine type of vehicles contributed pollution to both the point and slab blocks. No secondary organic aerosols were present since OC/EC ratio was less than 2. The good correlation EC and OC mass concentrations suggested OC and EC came from the same anthropogenic source.

For all the buildings, Na^+, NH_4^+, Ca^{2+}, K^+, Cl^-, NO_3^-, SO_4^{2-} and PO_4^{3-} were detected. Although studies have shown inorganic compounds can cause small adverse health effects to people, they may also facilitate the toxicity of other compounds. For example, sulphate does not act as a direct toxicant, but

facilitates the toxicity of reactive metal constituents e.g. it may play a role in the generation of ROS by functioning as a ligand for particle associated iron. WS trace metals such as Cr, Ni, Cd, Co and Pb were detected in all the samples of the point and slab blocks. IARC has classified Cr together with Ni, Cd and arsenic as known human carcinogens and two others, Pb and cobolt, as probable human carcinogens. Since WS trace metal compounds are present in the fine fraction, they can penetrate deep into the lungs and may cause serious pollution-related respiratory health problems. The dominant particulate PAHs measured at the buildings are Nap, Acy, BbF, Phe, Flt and BPe. Many studies have reported the mutagenic or carcinogenic effects of PAHs. IARC has identified BaA, BaP, DBA, BkF, Ind, BbF and Nap to be carcinogenic compounds. Chemical analysis of the traffic-generated particles shows the toxicity of these particles. For all the buildings, the nss-sulphates over the total sulphate in $PM_{2.5}$ were over 93% at the different floors of the buildings indicating a substantial anthropogenic origin. The concentrations of Na^+ and Cl^- showed both ions correlated well suggesting their origin may be due to sea salt.

The results in the point block showed that the seven major components accounted for about 88% of $PM_{2.5}$ mass for the low floor, 95% for the mid floor and 80% for the high floor of the block. The major components on site were organic matter (29 - 38%), elemental carbon (12 - 23%) and sulphate (9 - 14%). Carbonaceous species alone accounted for about 50% of $PM_{2.5}$ mass for the low floor, 61% for the mid floor and 41% for the high floor of the block. For the slab block, the seven major components of the reconstructed $PM_{2.5}$ mass accounted for about 89% of $PM_{2.5}$ mass for the low floor, 89% for the

mid floor and 90% for the high floor of the block. The major components of the site were organic matter (32 - 36%), elemental carbon (32 - 37%) and sulphate (7 - 12%). Carbonaceous species alone accounted for about 68% of $PM_{2.5}$ mass for the low floor, 70% for the mid floor and 69% for the high floor of the block. It can be seen that traffic-generated $PM_{2.5}$ contribute to a large extent to the toxicity of outdoor aerosols.

7.2.3 Third Objective

7.2.3.1 To study the effect of building configuration on the transmission of airborne $PM_{2.5}/NO_2$ to the buildings.

The study showed that two types of building configuration, slab and point blocks, do not have any effect on the vertical distribution profiles of $PM_{2.5}$ mass/number and NO_2 concentrations. The only difference between the vertical distribution profiles of $PM_{2.5}$ mass/number and NO_2 concentrations is that at corresponding floors, the mass or number concentration of $PM_{2.5}/NO_2$ for the slab block configuration was much higher than that of the point block configuration under similar traffic and meteorological conditions. This could be attributed to the configuration of the blocks. The observational data show the slab block tends to slow down the approaching wind, thus allowing the accumulation of the $PM_{2.5}/NO_2$ in front of the building.

7.2.4 Fourth Objective

7.2.4.1 To examine and recommend measures and design principles to minimize the transmission of traffic-generated pollution from expressways to naturally-ventilated residential buildings

After reviewing field and CFD results, the following measures and design principles are proposed as follow:

a) Trees help to intercept traffic-generated $PM_{2.5}/NO_2$ or modify the airflow patterns flowing towards the building resulting in highest concentration of $PM_{2.5}/NO_2$ to occur just above the tree tops i.e. about 1 - 3 storeys above the tree tops. In future buildings' design, it is recommended that residential buildings should have more free air passages at a storey or two above the tree tops levels like intermediate roof garden so as to suppress any $PM_{2.5}/NO_2$ peaks at these floors. Above the mid floors, dilution effect of the wind will help to further reduce the traffic-generated $PM_{2.5}/NO_2$ concentration as the height of the building increases.

b) Configuration of the buildings does not change the vertical distribution profiles of $PM_{2.5}/NO_2$ concentration. It was found that in a slab block design, the mass/number concentration of $PM_{2.5}/NO_2$ concentration was much higher than that of the point block at the corresponding floors. Comparatively, a point block configuration is a much better than that of a slab block in terms of potential respiratory health risk problems. Since a point block (4 households per horizontal floor of which only two households are facing the expressway) has lesser

households than a slab block (18 - 20 households per horizontal floor), lesser residents would be exposed to traffic-generated $PM_{2.5}/NO_2$ if the point block configuration was adopted for future housing designs close to major roads or expressways. To house more residents, taller point block designs could be considered.

c) The single row of trees and vegetation planted along the expressway has shown to be effective in mitigating the traffic-generated NO_2 at the low floors of the buildings. For example, there was a decrease of about 7 - 9% in the weekly mean concentration of NO_2 just before and after the trees and a further 6 - 17% from the trees to the building facades. The case studies cover distances from 15 - 20m. In order to mitigate traffic-generated $PM_{2.5}/NO_2$ inhalation, more rows of trees could be planted in between the expressways and buildings.

7.2.5 Fifth Objective

7.2.5.1 To assess the health risk of residents using health risk model due to exposure to traffic-generated $PM_{2.5}/NO_2$ in naturally-ventilated high-rise residential buildings close to expressways

The health risk model show for the point and slab blocks, infants to adults at the mid floors of the buildings have the highest health risk of contracting a respiratory disease due to $PM_{2.5}/NO_2$ inhalation. This was expected since the highest concentration of to $PM_{2.5}/NO_2$ concentration occurred at the mid floors of the buildings. Regardless the configuration of the block, teenage children of age 8 - 10yr had the lowest potential health risk due to $PM_{2.5}$ inhalation while infants, one year old children and adults had similar health risk. For NO_2

inhalation, one year old children in the point and slab blocks suffer from the highest health risk followed by 8 - 10yr old children. New born infants and adults had the least health risk. The health risk model results also showed that for the point block, NO_2 and the combined effect of $PM_{2.5}$ and NO_2 is about 2.3 and 3.3 times more risky than $PM_{2.5}$ respectively and for the slab block, NO_2 and the combined effect of $PM_{2.5}$ and NO_2 is about 2.1 and 3.2 times more risky than $PM_{2.5}$ respectively. Living in a slab block is about 1.37 times more risky due to $PM_{2.5}$ and about 1.27 times more risky due to NO_2 in contracting a respiratory disease compared to living in a point block.

7.3 Recommendations for Future Work

a) A study on the vertical distribution profile of traffic-generated $PM_{2.5}/NO_2$ in naturally-ventilated high-rise buildings at different downstream distances from the expressway would provide useful information at which downstream distance traffic-generated pollution becomes acceptable in terms of health risk of residents residing in the building. This study would be useful for policy makers.

b) Up drafts and airflow around the buildings need to be measured in detail so as to obtain a better picture of the airflow around the building.

c) CFD analysis would yield a better solution if trees were included in the simulation. A model with the capability of simulating how $PM_{2.5}$ dispersed and the migration from the motor vehicles to the different floors of the building should be developed to assist future study.

d) A comparative study on naturally-ventilated high-rise residential buildings surrounded with abundant greenery near the expressway with those in this study would yield useful information for policy makers and epidemiological studies.

e) For the health risk model, loael values for morbidity, inhalation volume and body weights of the various age groups in Singapore need to be determined for more accurate and representative estimates of health risk of residents living in naturally-ventilated high-rise residential buildings close to expressways.

REFERENCES

Airmetrics (2009). www.airmetrics.com.

American Lung Association (1994). The perils of particulates: An estimation of populations at risk of adverse health consequences from particulate matter in areas with particulate matter levels above the national ambient air quality standards of the Clean Air Act, American Lung Association: New York.

Andersen, I., (1972). Relationships between outdoor and indoor air pollution, Atmospheric Environment, Vol 6, pp. 275-278.

Appel, B. R., Tokiwa, Y., and Kothny, E.L., (1983). Sampling of carbonaceous particles in the atmosphere. Atmospheric Environment, Vol 17, pp. 1787-1796.

Balasubramanian, R, Qian, W.-B., Decesari, S., Facchini, M.C., and Fuzzi, S., (2003). Comprehensive characterization of $PM_{2.5}$ aerosols in Singapore, Journal of Geophysical Research,Vol 108(D16), pp. AAC 7-1.

Baron P.A., & Willeke, K. (Eds), (2001). Aerosol measurement: Principles, Techniques and Applications, New York: Wiley-Interscience.

Beak, S.O., Goldstone, M.E., Kirk, P.W.W., Lester, J.N., and Perry, R., (1991). Phase distribution and particle size dependency of polycyclic aromatic hydrocarbons in the urban atmosphere, Chemosphere, Vol 22, pp. 503-550.

Beckerman, B., Jerrett, M., Brook,J.R., Verma, D.K., Arain, M.A., Finkelstein, M.M., (2008). Correlation of nitrogen dioxide with other traffic pollutants near a major expressway, Atmospheric Environment, Vol 42, pp. 275-290.

Beckett, K.P., Freer-Smith, P., and Taylor, G., (2000). Effective tree species for local air quality management, Journal of Arboriculture, Vol 26(1), pp. 12-19.

Béghein, C., Y. Jiangm Y., and Chen, Q.Y., (2005). Using large eddy simulation to study particle motions in a room, Indoor Air, Vol 15(4), pp.281-90.

Benson, F.B., Henderson, J.J., and Caldwell, D.E., (1972). Indoor–outdoor air pollution relationships: a literature review, U.S. Environmental Protection Agency.

Berico, M., Luciani, A., and Formignani, M., (1997). Atmospheric aerosol in an urban area -measurements of TSP and PM_{10} standards and pulmonary deposition assessments, Atmospheric Environment, Vol 31, pp. 3659-3665.

Bérubé, K.A., Jones, T.P., Williamson, B.J., Winters, C., Morgan, A.J., and Richards, R.J., (1999). Physicochemical characterisation of diesel exhaust particles: Factors for assessing biological activity, Atmospheric Environment, Vol 33, pp.1599-1614.

Blocken, B., Stathopoulos, T., Saathoff, P., and Wang, X., (2008). Numerical evaluation of pollutant dispersion in the built environment: comparisons between models and experiments, Journal of Wind Eng. Ind. Aerodynamics Vol 96(10-11), pp. 1817-1831.

Bracho, L.R., Suh, H.H, Oyola, P., and Koutrakis, P., (2002). Measurements of children's exposures to particles and nitrogen dioxide in Santiago, Chile, The Science of the Total Environment, Vol 287, pp. 249-264.

Bree L. van, and Cassee, F.R., (2000). Toxicity of ambient PM10. A critical review of potentially caysitive PM properties and mechanisms associated with health effects, RIVM report no. 650010015.

Bruinen de Bruin, Y., Hanninen, O., Carrer, P., Maroni, M., Kephalopoulos, S., di Marco, G.S., and Jantunen, M., (2004). Simulation of working population exposures to carbon monoxide using EXPOLIS-Milan microenvironment concentration and time-activity data. Journal of Exposure Analysis and Environmental Epidemiology, Vol 14, pp.154-163.

Brunekreef B. (2000). Plenary lecture, European Aerosol Conference.

Burke, J.M., Zufall, M.J., and Ozkaynak, H., (2001). A population exposure model for particulate matter: case study results for PM2.5 in Philadelphia, PA, Journal of Exposure Analysis and Environmental Epidemiology, Vol 11, pp. 470-489.

Burnett, R.T., Cakmak, S., and Brook, J.R., (1998). The effect of the urban ambient air pollution mix on daily mortality rates in 11 Canadian cities, Canadian Journal of Public Health, Vol 89, pp. 152-156.

Burr, M.L., Karani, G., Davies, B., Holmes, B.A., and Williams, K.L., (2004). Effects on respiratory health of a reduction in air pollution from vehicle exhaust emissions, Occupational and Environmental Medicine, Vol 61, pp. 212-218.

Buzorius, G., Hämeri, K., Pekkanen, J., Kulmala, M., (1999). Spatial variation of aerosol number concentration in Helsinki city, Atmospheric Environment, Vol 33, pp. 553-565.

Cabada, J.C., and Pandis, S.N., (2002). Sources of atmospheric carbonaceous particulate matter in Pittsburgh, Pennsylvania, Journal of the Air & Waste Management Association, Vol 52, pp. 732-741.

Calvert, J.B., (2004). Wind: an exploration of the wind http://mysite.du.edu/~jcalvert/etuttle/weather/wind.htm.

Campbell, A., (2004). Inflammation, neurodegenerative diseases, and environmental exposures, Annals of New York Academy of Sciences, Vol 1035, pp.117-132.

Caselles, J., Colliga, C., and P. Zornoza, P., (2002). Evaluation of trace element pollution from vehicle emissions in petunia plants, Water, Air and Soil Pollution, Vol 136, pp.1-9.

Castellano, A.V., Cancio, J.L., Alemán, P.S., and Rodríguez, J.S., (2003). Polycyclic aromatic hydrocarbons in ambient air particles in the city of Las Palmas de Gran Canaria, Environment International, Vol 29, pp. 475-80.

Celis, J.E., Morales, J.R., Zaror, C.A., and Inzunza, J.C., (2004). A study of the particulate matter PM_{10} composition in the atmosphere of Chillán, Chile, Chemosphere, Vol 54, pp. 541-550.

Cerna, M., Jelinek, R., Janoutova, J., Kotesovec, F., Benes, I, and Leixner, M., (1998). Risk assessment of the common air pollutants in Teplice, Czech Republic, Toxicology Letters**,** Vol 96(97), pp. 203-208.

Chan, A.T., (2002). Indoor-outdoor relationships of PM and nitrogen oxides under different outdoor meteorological conditions, Atmospheric Environment, Vol 36, pp.1543-1551.

Chan, L.Y., and Kwok, W.S., (2000). Vertical dispersion of suspended particulates in urban area of Hong Kong, Atmospheric Environment, Vol 34, pp. 4403-4412.

Chao, C.Y.H., and Law, A., (2000). A study of personal exposure to nitrogen dioxide using passive samplers, Building and Environment, Vol 35, pp. 545-553.

Chao, C.Y.H., (2001). Comparison between indoor and outdoor air contaminant levels in residential buildings from passive sampler study, Building and Environment, Vol 36, pp. 999-1007.

Chao, C. and Wong, K., (2002). Residential indoor PM_{10} and $PM_{2.5}$ in Hong Kong and the elemental composition. Atmospheric Environment, Vol 36, pp. 265-77.

Chapman, R.S., Watkinson, W.P., Dreher, K.L., and Costa, D.L., (1997). Ambient particulate matter and respiratory and cardiovascular illness in adults: particle-borne transition metals and the heart-lung axis, Environment Toxicology Pharmacology, Vol 4, pp. 331-338.

Charron, A., and Harrison, R.M., (2000). Fine ($PM_{2.5}$) and coarse ($PM_{2.5-10}$) particulate matter on a heavily trafficked London highway: sources and processes, Occupatinal and Environmental Medicine, Vol 57, pp. 818-822.

Chaix, B., Gustafsson, S., Jerrett, M., Kristersson, H., Lithman, T., Boalt, A., and Merlo, J., (2006). Children's exposure to nitrogen dioxide in Sweden: investigating environmental injustice in an egalitarian country, Journal of Epidemiology and Community Health, Vol 60(3) , pp. 234-241.

Cheng, Z.L., Lam, K.S., Chan, L.Y.,Wang, T., and Cheng, K.K., (2000). Chemical characteristics of aerosols at coastal station in Hong Kong. I. Seasonal variation of major ions, halogens and mineral dusts between 1995 and 1996, Atmospheric Environment, Vol 34, pp. 2771-2783.

Chow, J.C.,Watson, J.G., Lu, Z., Lowenthal, D.H., Frazier, C.A., Solomon, P.A., Thuillier, R.H., Magliano, K., (1996). Descriptive analysis of $PM_{2.5}$ and PM_{10} at regionally representative locations during SJVAQS/AUSPEX, Atmospheric Environment**,** Vol 30, pp. 2079-2112.

Christchurch City Council (2009). City of Christchurch City Plan. Special Purpose (Road) Zone http://www.cityplan.ccc.govt.nz.

Chung, K.C., (1999). Three-dimensional analysis of airflow and contaminant particle transport in a partitioned enclosure, Building Environment, Vol 34, pp.7–17.

Churg, A., and Brauer, M.,(1997). Human lung parenchyma retains $PM_{2.5}$, American Journal of Respiratory and Critical Care Medicine, Vol 155, pp. 2109-2111.

Cleugh H.A., (1998). Effects of windbreaks on airflow, microclimates and crop yields, Agroforestry Systems, Vol 41, pp. 55-84.

Colls, J.J., and Micallef, A., (1997). Towards better human exposure estimates for setting of air quality standards, Atmospheric Environment, Vol 31, pp. 4253-4254.

Costabile, F., Wang, F., Hong, W., Liu, F., and I. Allegrini, I., (2006). Spatial distribution of traffic air pollution and evaluation of transport vehicle emission dispersion in ambient air in urban areas, JSME International Journal, Series 1, Vol 18, No. 1.

Cuhadaroglu, B., and Demirci, E., (1997). Influence of some meteorological factors on air pollution in Trabzon city, Energy and Buildings, Vol 25, pp. 179-184.

Danish, S., and Madany, I.M., (1992). Concentrations of nitrogen dioxide throughout the state of Bahrain, Environmental Pollution, Vol 77(1), pp. 71-8.

Department of Statistic, Singapore (2009). http://www.singstat.gov.sg.

Diabaté, (2000). Proceedings of the conference: Aerosol and health, Forschungszentrum Karlsruhe, Techniek and Umwelt, 28-29 June.

Dockery, D.W., Pope, C.A., III, Xu, X., Spengler, J.D., Ware, J.H., Fay, M.E., et al., (1993). An association between air pollution and mortality in six U.S. cities, New England Journal of Medicine, Vol 329(24), pp.1753–1759.

Doll, R., and Peto, R., (1981). The causes of cancer; quantitative estimates of the avoidable risks of cancer in the United States today, Journal of the National Cancer Institute (JNCI), Vol 66, pp.1191-1308.

Donaldson K., and MacNee, W., (1998). The mechanism of lung injury caused by PM_{10}. Issues in Environmental Science and Technology, Vol 10, pp. 21–32.

Donaldson, K., and Tran,C.L., (2002). Inflammation caused by particles and fibers, Inhalation Toxicology, Vol 14, pp. 5-27.

Duan, N., (1982). Models for human exposure to air pollution, Environment International, Vol 8, pp. 305-309.

Duffin, R., Tran, L., Brown, D., Stone, V., and Donaldson, K., (2007). Proinflammogenic effects of low-toxicity and metal nanoparticles in vivo and in vitro: highlighting the role of particle surface area and surface reactivity, Inhalation Toxicology, Vol 19(10), pp.849-856.

Ekberg, L.E., (1996). Relationships between indoor and outdoor contaminants in mechanically ventilated buildings, Indoor Air**,** Vol 6, pp. 41-47.

Eldred, R.A., Cahill, T.A., Pitchford, M., and Malm, W.C., (1988). IMPROVE-a new remote area particulate monitoring system for visibility studies, Proceedings of the 81st Annual Meeting of APCA, Dallas, Texas.

Elminir, H.K., (2005). Dependence of urban air pollutants on meteorology, Science of the Total Environment, Vol 350 (1–3) , pp. 225-237.

Encyclopedia of Britannica (2009). High-Rise Building.
http://www.britannica.com/EBchecked/topic/265364/high-rise-building.

Endalew, A.M., Hertog, M., Gebreslasie, M.G., Baelmans, M., Ramon, H., Nicolaï, B.M., and Verboven, P.,(2009). Modelling airflow within model plant canopies using an integrated approach, Computers and Electronics in Agriculture, Vol 66, pp. 9-24.

EPA Victoria (2009). Motor vehicle emissions and air quality, Environment Protection Authority Victoria's, Australia.
http://www.epa.vic.gov.au/air/vehicles/vehicle_emissions.asp.

Etkin, D.S. (1994). Particulates in the indoor environment: Characterization and health effects, Cutter Information Corp., MA, USA.

Fairley, D., (1999). Daily Mortality and Air Pollution in Santa Clara County, California: 1989-1996, Environmental Health Perspectives, Vol 107, pp.637-641.

Fang, G-C, Chang, K-F, Lu, C., and Bai, H, (2004). Estimation of PAHs dry deposition and BaP toxic equivalency factors (TEFs) study at Urban, Industry Park and rural sampling sites in central Taiwan, Taichung, Chemosphere, Vol 55, pp. 787-96.

Frampton, M.W., Ghio, A.J., Samet, J.M., Carson, J.L., Carter , J.D., and Devlin, R.B., (1999). Effects of aqueous extracts of PM10 filters from Utah Valley on human airway epithelial cells, American Journal on Physiology, Vol 277, pp. 960-967.

Fung, J.C.H., Yim, S.H.L., and Karl, A., (2009).Air ventilation assessment of the Oil Street Planning Area by CFD approach. http://envf.ust.hk/documents/oil_street_study_report.pdf.

Gao, Y., Nelson, E.D., Fielda, M.P., Ding, Q., Li, H., Sherrell, R.M., Gigliotti, C.L.,Van, D.A., Glenn, T.R., and Eisenreich, S.J., (2002). Characterization of atmospheric trace elements on $PM_{2.5}$ particulate matter over the New York-New Jersey harbor estuary, Atmospheric Environment, Vol 36, pp. 1077-1086.

Gietl, J.K., and Klemm, O., (1995). Analysis of traffic and meteorology on airborne particulate matter in Münster, northwest Germany, Journal of the Air & Waste Management Association (1995), Vol 59(7), pp.809-18.

Gilbert, N.L., Woodhouse, S., Stieb, D.M., and Brook, J.R., (2003). Ambient nitrogen dioxide and distance from a major highway. Science of the Total Environment, Vol 312, pp. 43-6.

Ghio, A.J., Stoneheurner, J., McGee, J.K., and Kinsey, J.S., (1999). Sulfate content correlates with iron concentrations in ambient air pollution particles, Inhalation Toxicology: International Forum for Respiratory Research, Vol 11, pp. 293-307.

Goldsmith, C. A., Imrich, A., Danaee, H., Ning, Y. Y., and Kobzik, L., (1998). Analysis of air pollution particulate-mediated oxidant stress in alveolar macrophages, Journal of Toxicology and Environmental Health, Part A, Vol 54, pp. 529-545.

Gordon, T., Nadziejko, C., Schlesinger, R., and Chen, L.C., (1998). Pulmonary and cardiovascular effects of acute exposure to concentrated ambient particulate matter in rats, Toxicology Letters, Vol 96-97, pp. 285-288.

Graham, S.E., and Burke, J.M.(2004). Human exposure modeling for air pollutants using SHEDS, Washington State University.

Grimm Technologies, Inc. (2009). www.grimm-aerosol.com.

Gross, (1987). A numerical study of the air flow within and around a single tree, Boundary-Layer Meteorology, Vol 40, pp.311-327.

Giugliano, M., Lonati, G., Butelli, P., Romele, L., Tardivo, R., and Grosso, M., (2005). Fine particulate matter ($PM_{2.5}$-PM_1) at urban sites with different traffic exposure, Atmospheric Environment, Vol 39, pp. 2421-2431.

Gunnarsen, L., and Fanger, P.O., (1992). Adaption to indoor air pollution, Environmental International, Vol 18, pp. 43-54.

Gupta, A., Cheong, K.W.D., and Wong, N.H., (2003). Characterization of particulate matter in the tropics, International Conference on Healthy Building, Vol 2, pp. 140-146.

Gupta, A., and Cheong, K.W.D., (2007). Physical characterization of particulate matter and ambient meteorological parameters at different indoor-outdoor locations in Singapore, Building and Environment**,** Vol 42, pp. 237-245.

Gupta, A.K., Patil, R.S., and Gupta, S.K., (2004). A statistical analysis of particulate data sets for Jawaharlal Nehru Port and surrounding harbour region in India, Environment Monitoring and Assessment, Vol 95 (1-3), pp. 295-309.

Gupta, A. K., Subhankar, N., and Mukhopadhyay U. K., (2006). Characterisation of PM_{10}, $PM_{2.5}$ and benzene soluble organic fraction of particulate matter in an urban area of Kolkata, India, Environmental Monitoring and Assessment, Vol 115, pp. 205-222.

Hagenbjork-Gustafsson, A., Forsberg, B., Hestvikg, G., Karlsson, D., Wahlberg, S., and Sandstrom, T., (1996). Measurements of indoor and outdoor nitrogen dioxide concentrations using a diffusive sampler, International Symposium on Modern Principles of Air Monitoring, Vol 121, pp. 1151-1304.

Hanninen, O., Kruize, H., Lebret, E., and Jantunen, M. (2003). EXPOLIS simulation model: $PM_{2.5}$ application and comparison with measurements in Helsinki, Journal of Exposure Analysis and Environmental Epidemiology, Vol 13**,** pp**.** 74-85.

Hänninen, O., Brüske-Hohlfeld, I., Loh, M., Stoeger, T., Kreyling, W., Schmid, O., and Peters, A., (2009). Estimation of health risks and safety margins due to inhalation of ultrafine particles and nanoparticles in selected occupational, consumer and environmental settings, Journal of Physics: Conference Series, Vol 170**.** 012031doi:10.1088/1742-6596/170/1/012031.

Hänninen, O., Lebret, E., Ilacqua, V., Katsouyanni, K., Künzli, N., Srám, R. J., and Jantunen, M .J. (2004). Infiltration of ambient $PM_{2.5}$ and levels of indoor generated non-ETS $PM_{2.5}$ in residences of four European cities, Atmospheric Environment, Vol 38, pp. 6411-6423.

Hargreaves, P.R., Leidi, A., Grubb, H.J., Howe, M.T., and Mugglestone, M.A., (2000). Local and seasonal variations in atmospheric nitrogen dioxide levels at Rothamasted, UK, and relationships with meteorological conditions, Atmospheric Environment Vol 34, pp. 843-853.

Harrison, R.M., (2004). Key pollutants-Airborne particles. Science of the Total Environment, Vol 334-335, pp. 3-8.

Harrison, R.M., Jones, A.M., and Barrowcliffe, R., (2004). Field study of the influence of meteorological factors and traffic volumes upon suspended particle mass at urban roadside sites of differing geometries, Atmospheric Environment, Vol 38, pp. 6361-6369.

Hazenkamp-von Arx, M.E., Götschi, T., Ackermann-Liebrich, U., Bono, R., Burney,P., Cyrys, J., Jarvis, D., Lillienberg, L., Luczynska, C., Maldonado,J.A., Jaén, A., Roberto de Marco, Mi, Y., Modig, L., Bayer-Oglesby,L., Payo, F., Soon, A., Sunyer, J., Villani, S., Weyler, J., and Künzli, N., (2004). $PM_{2.5}$ and NO_2 assessment in 21 European study centres of ECRHS II: annual means and seasonal differences. Atmospheric Environment, Vol 38, pp. 1943-1953.

Heal, M.R., Hibbs, L.R., Agius, R.M., and I.J. Beverland, I.J. (2005). Total and water-soluble trace metal content of urban background $PM_{2.5}$, PM_{10} and black smoke in Edinburgh, UK, Atmospheric Environment, Vol 39, pp. 1417-1430.

Hester, R.E. and Harrison, R.M., (1998). Air pollution and health, The Royal Society of Chemistry, UK. Zugriffsbedingungen.

Hien, P.D., Bac, V.T., Tham, H.C., Nhan, D.D., and Vinh, L.D., (2002). Influence of meteorological conditions on $PM_{2.5}$ and $PM_{2.5-10}$ concentrations during the monsoon season in Hanoi, Vietnam, Atmospheric Environment, Vol 36, pp. 3473-3484.

Hitchins, J., Morawska, L., Wolff, R., Gilbert, D., (2000). Concentrations of submicrometer particles from vehicle emissions near a major road, Atmospheric Environment, Vol 34, pp. 51-59.

Hitchins, J., Morawska, L., and M. Jamriska, M., (2001). Dispersion of particles from vehicle emissions around high- and low-Rise Buildings, Indoor Air, Vol 12, pp. 64-71.

Ho, K.F., Lee,S.C., Chan, C.K., Yu, J.C., Chow, J.C., and Yao, X.H., (2003). Characterization of chemical species in $PM_{2.5}$ and PM_{10} aerosols in Hong Kong, Atmospheric Environment, Vol 37, pp. 31-39.

Hobo® by onset (2009).www.thermastor.com/Meters-And-Data-Loggers.

Hochadel, M., Heinrich, J., Gehring, U., Morgenstern, V., Kuhlbusch, T., Link E et al., (2006). Predicting long-term average concentrations of traffic-related air pollutants using GIS-based information, Atmospheric Environment, Vol 40, pp.542-553.

Hoek, G., Schwartz, J.D., Groot, B., Eilers, P., (1997). Effects of ambient particulate matter and ozone on daily mortality in Rotterdam, The Netherlands, Archives of Environmental Health, Vol 52, pp. 455-463.17)

Hoek, G., Dockery, D.W., and Pope, A., (1998). Association between PM_{10} and decrements in peak expiratory flow rates in children, reanalysis of data from five panel studies, European Respiratory Journal, Vol 11, pp.1307-1311.

Hussein, T., Gltsos, T., Ondracek, J., Dohanyosova, P., Zdimal, V., Hämeri, K., Lazaridis, M., Smolik ,J., and Kulmala , M., (2006). Particle size characterization and emission rates during indoor activities in a house, Atmospheric Environment, Vol 40, pp. 4285-4307.

IARC (1999). Overall evaluations of carcinogenicity to humans. International Agency for Research on Cancer, Lyons, France.

IARC (2002). Monography on the evaluation of carcinogenic risk to humans, International Agency for Research on Cancer, Lyons, France.

ICRP (1994). International Commission on Radiological Protection: Human respiratory tract
model, Annals of ICRP, Vol 24, Issue 1.

IDEM (2009). Breathing zone. Indiana Department of Environmental Management. www.in.gov/idem.

Impens, R.A., and Delcarte, E., (1979). Survey of urban trees in Brussels, Belgium, Journal of Arboriculture, Vol 5(8), pp. 169-176.

Ishikawa, H,. Amano, S., and Yakushiji, K., (2006). Flow around a Living Tree, JSME International Journal Series B, Vol. 49 (4), Special Issue on Jets, Wakes and Separated Flows pp.1064-1069.

Janhäll, S., Molnár, P., and Hallquist, M., (2003). Vertical distribution of air pollutants at the Gustavii Cathedral in Göteborg, Sweden, Atmospheric Environment, Vol 37, pp. 209-217.

James, A.C., Stahlhofen, W., Rudolf, G., Egan, M.J., Nixon, W., Gehr, P. and Briant, J.K., (1991). The respiratory tract deposition model proposed by the ICRP task group, Radiation Protection Dosimetry, Vol 38, pp. 159-165.

Johnson, T.R., (1995). Recent advances in the estimation of population exposure to mobile source pollutants**,** Journal of Exposure Anaysis and Environmental Epidemiology , Vol 5(4)**,** pp**.**551-571.

Jones,M., Harrison, R.M., (1994). In: Non Biological Particles and Health, S. Holgate (Ed.) HMSO, London, pp. 15.

Jonsson, P., Bennet, C., Eliasson, I., and Lindgren, E.S., (2004). Suspended particulate matter and its relations to the urban climate in Dar es Salaam, Tanzania, Atmospheric Environment, Vol 38, pp.4175-4181.

Judd M.J., Raupach M.R. and Finnigan J.J., (1996). A wind tunnel study of turbulent flow around single and multiple windbreaks, Boundary-Layer Meteorology, Vol 80, pp. 127-165.

Jung, I., Kumar, S., John, K., (2004). Impact of meteorology on the fine particulate matter distribution in central and southeastern Ohio, 12th Joint Conference on the Applications of Air Pollution Meteorology with the Air and WasteManagement
http//ams.confex.com/ams/AFMAPUE/12AirPoll/abstracts/38553.htm.

Kakimoto H, Matsumoto Y, Sakai S, Kanoh F, Arashidani K, and Tang N, (2002). Comparison of atmospheric polycyclic aromatic hydrocarbons and nitropolycyclic aromatic hydrocarbons in an industrialized city (Kitakyushu) and two commercial cities (Sapporo and Tokyo). Journal of Health Science, Vol 48, pp. 370-375.

Kalaiarasan, M., Balasubramanian, R., Cheong, K.W.D., and Tham, K.W., (2009). Particulate-bound polycyclic aromatic hydrocarbons in naturally ventilated multi-storey residential buildings of Singapore: Vertical distribution and potential health risks, Building and Environment, Vol 44, pp. 418-425.

Kalaiarasan, M., Balasubramanian, R., Cheong, K.W.D., and Tham, K.W., (2008). Field-based investigation of traffic pollutants in multi-storey buildings in Singapore, Proceedings of IA2008, Copenhagen, Denmark.

Kalaiarasan, M., Balasubramanian, R., Cheong, K.W.D., and Tham, K.W., (2009). Traffic-generated airborne particles in naturally ventilated multi-storey residential buildings of Singapore: Vertical distribution and potential health risks. Special Issue of Building and Environment, Vol 44, pp. 1493-1500.

Kalaiarasan, M., Balasubramanian, R., Cheong, K.W.D., and Tham, K.W., (2009). Vertical distribution of airborne particulate matter in a tropical urban environment: Changes in physical and chemical characteristics. Approved for publication in the Springer Book 'Urban Airborne Particulate Matter: Origins, Chemistry, Fate and Health Impacts' in 2010. Editor: Professor Zereini, Institute for Atmospheric and Environmental Sciences, Goethe University, Frankfurt am Main, Germany.

Kamens, R., Lee, C.T., Weiner, R. and Leith, D., (1991). A study to characterize indoor particles in three non-smoking homes, Atmospheric Research, Vol 25, pp. 939-948.

Karthikeyan, S., Balasubramanian. R., and See, S.W., (2005). Optimization and validation of a low temperature microwave-assisted extraction method for analysis of polycyclic aromatic hydrocarbons in airborne particulate matter, Talanta, pp. 79-86.

Kastner-Klein, P., and Plate, E.J. (1999). Wind-tunnel study of concentration fields in street canyons, Atmospheric Environment, Vol 33(24-25), pp.3973-3979.

Kaur, S., and Nieuwenhuijsen, M.J., (2009). Determinants of Personal Exposure to $PM_{2.5}$, Ultrafine Particle Counts, and CO in a Transport Microenvironment, Environmental Science and Technology, Vol 43, pp 4737-4743.

Kim, K, Lee, M., Lee, G., Kim, Youn Y., and Oh, J., (2002). Observations of aerosol-bound ionic compositions at Cheju Island, Korea, Chemosphere, Vol 48, pp. 317-327.

Kirchstetter, T.W., Harley, R.A., Kreisberg, N.M., Stolzenburg, M.R., and Hering, S.V., (1999). On-road measurement of fine particle and nitrogen oxide emissions from light- and heavy-duty motor vehicles, Atmospheric Environment, Vol 33, pp. 2955-2968.

Kittelson, D.B., Johnson, J., Watts, W., Wei, Q., Drayton, M., Paulsen, D. and Bukowiecki, N., (2000). Diesel aerosol sampling in the atmosphere, SAE Paper No. 2000-01-2122.

Klepeis, N.E., (1999). An introduction to the indirect exposure assessment approach: Modeling human exposure using microenvironmental measurements and the recent National Human Activity Pattern Survey, Environmental Health Perspectives, Vol 107, pp. 365-374.

Koponen, I.K., Asmi, A., Keronen, P., Puhto, K., and Kulmala, M., (2001). Indoor air measurement campaign in Helsinki, Finland 1999 – the effect of outdoor air pollution on indoor air, Atmospheric Environment, Vol 35, pp. 1465-1477.

Kreyling, W., (1990). Interspecies comparison of lung clearance of "insoluble" particles, Journal of Aerosol Medicine, Vol 3(S1), pp. S93-S110.

Kruize, H., Hanninen, O., Breugelmans, O., Lebret, E., and Jantunen, M., (2003). Description and demonstration of the EXPOLIS simulation model: Two examples of modeling population exposure to particulate matter, Journal of Exposure Analysis and Environmental Epidemiology, Vol 13, pp. 87-99.

Kumar, R., Elizabeth, A., Gawane, A.G., (2006). Air quality profile of inorganic ionic composition of fine aerosols at two sites in Mumbai City. Aerosol Science and Technology, Vol 40, pp. 477-489.

Latini, G., Grifoni, R. C., and Passerini, G., (2002). Influence of meteorological parameters on urban and suburban air pollution, Air Pollution X, Transaction: Ecology and the Environment, Vol 53.

Laurinavičienė, D., (2008). Nitrogen dioxide concentration and their relation Kaunas, with meteorological conditions and some environmental factors in Kaunas, Environmental Research, Engineering and Management, Vol.1 (43), pp. 21-27.

Leitl, B.M., Kastner-Klein, P., Rau, M., and Meroney, R.N., (1997). Concentration and flow distributions in the vicinity of U-shaped buildings: wind-tunnel and computational data, Journal of Wind Eng. Ind. Aerodynamics, Vol 67&68, pp.745-755.

Le Tertre, A., Medina, S., Samoli, E., Forsberg, B. Michelozzi, P., Boumghar, A., Vonk, J.M., Bellini, A., Atkinson, R., Ayres, J.G., Sunyer, J., and Katsouyanni, K, (2002). Short-term effects of particulate air pollution on cardiovascular diseases in eight European cities, Journal of Epidemiology and Community Health, Vol 56 (10), pp. 773-779.

Lewin, E.E., R.G. de Pena, and Shimshock, J.P., (1986). Atmospheric gas and particle measurements at a rural northeastern US site, Atmospheric Environment, Vol 20, pp. 59-70.

Levy, J.I., Bennett, D.H., Melly, S.J., and Spengler, J.D., (2003). Influence of traffic patterns on particulate matter and polycyclic aromatic hydrocarbon concentrations in Roxbury, Massachusetts, Journal of Exposure Analysis and Environmental Epidemiology, Vol 13 (5), pp. 364-371.

Li, C.S., Lin, W.H., Jenq, F.T., (1993). Characterization of outdoor submicron particles and selected combustion sources of indoor particles, Atmospheric Environment, Vol 27(B) 4, pp. 413-424.

Li C.K., and Kamens, R.M., (1993). The use of polycyclic aromatic hydrocarbons as source signatures in receptor modelling, Atmospheric Environment, Vol 27, pp.523–32.

Li, W., and Meroney, R.N., (1983). Gas dispersion near a cubical model building. Part I. Mean concentration measurements, Journal of Wind Eng. Ind. Aerodynamics, Vol 12, pp.15-33.

Li , C., Fu, J., Sheng, G., Bi, X., Hao, Y.,Wang, X., and Mai, B.,(2005). Vertical distribution of PAHs in the indoor and outdoor $PM_{2.5}$ in Guangzhou, China, Building and Environment, Vol 40, pp. 329-341.

Logan, J.A., (1983). Nitrogen oxides in the troposphere: global and regional budgets. Journal of Geophysical Research, Vol 88, pp. 10785-10807.

Loomis, D., Castillejos, M., Gold, D.R., (1999). Air pollution and infant mortality in Mexico City, Epidemiology, Vol 10, pp. 118-123.

Lonati, G., Giugliano, M., Butelli, P., Romele, L., and Tardivo, R., (2005). Major chemical components of $PM_{2.5}$ in Milan (Italy), Atmospheric Environment, Vol 39, pp. 1925-1934.

LTA (2009). www.lta.gov.sg. Land and Transport Authority of Singapore.

LTP (2006). Air Quality Strategy, West Midlands Local Transport Plan, UK.http://www.westmidlandsltp.gov.uk.

MacIntosh, D.L., Xue, J.P., Ozkaynak, H., Spengler, J.D., and Ryan, P.B. (1995). A population-based exposure model for benzene, Journal of Exposure Analysis and Environmental Epidemiology, Vol 5(3), pp. 375-403.

McNaughton K.G., (1988). Effects of windbreaks on turbulent transport and microclimate. Agriculture, Ecosystems and Environment, Vol 22/23, pp.17-39.

Manno, E., Varrica, D., and Dongarrà, G., (2006). Metal distribution in road dust samples collected in an urban area close to a petrochemical plant at Gela, Sicily, Atmospheric Environment, Vol 40, pp. 5929-5941.

Maruo, Y.Y., Ogawa, S., Ichino, T., Murao, N., and Uchiyama, M., (2003). Measurement of local variations in atmospheric nitrogen dioxide levels in Sapporo, Japan, using a new method with high spatial and high temporal resolution, Atmospheric Environment, Vol 37, pp. 1065-1074.

Massachusetts General Laws (2009). General Provisions Relative to Real Property-Chapter 184, Section 30.

McCurdy, T., (1995). Estimating human exposure to selected motor vehicle pollutants using the NEM series of models: Lessons to be learned. Journal of Exposure Analysis and Environmental Epidemiology, Vol 5(4), pp.533-550.

Menichini E, (1999). Current legislation and guidelines on PAHs in ambient air: the Italian experience, Fresenius Environ Bull, Vol 8, pp.512–7.

Millero, F.J., and Sohn, M.L., (1992). Chemical oceanography, CRC press, Boca Raton FL, pp.531.

Minnesota Department of Health (2009). Air Quality: Particles and your health, http://www.health.state.mn.us/divs/eh/air/pm.htm.

Ministry of Health, Singapore, (2009). http://www.moh.gov.sg/mohcorp/statistics.

Modig, L., Järvholm, B., Rönnmark, E., Nyström,L., Lundbäck, B., Andersson, C., and Forsberg, B., (2006). Vehicle exhaust exposure in an incident case-control study of adult asthma. European Respiratory Journal, doi:10.1183/09031936.06.00071505.

Monn, Ch., Fuchs, A., Kogelschatz, D. and Wanner, H.-U., (1995). Comparison of indoor and outdoor concentrations of PM-$_{10}$ and PM-$_{2.5}$. Journal of Aerosol Science, Vol 26, pp. S515-S516.

Monn, C,H., Fuchs, A., Högger, D., Junker,M., Kogelschatz,D., Roth, N., and Wanner, H.U., (1997). Particulate matter less than 10 μm (PM_{10}) and fine particles less than 2.5 μm ($PM_{2.5}$): relationships between indoor, outdoor and personal concentrations, Science of the Total Environment, Vol 208, pp. 15-21.

Morawska, L., Bofinger, N.D., Kocis, L. and Nwankwoala, A., (1998). Submicron and supermicron particles from diesel vehicle emissions, Environmental Science and Technology, Vol 32, pp. 2033-2042.

Morawska,L., Thomas, S., Gillbert, D., Greenaway, C. and Rijnders, E., (1999). A study of the horizontal and vertical profile of sub micrometer particles in relation to a busy road, Atmospheric Environment, Vol 33, pp. 1261-1274.

Morawska, L., Johnson, G., Ristovski, Z.D., Agranovski, V., (1999). Relation between particle mass and number for submicrometer airborne particle, Atmospheric Environment, Vol 33, pp.1983-1990.

Morawska, L., He, C., Hitchens, J., Gilbert, D., and Parappukkaran, S., (2001). The relationship between indoor and outdoor airborne particles in the residential environment, Atmospheric Environment, Vol 35, pp. 3463-73.

Morawska. L., and Zhang, J.J., (2001). Combustion sources of particles. 1. Health relevance and source signatures, Chemosphere, Vol 49, pp. 1045-1058.

Morawska, L., He, C., Hitchins, J., Mengersen, K., Gilbert, D., (2003). Characteristics of particle number and mass concentrations in residential houses in Brisbane, Australia. Atmospheric Environment, Vol 37, pp. 4195-4203.

Mueller, P. K., Mosley,R., and L. Pierce, L., (1972). Chemical composition of Pasadena aerosol by particles size and time of day, IV, Carbonate and noncarbonated carbon content. Journal of Colloid and Interface Science, Vol 39, pp. 235-239.

NAAQS (2009). National Ambient Air Quality Standard. US Environmental Protection Agency. www.epa.gov.

Namdeo, A.K., Colls, J.J., and Baker, C.J., (1999). Dispersion and re-suspension of fine and coarse particulates in an urban street canyon, The Science of the Total Environment, Vol 235, pp.3-13.

NASA Goddard Space Flight Centre (2010). NO_2 concentration over the United States from September 24, 2004, through November 7, 2004. http://svs.gsfc.nasa.gov.

Nazaroff, W.W.,Gadgil, A.J.,Weschler, C.J.,(1993). Critique of the use of deposition velocity in modeling indoor air quality. Niren,L.,Nagda (Ed.),Modeling of Indoor Air Quality and Exposure,ASTM STP 1205. American Society for Testing and Materials, Philadelphia, pp. 81-104.

NEA (2005). Annual Report, National Environmental Agency of Singapore, http://www.nea.gov.sg.

NEA (2007). MET services, National Environment Agency of Singapore, www.nea.gov.sg.

Neuberger, M., Moshammer, H., and Kundi, M., (2002). Declining ambient air pollution and lung function improvement in Austrian children, Atmospheric Environment Vol 36, pp. 1733-1736.

Neuberger et al., (2002), Neuberger, Moshammer, H., and Kundi, M., (2002). Declining ambient air pollution and lung function improvement in Austrian children, Atmospheric Environment Vol 36, pp. 1733-1736.

Neuberger, M., Schimek, M., Horak Jr., F., Moshammer, H., Kundi, M., and T. Frischer et al., (2004). Acute effects of particulate matter on respiratory diseases, symptoms and functions: epidemiological results of the Austrian Project on health effects of particulate matter (AUPHEP), Atmospheric Environment Vol 38, pp. 3971-3981

Ng, E., Tam, I, Ng, A., Givoni, B., Katzschner, L., Kwok, K., Murakami, S., Wong, N.H., Wong, K.S., Cheng, V., Davis, A., Tsou, J.Y., and Chow, B., (2004). Final report: Feasibility study for establishment of air ventilation assessment system, technical report for Planning Department, HKSAR.

Ng, E., (2009). Policies and technical guidelines for urban planning of high-density cities – air ventilation assessment (AVA) of Hong Kong. Building and Environment, Vol 44, pp. 1478-1488.

Nisbet, and LaGoy, P., (1992) Toxic equivalency factors (TEFs) for polycyclic aromatic hydrocarbons (PAHs), Regulatory Toxicology Pharmacology, Vol 16, pp. 290-300.

NRC (1998). Research priorities for airborne particulate matter, Intermediate priorities and a long-range research portfolio, National Academy Press, Washington.

Oberdörster, G., Ferin, J., and Morrow, P., (1992a). Volume loading of alveolar macrophages (AM): A possible basis for diminished AM-mediated particle clearance, Experimental Lung Research, Vol 18, pp. 87-104.

Oberdörster, G., Ferin, J., Gelein, R., Soderholm, S.C., and Finkelstein, J., (1992b). Role of the alveolar macrophage in lung injury: studies with ultrafine particles, Environmental Health Perspective, Vol 97, pp.193-199.

Oberdörster, G., (1995). Lung particle overload: implications for occupational exposures to particles, Regulatory Toxicology and Pharmacology, Vol 21, pp. 123-135.

Oberdörster, G., and Utell, M.J., (2002). Ultrafine particles in the urban air: to the respiratory tract—and beyond, Environmental Health Perspect**,** Vol 110(8), pp. A440-1.

Ogawa & Company USA, Inc.(2009). www.ogawausa.com.

Ott, W.R., (1985). Total human exposure, Environmental Science and Technology, Vol 19, pp. 880-886.

Owen, M.K., and Ensor, D.S., (1992). Airborne particle sizes and sources found in indoor air, Atmospheric Environment **,** Vol 26, pp. 2149-2162.

Ozkaynak, H., Zufall, M., Burke, J., Xue, J., and Zidek ,J., (1999). A probabilistic population exposure model for PM_{10} and $PM_{2.5}$, Epidemiology, Vol 10**,** pp. S79-S79.

Pakkanen, T.A., Kerminen, V.M., Korhonon, C.H., Hillamo, R.E., Aarnio, P., Koskentalo, T., and Maenhaut, W., (2001). Urban and rural ultrafine (PM0.1) particles in the Helsinki area, Atmospheric Environment*,* Vol 35, pp.4593-4607.

Palmgren, F., Wahlin, P., Kildeso, J., Afshari, and A., Fogh, C.L., (2003). Characterisation of particle emissions from the driving car fleet and the contribution to ambient and indoor particle concentrations, Physics and Chemistry of the Earth, Vol 28(8), pp. 327-334.

Pandey, J.S., Kumar, R., and Devotta, S., (2005). Health risks of NO_2, SPM and SO_2 in Delhi (India), Atmospheric environment**,** Vol 39, pp. 6868-6874.

Peters, A., Wichmann, H.E., Tuch, T., Heinrich, J., and Heyder, J., (1997). Respiratory effects are associated with the number of ultrafine particles, American Journal of Respiratory and Critical Care Medicine, Vol 155, pp. 1376-1383.

Peters, A., von Klot, S., Heier, M., Trentinaglia, I., Hormann, A., Wichmann, H.E., et al., (2004). Exposure to traffic and the onset of myocardial infarction, New England Journal of Medicine, Vol 351(17), pp.1721-1730.

Petry, T., Schmid, P., and Schlatter, C., (1996). The use of toxic equivalency factors in assessing occupational and environmental health risk associated with exposure to airborne mixtures of polycyclic aromatic hydrocarbons (PAHs), Chemosphere,Vol 32, pp.639-48.

Penttinen, P., Timonen, K.L., Tiittanen, P., Mirme, A., Ruuskanen, J., and Pekkanen, J., (2001). Number concentration and size of particles in urban air: effects on spirometric lung function in adult asthmatic subjects, Environmental Health Perspect Vol 109, pp. 319-323.

Planning Department of Hong Kong SAR (2007). Air ventilation assessment report, Oil Street site, Executive summary.

Platek, S. M., Gallup, G. G., and Fryer, B. D., (2002). The fireside hypothesis: was there diffential selection to tolerate air pollution from human evolution? Medical Hypotheses, Vol 58(1), pp. 1-5.

Pope III , C.A., (1996). Adverse health effects of air pollutants in a non-smoking population. Toxicology . Vol 111, pp. 149-155.

Pope III, C.A., Burnett, R.T., Thun, M.J., Calle E.E., Krewski, D., Ito, K., and Thurston, G.D., (2002). Lung cancer, cardiopulmonary mortality and long-term exposure to fine particulate air pollution, Journal of the American Medical Association, Vol 287, pp.1132-1141.

Pope III ,C. A., and Dockery, D., (2006). Health Effects of Fine Particulate Air Pollution: Lines that Connect, JAMA, Vol 56, pp. 709.

Quackenboss, J.J., Spengler, J.D., Kanarek, M.S., Letz, R., and Duffy, C.P., (1986). Personal exposure to nitrogen dioxide: relationship to indoor/outdoor air quality and activity patterns. Environmental Science and Technology, Vol 20, pp. 775-783.

Quackenboss, J.J., Lebowitz, M.D. and Crutchfield, C.D., (1989). Indoor-outdoor relationships for particulate matter: exposure classifications and health effects, Environmental International, Vol 15, pp. 353-360.

Raducan, G., and Stefan,S., (2009). Characterization of traffic-generated pollutants Bucharest, Atmosfera, Vol 22(1), pp. 99-110.

Rastogi, N., and Sarin, M., (2005). Long-term characterization of ionic species in aerosols from urban and high-altitude sites in western India: Role of mineral dust and anthropogenic sources, Atmospheric Environement, Vol 39, pp. 5541-5554.

Ratt, W.K. de, (1994). Mutagens and polycyclic aromatic hydrocarbons in ambient airborne particles, PhD thesis, RU Leiden, Eburon, Delft.

Risom, L., Moller, P., and Loft, S., (2005). Oxidative stress-induced DNA damage by particulate air pollution, Mutation Research, Vol 592, pp. 119-137.

Ristovski, Z., Morawska, L. and Hitchins, J., (1998). Submicrometer and supermicrometer particulate emission from spark ignition vehicles. Environmental Science and Technology 32, pp. 3845-3852.

Rogak S.N., Green, S.I., and Robin C., (1994). A study of vehicle emissions in a traffic tunnel in Vancouver, B.C. Presented in the Annual Meeting of the Pacific Northeast Chapter of the Air and Waste Management Association, Eugene Oregon.

Rombout, P.J.A., Th Bloemen, H.J., Bree, L. van, Buringh, E., Cassee, F.R., Fischer, P.H., Freijer, J.I., Kruize, H., Marra, M., Opperhuizen, A., (2000). Health risks in relation to air quality, especially particulate matter, RIVM report 650010020, Bilthoven, The Netherlands.

Roorda-Knappe, M.C., Janssen, N.A.H., J.J. de Hartog, Van Vliet,P.H.N., Harssema, H., and Brunekreef, B., (1998). Air pollution from traffic in city districts near major motorways, Atmospheric Environment, Vol 32 , pp 1921-1930.

Rosenfeld, M., Marom, G., and Bitan, A., (2010). Numerical Simulation of the Airflow Across Trees in a Windbreak, Boundary-laler Meteorology, doi 10.1007/s10546-009-9461-8.

Ross, D.I., Upton, S.L., Hall, D.J. Bennett, I.P., (1999). Preliminary measurement of ultrafine aerosol emission from gas cooking, The Proceedings of the Eighth International Conference on Indoor Air Quality and Climate, Vol. 4, pp. 1043-1048.

Ross, D., (1996). Continuous monitoring of NO_2, CO, temperature and humidity in UK homes, Proceedings of the Seventh International Conference on Indoor Air Quality and Climate, pp. 513-518.

Rubino,F.M., Floridia, L., Tavazzani, M., Fustinoni, S., Giampiccolo, R., and Colombi, A., (1998). Height profile of some air quality markers in the urban atmosphere surrounding a 100m tower building, Atmospheric Environment, Vol 32, pp. 3569-3580.

Ryan, W.A., Hugh, W.D., Martin, A.C., Gary, M., Joel, D.K., and Sara, D.A.,(2009). The spatial relationship between traffic-generated air pollution and noise in 2 US cities, Environmental Research,Vol 109 , pp. 334-342 .

Sartorius AG, Goettingen, Germany (2009). http://sartorius.balances.com.

Schwartz, J., (1994). What are people dying of on high air pollution days, Environmental Research, Vol 64, pp. 26-35.

Seinfield, J.H., (1986). Atmospheric chemistry and physics of air pollution, Wiley-Interscience, New York.

Shair, F.H., and Heitner, K.L., (1974). Theoretical model for relating indoor pollutant concentrations to those outside, Environmental Science and Technology, Vol 8, pp. 444-451.

Shi, J.P., Evans,D.E., Khan, A.A., and Harrison, R.M., (2001). Sources and concentration of nanoparticles (10nm diameter) in the urban atmosphere, Atmospheric Environment, Vol 35, pp. 1193-1202.

Shi, Z., Shao,L., Jones,T.P., Whittaker,A.G., Lu, S., and K.A. Bérubé et al.,(2003). Characterization of airborne individual particles collected in an urban area, a satellite city and a clean air area in Beijing, 2001, Atmospheric Environment, Vol 37, pp. 4097-4108.

Shimada, M., Okuyama, K., Okazaki, S., Asai, T., Matsukura, M., Ishizu,Y., (1996). Numerical simulation and experiment on the transport of fine particles in a ventilated room, Aerosol Science Technology Vol 25(3) pp. 242-255.

Slooff W, Janus J.A., Matthijsen A.J.C.M., Montizaan, G.K., and Ros J.P.M.,(1989). Integrated Criteria Document PAHs, Report No. 758,474,011, The Netherlands National Institute of Public Health and Environmental Protection Bilthoven.

Sohn, D.H., Shin, W.K., Jung, S.Y., Jung , and W.T., (1995). Determination of indoor air pollution of Seoul by nitrogen dioxide using a Palmes tube air sampler, Jap. Journal of Toxicology and Environmental Health, Vol 41(2), pp.127-133.

Spengler, J.D., Dockery, D.W., Turner, W.A., Wolfson, J.M. and Ferris Jr., B.G., (1981). Long-term measurements of respirable sulfates and particles inside and outside homes, Atmospheric Environment**,** Vol 15**,** pp. 23-30.

Spengler, J., Schwab, M., Ryan, P., Colome, S., Wilson, A.L., Billick, I., and Becker, E., (1994). Personal exposure to nitrogen dioxide in the Los Angeles Basin, Journal of Air and Waste Management Association, Vol 44, pp. 39-47.

Spindler, G., Müller, K., Brüggemann, E., Gnauk, T., and Herrmann, H., (2004). Long-term size-segregated characterization of PM_{10}, $PM_{2.5}$, and PM_1 at the IfT research station Melpitz downwind of Leipzig (Germany) using high and low-volume filter samplers. Atmospheric environment, Vol 38, pp. 5333-5347.

Steiner, M., Boller, M., Schulz, T., and Pronk, W., (2007). Modelling heavy metal fluxes from traffic into the environment, Journal of Environmental Monitoring**,** Vol 9, pp. 847-854.

Stelson, W.T., and Seinfeld, J.H., (1982). Relative humidity and temperature dependence of the ammonium nitrate dissociation constant, Atmospheric Environment, Vol 16, pp. 983-992.

Stölzel, M., Breitner, S., Cyrys, J., Pitz, M., Wölke, G., Kreyling, W., Heinrich, J., Wichmann, H. E. and,Peters, A., (2007). Daily mortality and particulate matter in different size classes in Erfurt, Germany, Journal of Exposure Science and Environmental Epidemiology, Vol 17, pp. 458.

Sun, Y., Zhuang, G., Wang, Y., Han, L., Guo, J., Dan, M., Zhang, W., Wang, Z., and Hao, Z., (2004). The air-borne particulate pollution in Beijing-concentration, composition, distribution and sources, Atmospheric Environment, Vol 38, pp. 5991-6004.

Sunyer, J., Antó, J.M., Murillo, C., and Saez, M., (1991). Effects of urban air pollution on emergency room admissions for chronic obstructive pulmonary disease, American Journal of Epidemiology, Vol 134, pp. 277-286.

Sunyer, J., Castellsague, J., Saez, M., Tobias, A. and Anto, J.M., (1996). Air pollution and mortality in Barcelona. Journal of Epidemiology and Community Health, Vol 50 Suppl. 1, pp. 76-80.

Swami, K., Judd, C.O., Orsini, J.,Yang, K.X., and Husain, L., (2001). Microwave Assisted Digestion of Atmospheric Aerosol Samples Followed by Inductively Coupled Plasma Mass Spectrometry Determination of Trace Elements. Journal of Analytical Chemistry, Vol 369, pp. 63-70.

Tai, C.C. and Chong, K.C.,(1998). Development of Singapore's Rapid Transit System and the Environment. Railways and the Environment (Part 2).

Takahashi, M., and Higaki, A., Nohno, M., Kamada, M., Okamura, Y., Matsui, K., Kitani, S., and Morikawa, H., (2005). Differential assimilation of nitrogen dioxide by 70 taxa of roadside trees at an urban pollution level, Chemosphere, Vol 61(5), pp. 633-639.

Talebi, S.M., and Abedi, M., (2005). Determination of atmospheric concentrations of inorganic anions by ion chromatography following ultrasonic extraction, Journal of Chromatography A, Vol 1094, pp. 118-121.

Thatcher, T.L., and Layton, D.W.,(1995). Deposition, resuspension, and penetration of particles within a residence, Atmospheric Environment**,** Vol 29, pp. 1487-1497.

Thompson, C.R., Hensel, E.G., and Kats,G., (1973). Outdoor-Indoor levels of six air pollutants, Journal of the Air Pollution Control Association, Vol 23(10), pp. 881-886.

Tominaga, Y., and Stathopoulos, T., (2007a). Numerical simulation of dispersion around an isolated cubic building - influence of turbulence models and turbulent Schmidt number, Proc. 12th International Conference, Wind Engineering, Cairns, Australia.

Tominaga, Y., and Stathopoulos, T., (2007b). Turbulent Schmidt numbers for CFD analysis with various types of flowfield, Atmospheric Environment Vol 41(37), pp.8091- 8099.

Tominaga, Y., and Stathopoulos, T., (2008). Numerical simulation of plume dispersion around an isolated cubic buildings: comparisons between RANS and LES computations, BBAA VI International Colloquium on: Bluff Bodies Aerodynamics.

Turkoglu, N., Cicek, I., and Gurgen,G., (2004). Analysis of effects of meteorological factors on air pollutant concentrations in Ankara, Turkey, Nuovo Cimento Della Societa Italiana Di Fisica C-Geophysics and Space Physics, Vol 27 (4), pp. 347-358.

Turpin, B.J., Cary, R.A., and J.J. Huntzicker, J.J., (1990a and 1990b). An in-situ, time-resolved analyzed for aerosol organic and elemental carbon, Aerosol Science and Technology, Vol 12, pp.161-171.

Turalioglu, F.S., Nuhoglu, A., and Bayraktar, H., (2005). Impacts of some meteorological parameters on SO_2 and TSP concentrations in Erzurum, Turkey, Chemospere Vol 59 (11), pp. 1633-1642.

Turkoglu, N., Cicek, I., and Gurgen, G., (2004). Analysis of effects of meteorological factors on air pollutant concentrations in Ankara, Turkey. Nuovo Cimento Della Societa Italiana Di Fisica C-Geophysics and Space Physics**,** Vol 27 (4), pp. 347-358.

UNIPHIZ Lab software (2009). FindGrapgh software. www.uniphiz.com

United Nations (1979). Fine particulate pollution : A report of the United Nations Economic Commission for Europe. Oxford, New York, Pergamon Press.

US EPA (1996). PM Air Quality Criteria Document, US Environmental Protection Agency.

US EPA (2000). Air quality criteria for particulate matter. US Environmental Protection Agency, EPA 600/P-99/002b.

US EPA (2005). Particulate Matter: Nature and sources of the pollutant, US Environmental Protection Agency.

US EPA (2005). Total risk integrated methodology (TRIM) air pollutants exposure model documentation (TRIM.Expo / APEX Version 4) Volume I: User's guide. Research Triangle Park, NC, Office of Air Quality Planning and Standards.

US EPA (2009). National Ambient Air Quality Standards for Particulate Matter, US Environmental Protection Agency.

US EPA (2009). Air Pollutants, US Environmental Protection Agency.

US EPA (2009). Priority pollutant polycyclic aromatic hydrocarbons (PAHs). US Environmental Protection Agency.

US EPA (2010). Health Effects Associated with Nitrogen Dioxide, US Environmental Protection Agency.

Vaisala (2009). www.vaisala.com.

Vermeulen, A., Bakker, F., Geusebroek, M., Khlystov, A., Erisman, J.W., and ECN. Brandstoffen, Conversie en Milieu [BCM], (1999). Volatile organic compounds and aerosols in air: Development of sampling methods, chemical analysis and modeling. ECN-R-99-001, Petten, April.

Venkataraman, C., Lyons, J.M., and Fiedlander, S, (1994). Size distribution of aromatic hydrocarbons and elemental carbon, sampling measurement methods and source characterization, Environmental Science Technology, Vol28, pp. 535-562.

Wallace, L., (1996). Indoor particles: A review. JAMA, Vol 46, pp. 98-126.

Walmsley, J.L., Wesely, M.L., (1996). Modification of Coded Parametrizations of Surface Resistances to Gaseous Dry Deposition, Atmospheric Environment, Vol 30(7), pp. 1181-1188.

Wang, G., Wang, H., Yu, Y., Gao,S., Feng, J., Gao, S., Wang, L., (2003). Chemical characterization of water-soluble components of PM_{10} and $PM_{2.5}$ atmospheric aerosols in five locations of Nanjing, China, Atmospheric Environment, Vol 37, pp. 2893-2902.

Wehner, B., Birmili, W., Gnauk, T., and Wiedensohler, A., (2002). Particle number size distribution in a street canyon and their transformation into the urban-air background: measurements and a simple model study, Atmospheric Environment, Vol 36, pp. 2215-2223.

Wehner, B., and Wiedensohler, A., (2003). Long term measurements of submicrometer urban aerosols: statistical analysis for correlations with meteorological conditions and trace gases, Atmospheric Chemistry and Physics, Vol 3, pp. 867-879.

Weingartner, E., Keller, C, Stahel, W.A., Burtscher, H., Baltensperger, U., (1997). Aerosol emission in a road tunnel. Atmospheric Environment, Vol. 31, pp.451-462.

Wesely, M.L,(1989). Parameterization of Surface Resistances to Gaseous Dry Deposition in Regional-Scale Numerical Models. Atmospheric Environment, Vol 23, pp. 1293-1304.

Wen-Whai, LI., Helmut, P., Hugo, M., and Julian, C., (2003). Correlations between short term indoor and outdoor PM concentrations at residences with evaporative coolers, Atmospheric Environment, Vol 37, pp.2691-2703.

WHO (1987). Air Quality Guidelines for Europe. WHO Regional Publications, European Series No. 23, Regional Office for Europe, Copenhagen, Denmark.

WHO (2000). Air quality Guidelines for Europe, Second ed., Particulate matter WHO Regional Publications, Europe Series, No. 91, Copenhagen, Denmark, pp. 186.

WHO(2005). Air Quality Guidline. WHO Regional Publications, European Series No. 23, Regional Office for Europe, Copenhagen, Denmark.

Wilson, W. E. and Brauer, M., (2006). Estimation of ambient and non-ambient components of particulate matter exposure from a personal monitoring panel study, Journal of Exposure Science and Environmental Epidemiology, Vol 16, pp. 264-274.

Wikipedia (2009). Expressways of Singapore. http://en.wikipedia.org/wiki/Expressways_of_Singapore.

Winchester, J.W., Lu,W., Ren,L., Wang, M., and Maenhaut, W., (1981). Fine and coarse aerosol composition from a rural area in north China, Atmospheric Environment, Vol 15, pp. 933-937.

Wong, A.K., and Yeh, S., (1985). Housing a Nation: 25 Years of public housing in Singapore, Singapore: Maruzen Asia.

Wu,Y., Hao,J., Fu, L., Wang, Z., and Tang, G., (2002). Vertical and horizontal profiles of airborne particulate matter near major roads in Macao, China, Atmospheric Environment, Vol 36, pp. 4907-4918.

Xiao, H., and C. Liu, C., (2004). Chemical characteristics of water-soluble components in TSP over Guiyang, SW China, Atmospheric Environment, Vol 38, pp. 6297-6306.

Xu, X., Ding, H. and Wang, X., (1995). Acute effects of total suspended particles and sulphur dioxides on pre-term delivery: a community-based cohort study, Arch. Environ. Health Vol 50, pp. 407-415.

Yang, K.X.,Swami, K., and Husain, L., (2002). Determination of Trace Metals in Atmospheric Aerosols with a Heavy Matrix of Cellulose by Microwave Digestion-Inductively Coupled Plasma Mass Spectroscopy, Spetrochimica Acta Part B, Vol 57, pp. 73-84.

Yu, J., (2002). Chemical characterization of water soluble organic compounds in particulate matters in Hong Kong, A final report submitted for the provision of service to the Environmental Protection Department, HKSAR.

Zappoli,S., Andracchio,A., Fuzzi, S., Facchini, M.C., Gelencsér, A., Kiss, G., Krivácsy, Z., Molnár, A., Mészáros, E., Hansson, H. -C., Rosman, K., Zebühr, Y., (1999). Inorganic, organic and macromolecular components of fine aerosol in different areas of Europe in relation to their water solubility, Atmospheric Environment, Vol 33, pp. 2733-2743.

Zhu, Y., Hinds, W.C., Kim, S., and Sioutas, C., (2002). Concentration and size distribution of ultrafine particles near a major highway, JAMA, Vol 52, pp. 1032-1042.

Zidek, J.V., Shaddick, G., White, R., Meloche, J., and Chatfield, C., (2005). Using a probabilistic model (pCNEM) to estimate personal exposure to air pollution, Environmetrics, Vol 16**,** pp**.** 481-493.

Zou, X., Shen, Z., Yuan, T., Yin, S., Cai, J., Chen, L., and Wang, W., (2006). Shifted power-law relationship between NO_2 concentration and the distance from a highway: A new dispersion model based on the wind profile model, Atmospheric Environment, Vol 40, pp. 8068-8073.

APPENDIX A

Table A1 Specifications Grimm Dust Monitor

Particle Size	0.30, 0.40, 0.50, 0.65, 0.80, 1.0, 1.6, 2.0, 3.0, 4.0,5.0, 7.5, 10, 15, 20 µm
Count Range	1 to 2,000,000 counts/liter
Mass Range	1 to 100,000 µg/m^3
Size channels	16 channel sizes, mass in µg/m^3 and particle counts/liter
Sensitivity	1 particle/liter
Sample Flow Rate	1.2 liters/minute, flow controlled
Reproducibility	± 2%
PTFE Filter Size	47mm
Operating Temperature Range	4^{o}C to 45^{o}C

Table A2 WS425 Vaisala Ultrasonic Wind Sensor

Wind Speed	
Measurement range	
a)serial output	0 - 65 m/s
b)analog output	0 - 56 m/s
Starting threshold	virtually zero
Delay distance	virtually zero
Resolution	0.1 m/s
Accuracy (range 0-65 m/s)	± 0.135 m/s or 3% of the reading, whichever is greater
Wind Direction	
Measurement range	0 - 360°
Starting threshold	virtually zero
Delay distance	virtually zero
Resolution	1°
Accuracy (wind speed over 1 m/s)	± 2°
Inputs and Outputs	
Operating power supply for heated model	10-15 VDC, 12 mA typical (analog) 36 VDC ±10%, 0.7 A
Digital outputs	RS232, RS422 or RS48 SDI-12 Standard Data Interface
Analog outputs wind speed	
a)frequency	5 Hz/mph
b) voltage	8.0 mV/mph
Wind direction simulated	0-V_{ref} represents 0-359°
Operating Temperature	
Non-heated	-40 to 55 °C
Heated	-55 to 55 °C
Operating Temperature Range	4^{o}C to 45^{o}C

Table A3 Metrohm Ion Chromatography System Operating Parameters

Analysis	Anion	Cation
Column	Metrosep Anion Dual 2	Metrosep C2 -100
Eluent	Sodium hydrogen carbonate 336 mg/2L	Tartaric acid 1200 mg/2L
Eluent Flow rate	0.8 mL/min	1.0 mL/min
Suppressor	Yes	No
Detector	Metrohm 732 IC Detector	Metrohm 732 IC Detector
Sample Loop Volume	20 µL	20 µL
System Operating	6~9 MPa	5~7 MPa
Total Elution Time	Approx. 16 minutes	Approx. 14 minutes

Table A4 ICP-MS operating conditions and measurement parameters for the determination of trace elements in acid digested filter samples

Sample introduction	
Sample uptake	1 ml min^{-1}
Nebulizer	Cross-flow
Nebulizer gas	Argon, 0.93 l min^{-1}
(transport gas)	
Plasma conditions	
Rf power	1100 W
Plasma gas	Argon, 16 l min^{-1}
Auxiliary gas	Argon, 0.9 l min^{-1}
Spray chamber	Rytone Scott
Measurement parameters	
Data acquisition	Peak hopping
Isotopes measured	^{107}Ag, ^{27}Al, ^{111}Cd, ^{52}Cr, ^{59}Co, ^{63}Cu,
	^{57}Fe, ^{55}Mn, ^{60}Ni, ^{208}Pb, ^{64}Zn, ^{51}V, ^{48}Ti etc.
Dwell time	50 -150 ms
Sweeps per reading	20
Reading per replicate	1
Data acquisition	Peak hopping

Table A5 Toxicity Equivalence Factors

PAH	Individual TEF values
Naphthalene(Nap)	0.001
Acenaphthene (Ace)	0.001
Acenaphthylene (Acy)	0.001
Fluorene (Flu)	0.001
Phenanthrene (Phe)	0.001
Anthracene (Ant)	0.01
Fluoranthene (Flt)	0.001
Pyrene (Pyr)	0.001
Benzo[*a*]anthracen(BaA)	0.1
Chrysene (Chr)	0.01
Benzo[*b*]fluoranthene (BbF)	0.1
Benzo[*k*]fluoranthene (BkF)	0.1
Benzo[*a*]pyrene (BaP)	1
Indeno[*1,2,3,cd*]pyrene (Ind)	0.1
Dibenzo[*a,h*]anthracene (DBA)	5
Benzo[*g,h,i*]perylene (BPe)	0.01

(Source: Nisbet and LaGoy 1992)

APPENDIX B

INTERNATIONAL CONFERENCE ABSTRACTS

FIELD-BASED INVESTIGATION ON VERTICAL DISTRIBUTION OF AIRBORNE PARTICULATE MATTER IN MULTI-STOREY BUILDINGS

K. W. D. Cheong[1], R. Balasubramanian[2] and M. Kalaiarasan[1]

[1]Department of Building, National University of Singapore, Singapore
[2] Division of Environmental Science and
e-mail: mano_kalaiarasan@yahoo.com.sg
Engineering, National University of Singapore, Singapore

Keywords: Outdoor, IAQ, Fine particulate matter, Vertical transport

Abstract

The aim of the study is to quantify the concentration levels of fine particulate matter ($PM_{2.5}$; PM with diameter ≤ 2.5μm) at various heights of a typical high-rise building in close proximity to a major expressway in Singapore. For this work, a 22 - storeys naturally-ventilated high-rise residential building located within 30m from a major expressway was selected. Three different floors in the building were selected for the $PM_{2.5}$ measurements namely, the fourth storey which represented the lower floors, tenth storey which represented the mid floors and seventeenth storey which represented the upper floors of the building. Objective measurements namely, particle size, particle count, wind speed, wind direction, ambient temperature and relative humidity were conducted at the selected floors. The experimental results show that $PM_{2.5}$ count concentration was highest at the mid floors of the building when compared to its upper and lower floors during peak and

off peak hours. This could be due to the tree canopies planted alongside the expressway which deflected some of the traffic-polluted air from the lower floors towards the mid floors of the building thus contributing to the increase in the particle count concentration at the mid floors of the building. The lower floors had the second highest $PM_{2.5}$ count concentration due to its proximity to traffic emissions while the upper floors had the least fine particulate matter count concentration due to dilution.

FIELD-BASED INVESTIGATION ON VERTICAL DISTRIBUTION OF TRAFFIC POLLUTANTS IN MULTI-STOREY BUILDINGS IN SINGAPORE

M. Kalaiarasan[1*], R. Balasubramanian[2], K. W. D. Cheong[1] and K.W. Tham[1]

[1]Department of Building, National University of Singapore, Singapore
[2]Division of Environmental Science and Engineering, National University of Singapore, Singapore

*e-mail: mano_kalaiarasan@yahoo.com.sg or g0403455@nus.edu.sg

Keywords: Outdoor NO_2, Indoor NO_2, Vertical Transport, Vertical Distribution Profile

Abstract

The aim of this study is to determine and quantify the I/O ratio of traffic-generated NO_2 at various heights of a 20 - storeys naturally-ventilated high-rise building located within 30 meters from a major expressway in Singapore. Indoor and outdoor NO_2 measurements were conducted at every third floor of the building over a period of 5 weeks which was hot and sunny during the Northeast monsoon season. Key meteorological measurements namely, wind speed, wind direction, temperature and relative humidity were

also conducted at the selected floors. Results showed the weekly mean indoor and outdoor NO_2 concentration levels were highest at the mid floors of the buildings when compared to those measured at their upper and lower floors in a typical week. This trend could be due to the presence of dense tree canopies planted alongside the expressway that possibly deflected some of the traffic-polluted air from the lower levels towards the mid floors of the building as it traversed from the expressway towards the building. The I/O ratios of traffic-generated NO_2 concentration levels in the residential apartments ranged from 0.84 - 0.98.

EXPOSURE LEVELS OF TRAFFIC GENERATED PARTICLES IN NATURALLY-VENTILATED HIGHRISE RESIDENTIAL APARTMENT BUILDINGS IN SINGAPORE

M. Kalaiarasan[1*], K. W. D. Cheong[1] R. Balasubramanian[2] and K.W. Tham[1]

[1]Department of Building, National University of Singapore, Singapore
[2]Division of Environmental Science and Engineering, National University of Singapore, Singapore

*e-mail: mano_kalaiarasan@yahoo.com.sg or g0403455@nus.edu.sg

Keywords: Health, Vertical Distribution Profile, Traffic Particles

Abstract

The aim is to quantify the traffic-generated particle mass and particle number concentrations at various heights of a typical 22 - storeys high-rise building located in close proximity i.e. within 30 meter and along a busy major expressway in Singapore. Three representative floors were selected to

represent the lower, the mid and upper floors of the buildings for the $PM_{2.5}$ measurements including samples for chemical analysis to determine the organic carbon (OC) and elemental carbon (EC) mass concentrations and the ratio between these species i.e. OC/EC ratio was evaluated for real traffic emissions. The OC/EC ratio at the various floors of the building ranged from 1.20 - 1.81. This was within the expected value of 3.7 for traffic emissions and the lower values obtained suggested the expressway was dominated by vehicles with catalytic converter. The experimental results also show that $PM_{2.5}$ mean mass/number concentration was highest at the mid floors of the building when compared to its upper and lower floors. This could be due to the dense tree canopies planted alongside the expressway that deflected some of the traffic-polluted air from the lower levels towards the mid floors of the building as it traversed from the expressway towards the building. Although the lower floors were closest to traffic emissions, the mean particle mass/number concentration was lower there than at the mid floors due to losses from deflected traffic-polluted air and the tree canopies could have trapped $PM_{2.5}$ particles. The upper floors had the least fine particulate matter mass/number concentration due to dilution following pronounced mixing of the traffic-polluted air with ambient air. This study suggests residents at the mid floors are more susceptible to be affected by respiratory health problems due to higher exposure levels of traffic particles compared to those residents at the other floors of the building.

REFERRED INTERNATIONAL JOURNALS ABSTRACTS

TRAFFIC-GENERATED AIRBORNE PARTICLES IN NATURALLY-VENTILATED MULTI-STOREY RESIDENTIAL BUILDINGS OF SINGAPORE: VERTICAL DISTRIBUTION AND POTENTIAL HEALTH RISKS

(SPECIAL ISSUE)

M. Kalaiarasan[1], R. Balasubramanian[2] , K. W. D. Cheong[1], K.W. Tham[1]

[1]Department of Building, National University of Singapore, Singapore
[2] Division of Environmental Science and Engineering, National University of Singapore, Singapore

Keywords: Vertical Distribution Profile, Fine Particulate Matter, Dose-response, Health risks

Abstract

The main objective of the study is to quantify the mass concentration exposure levels of fine traffic-generated particles ($PM_{2.5}$) at various heights of typical multi-storey public housing buildings located in close proximity i.e. within 30m and along a busy major expressway in Singapore. The secondary objective is to compare the potential health risks of occupants in the buildings, associated with inhalation exposure of fine traffic-generated particulate matter, based on estimated dose rates and the lowest observed adverse effect levels (loael) at the various floors of these buildings. Two typical public housing buildings, both naturally-ventilated residential apartment blocks, of point block configuration (22-storeys) and slab block configuration (16-storeys) were selected for the study. Particulate samples were collected for both mass and chemical analysis (OC/EC ratio) at three representative floors: the lower, the mid, and upper floors of the buildings.

Key meteorological parameters such as wind speed, wind direction, ambient temperature, and relative humidity were also concurrently measured at the sampling locations. For the potential health risk analysis, the occupants have been divided into four age categories namely, infants, children (1 yr), children (8 - 10 yr) and adults. The analysis takes into account age-specific breathing rates, body weights for different age categories. Experimental results explicitly showed that $PM_{2.5}$ mean particle mass concentration was highest at the mid floors of both buildings when compared to those measured at upper and lower floors during a typical day. Although the lower floors were closest to traffic emissions, the mean particle mass concentration was lower there than that at the mid floors, which could presumably be due to the interception of $PM_{2.5}$ particles by tree leaves or the inflow of clean and drier air from higher altitude with lower aerosol burden mixing with the traffic-polluted air at the lower levels or both. The upper floors had the least fine particulate matter mass concentration due to dilution following pronounced mixing of traffic-polluted air with ambient air. The only difference between both blocks is that at corresponding floors, the mass concentration levels for slab block is much higher than that of point block. This could be attributed to the configuration of the blocks. Observational data shows the slab block tends to slow down the approaching wind thus allowing the accumulation of the fine traffic-generated particulate matter in front of the building. For point block, the HR values at the mid and lower floors suggest that occupants living in these floors experience 1.81 and 1.34 times more health risk, respectively, in contracting respiratory diseases when compared to those living at the upper floors for all age categories. Similarly, for the slab block,

occupants living in the mid and lower floors had 1.62 and 1.28 times more risk, respectively, in contracting respiratory diseases when compared to those living at the upper floors for all age categories.

PARTICULATE-BOUND POLYCYCLIC AROMATIC HYDROCARBONS IN NATURALLY-VENTILATED MULTI-STOREY RESIDENTIAL BUILDINGS OF SINGAPORE: VERTICAL DISTRIBUTION AND POTENTIAL HEALTH RISKS

M. Kalaiarasan[1], R. Balasubramanian[2] , K. W. D. Cheong[1], K.W. Tham[1]

[1]Department of Building, National University of Singapore, Singapore
[2] Division of Environmental Science and Engineering, National University of Singapore, Singapore

Keywords: PAHs, Fine Particulate Matter, Health Effects of Aerosols, Vertical Distribution Profile

Abstract

The main objective of the study is to quantify the polycyclic aromatic hydrocarbons (PAHs) concentration levels (US EPA priority components) in fine traffic generated particles ($PM_{2.5}$) at various heights of typical multi-storey public housing buildings located in close proximity i.e. within 30m and along a busy major expressway in Singapore. The secondary objective is to estimate the potential health risks associated with inhalation exposure, based on the toxicity equivalency factors (TEFs) at the various floors of these buildings. Two typical public housing buildings, both naturally-ventilated residential apartment blocks, of point block configuration (22 - storeys) and slab block configuration (16 - storeys) were selected for the study. Particulate samples were collected for chemical analysis at three

representative floors: the lower, the mid and upper floors of the buildings. Key meteorological parameters such as wind speed, wind direction, ambient temperature, and relative humidity were also measured at the representative floors. All samples were analyzed for the 16 PAH priority pollutants listed by US EPA. The vertical PAH distribution profile varies with height of building depending on the type of block configuration. The total mean concentrations of particulate PAHs for point and slab blocks are 3.32 ± 1.76ng/m^3 (0.56 - 7.2ng/m^3) and 6.0 ± 1.88ng/m^3 (3.19 - 10.26ng/m^3) respectively. For the point block, the highest mean total PAH concentration occurred at the mid floor followed by the upper floor. The lower floor had the least mean total PAH concentration. For the slab block, the highest mean total PAH concentration occurred at the lower floor and remained almost constant up to the mid floor and thereafter gradually decreased from mid floor to upper floor of the building. These results suggest that the building configuration influences the vertical distribution of particulate PAHs. The dominant particulate PAHs measured at the point block are naphthalene, acenaphthylene, benzo (b) fluoranthene, and benzo (g,h,i) perylene while those for the slab block, the main particulate PAHs are naphthalene, phenanthrene, fluoranthene, and benzo (g,h,i) perylene. The Bpe / Ind ratio for both blocks ranged from 0.92 ± 0.2 - 1.63 ± 0.6 indicating particulate PAHs are contributed by a mixture of both diesel and petrol engine type of vehicles, with diesel engine vehicles contributing a higher percentage of particulate PAHs to the different floor levels of both buildings. The total BaPeq concentrations for point and slab blocks are 1.06 ± 0.64ng/m^3 (0.14 - 2.45ng/m^3) and 0.94 ± 1.22ng/m^3 (0.10 - 4.59ng/m^3) respectively. The total

BaPeq equivalency results showed the potential health risk to cancer due to inhalation exposure is of concern for residents living in both blocks since the total BaPeq concentrations for both blocks were very close to, or slightly exceeded the maximum permissible risk level of 1ng/m^3 of benzo (a) pyrene.

SPRINGER BOOK PUBLICATION (2010)

VERTICAL DISTRIBUTION OF AIRBORNE PARTICULATE MATTER: PHYSICAL AND CHEMICAL CHARACTERISTICS

BOOK: URBAN AIRBORNE PARTICULATE MATTER: ORIGINS, CHEMISTRY, FATE AND HEALTH IMPACTS

M. Kalaiarasan[1], R. Balasubramanian[2] , K. W. D. Cheong[1], K.W. Tham[1]

[1]Department of Building, National University of Singapore, Singapore
[2] Division of Environmental Science and Engineering, National University of Singapore, Singapore

0.1.1 Introduction

Air pollution has become a subject of great interest on the global scale from both the regulatory and the scientific points of view. This is a result of the expanding economies, increasing population and urbanization. Particulate matter pollution has become a serious concern in urban areas due to its adverse impacts on human health (US EPA, 2009). Most of the previous studies reported in the literature on particulate air pollution deal with its temporal and spatial distributions as part of routine air quality monitoring (Hitchin et al. 2000; Wu et al. 2002; Levy et al. 2003; Morawska et al. 1999 and Zhu et al. 2002), but little work has been done on its vertical distribution in the vicinity of buildings. The horizontal distribution of particles is of interest because it helps town planners to decide on the location of buildings and amenities considering the degree of exposure of occupants to fine and ultra fine particles. In addition to those studies, the vertical distribution of particles also merits consideration because it provides an understanding how

particles are distributed with respect to the height of a building so that one can decide on the location of the natural air intake of the building, or the building orientation based on the source of particulate matter pollution. Several studies in urban areas show that motor vehicular emissions constitute the most significant source of ultrafine (particle's aerodynamic diameter less than 0.1 μm) and fine particles ($PM_{2.5}$) in urban environments (Zhu et al. 2002; Shi et al. 2001; Charron and Harrison, 2003). It was found that the daily concentrations of inhalable particles have been linked with cardio-respiratory health effects and even with mortality (Le Tertre et al. 2002; Schwartz, 1994 and Dockery et al. 1993); Pope et al. (2002) reported the correlation between long-term exposures to combustion related fine particulate matter and health effects. Long term exposure has been found to be an important environmental risk factor for cardiopulmonary and lung cancer mortality. A study reported that ultra fine particles in motor vehicle emissions have the largest surface area and the highest content of potentially toxic hydrocarbons among all particulate matter sources (Oberdörster and Utell, 2002). Studies show the majority of particles from the vehicle exhausts were found to be in the range 0.02 - 0.13μm diesel and 0.04 - 0.06μm petrol vehicles (Morawska et al. 1998 and Ristovski et al. 1998). A small fraction of the total emissions is in the coarse mode which is generally less than 30% (Rogak et al. 1994 and Weingartner et al. 1997). Thus a large number of the emitted particles have a high chance of depositing in the vulnerable parts of the respiratory system of human. The particles present in diesel engine exhaust are composed mainly of elemental carbon (EC), adsorbed organic material and traces of metallic compounds. The particles emitted from

gasoline engines are composed primarily of metallic compounds, elemental carbon and adsorbed organic material. Soluble organic fractions of the particles contain primarily polycyclic aromatic hydrocarbons, heterocyclic compounds, phenols, nitroarenes and other oxygen- and nitrogen-containing derivatives (IARC, 1989). Most of the studies and ongoing research on vertical distribution of fine particles in buildings are mainly done in the United States of America, Europe, Australia and Asian countries like Hong Kong and China (Morawska et al. 1999; Wu et al. 2002; Rubino et al. 1998; Chan and Kwok, 2000). Generally, the buildings are air-conditioned or partially airconditioned and the studies were done in temperate, semi tropical or in dry climatic conditions. However, no systematic studies have been conducted on vertical distribution of fine particles in buildings, influenced by the urban traffic in the tropics. A study on the vertical distribution of fine particles in buildings was conducted in Singapore which has tropical climate, characterized by hot and moist conditions year-round. Results obtained from this study are discussed in this book chapter. Changes in the physical as well as the chemical characteristics of the particles were measured at these buildings as described in Section X.X.3. The physical characteristics of particles determine in which part of the respiratory system the particles are likely to be deposited. Particles smaller than 10μm are inhalable.

Coarse particles and part of the fine particles in the size range 0.5 - 2.5μm are usually deposited in the extra-thoracic and trachea-bronchial parts of the lung system. Particles smaller than 1μm can penetrate into the pulmonary alveoli of the lungs, and end up in the interstitial spaces of the alveolar lung

tissue. Chemical characterization of particles helps to identify its toxicological constituents and provides as indication of the origins of $PM_{2.5}$ since certain compounds are characteristic of specific sources.

NOVA PUBLISHERS BOOK PUBLICATION (2011)

AIRBORNE PARTICULATE POLLUTION IN A TROPICAL URBAN ENVIRONMENT: HEALTH RISK ASSESSMENT OF RESIDENTS IN HIGH-RISE BUILDINGS

BOOK: PARTICULATE MATTER: SOURCES, EMISSION RATES AND HEALTH EFFECTS

M. Kalaiarasan[1], R. Balasubramanian[2] , K. W. D. Cheong[1], K.W. Tham[1]

[1]Department of Building, National University of Singapore, Singapore
[2] Division of Environmental Science and Engineering, National University of Singapore, Singapore

Abstract

A potential health risk assessment study was conducted in Singapore using an established health risk model. Singapore is highly urbanized and has a tropical climate, characterized by hot and moist conditions all year round. So far, there is no such comprehensive study done in a tropical climate. Several naturally-ventilated high-rise residential buildings at different parts of Singapore were selected for the study. These buildings were less than 30m from major expressways. Ogawa PS - 100 passive samplers were used to measure indoor and outdoor NO_2 concentration exposure levels of two typical building designs i.e. point and slab block designs. For both the block designs indoor/outdoor ratio at the various floors of the buildings were less

than unity suggesting the transport of NO_2 was from outdoors to indoors rather than internal sources. The outdoor source is mainly from the nearby traffic. The health risk assessment study show for both the point and slab block designs, residents at the mid floors of the buildings have the highest potential health risk for all age categories: infants, children (1 yr and under), children (8 - 10 yr) and adults in the mid floor compared to the high (lowest) and low floors (second highest) due to NO_2 inhalation. This was expected since the highest concentration of to NO_2 concentration occurred at the mid floors of the buildings. Children one year and under in both the blocks suffer from the highest health risk due to NO_2 inhalation followed by 8 - 10 yr old children. New born infants had the least health risk. Living in a slab block is about 1.27 times more risky due to NO_2 inhalation in contracting a respiratory disease compared to living in a point block. This was expected since the slab block tends to slow down wind speed thus allowing the accumulation of NO_2 concentration. Hence in terms of health concern, the point block is of a better design compared to the slab block. The health risk assessment study suggests a proactive design approach should be adopted in order to mitigate the health risk of residents living in these buildings.

1.0 Introduction

The two most prevalent oxides of nitrogen are nitrogen dioxide (NO_2) and nitric oxide (NO). Both are toxic gases with NO_2 being a highly reactive oxidant and corrosive Ambient air nitrogen dioxide is in large part derived from the oxidation of nitrous oxide, the major source of which is combustion emissions, mainly from motor vehicles. Evidence of the health effects of

NO_2 comes largely from toxicological studies and from observational studies on NO_2 exposure indoors. The current World Health Organization (WHO, 2005) guideline values for NO_2 are a 1-hour level of 200μg/m^3 and an annual average of 40μg/m^3. NO_2 acts mainly as an irritant affecting the mucosa of the eyes, nose, throat, and respiratory tract. A very high-dose exposure to the gas may result in pulmonary edema and diffuse lung injury. Prolonged exposure to high NO_2 concentration levels may contribute to the development of acute or chronic bronchitis whilst low concentration levels of NO_2 exposure may cause increased bronchial reactivity in some asthmatics, decreased lung function in patients with chronic obstructive pulmonary disease and increased risk of respiratory infections, especially in young children (US EPA, 2011). As people become increasingly concerned about air pollution issues, there is a need to study the impact of such traffic emissions on the environment and on human health. Most people spend their time indoors. Traffic emissions not only contribute to outdoor NO_2 concentration levels, but also to indoor levels. To address the health impact issues due to inhalation of NO_2, a potential health risk assessment study was conducted in Singapore which has a tropical climate, characterized by hot and moist conditions all year round. Results obtained from this study are discussed in this paper.